The Molecular Control of Fetal Wound Healing

Jacqueline Therese Teusner B.Biotech. (Hons)

Child Health Research Institute

Department of Surgery

Faculty of Medicine

University of Adelaide

South Australia

A thesis submitted for the degree of Doctor of Philosophy

July, 2001

Table of Contents

Table of Figures

Table of Tables

Abstract

The early to mid-gestation fetus has a striking capacity to heal skin wounds rapidly and without scarring, an ability that is lost as development proceeds. Since such physiological mechanisms are ultimately under genetic control, the major aim of this thesis was to identify genes that might be involved in fetal wound healing.

Preliminary experiments sought to investigate the ability of fetal skin to heal multiple excisional wounds *in vitro*. Full-thickness skin was dissected from the backs of embryonic day 17 (E17) and E19 rats, wounded many times using a 19-gauge needle, and suspended in serum-supplemented culture for up to 72 hours. Over this time, the dermis of wounds in E17 skin contracted on average to 34.7 ± 7.4 % of their original area and histology indicated that epidermal movement over the dermal margins of the wound also contributed to wound closure. In contrast, wounds created in E19 skin did not close but expanded slightly. These observations support previous *in vivo* findings that a developmental switch occurs in the mechanism of wound closure and establish a suitable *in vitro* model.

In order to detect mRNA transcripts that are differentially expressed during repair of open wounds inflicted at E17 and E19, a modified DD-PCR protocol was developed and optimised. Gene transcripts from four treatment groups, E17 t=0, E17 t=24 hours post-wounding, E19 t=0 and E19 t=24 hours post-wounding, were screened for differential expression. Of the 65 differentially expressed genes identified using this protocol, one 300bp PCR product that was apparently upregulated in the E17 t=24 hours post-wounding samples was isolated and cloned. Northern blot analysis using a sequence-specific probe identified a 3 kb mRNA and confirmed its upregulation in E17 but not E19 skin, in response to wounding.

The remaining sequence information of the differentially expressed transcript was obtained by 5' RACE. Analysis of the nucleotide sequence revealed a single long open

reading frame encoding a protein of 249 amino acids. Database analysis found the translated sequence has 61% amino acid identity globally with the human low affinity receptor for the Fc portion of IgG (FcγRIII). Moreover, the amino acid residues that contribute to FcγRIII structure and function are also conserved in the predicted protein, suggesting that it may be a novel member of the rat FcγR family. To date, no wound healing function has been ascribed to this family of receptors. Nevertheless, the scarless nature of wound healing in the mammalian fetus might be partly attributed to the upregulation of the FcγRIII-related gene in wound cells not previously known to express such receptors.

Statement of Originality

This work contains no material which has been accepted for the award of any other degree or diploma in any university or other tertiary institution and, to the best of my knowledge and belief, contains no material previously published or written by another person, except where due reference has been made in the text.

I give consent to this copy of my thesis, when deposited in the University Library, being available for loan and photocopying.

Jacqueline Therese Teusner

July, 2001

Acknowledgements

I must extend my gratitude to many people and organisations for the opportunity to undertake a PhD. Firstly, I would like to acknowledge The University of Adelaide for granting me The M.F and M.H Joyner Scholarship in Medicine and the Co-operative Research Centre for Tissue Growth and Repair for the provision of a supplementary scholarship to complete my Doctorate. I would also like to thank Gro*Pep* Ltd., particularly Dr. John Ballard, for granting me leave of absence to undertake post-graduate study.

Many thanks must go to Dr. David Belford, Dr. Chris Goddard and Dr. Barry Powell for their supervision throughout my project, for their insight and thought-provoking discussions, and for encouraging me to think laterally when faced with perplexing questions. I am deeply thankful to Dr. Vera Dunaiski and Dr. Allison Cowin for their invaluable technical advice, compassion with animal work, and support to keep me on track. I am also indebted to my partner in crime Mrs. Xenia Iona, who was always willing to assist me with everything in the lab and then some, and Mr Nick Hatzriodas for his technical assistance, particularly with animal work, and his great sense of humour.

I would like to extend thanks to Mrs. Kaylene Pickering for her expert help with histology; Mrs. Jo Cool for her help with image analysis and wound area calculations; Dr. Ian Nicholson for his help with all of the computer problems and his appreciated methods of stress-relief; Dr. Andy Dunbar of CSIRO Health Sciences and Nutrition, for assisting me with 5' RACE and allowing me the use of his lab; Mr. Sanford Boye of the Department of Pharmacology, Flinders Medical Centre for his expert advice and help with the phylogenetic analysis; Dr. Tony Simula of Gro*Pep* Ltd., for his help with WebAngis programs; Dr. John Wallace, Dr. Grant Brooker and staff of the Department of Biochemistry, University of Adelaide for allowing and helping me to use the Phosphor Imager; and Dr Grant Brooker again, for his knowledge and help in making protein structure and function predictions.

I extend a sincere thank-you to all the staff and students, too numerous to mention, of the Child Health Research Institute for making my life in the lab fun, there was never a dull moment; the Co-operative Research Centre for preparing me for post-doctorial life; and the CSIRO Division of Human Nutrition, Gro*Pep* Ltd. and the University of Adelaide for helping me out along the way.

Thankyou to my own family, the Drogemuller family, and my lifelong friends Christy, Ali, Leonie, Sarah, Penny, Suzanne, Stephanie, Rebeckah and Denis, for always lending a sympathetic ear and getting me out into the real word when I was in need. Thankyou to my brother Paul, even though it is hard for us to keep in touch I feel your kindness and know you will always be there for me.

I wish to pay tribute to Mum and Dad, Denise and Bob Teusner, for their willingness to assist me with anything I needed, for their undying support in the pursuit of my dreams and for their unconditional love.

The final and deepest thanks goes to my best friend, Christopher Drogemuller (aka Drugs), not just for his tolerance in putting up with me and keeping me on the right track, but also for his unfailing positive attitude, his patience and his enduring support throughout the duration of my PhD.

Abbreviations

aa	Amino acid
AAP	Abridged Anchor Primer
ADCC	Antibody-dependent cell-mediated cytotoxicity
aFGF	Acidic fibroblast growth factor
AIGF	Androgen-induced growth factor
AP	Adapter primer
APS	Ammonium persulfate
ASMA	Alpha smooth muscle actin
ATP	Adenosine triphosphate
AUAP	Abridged Universal Amplification Primer
bFGF	Basic fibroblast growth factor
BLAST	Basic Logical Alignment Search Tool
BMP	Bone morphogenetic protein
bp	Base pair(s)
CD44	Complementarity Determining 44
°C	Degrees Celsius
cDNA	Complementary DNA
COLIAI	Collagen I gene
cpm	Counts per minute
CS	Chondroitin sulfate
Da	Dalton(s)
dATP	Deoxyadenosine triphosphate
dCTP	Deoxycytosine triphosphate
DD-PCR	Differential display PCR

D-E	Dermal-epidermal
DNA	Deoxynucleotide 5'-triphosphate
DNase	Deoxyribonuclease
DEPC	Diethyl pyrocarbonate
DMEM	Dulbecco's Modified Eagles Medium
DMF	Dimethylformamide
dNTP	Deoxyribonucleic acid
DS	Dermatan sulfate
dsDNA	Double-stranded DNA
DTT	Dithiolthreitol
E.coli	Escherichia coli
E (e.g. E10)	Embryonic day (e.g. embryonic day 10)
EC	Extracellular
ECM	Extracellular matrix
EDTA	Ethylenediaminetetraacetic acid
EGF	Epidermal growth factor
ELISA	Enzyme-linked immunosorbent assay
EMBL	European Molecular Biology Laboratory
ES	Electronic subtraction
EST	Expressed sequence tag
FAP-α	Fibroblast activation protein-alpha
FBS	Fetal bovine serum
FcεR(s)	Receptor(s) for the Fc portion of IgE
FcγR(s)	Receptor(s) for the Fc portion of IgG
FcR(s)	Receptor(s) for the Fc portion of immunoglobulins

FPCL	Fibroblast-populated collagen lattice
g	Gram
g	Unit of gravity
G	Gauge
GAF	Glia-activating factor
GAG	Glycosaminoglycan
GPI-PL	Glycosyl phosphatidyinositol phospholipid
GR	Glucocorticoid receptor
HA	Hyaluronic acid
H&E	Haematoxylin and eosin
HASA	Hyaluronic acid stimulating activity
HB-EGF	Heparan binding-EGF
HCl	Hydrochloric acid
hFc1	Human Fc fragment of IgG1
HPLC	High performance liquid chromatography
h	Hour
HS	Heparan sulfate
HSPG	Heparan sulfate proteoglycan
Ig	Immunoglobulin
IgE	Immunoglobulin E
IGF	Insulin-like growth factor
IgG	Immunoglobulin G
IFN-γ	Interferon gamma
IL	Interleukin
IPTG	β-D-Isopropyl-thiogalactopyranoside
ITAM	Immunoreceptor tyrosine-based activation motif

kb	Kilobase(s)
KCl	Potassium chloride
kDa	Kilodalton(s)
KGF	Keratinocyte growth factor
L	Litre(s)
LAP	Latency-associated peptide
LB	Luria Bertani medium
LTBP	Latent TGFβ binding protein
M	Molar
µCi	MicroCurie(s)
MCS	Multiple cloning site
µg	Microgram(s)
mg	Milligram(s)
$MgCl_2$	Magnesium chloride
min	Minute(s)
mJ	Millijoule(s)
µL	Microlitre(s)
mL	Millilitre(s)
mm	Millimetre(s)
mM	Millimole(s)
MMP(s)	Matrix metalloproteinase(s)
mol	Mole(s)
MOPS	(N-morpholino) propanesulphonic acid
M6P	Mannose-6-phosphate
mRNA	Messenger RNA

MSF	Migration stimulation factor
MW	Molecular weight
NaCl	Sodium chloride
NaOH	Sodium hydroxide
NCBI	National Centre for Biotechnology Information
ng	Nanogram(s)
NK	Natural killer
nm	Nanometre(s)
nM	Nanomole(s)
nt	Nucleotide(s)
OD	Optical Density
ORF	Open reading frame
PA	Plasminogen activator
PAGE	Polyacrylamide gel electrophoresis
PAI	Plasminogen activator inhibitor
PCM	Pericellular matrix
PCR	Polymerase chain reaction
PDGF	Platelet-derived growth factor
pg	Picogram(s)
PI-PLC	Phosphatidylinositol-specific phospholipase C
PMN(s)	Polymorphonuclear leukocyte(s) (or neutrophils)
pmol	Picomole(s)
PTK(s)	Protein tyrosine kinases
PVA	Polyvinyl alcohol
RACE	Rapid amplification of cDNA ends
RHAMM	Receptor for HA-mediated motility

RNA	Ribonucleic acid
RNase	Ribonuclease
rRNA	Ribosomal RNA
RSP	Reverse sequencing primer
RT	Reverse transcription
SDS	Sodium dodecyl sulfate
sec	Second(s)
SH	Subtractive hybridisation
SH2	Src homology 2
SSC	Standard saline citrate
SSCP	Single-strand conformation polymorphism
TBE	Tris-borate EDTA buffer
TBR	Transforming growth factor beta receptor
TCR	T cell receptor
TE	Tris-EDTA buffer
TEM	Transmission electron microscopy
TEMED	N,N,N',N'-tetraethylethylenediamine
TGFα	Transforming growth factor alpha
TGFβ	Transforming growth factor beta
TIMP	Tissue inhibitor of MMP
TM	Transmembrane
TnC, R or X	Tenascin C, R or X
TNFα	Tumour necrosis factor alpha
tPA	Tissue-type plasminogen activator
Tris	Tri(hydroxymethyl)aminomethane

U	Units
uPA	Urokinase-type plasminogen activator
USP	Universal sequencing primer
UTR	Untranslated region
UV	Ultra violet
VEGF	Vascular endothelial growth factor
V	Volt(s)
(v/v)	Volume : volume ratio
(w/v)	Weight : volume ratio
www	World wide web
X-gal	5-Bromo-4-chloro-3-indolyl-β-galactopyranoside

Chapter One

Literature Review

1 Literature Review

1.1 GENERAL INTRODUCTION

Scarless healing of fetal wounds is one of the most dramatic observations in modern wound healing research. Although it has long been recognised that wound repair is an age-dependent process, many fundamental differences exist between healing in the mammalian fetus and the normal adult. The process of repair after dermal injury in the post-natal animal involves a series of well documented, organised events that usually result in the formation of a collagenous scar. In contrast, fetal skin wounds heal more rapidly, with minimal inflammation and without scarring.

This review provides a general background of the post-natal wound healing process, discusses aspects of fetal physiology and the fetal environment that may affect the cellular and extracellular processes involved in scarless wound healing, and considers research into the manipulation of adult repair to minimise scarring. The review covers the literature to the time that my research commenced, whereas citations relevant to this thesis published since then have been included in the appropriate chapters.

1.2 THE SKIN: STRUCTURE, FUNCTION AND RESPONSE TO INJURY

The skin of the fetus is less developed than adult skin. A summary of the structure and function of both adult and fetal skin is, therefore, essential prior to discussion of their different responses to wounding. The following section discusses the anatomy of human post-natal skin and human developing fetal skin. Although a fetal rat skin model was used in this thesis to study wound repair, the structure of human skin can generally be extrapolated to the rat with some differences noted, such as the presence of the panniculus carnosis in rat skin.

1.2.1 Anatomy of post-natal skin

The skin, also known as cutis or integument, constitutes almost one sixth of the total body weight, making it the largest organ of the body. Normal skin is essential for the survival of the animal and has the four major functions of protection, sensation, thermoregulation and metabolism.

The skin is not uniform, in that its appearance and thickness vary in different regions of the body according to different functional demands. Despite this, all skin types have the same basic structure. Human skin is composed of three distinct tissues, the epidermis, the dermis, and the hypodermis. The reader is directed to Burkitt *et al.* (1993) and Odland (1991) for a detailed review.

The epidermis is a keratinised, stratified squamous epithelium, containing five histologically distinct cell layers (see Figure 1.1). Superficially, the horny layer (stratum corneum) is comprised of flattened and fused cell remnants composed mostly of keratin. The next two cell types are the clear layer (stratum lucidum), which is only present in extremely thick skin, and the granular layer (stratum granulosum), which is made up of intracellular granules that contribute to keratinisation. In the prickle-cell layer (stratum

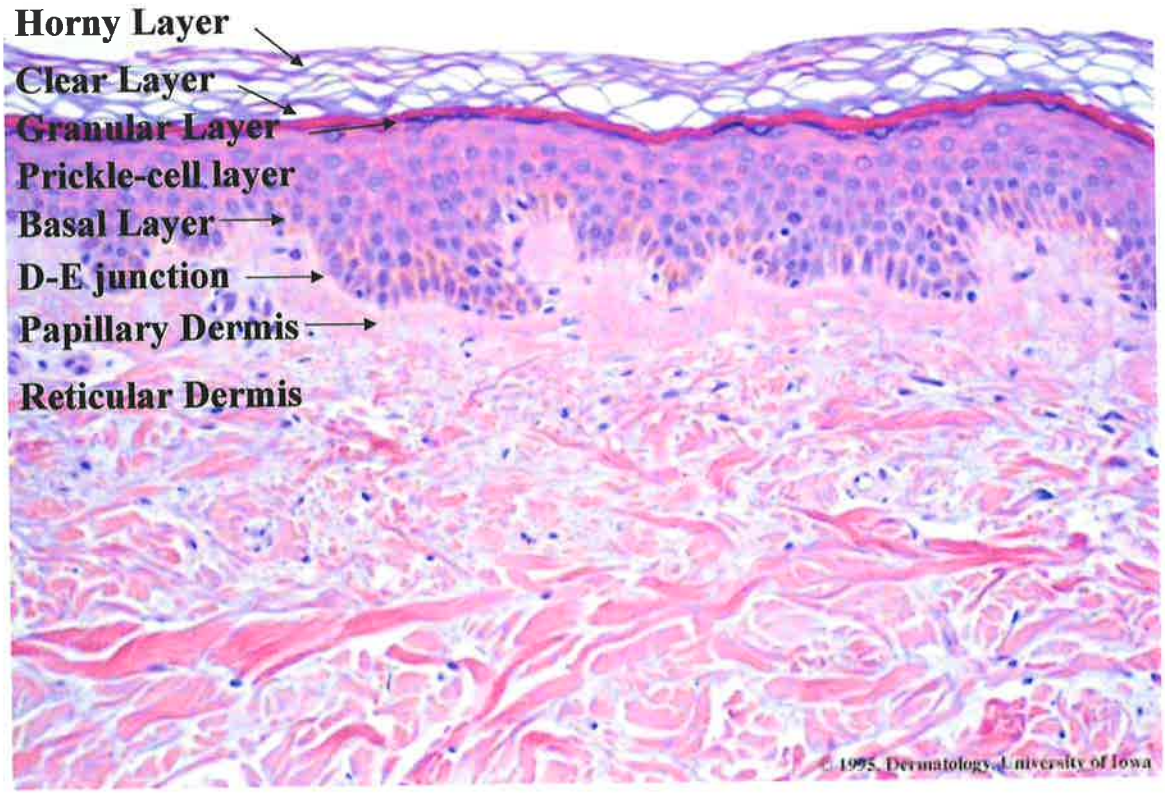

Figure 1.1 Low power photomicrograph of human post-natal skin.

The layers of the epidermis and dermis are indicated, as is the dermal-epidermal (D-E) junction. Figure is reproduced, with permission, from the DermPath Tutor© Images, Department of Dermatology, University of Iowa (tray.dermatology.uiowa.edu).

spinosum), cells are in the process of growth and early keratin synthesis, while the deepest basal layer (stratum germinativum) is the germinal layer of the epidermis. The outer keratinised layer is shed continuously and is replaced by the progressive movement and maturation of cells from the germinal layer. Therefore all the cells of this lineage are described as keratinocytes. The keratinocytes are attached to each other by highly developed cellular attachments, the desmosomes, but at the outermost horny layer, desmosomes are degraded prior to desquamation (Odland, 1991).

Cells of the epidermal basal layer and anchoring hemidesmosome structures abut upon the lamina lucida, which in turn lies on the lamina densa. The two layers comprise the basal lamina, the zone of attachment between the epidermis and dermis that is also known as the basement membrane or dermal-epidermal junction. This junction is characterised by downward folds of the epidermis called rete ridges that interdigitate with upward projections of the dermis called dermal papillae. This arrangement enhances the adhesion of the epidermis to the dermis (Burkitt *et al.*, 1993). Important molecular components of the basement membrane are type IV collagen, laminin and heparan sulfate proteoglycans. Anchoring fibrils of type VII collagen also loop from the lamina densa to the basal lamina and into the papillary dermis to enhance adhesion (Odland, 1991).

The dermis is a moderately dense fibroelastic connective tissue composed of collagen and elastic fibres, glycosaminproteoglycans, salt and water. The principal cells of the dermis are fibroblasts, but perivascular mast cells and variable numbers of tissue macrophages are also present. The dermis is divided into two zones. The more superficial papillary dermis (pars papillaris) is comprised of the dermal papillae and immediately subjacent tissue. This layer is highly vascularised with fine interlacing collagen fibres and accommodates numerous nerve endings and thermoreceptors. The deeper reticular dermis (pars reticularis) is relatively acellular and avascular compared to the papillary dermis and contains larger and more dense elastic and collagen fibres. Fibrillin and elastin constitute

the elastic fibres of the dermis, while the most abundant collagen is type I, then type III, with some type V and VI. The reticular layer also contains sweat and sebaceous glands and keratinising appendage structures of the skin (Mast, 1992). During embryological development, these appendages originate from downgrowths of epidermal epithelium into the dermis and hypodermis (Burkitt *et al.*, 1993). Smaller collagen fibrils, predominantly types III and V, appear as sheaths around the epithelial appendage structures, vessels and nerves throughout the papillary and reticular dermis and in the regions of the dermal-epidermal junction (Odland, 1991).

The hypodermis (or subcutis) consists largely of vascularised adipose tissue and is the anchoring layer attached to the underlying muscle fascia. Fibroblasts, histiocytes, plasma cells, lymphocytes and mast cells also exist in this subcutaneous layer. Many of these cells are involved in non-specific defence and the processing of foreign antigens that may be traumatically introduced into the skin (Mast, 1992).

1.2.2 Fetal skin histology

The skin of human embryos is far simpler than fetal or adult skin. The reader is directed to Holbrook (1991) for a detailed review. The primitive epidermis is established at 7-8 days as a single layered indifferent ectoderm. At the limb bud stages, between 4 to 8 weeks of gestation, the epidermis consists of a squamous peridermal layer overlying a cuboidal basal keratinocyte layer. This state of the epidermis persists during the embryonic period, which is the first 2 months of *in utero* life. Beneath the epidermis is a thin, loose and homogenous mesenchyme that has not yet differentiated into dermis (Martin and Nobes, 1992). The periderm, which exists between weeks 4 and 24 of human gestation, is the transient, protective covering of the epidermis that is sloughed into the amniotic fluid as soon as differentiation of the underlying epidermal layers is complete. It is unique to primates, has the appearance of multiple microvilli projecting off the surface of the skin and

may have an absorption function as an amniotic fluid dialysate membrane (Longaker and Adzick, 1991). At all stages, the epidermis is associated with a basal lamina and separated from it by a lamina lucida. Hemidesmosomes form at the end of the second month at the embryonic-fetal transition, coincident with the appearance of the first basal cell-derived intermediate cell layer between the periderm and the basal layer. Also after the embryonic-fetal transition, mesenchymal cells in the dermis become further separated as more fibrous material is secreted and by the end of the first trimester the reticular lamina increases in thickness (Holbrook, 1991).

During the fourth and fifth months, the amount of collagen increases to distinguish the papillary and reticular regions of the dermis. Anchoring fibrils, primarily consisting of collagen type VII, are recognised uniformly by 12 weeks' gestation. The size and number of hemidesmosomes and anchoring fibrils progressively increase during the second and third trimesters. Two to three more intermediate cell layers are also added to the epidermis in the second trimester of fetal life (see Figure 1.2). By six months a granular layer is established and the intermediate cells become known as spinous cells. The first stratum corneum develops at the end of the second trimester, superficial to the granular layer and beneath a few layers of incompletely keratinised cells. At first it consists of only a few cell layers, but it increases in thickness during the third trimester particularly near term, so that at birth the stratum corneum is equivalent to that of the adult. Coincident with the onset of keratinisation of the epidermis, the periderm becomes restricted to a thin layer and is gradually disrupted at sites where underlying cells have keratinised. Such desquamated periderm cells accumulate with other cellular debris and float freely in amniotic fluid until birth.

In the third trimester an adult-type, interlacing network of collagen fibre bundles is apparent in the dermis and there is an increase in diameter of both the individual fibrils and the collagen bundles. Elastic fibres are also clearly evident in both the papillary and

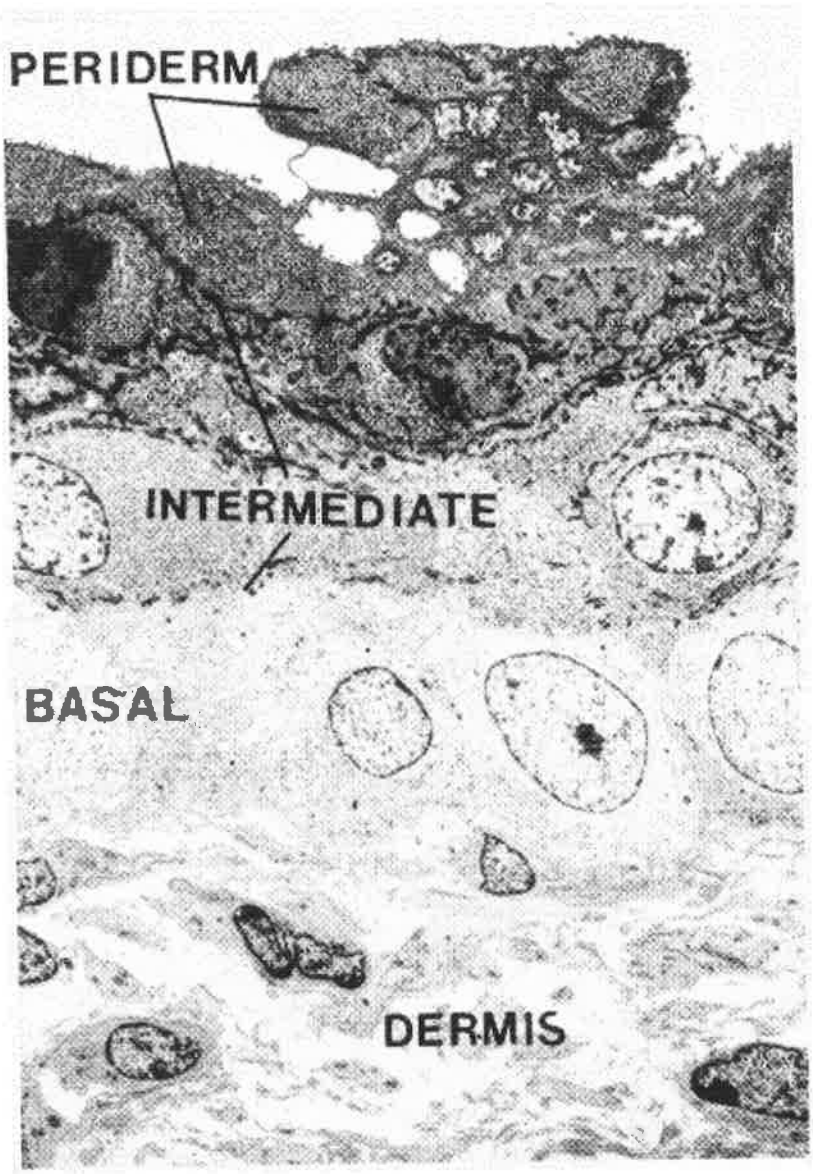

Figure 1.2 Photomicrograph of skin from a 104-day human fetus.

Three intermediate layers of the epidermis are seen underneath the periderm. Also indicated are the basal layer and the dermis (x 1900 magnification). Image was adapted from Holbrook (1991).

reticular dermis by 8 months' gestation. The dermal-epidermal junction is flat in nearly all parts of the body during the first two trimesters of development, as rete ridges do not form in the epidermis until the third trimester and are only weakly developed until after birth. At birth, the epidermis proper is fully established but the dermis is only approximately 60% of its adult thickness, is more highly cellular and fibre bundles are finer than that of the adult. The dermal water content remains high, the lower fetal ratios of collagen type I:III persist and much of dermal development takes place 3-5 months post-natally.

1.2.3 Wounding and scar formation

A wound can be defined as a disruption of normal anatomic structure and function (Lazarus *et al.*, 1994). Unlike some amphibians, the adult mammal has a limited capacity for regeneration, in the sense of restoring normal tissue architecture after injury (Longaker and Adzick, 1991). Only a few tissues like nerves and the liver show regenerative behaviour to a limited extent. Instead, wound healing usually results in fibrosis and the production of a collagenous scar to maintain the integrity and strength of the remaining tissue (Weeks and Nath, 1993). A fully developed skin scar can be defined as the macroscopic disturbance of normal skin structure and function as a consequence of wound repair (McCallion and Ferguson, 1996). Microscopically, a cutaneous scar appears as an excess of oriented, bundled collagen fibrils, instead of the basket-weave collagen matrix characteristic of unwounded dermis, with poor reconstitution of epidermal and dermal structures at the injury site (Nodder and Martin, 1997).

Scars can vary depending on the type of tissue injured, the extent of injury, genetic factors, and the presence of systemic disease in the host. Scarring may manifest itself as an elevated or a depressed site, with an alteration of skin texture, colour, vascularity, nerve supply, reflectance and elasticity (Ferguson *et al.*, 1996). A scar that exceeds the height of the surrounding tissue is termed a hypertrophic scar. One that exceeds both the height and

the boundaries of the surrounding tissue and that recurs after excision is known as a keloid (see Figure 1.3A). Keloids result from an abnormal connective tissue response to minor trauma, inflammation, burns or surgery. In contrast, hypertrophic scars develop from full thickness tissue loss such as third degree burn. Keloids rarely regress, whereas hypertrophic scars may involute and remain within the confines of the original wound (Murray and Pinnell, 1992).

Scarring and fibrosis can occur in nearly every aspect of medicine and surgery. Surgeons often must manage patients with pathologic processes in which excessive repair occurs, frequently resulting in loss of tissue function (Adzick and Longaker, 1992). Such conditions include adhesions limiting function after tendon repair, transmission loss after peripheral nerve injury and intraperitoneal fibrous adhesions after surgery (Mast *et al.*, 1992a). Some diseases are characterised by an abnormal deposition of collagen such as hepatic cirrhosis, pulmonary fibrosis, glomerulosclerosis, arteriosclerosis and scleroderma. Conversely, wound healing can be impaired in some cases, for instance in the disabled, the aged, those with diabetes, malnutrition, unsound circulation, or those on steroid or chemotherapy treatments. Pressure ulcers are an example of such chronic wounds (Lazarus *et al.*, 1994; see Figure 1.3B). Greater knowledge about the events surrounding wound repair is critical to understanding diseases and disorders such as those described above, with the ultimate aim of controlling the scarring process.

1.2.4 Overview of adult wound healing

Closure of cutaneous wounds involves the three mechanisms of reepithelialisation, connective tissue deposition and contraction. Reepithelialisation results in resurfacing of the wound, connective tissue deposition results in replacement of the damaged dermis and contraction brings the margins of open wounds together (Grinnell, 1994). A primarily closed skin incisional wound mainly heals by matrix deposition from the wound margins.

A

B

Figure 1.3 Examples of abnormal wound healing.

(A) Keloid; Shoulder region of 21 year old female patient (B) Unhealed ulcer; Lower leg of 40 year old male patient. Both figures are reproduced, with permission, from the Online Dermatology Image Atlas, University of Erlangen (www.dermis.net/doia).

This is healing by first intention. Partial thickness cutaneous wounds heal by reepithelialisation alone. A full thickness, open defect heals primarily by the deposition of a large volume of connective tissue and wound contraction, with some reepithelialisation. This is healing by second intention (Ehrlich and Krummel, 1996).

Although diversity exists in the types of wounds and in their depth of injury, normal healing consists of a predictable set of responses and is essentially the same at all post-natal ages. The normal adult repair response is considered to be the standard to which all other repair processes are compared. Thus, a summary of normal adult wound healing is essential prior to discussion of fetal tissue repair. By considering Schilling's categorisation, healing can be described in the four stages of haemostasis, inflammation, proliferation and remodeling (Schilling, 1976). Angiogenesis, reepithelialisation and the contraction of open wounds are also considered in the following discussion.

Haemostasis

Upon cutaneous injury, blood vessels are disrupted, causing local haemorrhage. Vasoconstriction, platelet aggregation, and fibrin formation are the mechanisms that the body initiates to counteract this haemorrhage. The newly formed clot then shields the denuded wound tissues and acts as a provisional matrix over which inflammatory cells can migrate throughout the repair process (Martin, 1997). The clot is composed of cross-linked fibrin fibres together with smaller amounts of fibronectin, vitronectin and thrombospondin (Clark, 1996a). Activated platelets embedded in this mesh of fibres degranulate and release growth factors. These substances are mitogenic and chemotactic for recruiting inflammatory cells into the injury site, and act to stimulate collagen deposition (see Figure 1.4A; Broker and Reiter, 1994).

Inflammation

Chemotaxis of polymorphonuclear leukocytes (PMNs) within 12 to 24 hours after injury constitutes acute inflammation. PMNs are recruited from the circulating blood after initial vasoconstriction gives way to vasodilation and increased capillary permeability (Mast *et al.*, 1992a). Besides growth factors, cues to initiate this influx of PMNs include formyl methionyl peptides cleaved from contaminating bacterial proteins and the by-products of proteolysis of fibrin and other extracellular matrix (ECM) components (Riches, 1996). Although PMNs phagocytose bacteria and foreign material, they may not be crucial for successful wound healing, as neutropenic patients seem to heal normally in the absence of infection (Broker and Reiter, 1994; Simpson and Ross, 1972).

Macrophages and lymphocytes gradually replace PMNs and continue the phagocytosis of any remaining pathogens and cell debris (Martin, 1997). The initial fibrin matrix is then degraded and replaced by proteoglycans (Mast *et al.*, 1992a). Macrophages are believed to be mandatory for successful wound healing as their depletion inhibits normal fibroplasia (Leibovich and Ross, 1975), the process of fibroblast recruitment to the injury site and ECM production (Clark, 1993). Like platelets, macrophages secrete growth factors including interleukin-1 (IL-1), basic fibroblast growth factor (bFGF or FGF-2), platelet-derived growth factor (PDGF), transforming growth factor alpha (TGFα) and transforming growth factor beta (TGFβ). These growth factors are in turn chemotactic and form a positive feedback loop to recruit more macrophages to the wound site and enhance the influx of fibroblasts.

Peripheral blood fibrocytes also rapidly enter sites of tissue injury (Bucala *et al.*, 1994). These cells express markers for bone marrow-derived cells, but synthesise the fibroblast products of vimentin, collagen I, collagen III and fibronectin, thereby contributing to connective scar formation. Fibrocytes express a distinct profile of growth factors and may attract and activate inflammatory and connective tissue cells (Chesney and Bucala, 1997).

Proliferation

The proliferation phase is characterised by multiplication of fibroblast, endothelial and epithelial cells present at the site of injury. Stimulated fibroblasts also produce TGFβ and PDGF in an autocrine positive feedback loop, similar to macrophages. Proliferation reaches its maximum levels 3 days after wounding when fibroblasts begin expressing specific integrins to mediate their adhesion to provisional matrix proteins (Clark, 1996a). By day 4, fibroblasts begin to migrate from the collagenous matrix of the dermis and the subcutaneous tissue into the provisional wound matrix as part of granulation tissue formation (Greiling and Clark, 1997). Reepithelialisation also occurs during the proliferative phase and neovascularisation becomes more prominent. By about one week after injury, fibroblasts in the wound are stimulated to synthesise collagen to replace the proteoglycan matrix (see Figure 1.4B; Mast *et al.*, 1992a).

Remodeling

Remodeling of the wound matrix completes the healing process, although it may continue for years after injury due to the ongoing synthesis and degradation of collagen (Doillon *et al.*, 1985; Levenson *et al.*, 1968; Madden and Peacock, Jr., 1968). An overabundance of matrix metalloproteinases (MMPs) compared to protein synthesis in the matrix is thought to soften, flatten and lighten the pigment of the maturing scar (Schaffer and Nanney, 1996). MMPs are derived from a variety of sources including PMNs, fibroblasts, endothelial cells, macrophages and keratinocytes (see Figure 1.4B). During remodeling these enzymes debride any fibrinous exudate in the wound and transform collagen III synthesised by wound fibroblasts into the more stable pre-injury phenotype of collagen I (Nwomeh *et al.*, 1999; Schaffer and Nanney, 1996). The fine collagen fibrils of young granulation tissue also undergo a condensation into thicker, denser fibres, organised into arrays parallel to the skin surface (Ehrlich and Krummel, 1996). Cross-linking and

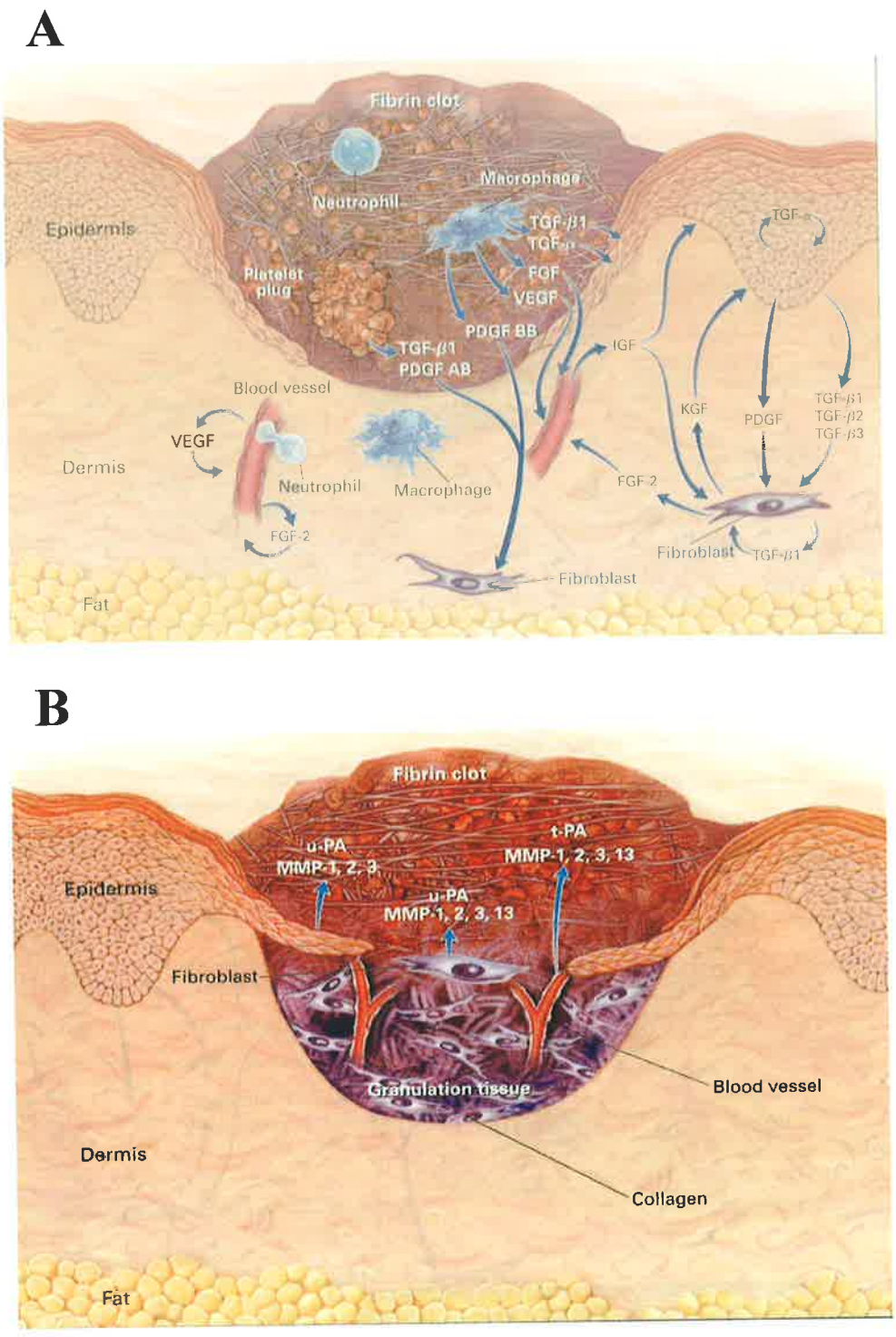

Figure 1.4 A post-natal cutaneous wound 3 days (A) and 5 days (B) after injury.

(A) Haemostasis and inflammation. Growth factors believed to be necessary for cell migration are indicated (TGFβ1, TGFβ2, TGFβ3 and TGFα denote transforming growth factors β1, β2, β3 and α; FGF fibroblast growth factor; VEGF vascular endothelial growth factor; PDGF platelet derived growth factor; IGF insulin-like growth factor; and KGF keratinocyte growth factor). (B) Proliferation, reepithelialisation and neovascularisation. Blood vessels are depicted sprouting into the fibrin clot as epidermal cells resurface the wound. Proteinases believed to be required for cell migration are indicated (u-PA is urokinase-type plasminogen activator; MMP-1, -2, -3 and –13 are matrix metalloproteinase-1, -2, -3 and -13). Both figures were adapted from Singer and Clark (1999).

structural modifications of the collagen fibrils are responsible for the increase in tensile strength of the healed wound, although the scar never regains the strength of normal tissue (Levenson *et al.*, 1968).

Angiogenesis

Angiogenesis, the process of new blood vessel formation, is stimulated primarily by vascular endothelial growth factor (VEGF) and bFGF, but acidic FGF (aFGF or FGF-1), epidermal growth factor (EGF), TGFα and TGFβ also play a role (McCallion and Ferguson, 1996). Basic FGF is released at the wound site by damaged endothelial cells, macrophages and from the ECM to initiate endothelial cells to migrate, proliferate and form tubules during granulation tissue formation. A later transition to a VEGF-mediated stimulus then allows for the more specific regulation of capillary growth and differentiation (Nissen *et al.*, 1998). VEGF is induced in wound-edge keratinocytes and macrophages in response to keratinocyte growth factor (KGF or FGF-7), EGF, TGFα and nitric oxide, and is highly specific for endothelial cell proliferation to allow a continual supply for capillary extension (Frank *et al.*, 1995 and 1998).

Besides chemotactic factors and growth factors, an appropriate ECM is also necessary for angiogenesis. In order to respond to wound angiogenic signals, endothelial cells upregulate their αvβ3 integrins, which recognise fibrin and fibronectin. These integrins are expressed at the tips of sprouting capillaries in the granulation tissue as they invade the fibrin clot (Clark, 1996a). As with the other cell migrations during the invasion phase, capillary morphogenesis is dependent on tightly regulated proteolysis of the surrounding matrix. Plasmin and MMP-8 are activated to digest the clot and basement membrane constituents to allow for endothelial cell migration (Fisher *et al.*, 1994).

Reepithelialisation

Reepithelialisation is a complex process involving the detachment, migration, reattachment, proliferation and differentiation of keratinocytes from the wound margin or from epithelial appendages deep within the dermis (Schaffer and Nanney, 1996). If a dermal injury leaves the stumps of hair follicles intact, they act like a cut epidermal wound edge and spread out to heal the epidermis. The appendages themselves are also regenerated. If, on the other hand, the wound is full thickness, then the healed region will not only be scarred but also lacking all appendages.

EGF and TGFα directly increase the rate of reepithelialisation (Brown *et al.*, 1986; Schultz *et al.*, 1987). Binding of these growth factors to the EGF receptor (erbB-1) is thought to suppress differentiation, increase proliferation and enhance migration during reepithelialisation (Hudson and McCawley, 1998). KGF is upregulated more than 100-fold within 24 hours by dermal fibroblasts at the wound margin, and specifically stimulates the proliferation of keratinocytes to indirectly affect the speed of reepithelialisation (Werner *et al.*, 1992). In addition, KGF is thought to enhance the capacity of the epithelial edge to cut through the clot by stimulating high PA and MMP-10 expression in motile keratinocytes (Madlener *et al.*, 1996; Tsuboi *et al.*, 1993). Also within the first day following injury, keratinocytes dissolve their α6β4 (laminin-binding) integrins and begin relocalising their α2β1 and α3β1 collagen/laminin receptors (Hodivala-Dilke *et al.*, 1998; Klein *et al.*, 1990; Schaffer and Nanney, 1996). Two major components of the normal basement membrane, laminin and type IV collagen, are lacking in the provisional matrix of skin wounds. Instead, epidermal cells grasp hold of and migrate over an irregularly thickened provisional matrix containing fibrin, fibronectin and diffuse deposits of vitronectin (Clark *et al.*, 1982). To do this, the leading edge keratinocytes project sheet-like lamellipodia and finger-like filopodia

and begin expressing the α5β1 fibronectin receptor, the α9β1 tenascin receptor and the αvβ5 vitronectin receptor (Cavani *et al.*, 1993; Hodivala-Dilke *et al.*, 1998).

Regulated changes in actin polymerisation and depolymerisation are the driving force for cell movement, directing protrusion at the front and retraction at the rear of the cell. The EGF receptor contains an actin-binding domain and is associated with the actin cytoskeleton upon ligand exposure, so it is thought that its activation can contribute to actin cytoskeletal reorganisation (Hudson and McCawley, 1998). Polymerised actin in a migrating cell is organised into different types of filamentous arrays, each linked to the underlying matrix via integrins. Lamellipodia, filopodia, and membrane ruffles are located at the leading edge of motile cells (Nobes and Hall, 1995). Positioned back from the leading edge are stress fibres and dorsal arc-like arrays of actin, which provide the driving force for forward movement of the rear of the cell. The co-ordinated organisation of actin filament assembly and disassembly is mediated by the GTPases Rac, Cdc42, Ras and Rho, and it is thought that reepithelialisation of post-natal skin wounds is dependent on their regulation of cell migration (Nobes and Hall, 1999; Ridley *et al.*, 1992; Ridley and Hall, 1992).

In order to migrate along the interface of the fibrin clot and the healthy dermis, the leading edge keratinocytes must dissolve the fibrin network ahead of them. For this, they upregulate expression of tissue-type plasminogen activator (tPA), urokinase-type plasminogen activator (uPA) and the specific receptor for uPA (McNeil and Jensen, 1990). Both of these activators convert plasminogen from the clot to the active fibrinolytic enzyme, plasmin (Martin, 1997). Some members of the MMP family are also upregulated by keratinocytes to aid migration and remodeling (Saarialho-Kere *et al.*, 1992; Salo *et al.*, 1994; Vaalamo *et al.*, 1997).

Forty eight to 72 hours after wounding, basal epidermal cells begin to proliferate to replace those cells lost during the injury. Migration and proliferation continue until contact with other epithelial cells occurs. When contact occurs, keratinocytes resume a basal cell

phenotype and begin to differentiate into a keratinised, stratified squamous epidermis (Schaffer and Nanney, 1996). Upon completion of wound reepithelialisation, fibrin and fibronectin gradually disappear and type IV collagen and laminin return (Clark *et al.*, 1982). When this basal lamina synthesis resumes, MMP expression ceases and new hemidesmosomes to the basal lamina reassemble (Martin, 1997).

Contraction

The task of reepithelialising a wound is facilitated by the underlying contractile granulation tissue, which concentrically decreases in size to bring the wound margins toward one another (Martin, 1997). There is currently some dispute as to the mechanism of wound contraction. One prevailing hypothesis is growth factors such as TGFβ1 and mechanical cues relating to the forces resisting contraction trigger a proportion of the wound fibroblasts to transform into myofibroblasts (Desmouliere *et al.*, 1993; Grinnell, 1994). These myofibroblasts resemble smooth muscle cells in that they both express α-smooth muscle actin (ASMA; Desmouliere *et al.*, 1993; Grinnell, 1994; Sappino *et al.*, 1990). ASMA is temporarily expressed during normal wound healing, and more persistently during fibrocontractive diseases, thus the myofibroblast is believed by some to generate the forces required for wound closure and contracture (Estes *et al.*, 1994). Evidence has also been put forward that contraction of open wounds can occur by direct fibroblast-collagen interaction, in the absence of myofibroblasts (Ehrlich, 1988; Ehrlich *et al.*, 1999). It was postulated that individual fibroblasts reorientate and reorganise the collagen fibrils associated with them into thicker bundles and this stressed matrix transmits the force necessary for wound closure. Another mechanism of wound contraction suggested that fibroblasts at the wound margins undergo a form of directed migration (Gross *et al.*, 1995). Regardless of its mechanism, contraction aids the repair of excisional wounds.

1.3 FETAL PHYSIOLOGY AND ENVIRONMENT

There are multiple intrinsic and extrinsic differences between the developing fetus and the post-natal animal that can influence wound repair. The aspects of fetal physiology and the fetal environment that may affect the cellular and extracellular processes involved in wound healing are discussed below.

1.3.1 Amniotic fluid

One major extrinsic difference between the fetal and the post-natal animal is that a sterile amniotic environment surrounds fetal skin wounds. It provides buoyant, thermally stable protection for the fetus and allows for unrestricted movement. Amniotic fluid contains nutritional substrates, trophic factors and ECM components required for fetal development (Dahl *et al.*, 1983; Harris *et al.*, 1988; Longaker *et al.*, 1989a; Mulvihill *et al.*, 1986). It is widely believed that amniotic fluid may modulate fetal skin wound healing by providing growth factors to stimulate fetal wound cells to synthesise a unique wound matrix (Longaker *et al.*, 1990a). Evidence of excellent healing by primary intention without inflammation or visible scarring in fetuses in contact with amniotic fluid has been published using rabbit, lamb and monkey models (Adzick and Longaker, 1991; Krummel *et al.*, 1987; Longaker *et al.*, 1991a). However, contraction of open wounds does not occur in fetal rabbit (Haynes *et al.*, 1995; Krummel *et al.*, 1987; Krummel *et al.*, 1989; Somasundaram and Prathap, 1970) and monkey (Sopher, 1975a and b) wounds bathed in amniotic fluid. Numerous observations have led to the conclusion that scarless healing is not solely dependent on contact with amniotic fluid, although it does appear to require a moist environment (Lin *et al.*, 1994; Longaker *et al.*, 1994a; Lorenz *et al.*, 1992; Lorenz *et al.*, 1995; Sancho *et al.*, 1997; Sullivan *et al.*, 1995a).

1.3.2 Oxygen tension

Tissue hypoxia seems important to angiogenesis induction, the activation of certain growth factors, and the stimulation of fibroblast and macrophage metabolism and division (McCallion and Ferguson, 1996). However, adult wound healing studies have shown that wound hypoxemia can result in delayed healing, impaired leukocyte function and increased infection (Jonsson *et al.*, 1991). It has also been shown that oxygen is required for the hydroxylation of proline and lysine during collagen synthesis and supplemental oxygen stimulates collagen deposition by adult fibroblasts (McCallion and Ferguson, 1996). Tissue oxygenation in the fetus is much less than that of adult tissue. For instance, the oxygen partial pressure of fetal lambs is 16 mmHg, while that of adult sheep is about 45 - 60 mmHg (Longaker and Adzick, 1991). The fetus compensates for its relative hypoxemia in many ways to heal wounds rapidly. Firstly, the fetus has a higher haemoglobin concentration than the adult. Secondly, fetal haemoglobin has a much higher oxygen affinity than adult haemoglobin. Thirdly, the cardiac output of the fetus per unit body weight is much greater than that of the adult. The lactic acid level of fetal blood, an indicator of anaerobic metabolism, is only slightly higher than in maternal blood (Pritchard, 1993). This is evidence that the fetus counteracts its hypoxemia well.

1.3.3 The immune system

One intrinsic difference between the fetus and the adult is the immune system. The fetus is significantly neutropenic and does not develop self/non-self immunologic identity until mid-gestation (Flake *et al.*, 1986). PMNs are absent in fetal wounds until late in gestation and although phagocytic capabilities gradually develop during the third trimester, chemotactic ability may be reduced (Adzick *et al.*, 1985a; Jennings *et al.*, 1991). Fetal wounds also heal without the formation of a fibrin clot (Somasundaram and Prathap, 1972), presumably due to the immature coagulation cascade and the fibrinolytic activity of

amniotic fluid. In adult wounds, the fibrin clot is thought to provide a reservoir of growth factors that contribute to scar formation that are not seen in the fetus (McCallion and Ferguson, 1996).

The absence of scarring in fetal wounds has been correlated with a sparse inflammatory response. For example, a markedly reduced macrophage and monocyte infiltrate accompanies scarless wound healing in the fetal marsupial, with inflammation becoming more prominent after pouch day 9, concomitant with scarring (Armstrong and Ferguson, 1995; McCallion and Ferguson, 1996). A similar lack of macrophage recruitment to the wound site is seen in the mouse fetus until relatively late in development at 14.5 days of gestation, coincident with when wounds begin to heal by scarring (Austyn and Gordon, 1981). Macrophages are first identified in the mouse embryo at embryonic day 10 (E10; Morris *et al.*, 1991), so even at fetal stages when macrophages have begun patrolling tissues, they still do not migrate to wounds until after closure.

The powerful chemotactic signals that attract macrophages to later stage and post-natal wounds may partly derive from platelet degranulation at the wound site, and platelets are not seen in early mouse embryos. Furthermore, the onset of macrophage recruitment seems to coincide with when platelets first appear in circulating blood (Nodder and Martin, 1997). Unlike the mouse, Olutoye *et al.* have found platelet counts and ultrastructure to be comparable in the E60 fetal pig (term = 114 days) and adult pig (Olutoye *et al.*, 1995; Olutoye *et al.*, 1996). However, numerous findings suggest that HA, the predominant GAG in fetal ECM (see section 1.3.5), inhibits platelet aggregation and cytokine release (Olutoye *et al.*, 1996; Olutoye *et al.*, 1997). Theoretically, this inhibition of platelet aggregation and degranulation may partly explain the minimal inflammation and scarless healing seen at the site of fetal dermal wounds.

In addition to the relative lack of macrophage infiltration (Austyn and Gordon, 1981; Cowin *et al.*, 1998; McCallion and Ferguson, 1996), an attenuated T lymphocyte response

(Adolph *et al.*, 1993), an absence of B lymphocytes (Cowin *et al.*, 1998), reduced angiogenesis and altered growth factor levels (Whitby and Ferguson, 1991a) have all been found at the fetal wound site. Despite neutropenia and immaturity of the immune system, it has been shown in rabbits that the fetus is capable of mounting a dose-dependent adult-like acute inflammatory response to avirulent bacteria introduced into the wound (Frantz *et al.*, 1993). Since there is no bacterial stimulus for leukocyte recruitment in the sterile amniotic environment that fetal wounds are bathed in, it was initially proposed that it might be responsible for scarless healing. This seems unlikely, since marsupial pouch young do not reside in a sterile environment and yet little inflammation is present in non-scarring pouch day 4 wounds (McCallion and Ferguson, 1996).

In short, inflammatory cells play a prominent role in normal adult wound repair. It is possible that the minimal inflammatory response seen in fetal wounds may cause the differences in matrix molecule synthesis and deposition that leads to scarless healing.

1.3.4 Growth factors and cytokines

Most polypeptide growth factors described to date are thought to be important regulators of post-natal wound healing. As described above, early fetal wounds seem to lack the two major sources of growth factors in adult wounds, degranulating platelets and invading macrophages. Consequently, fetal wounds have a reduced cytokine profile compared to that seen in adult wounds, which may lead to scarless repair. The major growth factors involved in post-natal wound healing are discussed below, as are their possible roles in fetal wound repair.

Transforming growth factor beta (TGFβ)

The TGFβ group of ubiquitous regulatory polypeptides are capable of stimulating or inhibiting proliferation and differentiation, depending on their concentration, presence of

other growth factors, and the cell type that they are acting on (Hill *et al.*, 1986). Three structurally and functionally related mammalian TGFβ isoforms have been identified, TGFβ1, TGFβ2 and TGFβ3. The TGFβ isoforms are secreted while noncovalently bound to a latency-associated peptide (LAP), and as such are unable to interact with their cell surface receptors. The LAP contains three oligosaccharide side chains, two of which have mannose-6-phosphate (M6P) as their terminal residues (McCallion and Ferguson, 1996). These M6P residues allow the inactive TGFβ-LAP complex to bind with high affinity to the cation-independent M6P/IGF-II receptor, which in effect activates the latent complex (Dennis and Rifkin, 1991). Plasmin, plasminogen activator and transglutaminase are also required for TGFβ activation (Coleman *et al.*, 1998; Kojima *et al.*, 1993). TGFβ1 acts through three receptors which are present on the membranes of most cells, TGFβ receptor I, II and III (TBRI, TBRII and TBRIII). TBRI and II are membrane spanning serine/threonine kinases. TBRIII, also known as betaglycan, appears to only serve in an auxiliary role by binding TGFβ and presenting it to TBRII. TBRII then binds to TBRI, forming a heteromeric complex with TGFβ and activating the signalling cascade. It is thought that signalling then proceeds through kinase pathways (Parrelli *et al.*, 1997).

TGFβ1 and TGFβ2 are released as early as one hour after wounding by platelets, lymphocytes and macrophages (Yang *et al.*, 1999) and are chemotactic for fibroblasts, monocytes and macrophages (Sporn and Roberts, 1992). TGFβ1 is involved in the initiation of fibrosis, whereby it stimulates the deposition of collagen and other ECM components by fibroblasts and prevents their degradation by proteolysis. In particular, it suppresses MMP-1, MMP-3 and plasminogen activators, and induces plasminogen activator inhibitor-1 (PAI-1) and tissue inhibitors of metalloproteinases (TIMPs; Cullen *et al.*, 1997; Overall *et al.*, 1989). Interestingly, TGFβ1 upregulates MMP-2 activity in cultured fibroblasts, which contrasts its inhibitory effects on MMP-1 and MMP-3 gene expression (Overall *et al.*, 1989

and 1991). Similarly, TGFβ1 modulates the protease profiles of fetal fibroblasts, demonstrating its possible role in fetal tissue remodeling (Cullen *et al.*, 1997).

TGFβ1 induces ASMA expression in fibroblasts, which correlates with scar formation and pathologic wound contraction (Desmouliere *et al.*, 1993). It is able to induce its own expression, by both increased recruitment and activation of macrophages and positive induction of the TGFβ1 promoter (Schmid *et al.*, 1993). This may be an important determinant in the progressive scarring characteristic of chronic diseases that result in the defacement of normal tissue architecture (Figure 1.5). A relationship between elevated TGFβ levels and scarring has been demonstrated in a number of fibrotic diseases, including cirrhosis, vitreoretinopathy, interstitial pulmonary fibrosis, glomerulonephritis, and scleroderma (Border *et al.*, 1990; Border *et al.*, 1992; Castilla *et al.*, 1991; Connor, Jr. *et al.*, 1989; Peltonen *et al.*, 1990; Roberts and Sporn, 1992). TGFβ1 consistently acts on cells to induce the deposition of matrix components and consequently is the chief isoform commonly associated with fibrosis (Sporn and Roberts, 1992).

The exogenous application of TGFβ1 has been shown to trigger scar formation not only in adult wounds (Ehrlich *et al.*, 1996; Mustoe *et al.*, 1987) but also in fetal wounds (Adolph *et al.*, 1993; Houghton *et al.*, 1995; Krummel *et al.*, 1988). It appears to induce an adult-like response in the usually non-scarring fetal tissue by increasing cellular infiltration, fibroplasia and collagen deposition.

Scarring has also been promoted in fetal human skin wounds by adding TGFβ1 that is infused in a slow release disk (Lin *et al.*, 1995; Sullivan *et al.*, 1995b). In these studies, the exogenous TGFβ1 appeared to stimulate the human fetal fibroblasts to upregulate TGFβ1 mRNA and protein expression. A direct interaction of TGFβ with fetal fibroblasts has been shown by *in vitro* cell surface binding studies (Durham *et al.*, 1989). Despite having a low constitutive expression of the collagen genes, exposure to TGFβ1 also induces collagen gene

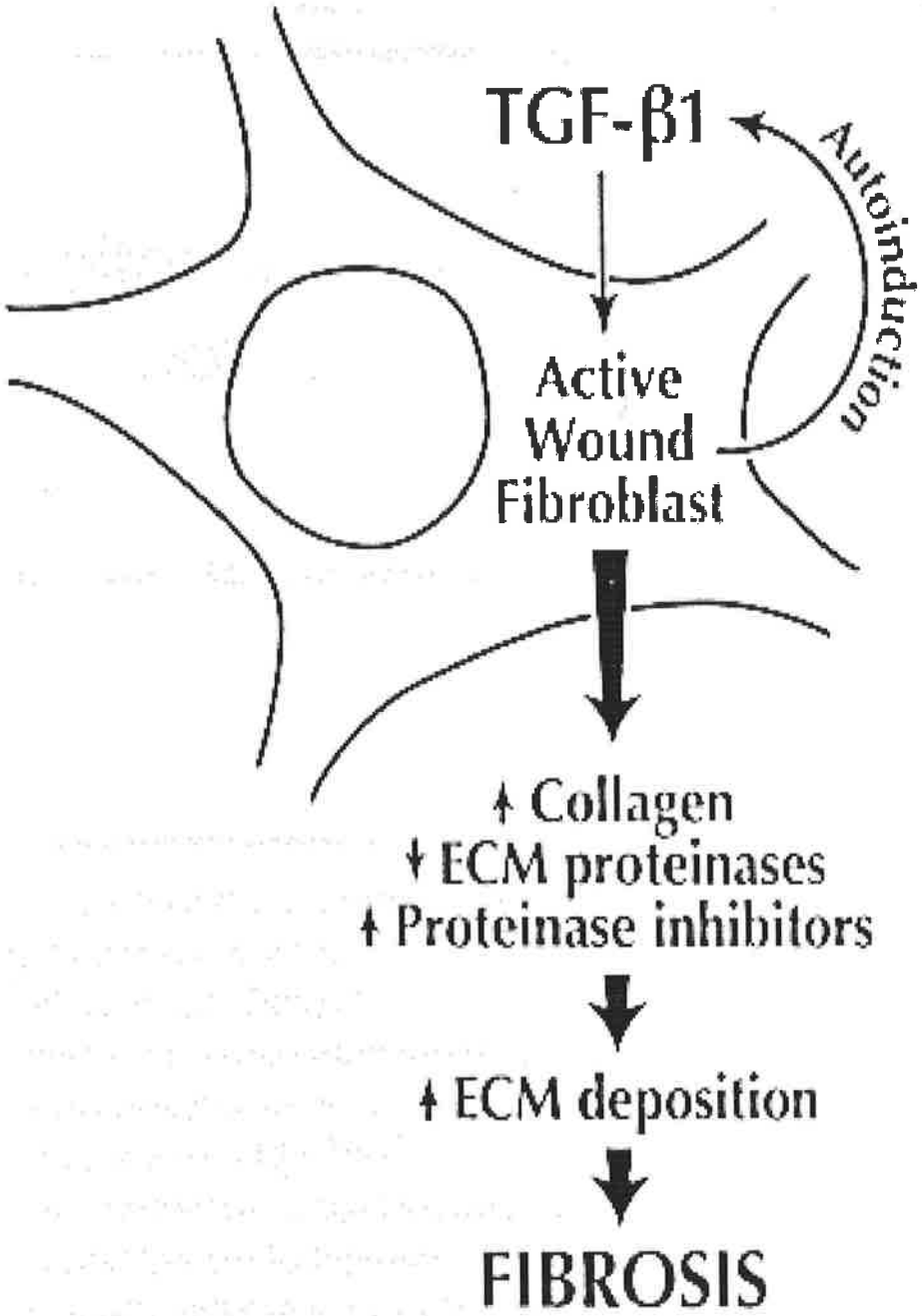

Figure 1.5 The role of TGFβ1 in the progression of fibrosis.

TGFβ1 can promote wound repair by stimulating local fibroblasts to produce collagen and other ECM proteins. It can also inhibit the production of ECM proteinases and induce the production of proteinase inhibitors. Through autoinduction, TGFβ1 can upregulate its own synthesis in fibroblasts so that these effects become amplified and fibrosis occurs. Adapted from Parrelli *et al.* (1997).

I and III expression in fetal dermal fibroblasts (Gallivan *et al.*, 1997; Lorenz *et al.*, 1993a). No such upregulation has been demonstrated in post-natal fibroblasts, which already show significant constitutive collagen gene expression in the inactivated state. More recently, Lanning *et al.* (1999) demonstrated that the administration of TGFβ1 in a sustained manner induces contraction, inflammation, fibrosis and an upregulation of collagen gene expression in excisional wounds in the fetal rabbit. Taken together, these reports support the view that the cellular and matrix machinery required for scar formation are present in fetal wounds, and fetal cells are capable of responding to growth factors in a way similar to adult cells. Indeed, embryonic fibroblasts have been reported to have more TGFβ cell surface receptors than adult fibroblasts (Durham *et al.*, 1989), thus, the lack of TGFβ-mediated fibrosis is not due to the inability of the fetal fibroblast to respond to TGFβ. Instead, as is discussed below, sustained TGFβ levels for the induction of collagen gene expression and excess collagen deposition are not present in fetal wounds.

Fibroblasts are not only capable of responding to TGFβ, they can also synthesise and secrete this growth factor. Under normal conditions, both fetal and adult fibroblasts can transcribe TGFβ1 mRNA, but fetal fibroblasts respond to hypoxia with a decrease in TGFβ1 transcription, while adult fibroblasts increase transcription (Chang *et al.*, 1993). It is thought that the low partial oxygen pressure of the fetal wound might downregulate TGFβ1 gene expression and contribute to scarless healing.

There have been many conflicting reports on the levels of both TGFβ mRNA and protein in fetal skin wounds. Early investigations found TGFβ to be apparently absent from fetal wounds (Lin *et al.*, 1995; Sullivan *et al.*, 1995b; Whitby and Ferguson, 1991a). Others found TGFβ to be expressed in the developing dermis but not upregulated in fetal wounds (Nath *et al.*, 1994a), or detected in activated epidermal and mesenchymal cells at the wound margin during the early phase of repair but rapidly cleared before wound closure (Martin *et*

al., 1993; Nodder and Martin, 1997). These reports contrast the pattern of elevated and sustained TGFβ1 expression seen in adult wounds. On the other hand, evidence of increased TGFβ levels have been found in the fetal wound environment relative to the adult situation (Longaker *et al.*, 1991b; Longaker *et al.*, 1994b). The increase in TGFβ reported by these groups could represent the inactive form of the peptide, thus accounting for the lack of fibrosis seen in fetal wounds. Additionally, it is conceivable that more TGFβ regulatory molecules that may limit the availability of active TGFβ exist in the fetal environment than in the adult. Although TGFβ1 LAP protein has been detected in human adult wounds but not in fetal wounds (Sullivan *et al.*, 1995b), other endogenous inhibitors of TGFβ such as decorin, biglycan, fibromodulin and α2-macroglobulin may be present in the fetus.

Very recently, a rat model that exhibits a transition from scarless repair in E16 fetal rat skin to adult-type repair with scar in E18 and post-natal skin was used to more fully explore the roles of TGFβ ligands, receptors and potential modulators during wound healing (Soo *et al.*, 2000). During the E16 to E18 transition period, basal levels of TGFβ did not change, although the levels of the potential antifibrotic molecules TGFβ3, latent TGFβ binding protein-1 (LTBP-1) and fibromodulin decreased. After injury, however, E16 fetuses displayed decreased TGFβ1 and TGFβ2 induction and E19 animals exhibited increased induction of the two isoforms. This suggested that the degree of TGFβ induction after injury might be more relevant to the transition to scar-forming adult repair than basal TGFβ levels. As expected during post-natal wound healing, TGFβ1 and TGFβ3 and the type I, II and III receptors were upregulated. Surprisingly though, the potential TGFβ modulators LTBP-1, decorin and biglycan were upregulated during adult wound repair, with only fibromodulin levels downregulated. The increased LTBP-1, decorin and biglycan levels in adult wounds argue against their antifibrotic role and make them unlikely candidates for mediating scarless fetal repair. In contrast, the inverse relationship between fibromodulin

expression and scarring in both rat wounds suggested that fibromodulin might be a relevant modulator of TGFβ activity during repair.

In general, the prevailing view is that wounded fetal dermis transiently expresses TGFβ1 in the absence of macrophages and lymphocytes. The relative lack of active TGFβ in the fetal wound may reflect the minimal macrophage infiltrate to the wound, the apparent lack of platelet degranulation at the injury site, or the reduced TGFβ synthesis in fetal platelets (McCallion and Ferguson, 1996). In contrast, active TGFβ is present at higher and sustained levels in adult wounds. Recent work demonstrates that this expression pattern is age-dependent and that it may also be related to the ability of the scar-forming fibroblast to secrete stimulators of TGFβ synthesis (Coleman *et al.*, 1998).

Platelet derived growth factor (PDGF)

The PDGFs are disulphide-bonded homo- or hetero-dimers of the products of two genes, the A- and B-chain genes. These isoforms have overlapping biological activities, but their secretory behaviour is different. Alternate splicing of exon 6 in the A gene is used to switch from a short secreted isoform, PDGF-AA_S, to one that is matrix associated, PDGF-AA_L. PDGF-BB, on the other hand, is predominantly cell-associated (Raines and Ross, 1992). PDGF-AB is the commonest isoform and is released largely from the alpha granules of platelets activated by coagulation. Consequently, it is one of the earliest growth factors participating in the post-natal wound response.

The expression of PDGF by recruited macrophages and the binding of PDGF to components of the ECM may account for its continuing presence at the adult wound site (Whitby and Ferguson, 1991a). It is chemotactic for both inflammatory cells and fibroblasts, and is a fibroblast mitogen. As such, PDGF has been shown to accelerate wound inflammation, fibroplasia and collagen deposition in both normal and deficient

healing states (Grotendorst *et al.*, 1985). The direct delivery of PDGF cDNA into skin by particle bombardment has also resulted in significant increases in wound tensile strength compared to controls (Eming *et al.*, 1999). Previous studies indicated a role for PDGF in tissue remodeling, as it is capable of stimulating the synthesis and secretion of collagenases (Bauer *et al.*, 1985). In fetal wounds, PDGF appears to be only transiently expressed (Whitby and Ferguson, 1991a), but like TGFβ, it modulates the secretion of MMP-2 in a dose-dependent manner and stimulates the secretion of activated MMP-9, uPA and its inhibitor, PAI-1, by fetal fibroblasts (Cullen *et al.*, 1997). Also like TGFβ, the exogenous addition of PDGF to fetal wounds via SILASTIC® implants results in greater fibroblast infiltration, collagen deposition and neovascularisation (Haynes *et al.*, 1994).

Basic fibroblast growth factor (bFGF)

In the context of wound repair, bFGF (FGF-2) is the most studied heparin-binding member of the FGF family, which also includes the wound repair peptides acidic FGF (aFGF or FGF-1) and KGF. Basic FGF stimulates new capillary formation, fibroblast proliferation and ECM synthesis, normal components of adult wound repair (Rifkin and Moscatelli, 1989). The profuse neovascularisation of adult wounds is significantly different to the normal vascular pattern that is restored in fetal wounds (Whitby and Ferguson, 1991b). It is possible that the absence of angiogenic bFGF and VEGF in the fetal wound may cause the restoration of a vascular structure similar to normal, unwounded fetal tissue. The addition of bFGF to culture medium bathing embryonic mouse wounds has been shown to result in faster healing relative to controls, but surprisingly, increased vascularity was not a feature of these wounds (Nodder and Martin, 1997).

Basic FGF is unusual in that it lacks a normal amino terminal signal sequence, thus the mechanism of bFGF secretion into the ECM is still unclear. Basic FGF and aFGF strongly

interact with heparin-like molecules as heparin stabilises and protects them from heat, acid and proteolytic degradation (Abraham and Klagsbrun, 1996). Activated platelets and PMNs at the injury site can secrete heparanase to release bFGF that is bound to heparan sulphate proteoglycan in the ECM, or bFGF bound to syndecans on the surfaces of migrating and proliferating epidermal cells at the wound margin (Ishai-Michaeli *et al.*, 1990). Tissue macrophages also appear to be a continuing source of bFGF in the wound. These may both be mechanisms whereby bFGF can be activated at the adult wound by coagulation or inflammation, hence the absence of active bFGF from fetal wounds may be secondary to the minimal inflammatory response seen.

Epidermal growth factor (EGF)

EGF is a single-chained, 53 amino acid polypeptide known to be mitogenic for epidermal cells, endothelial cells and fibroblasts (Cohen, 1983). Although EGF is the most studied family member in wound healing, EGF-like regions are present in other EGF family members including TGFα and heparin-binding EGF-like growth factor (HB-EGF). Despite their limited sequence homology, EGF and TGFα interact with the same cell surface receptor with similar affinities, as does HB-EGF (Nimni, 1997). The presence of multiple EGF receptor ligands in the wound environment and the transient increase in EGF receptor expression during reepithelialisation suggest that the EGF receptor also actively regulates wound repair (Hudson and McCawley, 1998).

EGF has been demonstrated to accelerate adult wound healing by stimulating reepithelialisation and increasing dermal thickness, granulation tissue organisation, collagen content and wound protease activity (DeLozier *et al.*, 1987; Franklin and Lynch, 1979; Franklin *et al.*, 1986; Hennessey *et al.*, 1990a). The topical application of EGF has also been shown to decrease overall wound contracture by effecting a less random arrangement of wound fibroblasts (Franklin and Lynch, 1979). Similarly, EGF has been shown to inhibit

contraction of a collagen gel by fetal fibroblasts, despite the increase in cell number caused by this mitogen (Piscatelli *et al.*, 1994). Like its effect on adult wounds, EGF accelerates fetal wound reepithelialisation (DeLozier *et al.*, 1987). In contrast, treatment of fetal excisional wounds with TGFα results in the infiltration of mesenchymal cells without reepithelialisation (Longaker and Adzick, 1991). Further work is necessary to delineate if EGF has a role in the cellular proliferation, interaction and differentiation that contributes to the absence of scar formation in fetal wounds.

All in all, growth factors are important regulators of cell proliferation and migration as well as matrix synthesis and degradation at the adult wound site. It seems likely that the ability of fetal wounds to heal without scarring is, in part, a consequence of the low levels of active growth factors released by inflammatory cells. As a brief and final note, expression of the interleukin family of cytokines has recently been evaluated during fetal wound repair. Production of proinflammatory IL-6 and IL-8 appears to be diminished during scarless fetal wound repair compared to the adult situation and fetal fibroblasts were found to produce significantly less IL-6 and IL-8 when stimulated with PDGF (Liechty *et al.*, 1998 and 2000a). In contrast, the absence of IL-10 resulted in increased inflammation in the fetal wound (Liechty *et al.*, 2000b). It was proposed that diminished fetal production of IL-6 and IL-8, believed to be due to IL-10 expression, results in the reduction of mononuclear cell recruitment and subsequent inflammation observed during fetal wound repair. This in turn may be important in providing a permissive environment for scarless repair.

1.3.5 Components of the extracellular matrix

Fetal wounds synthesise most of the matrix molecules present in adult wounds, yet there are striking differences particularly in relation to the restoration of normal collagen fibre orientation and tissue architecture in scarless fetal wounds. These differences may influence

the migration and orientation of cells infiltrating the injury site, as well as fibrillogenesis, which in turn influence whether a wound heals in a scar-free or scarring fashion (McCallion and Ferguson, 1996). Therefore, the constituents of the ECM and their deposition in wounds are important parameters to consider when investigating scarless fetal wound repair.

Collagen

Collagens are the major structural proteins of connective tissue in both scars and dermis in the post-natal mammal. They form a network of fibres in the interstitium of tissues, linking cells to other structural components as well as to each other. Type IV collagen is the major component of basement membranes (Mutsaers *et al.*, 1997). Collagen types I and III make up about 95% of the collagen of scars, and are deposited in large, parallel bundles orientated perpendicular to the wound surface. Type VII collagen, a minor component of scars, anchors the epidermal surface to the underlying scar matrix. In normal skin, the attachment of the dermis to the epidermis involves both type VII collagen and rete pegs. Since there are no rete pegs in scars, the type VII collagen fibrils are more important in maintaining this attachment (Ehrlich and Krummel, 1996).

There has been some controversy as to the nature of collagen deposition in fetal wounds. Early studies reporting no collagen deposition in fetal rat wounds were supported by more recent studies in fetal rabbit wounds using PVA silastic implants, wherein no collagen hydroxyproline was detected (DePalma *et al.*, 1987; DePalma *et al.*, 1989; Krummel *et al.*, 1987). Other investigators have detected greater and more rapid collagen hydroxyproline synthesis in fetal wounds relative to adult wounds (Adzick *et al.*, 1985a; Burd *et al.*, 1990a; Siebert *et al.*, 1990). It is now known that collagen types I, III, IV, V and VI are present in both fetal and adult wounds, but their spatial and temporal distribution varies (Longaker *et al.*, 1990b; Lovvorn, III *et al.*, 1999; Whitby and Ferguson, 1991b). All five types of collagen appear more rapidly in fetal wounds and the normal collagen pattern is

restored, while a scar is seen in the adult. Furthermore, transmission electron microscopy (TEM) has shown that in the adult rabbit wound, collagen fibril diameter is only 45% of the diameter of normal dermal collagen, while fetal wound collagen fibrils are almost indistinguishable at 82% of the size of fetal dermal collagen (Mast *et al.*, 1997). Consequently, it is widely accepted that collagen is not necessarily deposited in higher amounts in fetal wounds but is deposited more rapidly than in adults, and in a reticular pattern that is indistinguishable from adjacent, healthy tissue (Longaker *et al.*, 1990b).

The alterations in collagen synthesis in response to wounding have been quantified in the fetal and adult rabbit. The synthesis of non-collagen protein and collagen type I mRNA and protein are significantly elevated during the first 5 days in fetal wounds relative to unwounded fetal skin (Frantz *et al.*, 1992; Nath *et al.*, 1994b). The upregulated non-collagen proteins are likely to include collagenases and other ECM enzymes to control remodeling, cross-linking and the orderly deposition of collagen. Adult wounds produce higher levels of collagen I mRNA and protein than the adjacent unwounded tissue from 5 to 10 days post-wounding. These results correlate well with previous findings of accelerated collagen deposition in fetal wounds. Fetal wounds appear to produce more collagen by attracting already active cells from surrounding unwounded tissue to increase the cell density of the wound. Conversely, adult wounds show both fibroblast migration and upregulation of collagen gene transcription, implying multilevel regulation (Nath *et al.*, 1994b).

Unwounded fetal skin contains high levels of collagen III compared to unwounded adult tissues. Collagen III has a smaller, reticulin structure and a greater propensity to cross-link than type I collagen (Cass *et al.*, 1997a). As the fetus develops, the ratio of collagen type III/type I decreases (Lovvorn, III *et al.*, 1999). Although both fetal and adult wounds show significant elevation of collagen type I and III, type I is the major constituent of both wounds and is the mature form that ultimately replaces type III to form scars (Dostal and

Gamelli, 1993). Non-crosslinked forms of collagen type I have been shown to diminish rapidly in fetal sheep after 90 days' gestation, as crosslinked peptides become more prevalent in fetal skin beyond 120 days' gestation (Lovvorn, III *et al.*, 1999). This corresponds with the transition to scarring of fetal sheep wounds. In the same study, type V collagen was found to be the first chain to appear at the injury site. Despite type V comprising less than 2% of skin collagen, a developmental switch also occurred after 120 days' gestation from a predominance of α_1(V) chains in the fetus to α_2(V) chains in the adult. These differences between collagen in the fetal and adult dermis may be important determinants of the wounding response. Finally, it is interesting to note that small diameter collagen I fibrils with a high turnover and a similar configuration to fetal collagen occur adjacent to the epidermal/dermal junction in adult skin, the area which shows the least scarring in wounds (Fleischmajer *et al.*, 1990).

Adhesion glycoproteins

The adhesion glycoproteins, fibronectin, tenascin, laminin and vitronectin are other important components of the ECM. Fibronectins are dimeric glycoproteins that undergo splicing in three regions to form at least 20 different isotypes (Hynes, 1985; Yamada and Clark, 1996). Distinct patterns of expression for the different chain variants of fibronectin mRNA, including an embryonic form, are seen during adult wound healing (Ffrench-Constant and Hynes, 1989). This suggests different forms of fibronectin are possibly present in fetal and adult wounds. Fibronectin is synthesised by fibroblasts, macrophages and endothelial cells locally in the wound bed, but is also brought to the adult wound by the fibrin clot, platelet alpha granules and serum, and to the fetal wound by amniotic fluid (Broker and Reiter, 1994). Apart from stimulating the migration and proliferation of all the major cell types into the wound, fibronectin opsonises tissue debris after injury and is a component of the provisional matrix for ECM assembly (McCallion and Ferguson, 1996;

Whitby *et al.*, 1991). Furthermore, recent evidence suggests that nucleated cells expressing the α5β1 integrin bind to fibronectin within the blood clot to promote clot retraction and support cell shape change and spreading during wound contraction (Corbett and Schwarzbauer, 1999). Numerous immunohistochemical studies have implicated fibronectin as an earlier and transient signal for cell migration in the fetal wound compared to the adult (Longaker *et al.*, 1989b; Whitby *et al.*, 1991; Whitby and Ferguson, 1991b). It is thought that the early expression of fibronectin in the fetal wound may provide the scaffold on which keratinocytes and fibroblasts can migrate to rapidly repair the wound.

The tenascin family consists of Tn-C (cytotaxin), Tn-R (restrictin) and Tn-X (McCallion and Ferguson, 1996). Tenascin is reported to be sparsely and discontinuously distributed in the upper papillary dermis in unwounded skin (Filsell *et al.*, 1999; Mackie *et al.*, 1988). During wound repair a high transient expression of tenascin has been found to coincide with the initiation of cell proliferation and migration (Mackie *et al.*, 1988). An increase in tenascin expression is seen at the wound edge in all levels of skin, throughout the matrix of granulation tissue and particularly at the dermal-epidermal junction beneath migrating, proliferating epidermis. It is thought that inflammatory cytokines such as IL-4, tumour necrosis factor α (TNFα) and IFNγ, which are upregulated in healing skin, may induce epidermal tenascin expression during wound healing (Latijnhouwers *et al.*, 1998). Although the spatial pattern of tenascin distribution in fetal wounds appears to be the same as in adult wounds, the time that tenascin is first detected in the wound parallels the rate of reepithelialisation and wound closure, which is always more rapid in the fetus (Whitby *et al.*, 1991; Whitby and Ferguson, 1991b). It is conceivable that tenascin may aid wound closure in the fetus by antagonising the integrin-mediated adhesion of fibroblasts to fibronectin, allowing cells to detach from the wound matrix and migrate (Longaker and Adzick, 1991).

Vitronectin is a multifunctional glycoprotein found in plasma, extracellular matrices and fibrin clots. It mediates cell adhesion and migration, protects cells from cytosolic destruction by released activated complement complexes and can protect thrombin from inactivation by antithrombin III. Vitronectin also binds PAI-1 and stabilises its activity, which may help regulate its activity during tissue remodeling (Yamada and Clark, 1996).

Integrins are a large family of heterodimeric, transmembrane glycoproteins that function as cell adhesion receptors for extracellular matrix proteins and other cells. Each member of the integrin family consists of an α and a β chain, and more than 20 different αβ combinations have been recognised (Etzioni, 1999). It is the various combinations of the α and β subunits that confer receptor-binding specificities (Yamada *et al.*, 1996).

Integrins regulate a wide variety of cellular processes that are essential to epithelial repair, including spreading, migration, proliferation, differentiation and survival. Integrin ligation can also regulate the synthesis of growth factors, ECM proteins such as collagen, MMPs and other proteins that are critical to wound repair processes (Cass *et al.*, 1998; Gardner *et al.*, 1999). It appears that in the same way ECM proteins like fibronectin, tenascin and collagen are deposited more rapidly in fetal wounds compared to adult wounds, similar integrins are induced in both fetal and adult epidermal repair, but the rate is faster in the fetus. Epidermal integrin receptors specific for fibronectin and tenascin (α5, β6, αv, α9), collagen and laminin (α2, α3, α6, β4) are upregulated rapidly in the provisional matrix of fetal wounds, and this increase in expression continues until reepithelialisation is complete (Cass *et al.*, 1998). It has been hypothesised that early increased integrin expression may facilitate rapid fetal keratinocyte migration, proliferation and reepithelialisation.

Proteoglycans and glycosaminoglycans

Alterations in proteoglycan synthesis and in that of their constituent glycosaminoglycans (GAGs) correlates with the cell proliferation, migration, and collagen synthesis that accompany wound healing (Yeo *et al.*, 1991). Proteoglycans are polyanionic macromolecules that are made up of a protein core that can bind covalently to various linear, sulphated GAG chains, such as chondroitin sulphate (CS), dermatan sulphate (DS) and heparan sulphate (HS). Many functions are, in turn, related to the binding of proteoglycans or GAGs to other molecules. Some proteoglycans are components of the ECM, including versican, a large CS proteoglycan and decorin, a small DS proteoglycan (McCallion and Ferguson, 1996). The GAGs are able to combine with water to form bulky, viscous gels and help fill the space between collagen and elastin fibres, thereby providing mechanical resistance to tissue compression. Proteoglycans also have some regulatory functions influencing collagen fibrillogenesis and the three dimensional organisation of collagen (McGrath and Eady, 1997). Some proteoglycans have membrane-embedded core proteins, such as the syndecan family of heparan sulphate proteoglycans (HSPGs). All adherent cells express at least one syndecan, yet each syndecan family member is expressed selectively in cell-, tissue- and development-specific patterns (Kim *et al.*, 1994). Gallo and colleagues (1996) have shown that after injury, a large and transient induction of syndecans-1 and -4 is seen in the adult mouse and neonatal human skin, but not in human fetal skin. These observations correlate with the current knowledge that fetal skin heals without PMN infiltrate, fibrosis or apparent scarring. Thus, the investigators concluded that syndecans might bind molecules that enhance inflammation and fibrosis.

Hyaluronic acid (HA) is by far the most extensively studied GAG in wound healing. It is a linear polysaccharide that consists of alternating residues of N-acetylglucosamine and glucuronic acid (McCallion and Ferguson, 1996). HA is very large with a molecular weight of several million, is non-sulphated, and unlike the other GAGs, it probably does not bind to

proteins (Eschelbach *et al.*, 1998). HA is found in high concentrations during embryogenesis and whenever rapid tissue proliferation, regeneration and repair occur (Longaker *et al.*, 1989a).

Fetal wounds have an abundance of HA. It appears soon after wounding in both the fetus and the adult, but sustained deposition of HA is unique to fetal repair (DePalma *et al.*, 1989; Krummel *et al.*, 1987; Longaker *et al.*, 1991c; Sawai *et al.*, 1997; West *et al.*, 1997). The actual source of HA in the fetal wound is unknown. It is possible that this GAG is produced by fibroblasts or other cells in the wound bed. Alternatively, it may diffuse into the wound from the adjacent unwounded skin (Eschelbach *et al.*, 1998).

A decrease in HA content of fetal skin and the appearance of sulphated glycosaminoglycans, such as extracellular decorin and HS proteoglycan, correlates with the onset of scar formation that begins during late gestation (Freund *et al.*, 1993). Degradation of HA by hyaluronidase at the fetal wound site appears to cause an adult-like response with leukocyte infiltration, excessive fibroplasia, collagen deposition and neovascularisation (Mast *et al.*, 1992b). Conversely, HA has been reported to inhibit fibrosis and scar formation in healing adult wounds when applied topically (Hellstrom and Laurent, 1987). More recently, chronic additions of HA to incisional wounds of E18 fetal mouse limbs were demonstrated to induce scarless repair (Iocono *et al.*, 1998a). Forelimbs isolated from E18 fetal mice usually heal incisional wounds with scar. Thus, a prolonged presence of HA in fetal wounds may provide the matrix signal that orchestrates more organised healing by regeneration rather than by scarring.

The minimal immune response seen in fetal wound repair may in part be due to the inability of HA to provide an adequate matrix for lymphocyte adhesion and migration. Lymphocytes mediate the immune response in adult wounds by interacting with the glycoproteins and GAGs that compose the ECM. However, fetal lymphocytes are unable to bind to HA, the major constituent of the fetal wound ECM, hence they cannot migrate into

the zone of tissue injury (Dillon *et al.*, 1994). HA also inhibits cellular differentiation, and instead promotes cell proliferation and migration (DePalma *et al.*, 1989; Kujawa *et al.*, 1986; Kujawa and Tepperman, 1983). Due to its highly charged nature, HA can take on a large volume of hydration (Adzick and Lorenz, 1994). Furthermore, due to its large mass, cellular contact is blocked and hence so is contact inhibition of movement and growth. As a consequence, HA may stimulate mesenchymal cell infiltration by creating a low-resistance, hydrated matrix that releases cells from contact inhibition and restricted mobility (Eschelbach *et al.*, 1998). Its abundance may then prevent close interaction between the immature cells, thus inhibiting their differentiation into mature fibroblasts and preventing collagen deposition (see Figure 1.6).

HA is also known to affect collagen synthesis differently in various systems. For example, it elevates the deposition of small fibril type III collagen by cultured fibroblasts (Longaker *et al.*, 1991c). Scott and Hughes (1986) showed that early in chick and bovine tendon development, fetal collagen fibrils are smaller in diameter when HA is more abundant. Moreover, in this study a rapid increase in collagen fibril size during mid-gestation coincided with a decrease in HA and CS content. CS proteoglycan is present in fetal mouse wounds at the time of fibril formation but is absent in the adult wound (Whitby and Ferguson, 1991b). Since the ratio of type I to type III collagen determines the diameter of collagen fibrils (Glanville, 1982), it appears that fibril formation in the process of scarless fetal wound healing is modulated by the interactions of HA and CS with these collagens in the ECM.

Cell behaviour is chiefly regulated by HA through its principal receptor, a member of the CD44 family of cell surface glycoproteins (Culty *et al.*, 1990). Upon cell internalisation, HA is transported to a lysosome and digested while the 56 kDa receptor is recycled via a coated-pit pathway (Alaish *et al.*, 1994). Before this occurs, the HA receptor-ligand complex may trigger other events in the cell, such as changes in the cytoskeleton, HA

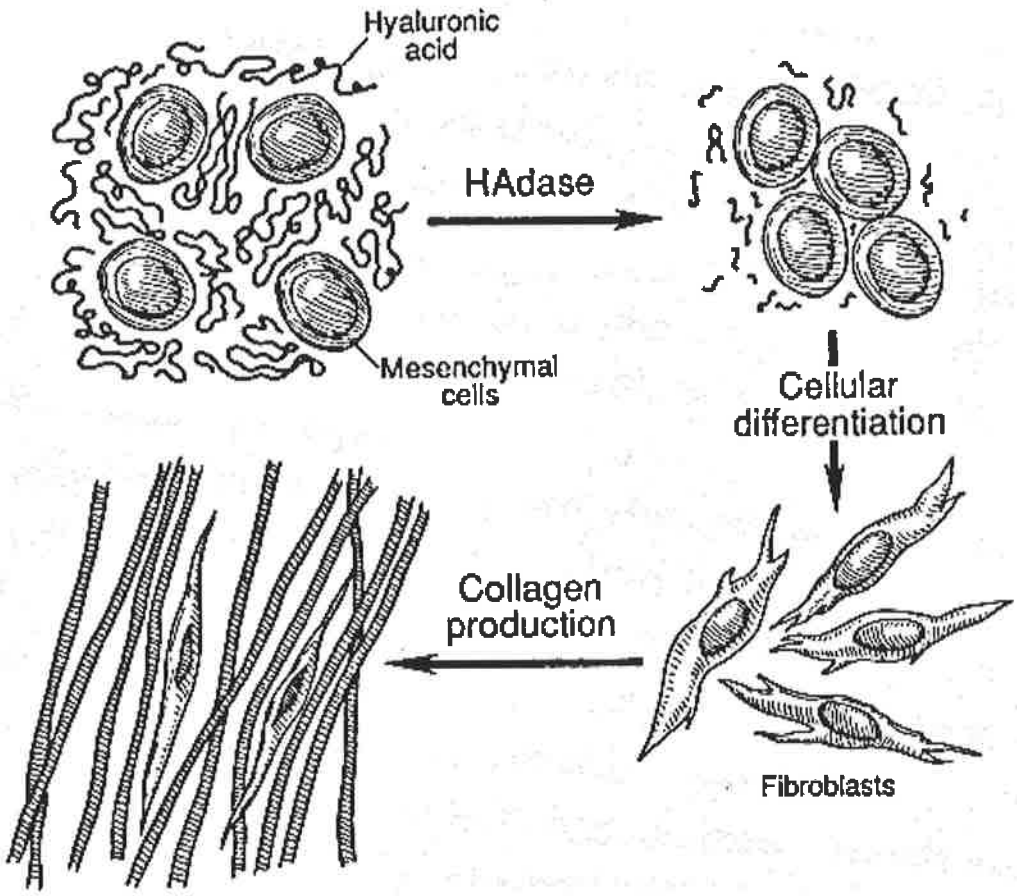

Figure 1.6 Illustration of a possible mechanism by which HA influences fetal wound repair.

The abundance of HA within fetal wounds may prevent differentiation of immature mesenchymal cells by preventing their close interactions. Hyaluronidase acting to reduce the HA content in wounds may promote the necessary interaction between these cells so that mesenchymal differentiation occurs, leading to fibroblast formation and collagen deposition. Alternatively, the reduction in HA may affect the supply or activity of growth factors that, in turn, affect the cellular activity. A final possibility is that HA directly affects collagen organisation by physicochemical interactions. Adapted from Mast *et al.* (1992b).

synthesis, and collagen and/or collagenase gene expression. The biological effects of HA are also mediated in part by RHAMM (receptor for HA-mediated motility). RHAMM is a critical regulator of cell locomotion and has been associated with cell migration after injury. Recently, a study by Lovvorn *et al.* (1998) demonstrated an increase in expression of both of the HA receptors in human and sheep fetal excisional wounds, correlating with fibroplasia and a reduced HA content. Incisional wounds that heal without scarring did not show an increase in HA receptor expression. This contrasts earlier findings that cultured fetal rabbit fibroblasts have four times the density of the cell surface HA receptor than adult fibroblasts (Alaish *et al.*, 1994). Consequently, it was speculated that strategies designed to limit the expression of HA receptors during post-natal wound healing might modify scar formation.

Amniotic fluid, fetal wound fluid, fetal urine, fetal serum and some fetal tissues contain a glycoprotein called HA-stimulating activity (HASA; Decker *et al.*, 1989; Longaker *et al.*, 1989a; Longaker *et al.*, 1989c; Longaker *et al.*, 1990a). Like HA, HASA is present in the fetal wound for a prolonged period of time and the level of HASA as a function of time after wounding appears to parallel that of HA, thus it may be a mechanism by which HA levels remain high in the fetus (Longaker *et al.*, 1991c). Evidence of an ontogenetic transition in wound HA and HASA levels, from elevated and sustained levels in the fetus to the small and transient increase seen in the adult, has been described (Estes *et al.*, 1993; Longaker *et al.*, 1990b). The relative lack of HASA in adult wound fluid implies that HA is deposited locally by platelets and the fibrin clot only during the earliest stages of adult wound healing (Longaker *et al.*, 1989c; Weigel *et al.*, 1986).

Different molecular species of HA, that is, the molecular size of HA and associated proteins, have been shown to have differential effects on contraction, angiogenesis and the evolution of wound strength (Arnold *et al.*, 1995). Many studies have implicated a role for HA in fetal wound healing as an inhibitor of angiogenesis (Eschelbach *et al.*, 1998). On the other hand, oligosaccharide degradation products of HA are thought to be important for

inducing new blood vessel formation in healing wounds (McCallion and Ferguson, 1996; Weigel *et al.*, 1986). Wound angiogenesis is tightly linked to the increased hyaluronidase activity and subsequent degradation of wound HA seen in the adult wound compared to the fetal wound (West *et al.*, 1997). Hyaluronidase is secreted by inflammatory cells such as macrophages that are attracted into the wound by the HA-fibrin matrix (Weigel *et al.*, 1986). The corresponding lack of HA degradation products at the fetal wound site is thought to contribute to the low angiogenesis levels seen, as fetal wounds that are treated with oligosaccharides generated by HA degradation show an increase in neovascularisation, fibroplasia and collagen deposition (Mast *et al.*, 1995). In summary, the sustained presence of HA in fetal wound fluid and tissue, thought to contribute to scar-free fetal wound repair, may be due to the effects of high HASA and low hyaluronidase activity compared to adult wounds.

Fibroblasts

Fibroblasts are responsible for the deposition and remodeling of the new ECM during wound healing. Adult fibroblasts are quite sparse and quiescent in normal, unwounded skin. Growth factors and the wound environment activate fibroblasts to acquire different phenotypes. In adult skin wounds, it is postulated that fibroblast proliferation is required for their change into migratory cells, at around 4 days post-wounding. Furthermore, it is thought that this change may involve development of a motor apparatus, loss of receptors for attachment to the ECM, and the expression of new motility receptors (Welch *et al.*, 1990). By 7 days post-injury, migrating fibroblasts completely fill the dermal defect and begin to produce type I collagen and fibronectin. Unlike adult fibroblasts that maximally produce collagen during quiescence, fetal fibroblasts normally exist in an active state and can proliferate and synthesise collagen simultaneously (Frantz *et al.*, 1992; Mast *et al.*, 1997). This may account for the faster rate of wound repair in the fetus.

At around day 9, the fibroblasts in the adult wound are largely replaced by myofibroblasts, which are thought to play a role in wound contraction (see section 1.2.4). The contractile properties of early gestation fetal skin fibroblasts appear to be qualitatively different from late gestation fetal and adult skin fibroblasts. The degree of collagen lattice contraction by mouse and lamb fibroblasts has been shown to increase with increasing gestational age. This *in vitro* data correlates with the onset of scarring and suggests that *in vivo* wound contraction may also increase with increasing gestational age (Coleman *et al.*, 1998; Piscatelli *et al.*, 1994).

Fetal and adult fibroblasts have been intensively studied for differences in growth factor expression. Several studies have provided evidence for reduced levels of growth factors such as TGFβ and bFGF in fetal wounds that heal without scarring (Broker *et al.*, 1999; Coleman *et al.*, 1998; Nath *et al.*, 1994a; Whitby and Ferguson, 1991a), while other studies have demonstrated that TGFβ is found in greater amounts in fetal wounds than in adult wounds (Chang *et al.*, 1993; Lee *et al.*, 2000; Martin *et al.*, 1993; Whitby *et al.*, 1994). For instance, despite finding that cultured adult fibroblasts express more mRNA for TGFβ1, bFGF and aFGF than cultured fetal fibroblasts in an earlier study, one group detected higher amounts of all three growth factor proteins in the cultured fetal fibroblasts compared to the adult fibroblasts (Lee *et al.*, 2000). Clearly, further investigation using both fibroblast cultures and wounding studies with different methods of detection are needed to better understand the complex growth factor profile of fibroblasts that exists during fetal wounds repair.

The regenerative nature of fetal wound repair has been suggested to result from the expression of particular phenotypic characteristics by fetal fibroblasts that are not shared by their adult counterparts. For example, wounded human fetal skin that is transplanted to a cutaneous location on an adult athymic mouse heals with scar formation and mouse

collagen, and is repaired by an influx of adult mouse fibroblasts and macrophages (Lin *et al.*, 1994). In contrast, wounded human fetal grafts in the subcutaneous location heal without scarring with human collagen, and are repaired by human fetal fibroblasts. No influx of inflammatory cells is seen. This supports the notion that the highly organised collagen deposition seen in scarless human fetal wound repair is intrinsic to the human fetal fibroblast and occurs in the absence of an adult-like inflammatory response.

Fetal fibroblasts also secrete migration stimulation factor (MSF), a 120 kDa protein that may be responsible for the cells' migratory capacity (Schor *et al.*, 1988). Despite their responsiveness to MSF, adult fibroblasts do not secrete this protein, except those of the adult oral mucosa. Since the oral mucosa heals more quickly and with less scarring than skin, it has been suggested that these cells represent a fetal-like subpopulation of adult fibroblasts (Schor *et al.*, 1996; Sloan, 1991). It has been shown that MSF secretion induces high and sustained synthesis of high molecular weight species of HA by both fetal and adult fibroblasts, which may increase fibroblast migration into the wound site (Schor *et al.*, 1989). Although MSF has been shown to be present in adult wound fluid, it is thought that the high levels of TGFβ in the adult wound may antagonise the action of MSF and inhibit the synthesis of high molecular weight HA (Ellis *et al.*, 1992). As a consequence, the low concentrations of high molecular weight HA and hence, restricted fibroblast motility, may contribute to scar formation. It is known that migrating fetal and adult fibroblasts have a similar dependence on HA (Ellis and Schor, 1996). This implies that their distinct migratory phenotypes result from differences in their constitutive levels of HA synthesis and, in turn, its modulation by cytokines such as TGFβ, rather than differences in their intrinsic migratory response to HA.

Moriarty *et al.* (1996) have found yet another intrinsic difference between fetal and post-natal fibroblasts. They have shown that both types of human fibroblasts produce a HA-dependent pericellular matrix (PCM), but the size of the PCM surrounding fetal fibroblasts

is significantly larger than that seen around post-natal cells. These PCMs require interaction with a HA-binding protein for assembly and maintenance. It is possible that the prolonged elevation of HA in fetal wounds might occur as a result of continual turnover of HA from fetal fibroblast PCMs. Besides the intrinsic ability of fetal fibroblasts to elaborate HA-dependent PCMs, there is evidence that extrinsic factors in the fetal environment also influence PCM size (Gallivan *et al.*, 1996). So the larger size and greater percentage of cells expressing PCMs may reflect another aspect of a unique fetal fibroblast phenotype.

Proteinases and their inhibitors

Proteolytic enzymes and their inhibitors are important regulators of ECM turnover and are believed to influence the structure and organisation of the remodeled matrix (Mignatti and Rifkin, 1993). Most proteinases belong to either the matrix metalloproteinase (MMP) or serine proteinase families, which function optimally at an extracellular pH and can act synergistically to digest the major molecules of the ECM (Knox *et al.*, 1987; Matrisian and Hogan, 1990). By acting on the various matrix molecules in the healing wound, proteases not only remodel structural proteins but are also necessary for altered cell functions such as migration and proliferation (Agren, 1999).

There are at least 17 members of the zinc-dependent matrix metalloproteinase family, and their type and activity vary spatially and temporally post-wounding (Kahari and Saarialho-Kere, 1997; Stricklin *et al.*, 1993; Vaalamo *et al.*, 1997). The collagenases (MMP-1, MMP-8 and MMP-13) degrade native collagen types I, II, III, VII and X to a form that is more susceptible to further digestion by other enzymes (Welgus *et al.*, 1981a, b and 1990). Gelatinase A and B (MMP-2 and MMP-9, respectively) digest denatured collagens, native type IV and V collagens, elastin and gelatin (Fessler *et al.*, 1984; Murphy *et al.*, 1991), while MMP-2 additionally digests native type X collagen (Welgus *et al.*, 1990). The stromelysins (MMP-3, MMP-10 and MMP-11) are not widely expressed but degrade many

ECM components such as proteoglycans, laminin, fibronectin, type IV and IX collagens and non-helical regions of collagens (Chin *et al.*, 1985; Matrisian, 1990; Murphy *et al.*, 1991; Woessner, Jr., 1991).

The metalloproteinases are secreted by fibroblasts, macrophages and keratinocytes into the ECM as zymogens that are incapable of proteolysis, and are activated by removal of an N-terminal propeptide. Secreted MMP proenzyme activation is regulated by proteinases and organomercurials, while inhibition is regulated by the non-specific α_2-macroglobulin and TIMPs (Airola *et al.*, 1998; Liu *et al.*, 2000; Matrisian, 1990; Matrisian and Hogan, 1990; Woessner, Jr., 1991). Like the MMPs, TIMPs are temporally and spatially regulated during post-natal cutaneous wound repair (Stricklin *et al.*, 1993; Vaalamo *et al.*, 1999). It is probable that ECM turnover and remodeling are regulated by the equilibrium between the synthesis of ECM proteins such as MMPs and their proteolytic enzymes and inhibitors.

Plasminogen activators (PA) are serine proteinases that specifically convert inactive plasminogen to plasmin, another serine protease (Matrisian and Hogan, 1990). There are two distinct types of plasminogen activators, urokinase-type (uPA, 50KDa) and tissue-type (tPA, 70KDa). Once activated, plasmin can either directly degrade ECM components such as laminin, fibronectin and fibrinogen, or it can activate other latent matrix proteinases (Murphy *et al.*, 1992). Proteolytic activity is dependent upon the synthesis of the pro-enzyme and its activator, as well as PAI. These inhibitors also act by forming a 1:1 complex with the enzyme (Matrisian and Hogan, 1990).

Uninjured adult skin shows little or no expression or activity of either the PA or MMP system. During the course of normal dermal repair, however, the temporal induction of PA and MMP mRNA expression, protein synthesis and proteolytic activity has been well-demonstrated (see section 1.2.4; Agren, 1999; Arumugam *et al.*, 1999; Knox *et al.*, 1987; Madlener *et al.*, 1998; Nwomeh *et al.*, 1998; Stricklin *et al.*, 1993). Moreover, just as the proteases and their inhibitors play a functional role in normal wound repair, dysregulation of

their activity seems to contribute to impaired wound healing (Madlener *et al.*, 1998). Despite being found at similar locations in both fetal and adult skin, the MMPs have been detected in fewer cells in the adult (Bullard *et al.*, 1997). This is not surprising, as rapidly growing fetal skin requires constant matrix turnover. It is also thought that increased proteinases found in fetal skin may also contribute to scarless healing. In contrast, the basal levels of uPA and its inhibitor, PAI-1, have been found to be significantly higher in neonatal fibroblasts compared to fetal samples (Cullen *et al.*, 1997). The high levels of uPA aid degradation of the fibrin clot and facilitate cell migration into the adult wound (Knox *et al.*, 1987). It is well established that fetal wounds do not form a fibrin clot (Somasundaram and Prathap, 1972), so this may account for the low levels of uPA secreted from the fetal fibroblasts.

The synthesis of MMP-1, -2 and MMP-9 is induced in both fetal and adult fibroblasts in response to injury (Gould *et al.*, 1997). However, the constitutive level of adult MMP-1 is 2-3 fold higher than in fetal fibroblasts and the induction of adult MMP-1 by mechanical injury is minimal. This observation has led to the development of a hypothetical model to explain the differential regulation of MMP activity in fetal and adult tissue. In the adult wound, platelets degranulate and release PDGF and TGFβ during haemostasis, which in turn promote fibroblast proliferation, type I collagen synthesis and inflammation (Olutoye *et al.*, 1996). MMP-2 and -9 then degrade basement membrane collagen type IV to enhance the migration of inflammatory cells to the injury site. However, the inhibition of collagenolysis by TGFβ, combined with the increased synthesis of collagen I, negates the higher constitutive level of adult MMP-1, resulting in a net deposition of collagen and subsequent scar formation in the adult animal. In the fetal situation, the cascade of cytokine release leading to fibroblast recruitment and inflammation is lacking, thus allowing the collagenolytic induction and activity to proceed unimpeded. The post-injury induction of fetal MMP-2 provides for a more fluid environment by degrading type IV basement

membrane collagen and type III collagen that is deposited by the fetal fibroblasts. Thus, remodeling is accelerated and occurs simultaneously with tissue repair in the fetus, resulting in the absence of scar (Gould *et al.*, 1997).

In summary, this review highlights firstly that there is probably no one factor solely responsible for scarless repair, secondly that the fetal environment is not crucial, and thirdly that the degree of differentiation of the fetus is a more important element in scar-free healing.

1.4 FACTORS INFLUENCING WHETHER A FETAL WOUND HEALS WITH OR WITHOUT SCARRING

1.4.1 Gestational age

Several studies have shown that the ability of a fetal wound to heal without scar formation is an intrinsic property of early to mid gestation skin. In fact, an *in utero* developmental transition from scar-free healing in the early fetus to scar-forming healing in late gestation has been described in the lamb, monkey, mouse and rat (Houghton *et al.*, 1995; Ihara *et al.*, 1990; Longaker *et al.*, 1990b; Lorenz *et al.*, 1993b; Soo *et al.*, 2000; Whitby and Ferguson, 1991c). In the lamb, scarless wound repair was seen at an age between E75 - E100, in the monkey at E75, in the mouse at E14 - E16 and around E16 – E17 in the rat fetus. Scar formation was observed by E100 – E120 in the lamb, by E107 in the monkey, by E18 in the mouse and by E18 - E19 in the fetal rat (term = 145 days, 165 days, 19 days and 21 days, respectively). Furthermore, the transition from fetal-like to adult–like healing occurring *in vivo* from E14 to E18 in the fetal mouse can be duplicated *in vitro* and in the absence of circulatory systemic elements (Chopra *et al.*, 1997). A similar developmental transition has been described *ex utero* in the marsupial *Monodelphis domestica* (Armstrong and Ferguson, 1995). Such ontogenetic consideration is important, especially if fetal surgery within the scar-free limits is to become a reality.

1.4.2 Magnitude of tissue damage

Most investigations comparing fetal scarless healing with gestational age have utilised a defined, incisional dermal wound. However, Horne *et al.* reported scarring of fetal lamb excisional wounds as early as 75 days' gestation (McCallion and Ferguson, 1996). This anomaly demonstrates the importance that the severity of the injury has on the scarring phenotype. Generally, the degree of scarring in the adult is proportional to the magnitude of

tissue damage. It follows that in a fetus at any given gestational age a greater amount of tissue damage will result in an increased likelihood of scar formation. This would be most pronounced at the transitional ages in outbred fetal animals, and may partly explain the controversies as to whether or not fetal lambs younger than E100 heal wounds with scarring (Estes *et al.*, 1994; Longaker *et al.*, 1990b). Indeed, a developmentally regulated, wound-size limit to the regenerative capabilities of the fetal lamb has been described (Cass *et al.*, 1997b). In short, it must be assumed that the greater the extent of damage to the tissue, the earlier in development wounding (e.g. surgery) must be performed to achieve scarless repair (Ferguson *et al.*, 1996).

1.4.3 Organ specificity

The majority of fetal wound repair studies have been largely confined to the integument. Besides the skin, other organ systems such as the skeletal, cardiovascular, gastrointestinal and respiratory systems can be injured or subjected to surgical manipulation. Scar formation in these organs may result in morbidity and mortality (Blewett *et al.*, 1997). It seems that not every fetal tissue heals in a regenerative manner. Linear diaphragmatic wounds in E100 fetal lambs repair with scar formation and without evidence of muscle regeneration (Longaker *et al.*, 1991d). Furthermore, incisional wounds created in the fetal lamb stomach and peritoneum always result in a pronounced scar, even at gestational ages when skin wounds heal without scarring (Adzick *et al.*, 1985b; Meuli *et al.*, 1995).

In contrast, the fetal skeleton is similar to fetal skin in its ability to heal more rapidly and perfectly than that in the adult. Adult skeletal tissues heal by regeneration of normal osseous tissue rather than fibrous scarring, but the injury is identified by the presence of a bony callus. Fractures have been observed to heal in the post-ossification E100 fetal lamb without callus formation (Longaker *et al.*, 1992a). Fetal lambs have also been used for monitoring tendon healing. Damage to the adult tendon generally leads to scarring and

impaired function as a result of slow healing and poor collagen reorganisation. Lesions in the E100 fetal tendon heal three times as fast as the adult and with no apparent scar formation nor loss of function (Nodder and Martin, 1997). Similarly, incisions performed on explant cultures of fetal mouse lung, at a gestational age of up to 18 days, heal rapidly and with complete reconstitution of tissue architecture (Blewett *et al.*, 1995). Airway mucosal healing has also been reported to be regenerative and scarless in fetal rabbits at 21 and 23 days of gestation (term = 31 days; Dohar *et al.*, 1998). Finally, cardiac explants from 14-day gestation mice are also able to repair incisional wounds in a regenerative fashion (Blewett *et al.*, 1997). Analogous to the dermis, this ability is lost as gestation progresses.

1.4.4 Species differences

It is clear from the review so far that numerous animal models have been employed to study fetal wound repair. Response to skin injury in all fetal species examined always seems to include a lack of significant inflammation, yet observations of wound closure are less consistent. This is best described in the case of the excisional wound. Adult excisional wounds heal by secondary intention, which includes wound contraction. Fetal rabbit wounds do not contain myofibroblasts, show a lack of reepithelialisation and lack of contraction when exposed to amniotic fluid (Haynes *et al.*, 1989; Krummel *et al.*, 1989). Instead, they appear to gape open and expand (Somasundaram and Prathap, 1970). When protected from amniotic fluid by a Silastic graft, however, fetal rabbit wounds show a pronounced cellular inflammatory response and heal with regeneration of epidermis, dermis and epidermal appendages (Ditesheim *et al.*, 1989; Morykwas *et al.*, 1991a; Somasundaram and Prathap, 1972). Moreover, fetal rabbit dermal fibroblasts contract fibroblast-populated collagen lattices (FPCLs) to a greater extent than their adult counterparts and a dose-dependent ability of rabbit amniotic fluid to inhibit contraction by both fetal and adult fibroblasts has been confirmed (Krummel *et al.*, 1989 and 1993). Therefore, the inability of

fetal rabbit wounds to close by secondary intention is not due to an inherent defect in the contractility of fetal fibroblasts or of the fetal collagen matrix, but likely to be due to contact with amniotic fluid. The relative scarcity of TGFβ at the fetal rabbit wound site may also be partly responsible for the lack of contraction seen, as administration of TGFβ to open fetal rabbit dermal wounds increases fibroblast density, induces ASMA protein expression, contraction, inflammation, fibrosis and upregulates collagen gene expression (Lanning *et al.*, 1999 and 2000).

Rapid and scarless repair of the neonatal opossum wound by contraction has been documented (Adzick and Longaker, 1991). At birth, the opossum is physiologically and anatomically a fetus and remains attached to the mother's nipple for 4 – 5 weeks before weaning. Therefore, the fetal development of the marsupial continues in the non-sterile environment of the pouch and in the absence of amniotic fluid. This further supports the idea that contact with amniotic fluid may be an important factor in the lack of wound closure seen in other fetal models such as the rabbit.

Burrington was the first to show that rapid healing, with evidence of contraction, does occur in fetal lamb excisional wounds (Burrington, 1971). Exposure to, or exclusion from, amniotic fluid has no effect on the ultimate wound size in the fetal lamb. In fact, sheep amniotic fluid does not inhibit but actually stimulates sheep and human fibroblasts to contract a FPCL in a dose-responsive fashion. The identification of 40 kDa protein factor in E125 sheep amniotic fluid that specifically stimulates this contraction has recently been reported (Rittenberg *et al.*, 1991).

It is still unknown if myofibroblasts mediate wound contraction and early closure, or play a role in matrix synthesis. Anti-muscle actin antibody and TEM has revealed that open E100 fetal lamb wounds contain myofibroblasts (Longaker *et al.*, 1991a). Myofibroblasts seem to participate in the early stages of excisional wound repair in fetal lambs, but by 14 days post-wounding they are relatively absent from wounds that heal without scarring, and

abundant in those with scarring (Cass *et al.*, 1997c). Moreover, ASMA expression appears only in myofibroblasts of wounds healing by scar formation and contraction, that is, in fetal lambs older than E100 (Estes *et al.*, 1994). In adult skin, TGFβ1 and 2, heparin, fibronectin, and other ECM molecules induce ASMA expression, but the factors that regulate ASMA in the fetus and the transition from fetal fibroblast to the myofibroblast phenotype remain unknown (Desmouliere *et al.*, 1993; Serini and Gabbiani, 1996).

Early fetal rat skin heals an open wound rapidly in culture and *in vivo* (Belford, 1997; Ihara *et al.*, 1990; Ihara and Motobayashi, 1992). Like the rat, excisional wound repair in the fetal chick and rodent seems to occur by a combined process of connective-tissue contraction and active movement of the epithelium over the dermal margins of the wound (Martin *et al.*, 1994; Martin and Lewis, 1992; McCluskey *et al.*, 1993; McCluskey and Martin, 1995). The presence of an actin cable surrounding the wound perimeter suggests that this movement is a consequence of actin filament contraction to effect a purse-string mechanism of wound closure. Additionally, unlike adult contractile granulation tissue, it appears that mouse embryonic connective tissue contraction does not require myofibroblasts (Nodder and Martin, 1997).

Care must be taken in extrapolating the findings of open wound healing in fetal animals to humans due to interspecies variation. One post-mortem examination of a spontaneously aborted human fetus of about 20 weeks' gestation showed that wounds caused by congenital amniotic bands healed by ingrowth of normally proliferating mesenchymal cells from surrounding tissue (Rowlatt, 1979). Additionally, an inhibitory effect of human amniotic fluid on lattice contraction has also been demonstrated using both human fetal and adult FPCLs (Wider *et al.*, 1993). This supports the notion that open human fetal wounds behave like wounds in the fetal rabbit and do not contract *in utero*.

In summary, the ability of the fetal excisional wound to close and its mechanism *in vivo* appears to be species dependent. Taken together, these studies highlight considerable differences between species when studying fetal wound healing.

1.5 CLINICAL IMPLICATIONS OF FETAL WOUND HEALING RESEARCH

1.5.1 Manipulation of adult wound healing to minimise scar formation

Research into the differences between fetal and post-natal wound healing contributes to understanding the biology of scar formation. Indeed, many aspects of adult wound repair have been manipulated to resemble the fetal response to injury, in the hope of possibly reducing or preventing scarring. The growth factor profile and the ECM constituents of the adult wound are the two major areas that have been modified to effect a more fetal-like phenotype.

Manipulation of growth factor profile

Since adult wounds have an excessive inflammatory response and growth factor profile compared to fetal wounds, a number of anti-inflammatory therapies were devised in an attempt to reduce the scarring associated with adult wound healing. An early experiment that inhibited the infiltration of monocytes and macrophages into the injury site resulted in a significant retardation of fibrosis and a severe lack of wound debridement, which were subsequently thought to be mediated by macrophages (Leibovich and Ross, 1975). However, this study used anti-macrophage serum for local elimination of tissue macrophages and hydrocortisone acetate to induce a prolonged monocytopenia, so other aspects of the wound healing response were also inhibited. Similarly, an anti-inflammatory drug called suramin, which blocks the binding of numerous growth factors to their receptors, was found to have significant side-effects and inhibit tissue repair when applied intradermally to rat wounds (Chamberlain *et al.*, 1995). The overall lack of success of such treatments confirmed that a degree of normal inflammation is required for healing, and that scarring is a consequence of a process that is more complex than a general inflammatory

response. Hence, the alteration of specific cytokine levels in adult wounds is now being considered as a basis for scar prevention strategies.

The topical application of several classes of growth factors has been shown to enhance all aspects of both normal and impaired tissue repair (Bennett and Schultz, 1993). Many studies have focussed on the effects of single growth factors such as TGFβ, PDGF, bFGF, EGF, IL-1 and IGF-1 (Greenhalgh *et al.*, 1990; Grotendorst *et al.*, 1985; Hennessey *et al.*, 1990b; Jyung *et al.*, 1994; Lawrence *et al.*, 1985; LeGrand *et al.*, 1993; McGee *et al.*, 1988; Mustoe *et al.*, 1987; Pierce *et al.*, 1989b; Pierce *et al.*, 1989a; Pierce *et al.*, 1992; Suh *et al.*, 1992; Uhl *et al.*, 1993). These factors have all been shown to enhance compromised healing states on the experimental animal. However, numerous wound-healing investigations have reported TGFβ as being the main growth factor important in scarring and fibrosis (see section 1.3.4). Therefore, more researchers have chosen to study TGFβ, particularly to determine if a reduction in TGFβ at the adult wound site reduces scar formation (see Figure 1.7).

The application of TGFβ1 and TGFβ2 neutralising antibodies to adult rat wounds has resulted in reduced scar formation (Shah *et al.*, 1992). Similarly, scar formation that normally occurs in wounded mouse E18 limbs grown in a serum-free culture system was abolished by the addition of neutralising antibodies to TGFβ (Houghton *et al.*, 1995). Neutralising the TGFβ levels immediately upon wounding may reduce the amount of active TGFβ and hence prevent its auto-induction and decrease macrophage recruitment in the wound site. Furthermore, it is thought that the more reticular orientation of collagen deposition is a consequence of increased fibrinolysis, possibly because neutralisation of TGFβ decreases the levels of PAI and increases the levels of plasminogen activator and plasmin (Shah *et al.*, 1994). Later studies using isoform-specific antibodies have shown that

neutralisation of both TGFβ1 and TGFβ2 has a greater, synergistic anti-scarring effect than neutralisation of either isoform alone (Shah *et al.*, 1995).

Although the injection of antibodies against TGFβ into wounds is an attractive anti-scarring therapy, other methods of reducing the levels of TGFβ in healing adult wounds have also been investigated. Decorin, a small proteoglycan that binds and inactivates each TGFβ isoform, has been shown to suppress the pathological increase in matrix synthesis observed in glomerulonephritis (Border *et al.*, 1992). The broad ability of decorin to inhibit TGFβ1, 2 and 3 might be a therapeutic advantage in the treatment of kidney, lung and liver fibrotic diseases, as decorin has a propensity to accumulate in these organs after intravenous administration. Similarly, M6P has been found to limit scar formation in rodent wounds, probably by binding to the M6P/IGF-II receptor and hence blocking TGFβ activation (Shah *et al.*, 1993). It is also thought that the binding of M6P to mannose receptors should modulate collagen synthesis during wound repair (McCallion and Ferguson, 1996).

The exogenous application of TGFβ3 at low concentrations has been shown to downregulate TGFβ1 and TGFβ2 levels in adult rodent incisional wounds, leading to reduced inflammation and more organised collagen deposition (Shah *et al.*, 1995). In the same study, exogenous application of a panspecific antibody to TGFβ, which binds all isoforms equally, had no beneficial effect on scar prevention in the healing wound. It is therefore likely that cutaneous scar formation is dependent on the ratio of TGFβ3 compared to TGFβ1 and TGFβ2. Hence, varying the TGFβ isoform profile within a healing wound may alter the cellularity and architecture of the repair process.

In contrast, Wu *et al.* (1997) recently reported molecular data contradicting the claim that TGFβ3 minimises wound scarring. Using a dermal ulcer model, they found that TGFβ3 increased granulation tissue formation, while in a hypertrophic scar model, they found no significant difference in the degree of scar formation in TGFβ3-treated wounds compared

with controls. Additionally, topical application of each of the isoforms of TGFβ resulted in a substantial upregulation of endogenous TGFβ1 mRNA at the wound site. In cultured human fibroblasts, TGFβ3 has been reported to increase DNA synthesis, collagen protein and collagen mRNA levels through TGFβ1-dependent and independent pathways (Murata *et al.*, 1997). Since interactions between TGFβ1 and TGFβ3 occurs during *in vivo* wound healing, it is possible that TGFβ3 may help regulate the total TGFβ activity at the injury site and hence help direct the overall fibrotic response.

Other anti-TGFβ strategies, such as flooding the wound with TGFβ receptors to compete with cellular binding sites have also been contemplated for their possible anti-scarring effects. Intradermal injection of antisense oligonucleotides to TGFβ1 and TGFβ2 has been found to reduce cutaneous scar formation in adult rat wounds, but not to the extent seen with the application of their respective neutralising antibodies or exogenous TGFβ3 (Chamberlain *et al.*, 1995; Choi *et al.*, 1996).

The design of transgenic mice with gene knockouts and interbreeding of knockout mice are also providing an insight into tissue repair mechanisms. Some candidate wound repair genes have been found to be critical to normal development, as the full gene knockouts were lethal to the embryo. This demonstrates that most wound signals control more than just one cellular activity (Martin, 1997). On the other hand, unexpectedly normal healing phenotypes have been reported (Guo *et al.*, 1996). This supports the notion that the cellular activities during wound repair are responses to more than just one signal. Basic FGF appears to be an exception to this school of thought, as knockouts have indicated it has a specific function in skin wound healing even though it is not essential for embryonic development (Ortega *et al.*, 1998).

Transgenic mice that express high levels of active TGFβ1 have also been designed to investigate the effect of elevated TGFβ1 on wound healing (Shah *et al.*, 1999).

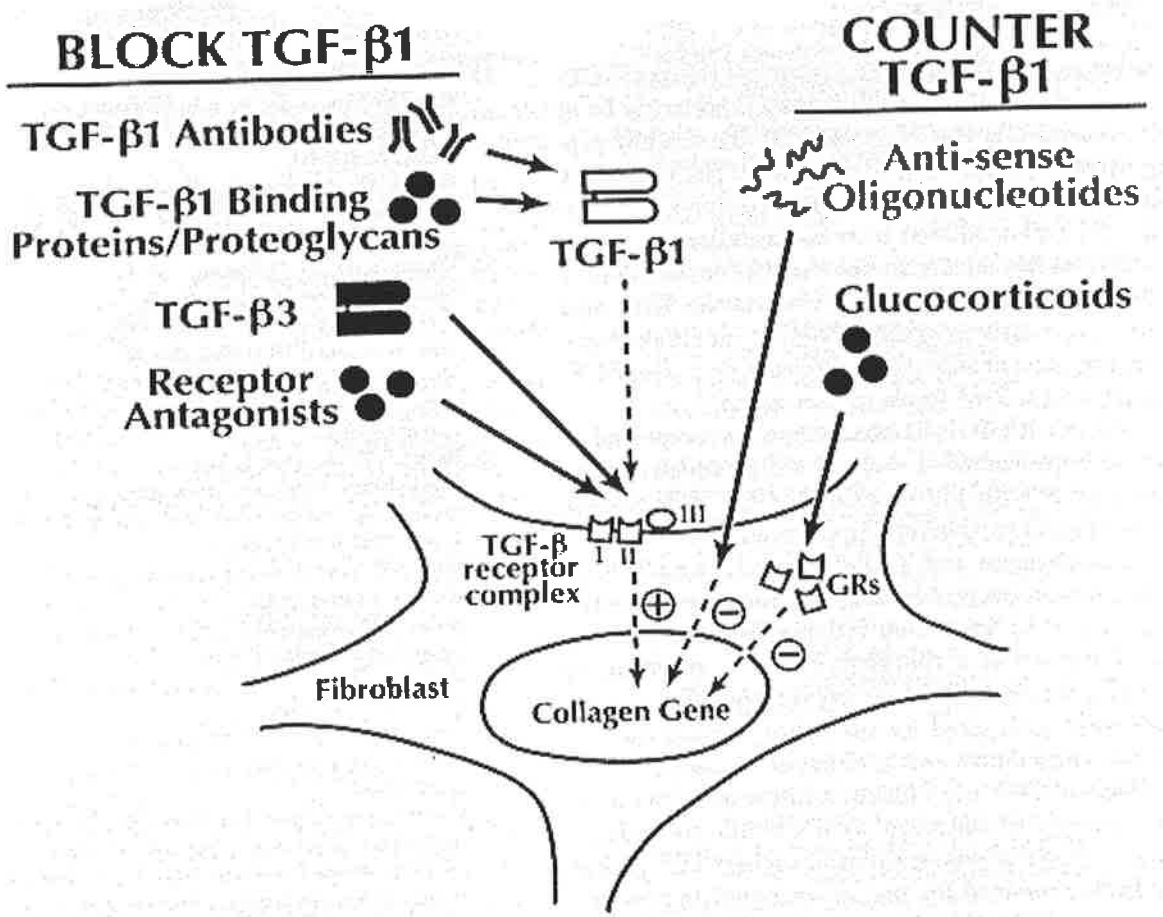

Figure 1.7 Anti-TGFβ1 strategies to reduce scar formation.

TGFβ1 binds to the TGFβ1 receptor complex (TBR I, II, and III), activating a signal cascade which results in upregulation of the collagen gene. Targeting TGFβ1 directly with either TGFβ1 antibodies or TGFβ1 binding proteins and proteoglycans could block this pathway. The receptor complex itself could be blocked with either receptor antagonists or TGFβ3, as TGFβ3 is believed by some to have a counteractive effect on TGFβ1 in wound healing. Alternatively, glucocorticoids, which act through glucocorticoid receptors (GRs), or anti-sense oligonucleotides targeted to the collagen gene could be used to down-regulate expression of the collagen gene, thus counteracting the effect of TGFβ1. Adapted from Parrelli *et al.* (1997).

Surprisingly, incisional cutaneous wounds in transgenic mice healed with less scarring along with greater immunostaining for TGFβ3 and TGFβ-receptor RII and less immunostaining for TGFβ1 compared to control mice. In the same study, subcutaneous PVA sponges implanted in the transgenic mice showed enhanced matrix deposition accompanied by an increase in the immunostaining for all TGFβ isoforms and their receptors compared to controls. These data demonstrate that increased circulating levels of TGFβ1 do not always result in increased expression or activity in target tissues and confirm that the cutaneous incisional wound model and the PVA implant model differ significantly in their host response patterns.

In summary, TGFβ is a key player in the treatment of impaired or excessive wound healing, but it is crucial to be able to control its bioavailability before it can be used as a therapeutic agent (Nimni, 1997).

Manipulation of ECM constituents

Scarring primarily results from the upregulation of collagen production, so blocking excess collagen synthesis using antisense oligonucleotides targeted to the collagen gene may be another method for preventing fibrosis. Alternatively, glucocorticoid steroids, which are anti-inflammatory and normally impair wound healing, may be used to reduce scarring. Glucocorticoids decrease PMN and macrophage infiltration into the wound site during the inflammatory phase and decrease collagen levels and synthesis (Leibovich and Ross, 1975). Since glucocorticoids have the opposite effect of TGFβ in dermal wound repair, they could be used to counteract the fibrotic effect of TGFβ. Promising studies have shown that treatment with the glucocorticoid, dexamethasone, decreases TGFβ1 secretion and mRNA levels in fibroblasts (Parrelli *et al.*, 1997).

Recently non-crosslinked collagen was shown to increase epidermal advance, blood vessel formation, and collagen synthesis and deposition in the granulation tissue relative to control wounds (Redlich *et al.*, 1998). The readily released collagen peptides are thought to have an immediate and rapid chemotactic effect on fibroblasts to enhance wound healing. Similarly, the rate of adult wound closure accelerates and the bursting strength of wounds in malnourished rats increases after the addition of exogenous fibronectin (Cheng *et al.*, 1988; Nakada *et al.*, 1998). The exogenous fibronectin might also be a source of extra chemotactic fragments that results in the more rapid accumulation of macrophages and fibroblasts into the wound site.

Therapy with the potent angiogenesis inhibitor TNP-470 induces a significant delay in murine cutaneous wound healing (Klein *et al.*, 1999). In the same study, topical application of bFGF was found to reverse the TNP-470 inhibition of wound healing. In the clinical setting, this beneficial effect of bFGF may be exploited to normalise the rate of wound closure in patients that are administered TNP-470 to treat neoplastic and angio-proliferative diseases.

Research in the area of fetal wound contraction may lead to discoveries that permit the control of otherwise pathologic scar contracture in the adult. Burn wound contracture and anastomotic stricture are two examples of compromised tissue architecture and anatomical function (Adzick and Longaker, 1992). As discussed in section 1.4.4, rabbit and human amniotic fluid can inhibit, while sheep amniotic fluid can stimulate FPCL contraction *in vitro* (Krummel *et al.*, 1989; Rittenberg *et al.*, 1991; Wider *et al.*, 1993). These early observations indicate a potential clinical application of the key contraction-inhibiting factors in rabbit and human amniotic fluid, or antibodies against the contraction-stimulating factors in sheep amniotic fluid, for treating pathologic wound contraction.

As discussed in section 1.3.5, there are several mechanisms by which the high levels of HA seen in fetal wounds may contribute to scarless repair. Accordingly, topical application

of HA to adult wounds has been reported to accelerate the rate of wound closure and reduce scarring (Abatangelo *et al.*, 1983; Burd *et al.*, 1989; Hellstrom and Laurent, 1987). However, the HA used in these studies was extracted from either rooster comb or human skin and was impure. In contrast, the exogenous addition of purified, synthetic HA has shown little effect on scar formation (Burd *et al.*, 1989; McCallion and Ferguson, 1996). Tissue-extracted HA can inhibit fibroblast replication in culture, while pure HA cannot, and the effect of tissue-extracted HA cannot be abolished by the addition of hyaluronidase (Burd *et al.*, 1991). It is possible that HA delivers certain proteins to the wound site, and it is these HA-protein complexes that influence the organisation of scar tissue. Therefore, rather than applying pure HA to adult wounds, the efficacy of applying agents which maintain a HA-rich adult wound environment must be further tested. The therapeutic addition of a depot form of HA to an acute wound, which allows the HA levels to remain elevated for an extended period of time, has already shown repair to proceed with diminished but more organised collagen deposition (Iocono *et al.*, 1998b).

In summary, it seems that during evolution, speed of healing under adverse conditions (e.g. contamination and pollution) was selected at the expense of scar quality. However, these studies indicate that, along with contemporary hygiene and wound care, it may now be possible to manipulate the adult injury response so as to improve the quality of healing without compromising speed of repair or wound strength.

1.5.2 Human fetal surgery

Apart from modulating adult wounds to make them heal in a more fetal-like, scar-free fashion, studies of fetal wound healing have other immediate relevant applications. Greater knowledge about the processes of *in utero* repair must be gained as the human fetus is now considered a surgical patient. Since 1981, surgeons have performed operations on the

human fetus at 18 - 28 weeks of gestation for anatomic defects that have progressive, deleterious physiologic consequences after birth (Adzick and Longaker, 1992). One such disorder that has been surgically resolved *in utero* is congenital diaphragmatic hernia. This disorder, where the fetal intestines have escaped into the thoracic space, procluding growth of the developing lung buds, may be lethal at birth if the lungs have not grown sufficiently for breathing. Other life-threatening anatomic malformations that have been corrected by hysterotomy and open fetal surgery include severe bilateral hydronephrosis, sacrococcygeal teratoma, and cystic adenomatoid malformation of the lung (Longaker and Adzick, 1991).

The clinical and experimental observations that fetal cutaneous wounds heal without scarring are also of great potential interest in the repair of craniofacial structures such as cleft lip and palate. Studies in the fetal lamb model have shown that cleft lip and palate, when iatrogenically produced and repaired at 70 days of gestation, heal without evidence of scar formation (Canady *et al.*, 1994; Estes *et al.*, 1992a and b; Longaker *et al.*, 1992b). Despite the recent interest, fetal surgery presently does not extend to treatment of craniofacial abnormalities due to inherent risks of open fetal surgery to both the mother and the fetus (Longaker *et al.*, 1991c; Longaker and Adzick, 1991). The transition later in gestation to adult-like healing with scarring is an important aspect of fetal repair that must be taken into account before attempting surgery on human fetal cleft palate. Further studies are required to determine the optimal time during gestation when surgery should be performed so that scar-free healing results, as there is currently no convincing data on whether or not such a transition exists in human fetal wound repair.

1.6 PROJECT OVERVIEW

This review of the literature illustrates the accumulating evidence suggesting that the regulation of both the dermal and epidermal components of fetal wound repair differs to that seen in the adult. In all species examined, adult cutaneous injury heals with the formation of scar tissue. In contrast, fetal skin heals faster and with complete restoration of dermal architecture such that no scar is formed. What is more important about early gestation fetal skin wound healing is that it is one of the few examples of mammalian tissue regeneration. Understanding this biology may be the key to unlocking an ability to regenerate lost or damaged tissue.

Central to the understanding of fetal skin wound repair is determining the factors responsible for scarless healing. A variety of clinical disorders call for research in this area, with perhaps the greatest application being the therapeutic manipulation of adult wound healing to reduce or eliminate scarring. Recent studies have gained much insight into the expression patterns of genes following wounding in the post-natal animal. Adult surface wound healing is regulated by several classes of growth factor and ECM signals that control the division, migration and biosynthetic capacity of the cells of wound repair. The review of the literature clearly shows that the differences between fetal and adult wound healing are multifaceted. Over recent years, increased knowledge about the growth factor profile, changes in the ECM and cellular movements into the fetal wound have contributed to the understanding of fetal wound repair. However, the full story is still not complete. Understanding the genetic regulation of scarless fetal wound healing is also of considerable scientific significance as all of the genes responsible for the scar-free phenotype, as well as those directly responsible for the fetal to adult transition in wound healing, are yet to be elucidated. In short, it is still unknown why a fetal skin wound heals without scarring up to a particular age of gestation but then beyond this age heals by scar formation.

This project studied the molecular events surrounding the fetal to adult transition in the mechanism of wound repair in fetal rats. I hypothesised that growth factors and ECM components commonly known to be involved in adult wound healing are not the only relevant influences on fetal wound healing and that other unidentified factors or known factors that have not yet been implicated in wound repair are also involved. The overall aim of this thesis was to identify genes involved in the fetal to adult transition in the mechanism of wound repair. Accordingly, the specific aims of this thesis were:

i) To establish a modified organ culture model based on that of Belford (1997) and confirm the healing of multiple wounds in E17 rat skin;

ii) To quantify the healing of multiple wounds in E17 rat skin;

iii) To set up the DD-PCR protocol as a means of detecting altered gene expression in E17 and E19 rat skin wounds; and

iv) To identify and characterise genes that are differentially expressed during the E17 to E19 transition in wound healing.

The outcome of this project may provide a rational basis for interventional therapies directed at reducing scar formation after dermal injury as well as fibrotic diseases of other organ systems.

Chapter Two

Measurement of Excisional Fetal Wound Repair *In Vitro*

2 Measurement of Excisional Fetal Wound Repair *In Vitro*

2.1 INTRODUCTION

The investigation of any physiological process is dependent on the use of models. Many mammals have been employed to study fetal wound repair. The response of non-human primates to wounding most closely resembles the situation in humans, but due to ethical reasons research using these animals has been restricted to just a few laboratories (Hallock *et al.*, 1987; Lorenz *et al.*, 1993b). The fetal sheep model is attractive to some researchers because the size of the animal and the long gestation period enable fetal manipulations to be more feasible (Burd *et al.*, 1990a; Burrington, 1971; Cass *et al.*, 1997c; Longaker *et al.*, 1990b). The main drawbacks are the low litter size per animal, the risk of zoonotic infection and the thick wool that can interfere with histological analysis of tissue sections. The pig is another larger animal with a long gestation period, but it has the added advantage over sheep in that there is usually a greater litter size and the skin closely resembles that of humans. The main disadvantage is the high abortion rate of the pig. Other investigators have used marsupial models to demonstrate the transition from scar-free to scar-forming phenotype in the ontogeny of skin and the ability of the fetus to heal in a non-sterile extrauterine environment (Armstrong and Ferguson, 1995; Morykwas *et al.*, 1991b). Yet, the most widely used model to study fetal wound repair is the rabbit, as it has a higher number of fetuses per animal (Adzick *et al.*, 1985a; DePalma *et al.*, 1987; Ditesheim *et al.*, 1989; Haynes *et al.*, 1989; Krummel *et al.*, 1987, 1989 and 1993; Siebert *et al.*, 1990; Somasundaram and Prathap, 1970 and 1972; Thomasson *et al.*, 1973). Tissue movements during embryonic wound closure have also been extensively studied using mouse and chick models (Martin *et al.*, 1994; Martin and Lewis, 1992; McCluskey *et al.*, 1993; McCluskey and Martin, 1995; Nodder and Martin, 1997). However, the shorter gestation period of the

rabbit, mouse and chick mean that there is less time for fetal manipulation and the fetuses are very small. For this thesis, rats were the preferred species for studying the transition in the mechanism of fetal excisional wound repair for two main reasons. Firstly, like rabbits and mice, they are inexpensive and easy to handle. Secondly, unlike the rabbit, the ability of the fetal rat to heal an excisional wound both *in vivo* and *in vitro* had previously been demonstrated (Ihara *et al.*, 1990; Ihara and Motobayashi, 1992; Krummel *et al.*, 1989; Somasundaram and Prathap, 1970).

To study the process of wound healing several *in vitro* and *in vivo* models have been used. For *in vivo* studies, the maternal animal usually undergoes a laparotomy and a hysterotomy is made to provide direct access to the fetus. The fetus is wounded while contained in the uterus, the hysterotomy is closed and the maternal animal is sacrificed prior to delivery (Nelson *et al.*, 1990). Alternatively in mice or rats, a hysterectomy can be performed so the fetuses continue their development in organ culture medium (Ihara and Motobayashi, 1992; Martin and Lewis, 1992; Martin and Nobes, 1992; McCluskey and Martin, 1995).

Histology, tensile properties, and quantification of contraction have all classically been used to evaluate wound repair. Although these methods allow descriptive evaluations of the wounds, they are not particularly sensitive to the cellular activities of wound healing and do not provide biochemical data representative of the various stages of repair. In order to delineate the tissue response and new growth associated with fetal and post-natal wound healing, numerous subcutaneous wound implants have been devised. These include the Hunt-Schilling chamber (Hunt *et al.*, 1967; Schilling *et al.*, 1959), the Cellstic device (Viljanto, 1976), the GoreTex™ tube (Goodson, III and Hunt, 1982), and the polyvinyl alcohol (PVA) implant (Cohen and Mast, 1990; Olutoye and Cohen, 1996). Various agents such as growth factors and antibodies can be placed into the wound implant to determine their effects on fetal wound healing. Although easy to implement, wound implants

themselves can directly influence the ECM composition by creating an inflammatory response (Alaish *et al.*, 1995) and therefore, may not accurately represent all aspects of normal repair. Furthermore, these models primarily measure granulation tissue formation and neglect the role of reepithelialisation and wound contraction. These elements should not be ignored, as the signals regulating migration and proliferation of epidermal cells, and their interactions with other cells in the wound, are still not well defined, and it is believed communications between epithelial and mesenchymal cells are important to successful wound repair. For example, KGF mRNA expression is dramatically induced in the dermis at the wound edge and the hypodermis below the wound just 1-day after injury to the post-natal animal, yet the receptor for this growth factor is predominantly expressed in the epidermis (Wearing and Sherratt, 2000; Werner *et al.*, 1992). This supports the notion that a KGF-mediated paracrine interaction may be important for the migration and proliferation of epidermal keratinocytes seen during adult wound repair. Furthermore, the organ culture of fetal rat skin at 16 days of gestation (E16) has been used to show that isolated epidermis and mesenchyme differ greatly in their injury response (Ihara and Motobayashi, 1992). When the two tissues were separated by treatment with Dispase immediately after wounding, the mesenchymal wound closed at essentially the same rate as that seen in full-thickness skin while the epidermal wound increased in size. This suggested that cellular activity in the mesenchyme is essential to wound closure in the fetus and that the close proximity with the epidermis may cause spreading of the epidermis along with the mesenchyme to effect closure. These observations are evidence that interactions between epithelial and mesenchymal cells are necessary for complete wound closure.

Numerous models have been used to demonstrate that scarless repair is not dependent upon contact with amniotic fluid. Longaker *et al.* (1994) showed that when adult sheep skin is placed in the fetal environment, that is, grafted onto a fetal lamb and returned to the uterus, incisional wounds still heal with scar formation. Furthermore, the intrinsic ability of

fetal skin to heal an incisional wound outside of the fetal environment has been demonstrated in many different species (Armstrong and Ferguson, 1995; Lin *et al.*, 1994; Lorenz *et al.*, 1992, 1993b and 1995; Sancho *et al.*, 1997). One model of fetal wound repair used in some laboratories involves the transplantation of early gestation human fetal skin into subcutaneous pouches on the backs of nude mice (Lin *et al.*, 1994; Lorenz *et al.*, 1992 and 1995). Another is the unperfused rat or mouse embryo hindlimb model, wherein once the limb bud is wounded, the whole embryo is cultured in roller bottles (Martin and Nobes, 1992; McCluskey *et al.*, 1993). By removing the influences of amniotic fluid, these models are amenable to biochemical manipulative experiments and provide a sensitive assay for wound healing agents so that the cell and tissue responses to injury can be directly analysed.

Several groups have investigated fetal wound repair using organ culture (Belford, 1997; Burd *et al.*, 1990b; Chopra *et al.*, 1997; Ihara *et al.*, 1990). One benefit of organ culture is that it allows direct manipulation of the healing environment without interference by the systemic circulatory factors that modulate *in vivo* wound repair. The ability to keep the cells in the wound area viable, without stimulating healing, by incubating the wounds in suboptimal serum concentrations allows the effects of different agents, such as growth factors, on the wound healing process to be studied. *In vitro* skin explant models offer a normal epidermal-dermal architecture but are limited in that angiogenesis and inflammation are absent. In truth, much research has indicated that inflammation is not a pre-requisite to healing, as the absence of scarring in fetal wounds correlates with the sparse inflammatory response (Austyn and Gordon, 1981; Krummel *et al.*, 1987; Longaker *et al.*, 1991a; McCallion and Ferguson, 1996). Consequently, these models are mostly used for the elucidation of the individual components that participate in scarless fetal skin repair.

Most of the models used to study fetal wound healing have looked at incisional wounds, and until recently, the repair of excisional wounds by fetal skin received considerably less attention. A full thickness open defect in post-natal skin heals primarily by the deposition of

a large volume of connective tissue and wound contraction, with reepithelialisation (Ehrlich and Krummel, 1996). In regard to embryonic excisional wounds, reepithelialisation and connective tissue contraction occur in some species but not others. Fetal rabbit and monkey wounds fail to contract and reepithelialise *in utero* (Krummel *et al.*, 1989; Somasundaram and Prathap, 1970; Sopher, 1975a and b), whereas open fetal lamb, opossum, and rat wounds do (see section 1.4.4; Adzick and Longaker, 1991; Burrington, 1971; Ihara *et al.*, 1990; Ihara and Motobayashi, 1992).

The fibroblast–populated collagen lattice (FPCL) is a model that has been widely used to study fetal and adult fibroblasts and their role in wound contraction under different conditions. Fetal rabbit dermal fibroblasts contract FPCLs to a greater extent than their adult counterparts, and a dose-dependent ability of rabbit amniotic fluid to inhibit contraction by these fibroblasts has been demonstrated (Krummel *et al.*, 1989 and 1993). Together, this suggests that the inability of fetal rabbit wounds to close by secondary intention is not due to an inherent defect in the contractility of fetal fibroblasts or of the fetal collagen matrix. An inhibitory effect of human amniotic fluid on lattice contraction has also been demonstrated using both human fetal and adult FPCLs (Wider *et al.*, 1993). Interestingly, sheep amniotic fluid does not inhibit but actually stimulates sheep and human fibroblasts to contract a FPCL in a dose-responsive fashion. The identification of 40 kDa protein factor in E125 sheep amniotic fluid that specifically stimulates this contraction has recently been reported (Rittenberg *et al.*, 1991). Taken together, these studies highlight considerable differences between species when studying fetal excisional wound healing.

Previous work in this laboratory showed an organ culture model to be effective for investigating the mechanism of fetal excisional wound repair in response to different growth factors (Belford, 1997). It was demonstrated that fetal rat skin at 17 days of gestation (E17) retains the ability to heal an excisional wound by dermal contraction and movement of the epithelium over the dermal margins of the wound. This response was observed in

suspension culture in the absence of an adhesive substrate over which to migrate and was dependent on the source of trophic factors. The substrate-dependent migration of epidermal cells is characteristic of adult wound repair (Stenn and Malhotra, 1992), thus the inability of skin taken from the day 19 (E19) fetus to heal *in vitro* suggested a developmental transition in the mechanism of wound reepithelialisation.

The work by Belford (1997) was the impetus for the current thesis as it clearly showed a difference, or transition, in the wound response of skin from the E17 and E19 rat fetus. Additionally, the transition of wound healing patterns is the same as that noted for intrauterine healing, with the fast wound-closing fetal mechanism replaced by an adult-type mechanism later in gestation (Houghton *et al.*, 1995; Ihara *et al.*, 1990; Ihara and Motobayashi, 1992; Soo *et al.*, 2000). One important issue that still remains unexplained is why E19 fetal skin lacks the wound closing capabilities *in vitro* of the E17 fetus. The divergent responses of the two skin types suggest that the two repair processes result from different changes in gene expression. Chapter 3 analyses such changes in gene expression induced in both E17 and E19 skin in response to wounding. With a view to amplify the wound response of fetal skin and hence, increase the number of differences seen in gene expression, the volume of wounded tissue was maximised in this study by creating many excisional wounds in each skin biopsy. Because of this, it was necessary to determine if E17 fetal rat skin also heals multiple wounds *in vitro*, or if there is a competitive advantage for some wounds to heal over others in a single skin biopsy. In order to achieve this, a modified version of the *in vitro* suspension culture model was employed (Belford, 1997; Ihara *et al.*, 1990).

The organ culture system was chosen to study the molecular mechanisms of fetal wound repair so as to limit the comparison to the epidermal and dermal wound responses of E17 and E19 skin. Moreover, by excluding systemic factors that are normally induced *in vivo*, the sample variability should be minimised, thus enabling the key factors controlling

efficient tissue repair in the fetus to be dissected out. The use of the organ culture model is also valid given the intrinsic property of early to mid-gestation skin to heal a wound outside of the fetal environment.

In summary, as a first step toward elucidating the molecular mechanisms involved in the transition from the fetal to the adult–like pattern of wound repair, the aims of the research described in this chapter were:

i) To determine whether multiple excisional wounds created in isolated E17 rat skin close; and

ii) To quantify the extent of dermal wound closure in E17 skin compared to equally wounded skin isolated from the E19 rat fetus.

2.2 MATERIALS AND METHODS

General laboratory chemicals were molecular biology grade and purchased from either Sigma Aldrich Pty. Ltd. (Castle Hill, NSW, Australia) or Merck Pty. Ltd. (Kilsyth, VIC., Australia).

2.2.1 Culture media

Dulbecco's modified Eagle's medium (DMEM, JRH Biosciences, Lenexa, KS, USA), and fetal bovine serum (FBS, CSL Ltd., Parkville, VIC., Australia) were used for the organ culture of fetal rat skin. The antibiotics penicillin and streptomycin (CSL Ltd.) and the amino acid glutamine (Sigma Aldrich Pty. Ltd.) were included in the tissue culture medium. All tissue grade flasks and multi-well plates were purchased from Cellstar® (Greiner Labortechnik, Frickenhausen, Germany).

2.2.2 Animals

Time-mated pregnant Sprague-Dawley rats were obtained from the University of Adelaide (Adelaide, SA, Australia). All experiments were approved by the Animal Care and Ethics Committees of the University of Adelaide and the Women's and Children's Hospital (North Adelaide, SA, Australia), following the Australian Code of Practice for the Care and Use of Animals for Scientific Purposes. The rats were housed in separate cages under constant temperature and humidity with 14-hour light/10-hour dark cycles. The day on which rats were smear-positive was designated as day zero of gestation. Pregnant rats were killed by CO_2 asphyxiation at either 17 or 19 days of gestation. Laparotomy and hysterectomy were performed, the fetuses removed from the uterus and their amniotic membranes, weighed, and placed in ice-cold sterile DMEM. All further procedures were undertaken in a laminar flow hood under sterile conditions.

2.2.3 Fetal skin cultures

Wounding and culture of fetal rat skin was undertaken as described in the legend to Figure 2.1. Colour images of the skin wounds were captured using a colour digital video camera (Sony Hyper HAD, Japan) connected to a Wild M32 dissecting microscope (Heerbrugg, Switzerland), and image analysis computer program (Image-Pro®-Plus, Media Cybernetics®, Silver Spring, MD, USA). Images were captured immediately after wounding, and at 24, 48 and 72 hours of culture.

2.2.4 Wound perimeter traces and area calculations

The perimeter of each whole skin explant and the dermal margin of its contained wounds at each time point were traced and the corresponding areas of each were calculated using the image analysis system. All wounds were traced at time zero for comparison. The epithelial wound margin was not traced for wound area calculations, as transillumination of the wound during closure did not enable reliable visualisation of the epithelial margin, although the dermal margin was always clearly seen. Nevertheless, fully reepithelialised wounds could be clearly distinguished from open wounds. From seventeen E17 skins, 200 wounds were traced after 24 hours and from four E17 skins 60 wounds were traced after 72 hours in serum-supplemented culture. Ninety-seven wounds were traced from six E19 skins after 72 hours in culture only. The data was saved as a Microsoft® Excel spreadsheet (Windows 99, Microsoft® Corporation) and the percent of skin removed by wounding for each explant was determined by the following formula:

$$(\text{Sum of wound areas})_{t=0} / (\text{area of whole skin explant})_{t=0} \times 100\%$$

The percent of dermal closure was determined in E17 and E19 fetal rat skin wounds by measuring the perimeter, and hence area, of the underlying dermis of the open wounds at

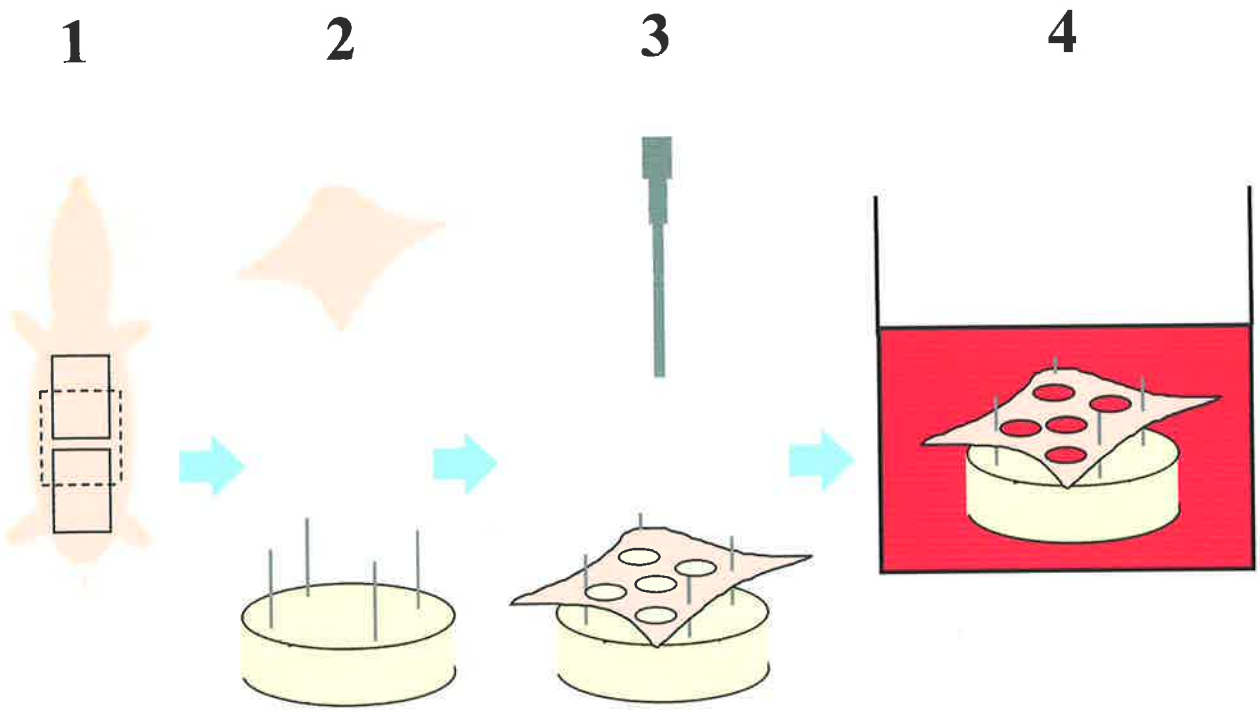

Figure 2.1 Flow diagram of fetal skin culture.

Step 1: A rat fetus was pinned to a dissecting board with injection needles (23G) and skin (approximately 1cm x 1cm) was dissected from its back using fine scissors and forceps (1 explant from E17 shown as broken line, 2 explants from E19 shown as solid lines). Step 2: The skin was floated in DMEM onto a 16mm Tuf-Bond™ Teflon®/Silicon disk (Pierce, Rockford, Illinois) and pinned at each corner with shortened injection needles (23G, 5mm high). Care was taken to preserve the natural tension of the skin and to ensure the skin floated above, not resting on, the disk. Step 3: Under a dissecting microscope, wounds of full thickness (approximately 1mm diameter) were created in the skin explant using a squared-off, sharpened 19G needle. Dipping the needle into a sterile solution of India ink before wounding marked the wound margins. Step 4: The skin explant was then placed into one well of a 12-well tissue culture dish containing 3mL DMEM supplemented with penicillin and streptomycin either with or without 10%(v/v) FBS. The culture was maintained in a humidified atmosphere at 37°C in 5% CO_2-air for up to 72 hours.

time zero and again after a given time in culture. The change in the area of the wounds from both skin types was expressed as the percent of original wound area, using the following formula:

$$(\text{Wound area})_{t=x} / (\text{wound area})_{t=0} \times 100\%$$

Where x = given time in culture

2.2.5 Histology

Wounded skin explants were fixed in methacarn (10% acetic acid / 30% chloroform / 60% methanol) for 2 hours before storage in 70% ethanol and processing by graded dehydration. The specimens were then embedded in paraffin, 3μm transverse sections were cut across the wounds and the sections were stained with haematoxylin and eosin (H&E). Colour images of sections were captured using a colour digital video camera connected to a light microscope (Olympus BH2, Olympus Australia Pty. Ltd., Mount Waverly, VIC., Australia) and image analysis program.

2.3 RESULTS

2.3.1 Healing of E19 fetal wounds in culture

By E19, the fetal rats used in this study were 2.59 ± 0.49 g in weight. At this stage of development the dorsal skin was strong enough to be easily removed without tearing using microscissors and forceps. Due to the size of the E19 fetus, two $1cm^2$ dorsal skin explants could be taken from each fetus. Skin explants to be cultured included the subcutaneous tissue (panniculus carnosus), as well as the dermal and epidermal layers. After the circular excisions of skin were removed, the dermal margins were clearly visible in all open wounds created in the skin pieces. Excisional wounds in skin harvested from E19 embryos did not heal in either the presence or absence of FBS (Figure 2.2). This was the case for all skin explants, regardless of whether they were wounded with one single excision (data not shown) or many punch wounds. After 72 hours in culture, all wounds remained open. Histological sections through the wounded fetal rat skin after 72 hours in culture in either the presence or absence of FBS showed no evidence of cell death or subepidermal liquefaction (Figure 2.3). Histology also showed no evidence of either epidermal or dermal cell migration into the wound, suggesting that no reepithelialisation or contraction took place. Image analysis quantitation of dermal wound size showed that 8.7 ± 1.3 % of skin was removed when multiple excisions (average of 20 wounds per explant) were made in E19 skin explants (n=6 skins). These wounds expanded to 118.9 ± 10.3 % of their original size over the 72 hour culture period (n=97 wounds, Figures 2.2 and 2.7).

2.3.2 Healing of E17 fetal wounds in culture

The E17 fetal rats used in this study were 0.93 ± 0.23 g in weight. By this stage of development the dorsal skin was still quite fragile, so care had to be taken to delicately

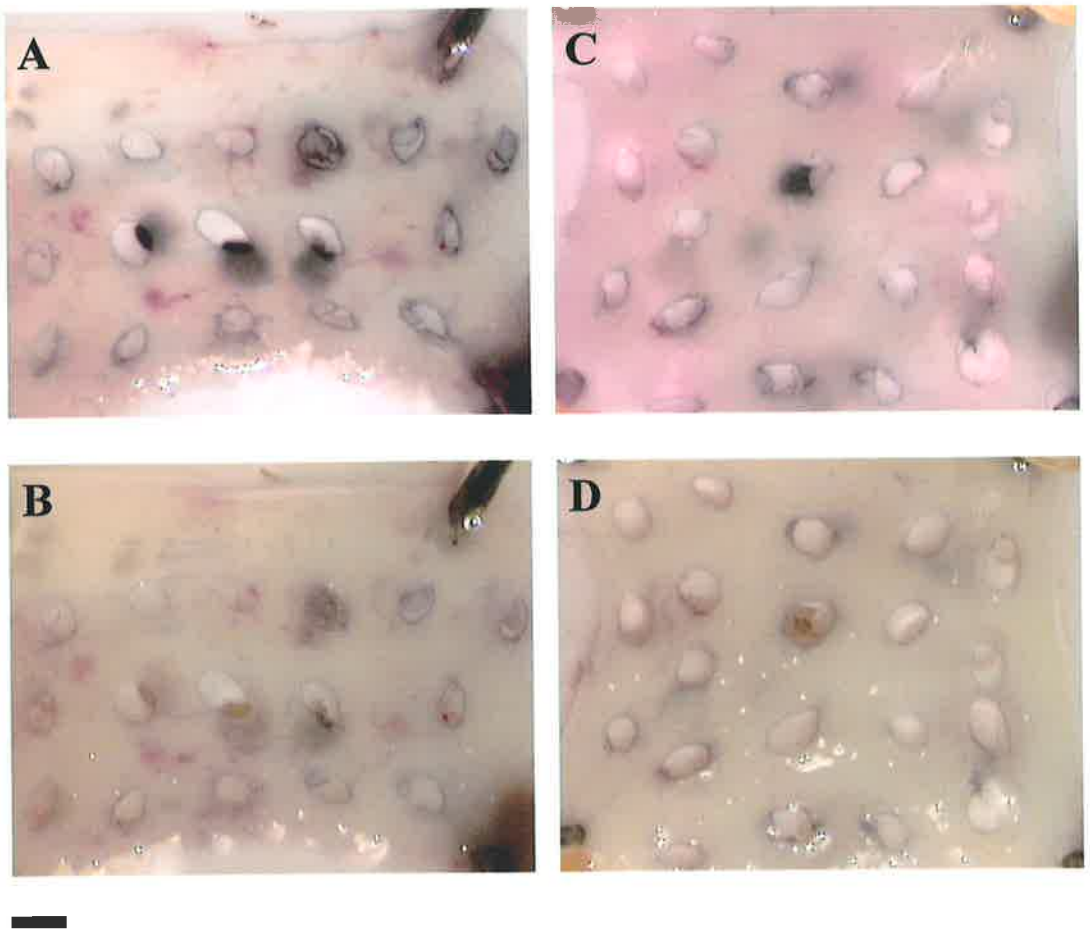

Figure 2.2 Response of excisional wounds in organ cultured E19 fetal rat skin.

Skins were dissected from the dorsum of E19 fetuses, wounded several times with a 19G cutting needle and cultured in DMEM supplemented with 10% FBS (A and B) or DMEM alone (C and D). Images of skins were captured at x 6.5 magnification as described in section 2.2.3 at the time of wounding (A and C) and after 72 hours in culture (B and D). Bar: 1mm.

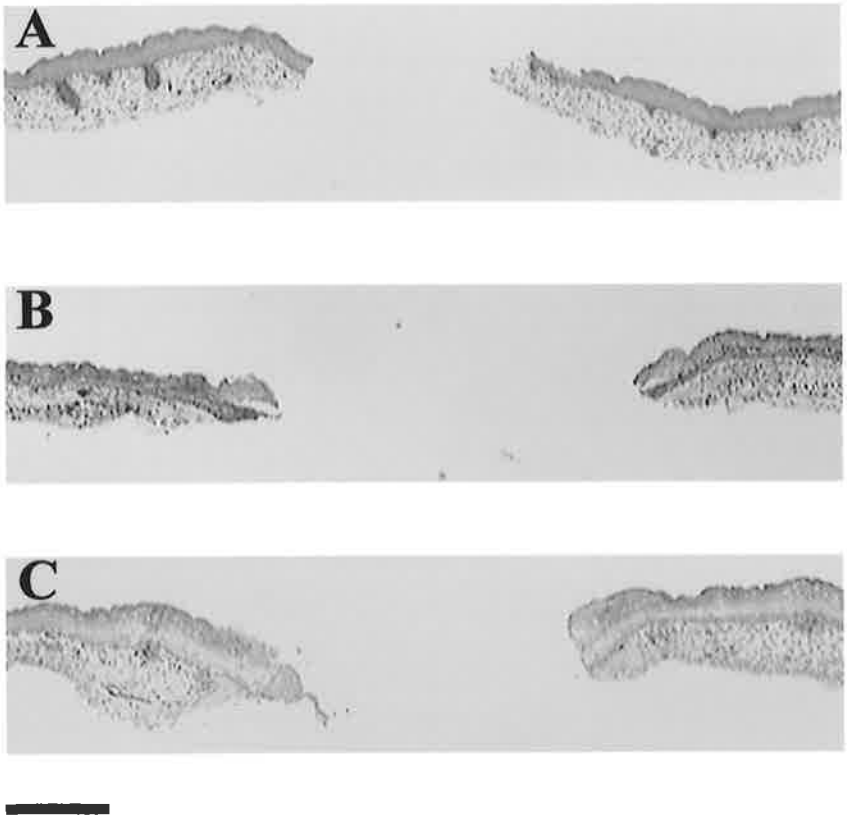

Figure 2.3 Histology of excisional wounds in organ cultured E19 fetal rat skin.

The wounded fetal skins were maintained in DMEM alone (A and B) or DMEM plus 10% FBS (C) and fixed in methacarn at 0 (A) or 72 hours of culture (B and C). Vertical sections cut across the wound centres were prepared and stained with H&E. Bar: 0.25mm.

dissect it from the back of the fetus without tearing. Only one skin piece was dissected from each fetus due to their small size, and each included the dermal and epidermal layers. As with the E19 skins, the dermal margin was clearly visible in all open wounds created in the skin pieces. Photomicrographs of wounds created in skin taken from the E17 rat and cultured in the presence or absence of serum are shown in Figure 2.4. In serum-free medium, all wounds contracted only slightly and never closed (Figures 2.4E and F). The presence of 10% FBS in the culture medium promoted closure in multiple wounds created in the E17 skin after just 24 hours (Figures 2.4A and B). After 72 hours in serum-supplemented culture the area of the wounds had further decreased, but not all wounds had healed. Figure 2.4C shows a representative skin explant with 18 excisional wounds at time zero and Figure 2.4D shows that 2 of the wounds in the same explant have not completely healed after 72 hours in culture. A consistent observation was that with time, the wounded skin becomes less elastic. At the beginning of culture the skin is jelly-like and the wounds appear loose. By 24 hours post-wounding the excisions not only appear to be smaller, but also taught and more rounded. As time proceeds, the isolated skin itself also seems to retract as the wounds close and this is especially evident at the sites of pinning. Some wounds also appear to close at the expense of others that remain open due to the tension placed on the skin. Figure 2.5 shows another example wherein this loss of elasticity is particularly evident. The explant shown was wounded with 4 excisions (Figure 2.5A). After 72 hours in serum-supplemented culture, 3 wounds appear to have healed in part by dermal contraction but this appears to be at the expense of the fourth wound, whose dermal area has increased (lower right wound, Figure 2.5B).

Observation of the movement of ink particles, used in some instances to tattoo the wound margin (see Figure 2.5), also suggested the mechanism of wound closure in E17 skin. Ink particles that were originally at the wound margin at the time of culture progressed inwards towards the centre of each wound by 72 hours of culture. An outer ring of ink

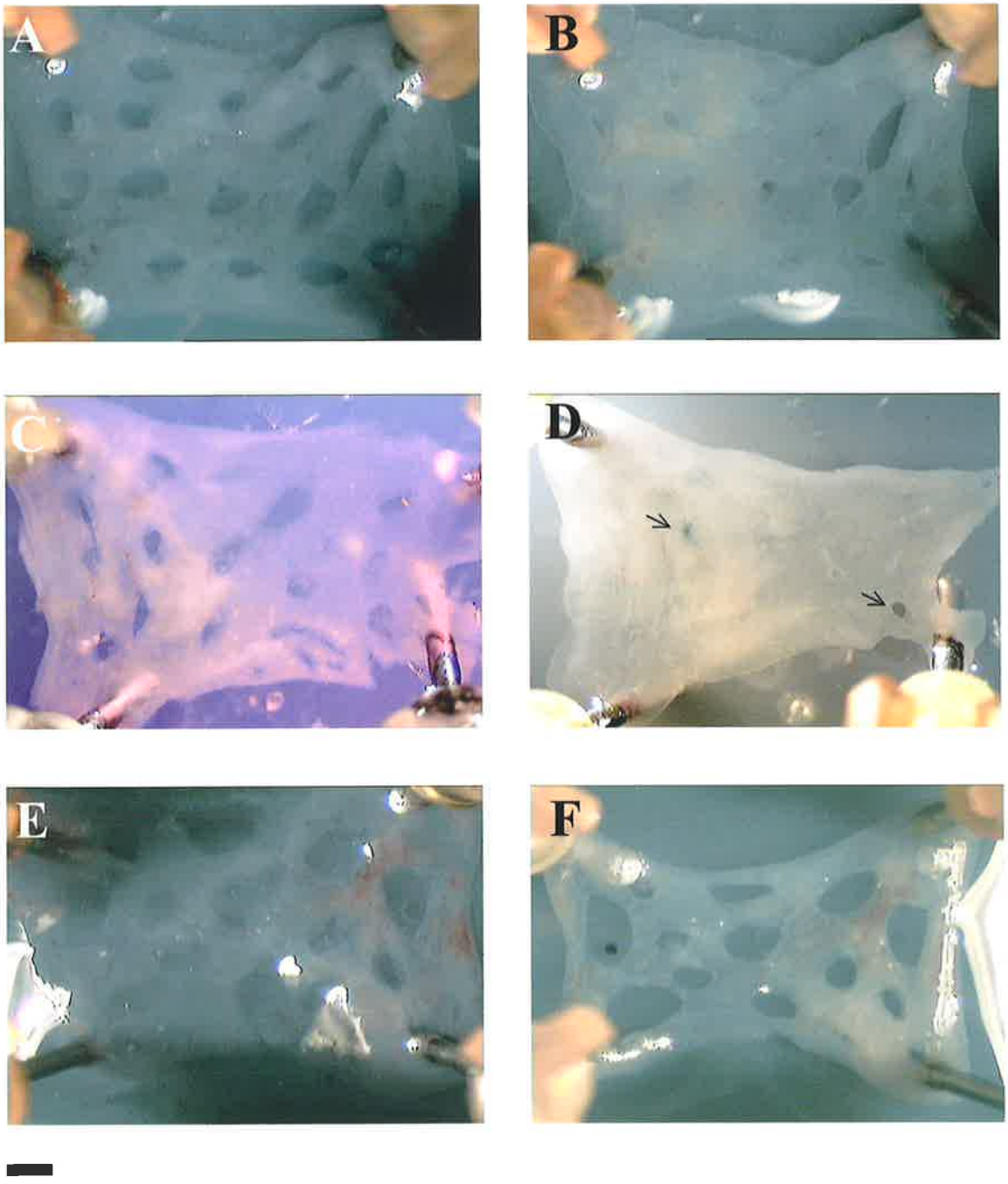

Figure 2.4 Response of excisional wounds in organ cultured E17 fetal rat skin.

Skins were dissected from the dorsum of E17 fetuses, wounded several times with a 19G cutting needle and cultured in DMEM supplemented with 10% FBS (A, B, C and D) or DMEM alone (E and F). Images of skins were captured at x 6.5 magnification as described in section 2.2.3 at the time of wounding (A, C and E), after 24 hours (B) and after 72 hours in culture (D and F). Arrows shown on (D) point to wounds that have not completely closed. Bar: 1mm.

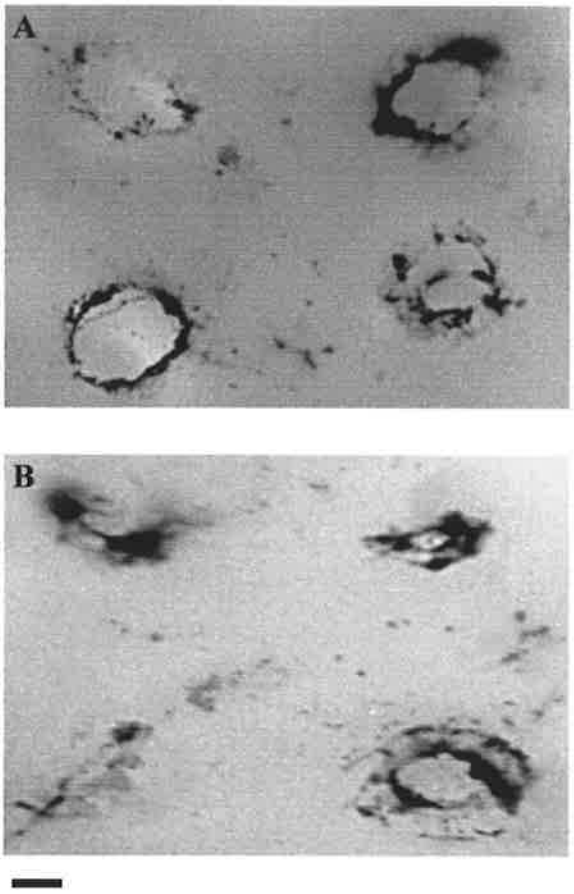

Figure 2.5 Response of excisional wounds in organ cultured E17 fetal rat skin.

Skin was dissected from the dorsum of an E17 rat and wounded with 4 full thickness excisions using a sterile 19G diameter-cutting needle. Dipping the needle into India Ink immediately before wounding marked the wound margin. The skin was cultured in DMEM plus 10% FBS and photographed at x 16 magnification at the time of wounding (A) and after 72 hours in culture (B). Bar: 0.5mm.

particles was often seen enclosing a much smaller inner ring. The outer ring of ink appeared to line the mesenchymal layer, with the inner ring lining the epidermal margin that is thought to move over the dermal layer during reepithelialisation.

Wound histology of the E17 skin explants is shown in Figure 2.6. Wounded E17 skin maintained in serum-free medium for 72 hours showed no evidence of epidermal or dermal movement into the wound defect, but the epithelial edges of the wound did appear to round up compared to the scabrous edges of the E19 wounds (compare Figure 2.3D and Figure 2.6B). In contrast, histological sections through the wounded skins after 72 hours in serum-supplemented medium revealed an epidermal bridge spanning the dermal margins of the wound (Figure 2.6C). This confirmed the ink movement observations above that the epithelial layer had migrated over the dermal margins of the wound to effect final closure. Ink particles remaining on the dermal margin of the wound are visible. Histology of a representative E17 wound that did not completely reepithelialise after 72 hours of culture in serum-supplemented medium is shown in Figure 2.6D. This wound was adjacent to other wounds that had closed, and the skin explant possibly had reduced plasticity comparable to that described in Figure 2.5. Despite not closing, a thickening of the epidermis at the wound margins and a tongue-like protrusion of epidermis from the margin were both seen. This suggests that even though such skin wounds were under too much tension from competing wounds nearby to contract, an epithelial response was still initiated.

Image analysis quantitation of wound size showed that 12.2 ± 4 % of skin was removed by multiple wounding (average of 14 wounds per explant) in E17 skin explants (n=21 skins). The dermis of these wounds contracted to 43.6 ± 12.4 % of their original size after 24 hours in serum-supplemented culture (n=202 wounds), and to 34.7 ± 7.4 % of their original size after 72 hours in serum-supplemented culture (n=60 wounds; Figure 2.7).

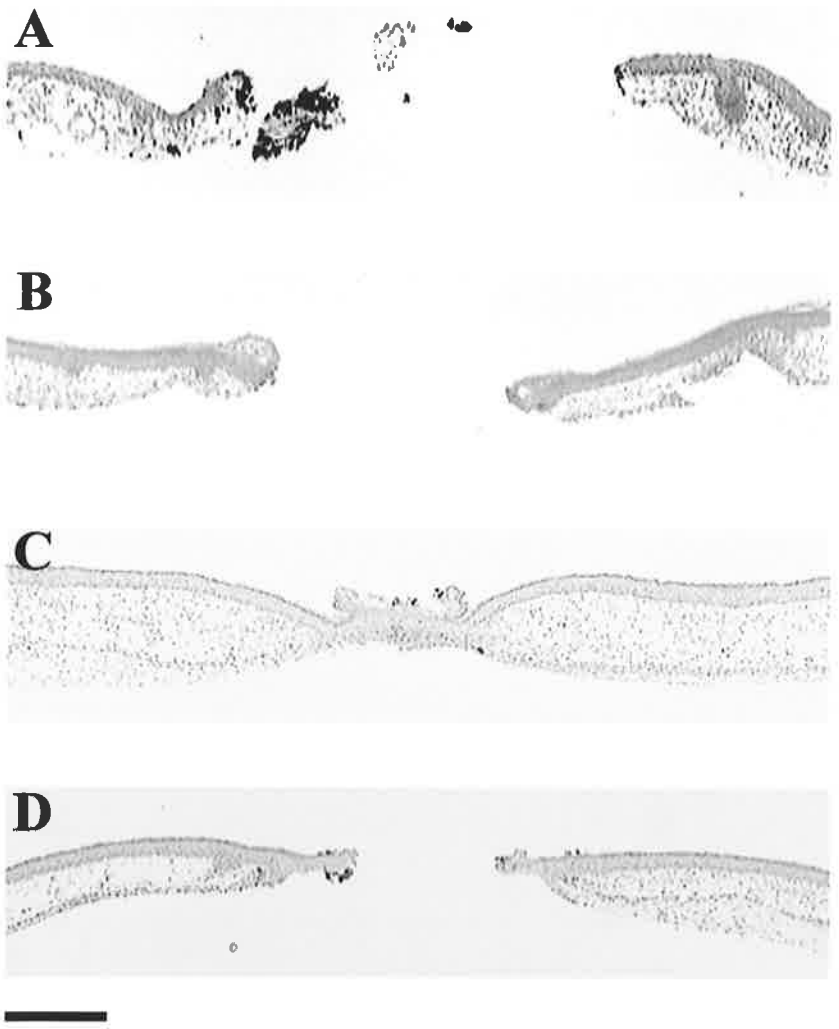

Figure 2.6 Histology of excisional wounds in organ cultured E17 fetal rat skin.

The wounded fetal skins were maintained in DMEM alone (A and B) or DMEM plus 10% FBS (C and D) and fixed in methacarn at 0 (A) or 72 hours of culture (B, C and D). Vertical sections cut across the wound centres were prepared and stained with H&E. Some black ink particles can be seen at the wound margins. Bar: 0.25mm.

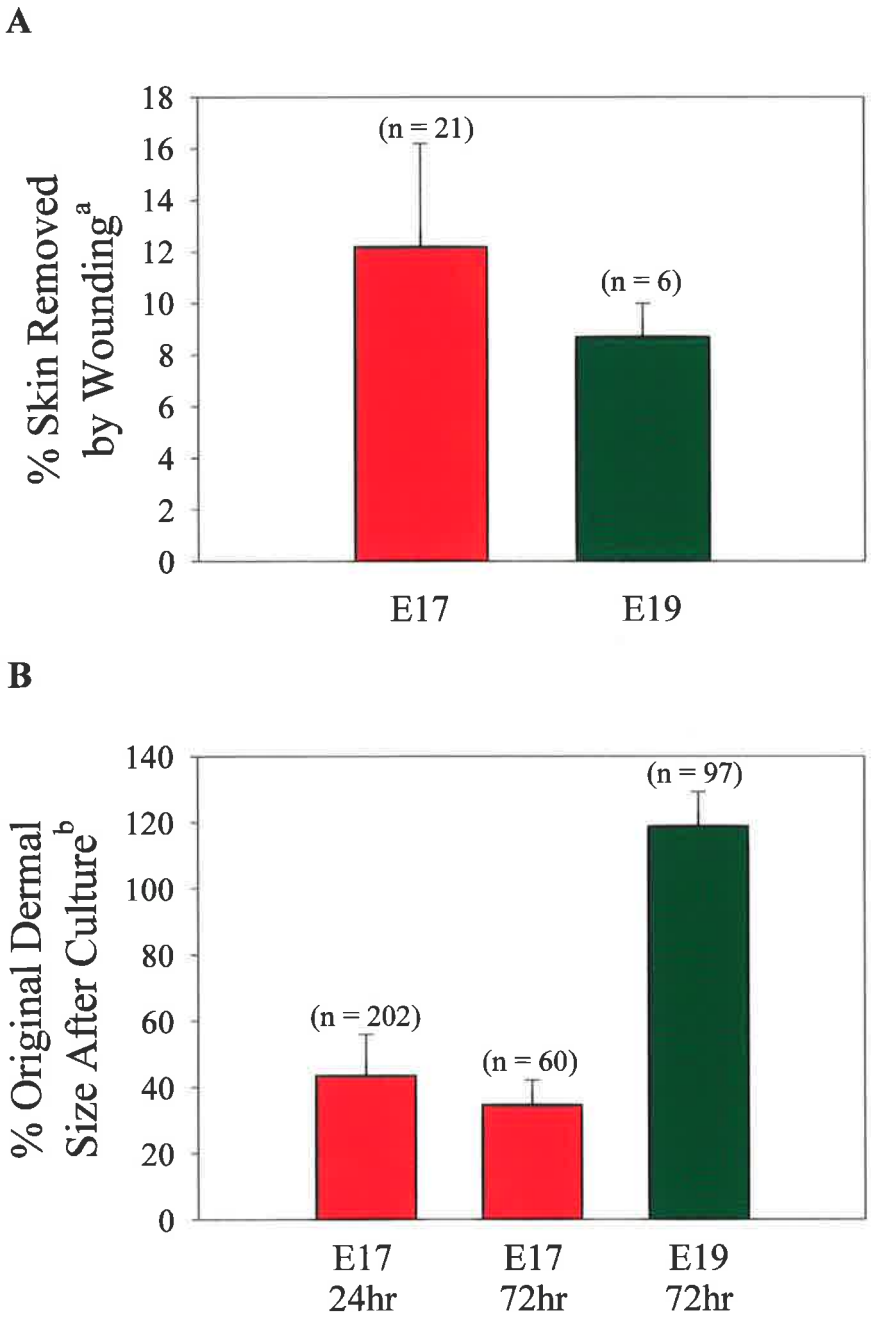

Figure 2.7 Summary of wound calculations.

The perimeter of each whole skin piece and the dermal perimeter of its contained wounds at each time point were traced and the corresponding areas of each were calculated as described in section 2.2.3. The average values for the percent of skin removed by wounding and the percent of wound size after a given time in culture are given. Figure was produced using SigmaPlot® for Windows™ Version 4.00 (Jandel Scientific, San Rafael, CA, USA).

[a] Data represent the mean ± SD of n skins cultured for 72 hours.

[b] Data represent the mean ± SD of n wounds after the given time in culture.

2.4 DISCUSSION

Although numerous techniques and models have been used to investigate incisional wound repair in the fetus, the repair of fetal excisional wounds has received less attention. However, previous studies have demonstrated that the processes of reepithelialisation and contraction are both present during fetal excisional wound repair *in vitro* (Belford, 1997; Ihara *et al.*, 1990). In this study, histological analysis and wound area calculations demonstrated that skin isolated from the E17 rat fetus retains the ability to heal numerous excisional wounds in serum-supplemented culture by

1) movement of the epithelium over the dermal wound margins and
2) dermal contraction.

Satisfactory *in vitro* experiments were impossible on fetuses of E16 or earlier due to the small size and fragility of the skin. The embryonic integument, however, is likely to retain its plasticity and rapid-closure mechanism at least from E10 to E17, as rapid closure of incisional wounds inflicted in E10 rats has been demonstrated using whole embryo culture (Smedley and Stanisstreet, 1984). E19 fetal skin was used as a model of adult wound repair in the current study because it is difficult to culture adult skin. Firstly, unlike fetal skin that can be harvested and handled under completely sterile conditions, skin harvested from the adult animal is not sterile. Secondly, the subepidermal liquefaction that results from collagenase activity destroys the normal architecture of adult skin. Thirdly, the absence of systemic factors has clear implications for adult wound repair *in vitro*, as the healing response can only be mounted by resident cellular elements. This was demonstrated by Greenwald *et al.* (1992), where skin incisions made on rats that were closed immediately and allowed to heal for up to 96 hours then placed into tissue culture for 6 weeks were much weaker than those wounds left on the animal for the same duration.

The current study not only showed that E17 excisional wounds contract after 72 hours in serum-supplemented culture, but most of the contraction occurred after just 24 hours. This ability of E17 fetal skin wounds to close *in vitro* must be partly attributed to the properties of FBS, rather than just being intrinsic to the fetal cells themselves, as wounds that were maintained in DMEM alone remained unhealed after 72 hours in culture. The components in FBS that control the progression of wound closure are still unknown but are thought to be complex mixtures of growth and cell migration factors. Earlier attempts to reproduce the response of E17 wounds to serum using individual growth factors have been unsuccessful (Belford, 1997). In contrast to E17 skin, the excisional wounds created in the E19 rat skin did not contract or reepithelialise when cultured in serum-supplemented medium, but actually expanded. This extends the previous observation that a single excisional wound does not close in E19 skin (Belford, 1997). Using a similar suspension culture model, Ihara *et al.* (1990) demonstrated that E18 rat skin was not able to close an open wound but compensated by forming a thin acellular network of cross-linked fibrin that served as a scaffold for the ingrowth of fibroblast-like cells from the surrounding skin. No acellular network was seen in the wound space of the E19 fetal skin of the current study. Nevertheless, the healing variation noted between the E17 and E19 fetuses suggests that the rat undergoes a fetal to adult switch in the mechanism of wound closure over this developmental period, as shown by Ihara *et al.* (1990).

When wounded with many excisions, the E17 skin appears to lose some of its elasticity over time in culture. At the time of wounding the skin is gelatinous and loose, but with time, tension is set up so that the perimeter of the isolated skin also seems to retract as the wounds close. Martin and Lewis (1992) observed a similar retraction with isolated embryonic skin. When a small patch of embryonic skin was grafted onto their denuded chick wing bud model, the grafted epidermis did not expand over the adjacent vacant surface but actually retracted, leaving its own mesenchyme exposed. This behaviour seemed to be

the opposite of that observed during wound closure, but they reasoned that the circumferential tension in the free edge of the epithelium, acting like a purse string, could drive both the contraction of the isolated skin as well as the closure of a wound. In the current model looking at multiple excisions in a single E17 skin biopsy, the wounds appear to close by contraction as well as contraction of the isolated skin. Wound closure has previously been shown to be independent of cell proliferation, as the addition of hydroxyurea to the wounds does not inhibit wound closure *in vitro* (Allison Cowin, personal communication; Ihara and Motobayashi, 1992). Since multiple wounds result in a large loss of tissue that is not recovered by cell proliferation, contraction of the skin may be at the expense of other wounds nearby that may expand even more, particularly in the underlying dermis. Histological analysis of such incompletely healed wounds demonstrated thickening of the epidermis at the wound margins and a tongue-like protrusion of epidermal cells from the margin. This suggests that even in situations where healing by dermal contraction is compromised, the reepithelialisation response is still mounted. Therefore, the statement that the epithelial component of repair of a single excisional wound proceeds in organ cultured fetal skin (Belford, 1997) can be extended to include multiple wounds.

The findings of the current study support observations in the fetal chick and rodent whereby excisional wounds were shown to heal by both mesenchymal contraction and active movement of the epithelium over the dermal margins of the wound (Martin and Lewis, 1992; McCluskey *et al.*, 1993; McCluskey and Martin, 1995). These authors found that unlike in post-natal wounds, no lammelipodia were seen on the migrating epithelial cells, instead, wound-edge cells remained blunt-faced and adherent to the underlying basal lamina, which is drawn along with the forward-moving epithelial cells. Embryonic epidermal cells have no need to alter their integrins and hence, begin moving promptly, without a lag phase. The presence of an actin cable in the basal epidermis at the wound perimeter suggested that this movement was the result of the co-ordinated expression and

action of actin filaments to effect a purse-string mechanism of wound closure (Martin and Lewis, 1992; McCluskey and Martin, 1995). This actin cable is thought to join adjacent cells via adherens junctions to enable the leading cells in a fetal wound to migrate forward while concomitantly towing their epithelial cell neighbours. Other studies have indicated that these cables also contain myosin and act in a zipper-like manner to close incisional wounds in the fetus (Brock *et al.*, 1996).

Although the repair mechanism of the multiple wounds created in E17 skin was not studied in this project, our group has found actin polymerisation to occur in the epithelium of single E17 rat skin wounds after just 3 hours post-wounding (Allison Cowin, personal communication). Over the following 48 – 72 hours, the actin further condenses around the wound margins, suggesting it is causing the wounds to contract and close. Furthermore, chemical or mechanical disruption of the actin cable prevents wound closure. No actin cables were detected in the epithelial margins of the non-closing E19 rat wounds, although actin filaments were seen at the dermal wound margin. This data suggests that a component of the fetal to adult transition in the mechanism of repair is a loss in the ability of the fetal epidermal cell to respond to wounding by migrating over the mesenchyme according to a substrate-independent purse-string mechanism. Moreover, the ability of the E17 but not E19 epidermis to form the actin cable suggests that differences in cell signalling exist to activate these responses. It is known that, in contrast to the Rac- and Cdc42-mediated lamellipodial crawling of post-natal keratinocytes (see section 1.2.4), Rho mediates the signals regulating reepithelialisation in the embryo, including actin cable formation (Brock *et al.*, 1996; Nobes and Hall, 1999; Ridley *et al.*, 1992; Ridley and Hall, 1992). Further investigation into the signals regulating reepithelialisation, as well as the role of actin and its associated contractile binding proteins during fetal excisional wound healing, is currently underway in a separate project in our laboratory. Nevertheless, this purse-string mechanism of wound closure *in vitro* fits the observations of others who have investigated embryonic wound healing using

in vivo models, and hence, further supports the suitability of the skin culture model for studying fetal excisional wound repair.

As mentioned in section 1.4.4, the ability of fetal excisional wounds to close and the mechanism *in vivo* appears to be species dependent. Fetal rabbit wounds show a minimal inflammatory response (Morykwas *et al.*, 1991a), a lack of reepithelialisation and lack of contraction when exposed to amniotic fluid (Krummel *et al.*, 1989), instead, they appear to gape open and expand (Somasundaram and Prathap, 1970). When protected from amniotic fluid by a Silastic graft, however, fetal rabbit wounds do close (Somasundaram and Prathap, 1972). In contrast, rapid and scarless repair of the neonatal opossum wound by contraction has also been documented (Adzick and Longaker, 1991). Since the fetal development of this marsupial continues in the non-sterile environment of the pouch, contact with amniotic fluid is not important for wound closure. Additionally, early fetal rat and lamb skin both heal open wounds rapidly *in vivo* (Burrington, 1971; Ihara *et al.*, 1990; Ihara and Motobayashi, 1992). Moreover, exposure to, or exclusion from, amniotic fluid has no effect on the ultimate wound size in the lamb. There is also mounting evidence that myofibroblasts, the cell type that may be responsible for generating the forces required for adult wound contraction, are abundant in fetal lamb wounds that heal by scar formation (Cass *et al.*, 1997c; Estes *et al.*, 1994; Longaker *et al.*, 1991a). Although it is still unknown whether myofibroblasts mediate wound contraction and early closure in the younger lamb fetus that heals wounds scarlessly, evidence from studies in the embryonic mouse and rabbit suggests connective tissue contraction does not require myofibroblasts (Haynes *et al.*, 1989; Nodder and Martin, 1997).

In summary, E17 fetal rat skin retains the ability to heal multiple excisional wounds by a combined process of dermal contraction and movement of the epithelium over the dermal margins of the wound. Due to the tension placed on the skin by many wounds, however, this may be at the expense of some nearby competing wounds, which are unable to close.

Histology indicates that the epithelial response occurs in all wounds, but wounds under the greatest tension cannot close. This response is serum-dependent. Furthermore, although the extent to which the E17 and E19 skin explants were wounded was similar, this study clearly showed a difference in the wound response of skin from the E17 and E19 rat fetus. The epithelial and dermal response to wounding that was mounted in E17 skin was not seen in E19 skin wounds and this alone warrants more research. The inability of skin taken from the E19 fetus to heal multiple wounds *in vitro* supports the notion that there is a developmental transition in the mechanism of wound reepithelialisation and dermal contraction. This transition in wound response is sure to result from distinct changes in E17 skin gene expression that are not mimicked in the E19 fetus. Consequently, DD-PCR was the method employed to analyse the expected differences in gene expression and to identify candidate genes differentially expressed during repair following skin injury.

Chapter Three

Differential Display of Excisional Wound Repair in Fetal Rat Skin: Development of Methodologies

3 Differential Display of Excisional Wound Repair in Fetal Rat Skin: Development of Methodologies

3.1 INTRODUCTION

In the previous chapter, an *in vitro* suspension culture model was used to examine the different wound responses of E17 and E19 fetal rat skin. Skin isolated from the E17 rat fetus retained the ability to heal numerous excisional wounds in suspension culture while wounds created in E19 rat skin did not heal but rather increased in size. This difference in wound response supports previous findings that a developmental transition in the mechanism of wound closure occurs late in gestation. Despite all of the comparative studies of scarless fetal wound healing with the adult condition, the intrinsic molecular factors that regulate this transition are still not defined. Differential gene expression in both the dermal and epidermal components of adult and fetal skin tissue is currently an area of intense interest.

Differential gene expression is the basis of tissue specialisation (Franz *et al.*, 1998). Mammals have approximately 30,000 different transcribed genes in their genome (International Human Genome Sequencing Consortium, 2001; Venter *et al.*, 2001). Although any 2 tissues in an organism will express many of the same genes, tissue differences result from the differential expression of some genes. These differences not only include differences in cell type but also differences in metabolism of the same cell type under differing conditions. The level of expression of a given gene is also likely to change under various physiological or pathological states (Wang *et al.*, 1997). Therefore, changes in gene expression are thought to direct the course of normal cellular growth and differentiation, as well as pathological changes that arise in some disease states. To fully understand the molecular nature of disease and to devise rational therapies accordingly is

dependent on the ability to identify and characterise those genes that are differentially expressed.

Saturation and kinetic studies indicate that 99% of distinct messenger RNA (mRNA) species expressed in a cell are rare (Axel *et al.*, 1976; Bishop *et al.*, 1974). Furthermore, this 99% represents only 50% of the total mRNA mass, thus about 50% of the mRNA comprises a relatively small number of abundant mRNA species. Therefore, an optimal method is required to identify a differentially expressed mRNA independent of its prevalence in the mRNA population. At the time of this thesis the three most widely used methods for the study of differential gene expression were electronic subtraction (ES), subtractive hybridisation (SH) and DD-PCR.

ES involves the construction of complementary DNA (cDNA) libraries from the two or more cell populations being compared. This is followed by the sequencing of at least 1000 randomly picked cDNA species from each library, and a comparison of the redundancies of the sequences. Northern blot analysis then determines which genes are induced in one cell type only, and which are consequently differentially expressed. Subtractive hybridisation eliminates the need to sequence large numbers of clones by removing, via liquid hybridisation, cDNA species common to all cell types being compared. Following removal, the subtracted cDNA is used as a labelled probe to screen libraries, or to construct a subtracted cDNA library. Randomly selected cDNA clones are subsequently sequenced, and Northern analysis is performed to confirm their induction in one of the cell types (Wan *et al.*, 1996).

Since its conception in 1992 (Liang and Pardee, 1992), DD-PCR has emerged above ES and SH as the method of choice for detecting and characterising altered gene expression among two or more related cell populations. It has been successfully used to isolate genes differentially expressed in cancers (Koopman *et al.*, 1999; Liang *et al.*, 1992, 1993 and 1994; Orlandini *et al.*, 1996), the brain (Chen *et al.*, 1997; Sokolov and Prockop, 1994;

Wang *et al.*, 1999), and *Mycobacterium tuberculosis* (Rivera-Marrero *et al.*, 1998) as well as during chronic cardiac rejection (Utans *et al.*, 1994), cellular differentiation (Mashima *et al.*, 1999; Ryoo *et al.*, 1997; Verkoczy and Berinstein, 1998), development (Malhotra *et al.*, 1999), replicative senescence (Linskens *et al.*, 1995) and growth factor regulation (Battelino *et al.*, 2000; Eschelbach *et al.*, 1998; Frank *et al.*, 1997; Hsu *et al.*, 1993; Wan *et al.*, 1996). More recent reports have also demonstrated the utility of DD-PCR in wound healing (Darden *et al.*, 2000; Li *et al.*, 2000; Munz *et al.*, 1997 and 1999; Soo *et al.*, 1999; Werner *et al.*, 2000; Yi *et al.*, 2000).

DD-PCR is based on the principal that the steady-state mRNAs expressed in two or more cell types can be directly compared by amplifying partial cDNA sequences from subsets of mRNA using reverse transcription and PCR (Liang and Pardee, 1992). Figure 3.1 is a schematic diagram of DD-PCR, as it is used in this study. RNA is reverse transcribed using an anchored 3' primer, designed to bind to the 5' boundary of a poly A tail. The resulting cDNA is PCR amplified at a low annealing temperature with additional arbitrary 5' primers. This RT-PCR is repeated under controlled conditions for each of the tissue samples being compared that differ in spatial or temporal source, or by environmental influences. Pairs of primers are selected so that each will amplify DNA from 50–150 mRNAs. Arbitrary priming is sequence dependent, but the primer is not chosen based on a match with the template. The best primer-binding sites on the template often match only 6-8 bases out of 10 at the 3' end of the primer (McClelland *et al.*, 1995). For a 5' primer of arbitrary base sequence, annealing positions to cDNA should be randomly distributed in distance from the poly A tail. Therefore, the amplified PCR products from various mRNAs will differ in size, and a side by side comparison can be made between two or more related cell populations by resolving the products on a denaturing polyacrylamide gel. When closely related populations are compared the display gels show similar banding patterns. It is the RNA species governing housekeeping functions that produce identical banding patterns, while the

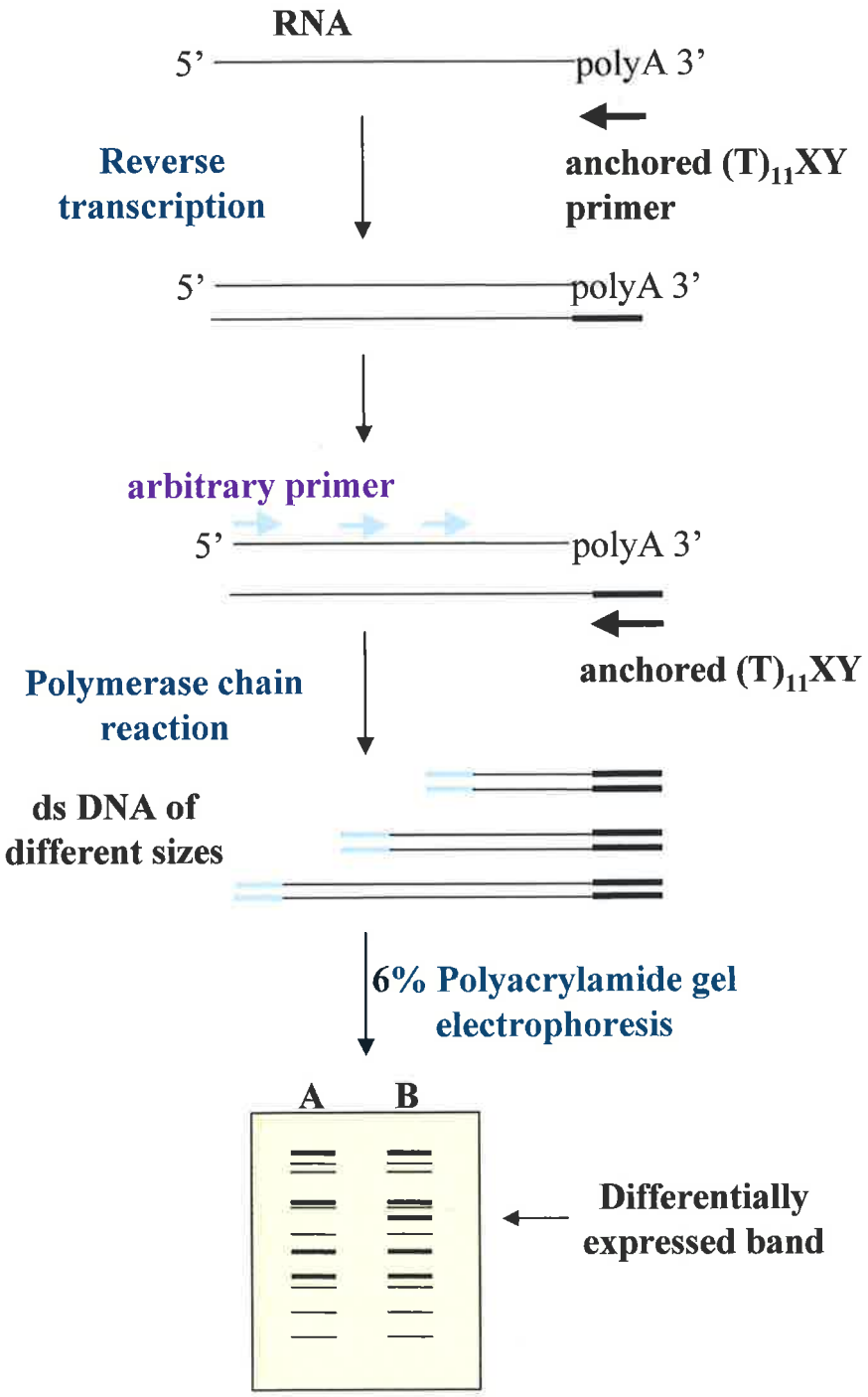

Figure 3.1 Overview of Differential Display PCR.

RNA is isolated from the fetal rat skin and reverse transcribed using one of four possible 3' anchored (T_{11})XY primers (where X = A + C + G and Y = A, C, G or T). The cDNA is PCR amplified using the same 3' primer and one of 20 different 5' arbitrary 10mer primers in the presence of ^{33}P-labelled dATP. The resulting products are resolved on a denaturing polyacrylamide gel and the expressed genes, including those that are differentially expressed, are displayed as a banding pattern by autoradiography.

differences in banding are most likely to represent differentially expressed genes involved in tissue-specific processes. Every combination of primer pairs has a certain chance of identifying a limited number of target gene sequences within the pool of reverse-transcribed cDNA. By using multiple primer combinations, DD-PCR has the potential to visualise all the expressed genes in a cell.

It is proposed here that novel factors exist in fetal tissue that play a regulatory role in the fetal healing process and that DD-PCR can be used to identify their cognate gene transcripts. Differential display may also detect genes that have already been identified and characterised in other processes but not previously thought involved in wound repair. Hence, the aims of the research described in this chapter are twofold:

i) To develop a DD-PCR protocol for examining the mRNA expression patterns of wounded fetal day 17 (E17) and E19 skin at two time points, the time of wounding and 24 hours post-wounding; and

ii) To isolate genes that are differentially regulated in E17 rat skin at 24 hours post-wounding when compared to the time zero and E19 skin samples.

This chapter describes the development of a DD-PCR protocol that is capable of identifying and isolating transcripts that are differentially expressed during the E17 to E19 transition of fetal wound healing.

3.2 MATERIALS AND METHODS

General laboratory chemicals were of molecular biology grade and, unless otherwise stated, purchased from either Sigma Aldrich Pty. Ltd. (Castle Hill, NSW, Australia) or Merck Pty. Ltd. (Kilsyth, VIC., Australia).

3.2.1 Bacterial strains and culture media

Competent *Escherichia coli* JM109 cells (Promega Corporation, Sydney, NSW, Australia) were used to subclone recombinant pGEM®-T vector constructs.

The genotype of the JM109 strain is *endA*1, *recA*1, *gyrA*96, *thi*, *hsdR*17 (r_k-, m_k+), *relA*1, *supE*44, Δ(*lac-proAB*), [F', *traD*36, *proAB*, *lacI*^{q}ZΔM15]. The *lacI*^{q}ZΔM15 marker provides α-complementation of the β-galactosidase gene, allowing for blue/white colour selection of recombinant clones.

Luria Bertani (LB) broth (including yeast extract and tryptone) and agar were used for the routine culture of the bacterial strain *E. coli* JM109 and were purchased in dehydrated form from Oxoid Ltd. (Basingstoke, Hampshire, UK). The substrates used for bacterial selection included β-D-isopropyl-thiogalactopyranoside (IPTG) and X-galactosidase (X-gal; Astral Scientific, Gymea, NSW, Australia) and the antibiotic ampicillin (Sigma Aldrich Pty. Ltd).

3.2.2 Molecular reagents

RNA was isolated from cultured fetal rat skin using either RNAzol™B from Tel-Test, Inc. (Friendswood, TS, USA) or the RNeasy™ mini kit from Qiagen (Clifton Hill, VIC., Australia).

The pGEM®-T Vector System II cloning kit, RNAsin® and T4 DNA Ligase were also purchased from Promega. DNase I and SuperScript™II reverse transcriptase were both purchased from Gibco BRL Life Technologies (Grand Island, NY, USA) and the RNase-free DNase set (for use with RNeasy™ columns) from Qiagen. *FPLC*pure™ T4 polynucleotide kinase and One-Phor-All *PLUS* buffer was obtained from Amersham Pharmacia Biotech (Castle Hill, NSW, Australia). Amplitaq® DNA polymerase and the Stoffel fragment of *Taq* DNA polymerase were purchased from Perkin/Elmer (Branchburg, NJ, USA) while *Taq* DNA polymerase was purchased from Qiagen. All enzymes were supplied with their associated buffers. PCR products were purified directly from reactions using the BresaSpin® kit from GeneWorks Ltd. (Adelaide, SA, Australia) or after agarose gel resolution using GENECLEAN® spin columns (BIO101, Vista, CA, USA).

The radiolabelled nucleotides used, [α-^{33}P]-dATP, [γ-^{33}P]-ATP, [α-^{32}P]-dCTP, [α-^{32}P]-dATP and [γ-^{32}P]-ATP, were supplied at a concentration of 10mCi/mL and were purchased from GeneWorks Ltd.

Electrophoresis reagents included agarose (ScientifiX Scientific supplies, Cheltenham, VIC., Australia), ethidium bromide (Sigma Aldrich Pty. Ltd), SequaGel-6 (National Diagnostics, Atlanta, GA, USA), 30% bis-acrylamide (19:1), N,N,N'N'-tetra-methylethylenediamine (TEMED, Bio-Rad, Hercules, CA, USA) and ammonium persulfate (APS; Eastman Kodak Company, Rochester, NY, USA). The DNA markers used were Molecular Weight Marker VIII (Boehringer Mannheim, Castle Hill, NSW, Australia), λ DNA HEH digest (GeneWorks Ltd.) pBR322 HaeIII digest (Sigma Aldrich Pty. Ltd) and 1 kb DNA Ladder (Promega). The RNA markers used were the 0.24 - 9.5 kb RNA ladder (Gibco BRL Life Technologies). The tracking dyes, bromophenol blue and xylene cyanol, were obtained from Bio-Rad. The SILVER SEQUENCE™ system was purchased from

Promega. BioMax X-ray and XOMAT AR autoradiographic films were obtained from Kodak.

3.2.3 Oligonucleotides

M13 universal sequencing primer (USP), reverse sequencing primer (RSP) and β-actin primers for control reverse transcription (RT) and polymerase chain reactions (PCR) were purchased from GeneWorks Ltd. The 5' arbitrary 10mer DD-PCR primer kit OPA and the 3' anchored poly T primer kit SK010 were purchased from Operon Technologies (Alameda, CA, USA). The adapter primers, A21 and A20, and the modified DD-PCR primers HindIIIOPA-2 and HindIII$(T)_{11}$VG were synthesised by Gibco-BRL Life Technologies.

3.2.4 Trial and modification of DD-PCR conditions

3.2.4.1 Isolation of RNA from fetal rat skin

Skin was removed from each E19 and E17 fetus and wounded as described in section 2.2.3. After culture, the skin was either immediately snap-frozen in liquid nitrogen or stored in RNAlater™ (Ambion Inc., Austin, TX, USA) at -70°C. RNA was isolated from fetal rat skin using RNAzol™B or the RNeasy™ mini kit. In order to obtain high yields of RNA, two to three skins from each sample condition were pooled before extraction. For the RNAzol™B protocol, 1mL of RNAzol™B was added to those skins that weighed less than 100mg (usually E17 skins), while 2mL was added to those greater than 100mg (always pools of E19 skins). The skins were homogenised for about 2 minutes at 17000rpm on ice using a DIAX 600 homogeniser motor and TYP 6 drill (Heidolph, Germany). Further steps in the extraction process were carried out according to the manufacturer's instructions. When using the RNeasy™ kit, 350-600μL of lysis buffer was added to the pooled skins for

homogenisation on ice, then extractions proceeded according to the supplier's protocol. DNase-I treatment was also performed on-column when using the RNeasy™ kit. This minimised the chance of contaminating DNA being present in each RNA preparation.

The concentration of all RNA samples was determined by measuring the absorbance at 260nm and the purity was determined by the 260nm:280nm ratio. The integrity of each RNA sample was verified by agarose gel (1.5%) electrophoresis with ethidium bromide staining. RNA samples were stored in DEPC-treated water at -80°C.

3.2.4.2 Reverse transcription

Reverse transcription was carried out on triplicate RNA samples from four different categories of fetal rat skin: E17 t=0, E17 t=24 hours, E19 t=0, and E19 t=24 hours post-wounding. The primers used were the 3' anchored poly T SK010 primers, $(T)_{11}XY$ (where X is a mix of A, C and G and Y may represent A, C, G or T, see Table 3.1), or the HindIII$(T)_{11}$VG primer (GAGCAAGCTT$(T)_{11}$VG, where V is also a mix of A, C and G). Briefly, 0.5 - 1µg total RNA in a volume of 12µL containing 20 Units (U) RNAsin® and 250ng 3' primer was denatured at 70°C for 10 minutes then snap-cooled on ice for 5 minutes. Four microlitres of 5 x RT buffer (250mM Tris-HCL pH 8.3, 15mM $MgCl_2$, 375mM KCl), 2µL of 0.1mM dithiolthreitol (DTT) and 1µL 10mM dNTP mix was added to the denatured RNA and incubated at 42°C for 2 minutes. Finally, 1µL (200U) of SuperScript™ II reverse transcriptase was added to the reaction mix before incubation at 42°C for 50 minutes. The reactions were then incubated at 70°C for 15 minutes to inactivate the reverse transcriptase and stored at 4°C. A control RT reaction without added reverse transcriptase was always performed on each RNA sample. Subsequent amplification using β-actin specific primers that did not result in the detection of β-actin DNA confirmed the RNA samples were free from contaminating DNA.

Table 3.1 Sequence of DD-PCR primers in the 3' anchored poly T SK010 kit.

These primers were originally described by Liang and Pardee (1992). All primer sequences are shown 5' to 3' and consist of 11 thymine bases plus two additional bases which provide specificity.

Anchored 3' poly T DDPCR primers:			
$(T)_{11}AA$	TTTTTTTTTTAA	$(T)_{11}CG$	TTTTTTTTTTCG
$(T)_{11}AC$	TTTTTTTTTTAC	$(T)_{11}CT$	TTTTTTTTTTCT
$(T)_{11}AG$	TTTTTTTTTTAG	$(T)_{11}GA$	TTTTTTTTTTGA
$(T)_{11}AT$	TTTTTTTTTTAT	$(T)_{11}GC$	TTTTTTTTTTGC
$(T)_{11}CA$	TTTTTTTTTTCA	$(T)_{11}GG$	TTTTTTTTTTGG
$(T)_{11}CC$	TTTTTTTTTTCC	$(T)_{11}GT$	TTTTTTTTTTGT

3.2.4.3 Differential display PCR

The reverse transcribed cDNA to be used in DD-PCR was generated as described above. All DD-PCR reactions were performed in duplicate with the same amount of template cDNA to avoid the possibility of losing rarer mRNAs and to minimise errors in the procedure that may lead to spurious bands. Although the RNA preparations were confirmed to be DNA-free, in situations where it was suspected that other PCR components might be contaminated with DNA, PCR mixes were treated with ultraviolet (UV) irradiation directly before adding the primers or template DNA (Cimino *et al.*, 1990; Sarkar and Sommer, 1990a and b). The sequences of the arbitrary 10mer primers used are shown in Table 3.2. Note that a random primer is a mixture of all four bases at each position whereas an arbitrary primer has a single base at each position. Two additional arbitrary primers termed HindIIIOPA-2 (5'-GAAGAAGCTTTGCCGAGCTG) and HindIIIOPA-3 (5'-GAAGAAGCTTAGTCAGCCAC), made by adding 5'-GAAGAAGCTT to the 5' end of OPA-02 and OPA-03, respectively, were synthesised for high stringency PCR in combination with the anchor primer HindIII$(T)_{11}$VG. All three primers were analysed for

the absence of any obvious hairpin structures and stable primer-dimers, and their dissociation temperatures were close to 60°C, determined using Oligo 4.0 software (National Biosciences, Inc., Plymouth, MN, USA).

Table 3.2 Sequence of primers in the 5' arbitrary 10mer OPA kit used in DD-PCR.

All primer sequences are shown 5' to 3'.

Arbitrary 5' DDPCR primers:			
OPA-01	CAGGCCCTTC	OPA-11	CAATCGCCGT
OPA-02	TGCCGAGCTG	OPA-12	TCGGCGATAG
OPA-03	AGTCAGCCAC	OPA-13	CAGCACCCAC
OPA-04	AATCGGGCTG	OPA-14	TCTGTGCTGG
OPA-05	AGGGGTCTTG	OPA-15	TTCCGAACCC
OPA-06	GGTCCCTGAC	OPA-16	AGCCAGCGAA
OPA-07	GAAACGGGTG	OPA-17	GACCGCTTGT
OPA-08	GTGACGTAGG	OPA-18	AGGTGACCGT
OPA-09	GGGTAACGCC	OPA-19	CAAACGTCGG
OPA-10	GTGATCGCAG	OPA-20	GTTGCGATCC

DD-PCR with Stoffel fragment of Taq DNA polymerase (Perkin/Elmer):

One microlitre of the undiluted cDNA was used as template in 30µL reactions containing 2.5mM $MgCl_2$, 1 x Stoffel buffer (1mM Tris-HCl pH 8.3, 5mM KCl), 200µM dNTPs, 1µM 3' poly T anchored primer, 0.2µM 5' arbitrary primer and 3.6U Stoffel fragment of *Taq* DNA polymerase. The DD-PCR reactions were amplified in a thermal cycler (Corbett Research model PC-960, Mortlake, NSW, Australia) under the following

conditions: 94°C for 1 minute, 40 cycles of 94°C for 30 seconds, 40°C for 2 minutes, 72°C for 30 seconds and 72°C final extension for 5 minutes.

After amplification the DD-PCR samples were dried down in a SpeedVac Concentrator SVC200H (Savant Instruments Inc., Farmingdale, NY, USA) for 2 hours then resuspended to a final volume of 20µL in loading buffer (6% glycerol, 0.01% bromophenol blue, 0.01% xylene cyanol). Five microlitres of each duplicate sample was heated at 70°C for 5 minutes, snap-cooled on ice and electrophoresed in parallel on 8M urea / 6% polyacrylamide gels (see section 3.2.5.2). The SILVER SEQUENCE™ system was used for the detection of amplification products by silver staining according to the manufacturer's protocol.

DD-PCR with Amplitaq® DNA polymerase (Perkin/Elmer):

The undiluted cDNA (1-2µL) was used as template in 20µL reactions containing 1.5mM $MgCl_2$, 1 x Amplitaq® buffer (1mM Tris-HCl pH 8.3, 5mM KCl), 200µM dNTPs, 1µM 3' poly T primer, 0.2µM 5' arbitrary primer, 4µCi [α-^{33}P]-dATP (specific activity 2000Ci/mmol) and 1.25U Amplitaq® polymerase. The DD-PCR reactions were amplified in a thermal cycler under the same conditions given above using the Stoffel fragment of *Taq* DNA polymerase.

For gradient PCR, eight different annealing temperatures were evaluated that varied by 2°C from 42°C to 56°C. Amplification was performed in a Robocycler® Gradient 40 temperature cycler (Stratagene, La Jolla, CA, USA) under the following conditions: 94°C for 1 minute, 40 cycles of 94°C for 45 seconds, 42-56°C for 2 minutes, 72°C for 1 minute and 72°C final extension for 5 minutes.

After amplification, 6µL of each duplicate sample was mixed with 3µL formyl loading buffer (90% formamide, 20mM ethylenediaminetetraacetic acid (EDTA), 0.05% bromophenol blue, 0.05% xylene cyanol FF), boiled at 95°C for 2 minutes, snap-cooled on

ice and electrophoresed in parallel on 8M urea / 6% polyacrylamide gels (section 3.2.5.2). The gels were fixed with 20% ethanol / 12.5% acetic acid to remove excess urea, transferred to 3MM Whatmann paper and dried at 70°C under vacuum in a slab gel dryer (DrygelSR, model SE 1160, Hoefer Scientific Instruments, San Francisco, CA, USA) for 45 minutes. Gels were taped down in an autoradiographic cassette with intensifying screens and BioMax X-ray film was carefully aligned to the top left corner of the cassette for exposure for 1 to 3 days at room temperature. Bromophenol blue and xylene cyanol dye migration were used as markers of product sizes.

DD-PCR with Taq DNA polymerase (Qiagen):

The undiluted cDNA (1µL) was used as template in 20µL reactions containing 1.5mM $MgCl_2$, 1 x PCR buffer and Q-Solution (proprietary solution supplied by Qiagen), 200µM dNTPs, 1µM 3' poly T anchored primer, 0.2µM 5' arbitrary primer, 4µCi [α-^{33}P]-dATP and 1.25U *Taq* DNA polymerase. The DD-PCR reactions were amplified in a thermal cycler and products electrophoresed on 6% denaturing gels as described above for Amplitaq® polymerase. For high stringency PCR with the longer *HindIII* primers, the reactions were amplified as followed: 94°C for 1 minute; 5 cycles of 94°C for 30 seconds, 40°C for 2 minutes, 72°C for 30 seconds; 40 cycles of 94°C for 30 seconds, 55°C for 2 minutes, 72°C for 30 seconds; and 72°C final extension for 5 minutes.

3.2.5 Gel electrophoresis

3.2.5.1 Agarose gels

Agarose gels for DNA or RNA analysis were prepared by dissolving 1-2g of agarose per 100mL of 0.5 x TBE buffer (45mM Tris-borate, 1mM EDTA) in a microwave on high

power for about 1 minute. When the solution had cooled to about 60°C, ethidium bromide was added to a final concentration of 2μg/mL in order to visualise the nucleic acids under medium wavelength (312nm) UV light. The gel was poured, allowed to set, and the combs were removed before it was placed in a tank of 0.5 x TBE for electrophoresis. An appropriate volume of 6 x gel loading buffer (30% glycerol, 0.25% bromophenol blue, 0.25% xylene cyanol FF) was added to each sample before loading onto the gel. Electrophoresis proceeded at 60-100V and after sufficient nucleic acid separation the gel was photographed under UV light.

3.2.5.2 Denaturing gels

8M Urea / 6% polyacrylamide gels (35cm x 40cm x 0.4cm) were prepared using SequaGel-6 solutions according to the manufacturer's instructions. Briefly, 64mL of Sequagel-6 was mixed with 16mL of Sequagel-6 complete buffer and 640μL of 10% APS. The solution was poured between two glass plates, one of which was siliconised with Rain-X® (Unelko, Scottsdale, AZ, USA) to allow easy separation after electrophoresis, and allowed to polymerise for at least 2 hours. Upon setting, the combs were removed from the gels and the wells were washed with 1 x TBE (89mM Tris-borate, 2mM EDTA, pH 8.3) to flush out any unpolymerised acrylamide. The gels were pre-electrophoresed in a vertical gel apparatus in 1 x TBE buffer for 30 minutes at 40W, the combs reinserted, and the wells again flushed with 1 x TBE before loading the samples. Electrophoresis of the samples proceeded at 40W until the xylene cyanol dye had migrated at least three quarters of the length of the gel. Silver staining or autoradiography was used to detect differentially expressed DNA bands in the gels after electrophoresis (see section 3.2.4.3).

3.2.6 Recovery and reamplification of DD-PCR products

Autoradiographs were carefully examined and bands from gels showing a differential expression pattern were counted. Only bands that showed differential expression in duplicate sample lanes of the gel, and in all triplicate samples for that category of skin, were selected for reamplification. To provide exact registration for locating the products of interest, the film was carefully realigned to the top left corner of the cassette over the dried gel. Needle holes (26G) were punched in the autoradiographic film surrounding the individual bands and the position of the DD-PCR products were marked through the holes with a fine pencil. Gel/Whatmann paper slices were excised from the marked regions of the dried gel using a sterile razor blade and the DD-PCR products were eluted in 100µL of elution buffer (10mM Tris-HCl (pH 9), 50mM KCl, 1.5mM $MgCl_2$, 0.1% Triton® X-100; Sanguinetti *et al.*, 1994) at 95°C for 20 minutes. The eluted PCR products were then centrifuged at 13000*g* for 5 minutes at room temperature to pellet the acrylamide. One microlitre of eluted DD-PCR products were then either directly reamplified, or the DNA in the eluate was further purified by standard phenol/chloroform extraction and sodium acetate/ethanol precipitation (Sambrook *et al.*, 1989). Briefly, an equal volume of phenol/chloroform (1:1) was added to the eluate, vortexed, and centrifuged at 13000*g* on a bench top centrifuge for 5 minutes. The resulting aqueous layer was precipitated with 1/10 volume of 3M sodium acetate (pH 5.2) and 3 volumes of 100% ethanol in the presence of 50µg glycogen at -80°C overnight. After centrifuging for 15 minutes at 13000*g*, the pellet was washed with 400µL ice cold 70% ethanol by quick vortex, spun as before and resuspended in 5-10µL of water. When eluted DD-PCR products were precipitated, the entire amount was used as the template in reamplifications.

Fifty microlitre DD-PCR reamplifications proceeded under the same conditions as the original DD-PCR, except 2.5U of *Taq* polymerase was used and the radioisotope was

omitted. As with DD-PCR, in instances when DNA contamination was suspected, PCR mixes were treated with UV irradiation directly before adding the primers or template DNA (Cimino *et al.*, 1990; Sarkar and Sommer, 1990a and b,). Five microlitres of each reamplified product was checked by agarose gel (1.5%) electrophoresis with ethidium bromide staining, while the remainder was purified using the BresaSpin® kit according to the manufacturer's instructions. The purified products were then used directly for subcloning into pGEM®-T (see section 3.2.8).

3.2.7 Specific reamplification of DD-PCR products using adapter primers

In order to specifically reamplify extremely low amounts of eluted DD-PCR transcripts, the complementary adapter primers, A20 and A21, were synthesised. These primers should not misprime onto themselves and can be annealed together and ligated to the ends of PCR products for specific reamplification (see Table 3.3). This takes advantage of their T nucleotide overhang and the single A nucleotide overhang added to the 3' end of PCR products by *Taq* polymerase (i.e. the same principle as the pGEM-T vector).

Table 3.3 Sequence of adapter primers used for specific amplification of eluted DD-PCR transcripts.

Both primers are shown 5' to 3'.

Complementary adapter primers:	
A20:	TCACTATGGTCGACTAACTG
A21:	CAGTTAGTCGACCATAGTGAT

3.2.7.1 Synthesis of adapter duplex

A20 was phosphorylated at the 5' end with ^{32}P as follows:

50pmol of A20 was combined with of 1 x One-Phor-All *PLUS* buffer, 50pmol of ATP, 10μCi of [γ-^{32}P]-ATP (3000Ci/mmol), 20U of *FPLC*pure™ T4 polynucleotide kinase in a final volume of 50μL. The reaction was incubated at 37°C for 30 minutes then 5μL of 0.25M EDTA (pH 7) was added to stop the reaction.

The end labelled oligonucleotide was purified by phenol/chloroform extraction and ethanol precipitation as described in section 3.2.6, except precipitation was at -80°C for 1 hour with 20μg of glycogen as a carrier. The phosphorylated oligonucleotide (50pmol) was allowed to anneal to the A21 oligonucleotide (50pmol) in 1 x One-Phor-All *PLUS* buffer in a final volume of 20μL at 85°C for 2 minutes, 65°C for 15 minutes, 37°C for 15 minutes, 25°C for 15 minutes and 4°C for 15 minutes.

The annealed adapter duplex was purified from excess oligonucleotide by separation on a 15 % non-denaturing polyacrylamide gel (Sambrook *et al.*, 1989). Briefly, the duplex was diluted in an appropriate volume of 6 x gel loading buffer and electrophoresed at 250V until the bromophenol blue dye had migrated down 75% of the gel. As a control, 5μL of the annealed adapter was diluted in an appropriate volume of formyl loading buffer and denatured by heating at 95°C for 5 minutes before loading onto the gel. The wet gel was covered in Glad wrap and exposed to XOMAT AR X-ray film for 3 minutes. The gel was carefully traced onto the film to mark its alignment.

After developing, the film was carefully realigned to the gel and the gel band corresponding to the annealed adapter was excised. The A20/A21 duplex was eluted from the gel in 100μL of elution buffer at 37°C for 3 hours, then the acrylamide gel was pelleted at 13000*g* for 1 minute at room temperature. Two volumes of 100% ethanol and 20μg of glycogen were added to the supernatant and it was placed at 4°C overnight. The duplex adapter was centrifuged at 13000*g* for 10 minutes, resuspended in 200μL of TE (10mM Tris / 1mM EDTA, pH 8), then precipitated once more in 1/10 volume 3M sodium acetate (pH

5.2) and 2 volumes of 100% ethanol on ice for 30 minutes. After a 10 minute spin at 13000*g*, the pellet was washed with 400µL ice cold 70% ethanol, pelleted as before and resuspended in 25µL of TE.

3.2.7.2 Ligation of adapter duplex to control DNA

To determine if the A20/A21 duplex could ligate onto the ends of a DNA insert, two PCR products available from within the laboratory were used. These were a 250 base pair (bp) human BarX2 and a 550 bp collagen III PCR product. Decreasing amounts of both insert and adapter duplex and decreasing molar ratios of the two were set up to determine the lowest amount of insert necessary for successful ligation. Briefly, ligation reactions contained 1.6pg-1.6ng of adapter duplex, 2pg-2ng PCR product insert, ligation buffer (50mM Tris-HCl pH 7.4, 10mM $MgCl_2$, 10mM DTT, 1mM ATP) and 3 Weiss units T4 DNA ligase in a total volume of 10µL. All ligations were incubated at 4°C overnight then inactivated by heating at 65°C for 15 minutes.

3.2.7.3 Ligation of adapter duplex to DD-PCR product

Ligations contained 10pg of A20/A21 duplex, 6µL of purified DD-PCR product, ligation buffer and 3 Weiss units T4 DNA ligase in a total volume of 10µL. All ligations were incubated at 4°C overnight then inactivated by heating at 65°C for 15 minutes.

3.2.7.4 Specific amplification of ligated DNA products

To determine if the ligations were successful, a PCR was performed using the A21 oligonucleotide as both the forward and reverse primer. Five microlitres of the ligation was used as template in 20µL reactions containing 1.5mM $MgCl_2$, 1 x PCR buffer (Tris-HCl pH 8.7, KCl, $(NH_4)_2SO_4$), 1 x Q-Solution, 200µM dNTP mix, 100pmol A21 primer, and 1.25U

Taq DNA polymerase (Qiagen). The reactions were amplified in a thermal cycler under the following conditions: 94°C for 1 minute, 40 cycles of 94°C for 30 seconds, 55°C for 2 minutes, 72°C for 30 seconds and 72°C final extension for 5 minutes. The reactions were run on agarose gels as described in section 3.2.5.1.

3.2.8 DD-PCR cloning procedures

3.2.8.1 Cloning vectors

The reamplified DD-PCR products were cloned into the pGEM®-T vector, which contains single 3' thymine overhangs at both ends of the insertion site. Ligation takes advantage of the template–independent addition of a single adenosine to the 3' end of PCR products by *Taq* polymerase. The pGEM®-T vector contains T7 and SP6 RNA polymerase promoters that flank a multiple cloning region within the α-peptide coding region of the enzyme β-galactosidase. Insertional inactivation of the α-peptide allows recombinant clones to be identified by blue/white colour screening on indicator plates.

3.2.8.2 DNA ligation reactions

DNA ligations were carried out using various molar ratios of vector : insert ranging from 1:1 to 1:10 for each experiment. Typically, ligation reactions contained 50ng of pGEM®-T vector, 30-100ng DNA insert, ligation buffer (50mM Tris-HCl pH 7.4, 10mM $MgCl_2$, 10mM DTT, 1mM ATP) and 3 Weiss units T4 DNA ligase in a total volume of 10μL. All ligations were incubated at 4°C overnight. Ligation mixes were transformed into competent bacterial cells as described below.

3.2.8.3 Transformation of competent bacterial cells

Two microlitres of each completed ligation reaction or plasmid DNA (100ng) was added to 50µL of thawed *E.coli* JM109 competent cells and placed on ice for 20 minutes. The cells were heat-shocked at 42°C for 2 minutes, returned to ice for 2 minutes, then incubated in 950µL of SOC medium (2% bactotryptone, 0.5% bacto yeast extract, 0.05% NaCl (w/v), 10mM $MgCl_2$, 20mM glucose, pH 7) at 37°C for 2 hours with shaking. The cells were centrifuged at 1000*g* for 10 minutes and the supernatant decanted. The cells were resuspended in 200µL of SOC medium, 100µL were spread aseptically onto duplicate LB agar plates (1% bactotryptone / 0.5% bacto yeast extract / 1% NaCl (w/v) / 1.5% agar pH 7) containing ampicillin (100µg/mL) and transformant colonies were allowed to grow overnight at 37°C. Where blue/white colour selection was required, plates were also spread with 100µL IPTG (0.1M) and 50µL X-Gal (50mg/mL in dimethylformamide).

3.2.8.4 Storage of bacteria

For long term storage, bacteria from inoculated overnight cultures were stored as 40% glycerol stocks at -80°C. For short term storage (4 weeks), bacteria were streaked onto agar plates, incubated overnight at 37°C and stored at 4°C.

3.2.8.5 Colony PCR screening of transformants

A bacterial colony PCR screening procedure was employed to identify cDNA-containing clones that used vector-specific rather than insert-derived primers. For each DD-PCR band ligated into the pGEM®-T vector, at least 16 clones were analysed. Single ampicillin resistant transformant colonies were picked with sterile pipette tips, streaked onto LB plates containing ampicillin and allowed to grow overnight at 37°C. The colony on each tip was then resuspended in a 20µL PCR containing 1 x PCR buffer, 1 x Q-Solution, 1.5mM

$MgCl_2$, 200μM dNTP mix, 100ng USP, 100ng RSP and 1.25U *Taq* DNA polymerase (Qiagen). The M13 primers flank the multiple cloning site (MCS) in the pGEM®-T vector (see Table 3.4). The reactions were amplified in a thermal cycler using the following parameters: 94°C for 10 minutes, 30 cycles of 94°C for 1 minute, 55°C for 1minute, 72°C for 1 minute, and then a final extension of 72°C for 5 minutes. Two microlitres of each PCR product was checked by agarose gel (1.5%) electrophoresis with ethidium bromide staining. Using these primers, a PCR product of 236 bp, corresponding to vector sequence only, was observed for clones lacking an insert, whereas colonies containing DD-PCR inserts produced bands greater than 236 bp. The remainder of each colony PCR product was stored at -20°C for dot-blot hybridisation analysis (see section 4.2.4).

Table 3.4 Sequence of M13 primers used for DNA sequencing and amplification of inserts in the pGEM®-T vector.

These primers hybridise to pUC/M13 regions in the M13 *lac* cloning vector pGEM®-T, which are found on either side of the polylinker. Both primer sequences are shown 5' to 3'.

General sequencing primers:	
M13 USP:	GTAAAACGACGGCCAGT
M13 RSP:	CACACAGGAAACAGCTATGACCATG

3.3 RESULTS

3.3.1 Development, trial and modification of DD-PCR conditions

3.3.1.1 Detection of DD-PCR products

Initially, the detection of DD-PCR amplification products was performed using the SILVER SEQUENCE™ system, as it allows the direct detection of amplified fragments on the gel. In turn, the silver-stained bands can be excised directly from the gel and no careful alignment of an autoradiograph with the gel is required. However, a very low signal was obtained from DD-PCR reactions using silver staining (see Figure 3.2). Subsequently, a ^{32}P-labelled dNTP was included in the PCR so that the display pattern could be visualised by autoradiography. As expected, the sensitivity of ^{32}P was much greater than silver staining but the band resolution did not improve (data not shown). The use of a ^{33}P-labelled dNTP in place of ^{32}P was found to increase the resolution of the display patterns after gel electrophoresis (see Figure 3.4).

3.3.1.2 DD-PCR reaction parameters

dNTP concentration

Once the detection method was finalised, the most robust fingerprinting conditions were determined to improve the reproducibility of DD-PCR for analysing the fetal rat skin wound-healing model. Several of the reaction parameters were examined and different amounts of each DD-PCR reaction component were tested. Keeping all other reagents constant, four dNTP concentrations of 20, 50, 100 and 200μM were considered. The clearest pattern was seen when 200μM of dNTPs was used (data not shown). The lower amounts of unlabelled dNTPs gave too dark a background, presumably as more ^{33}P-dATP

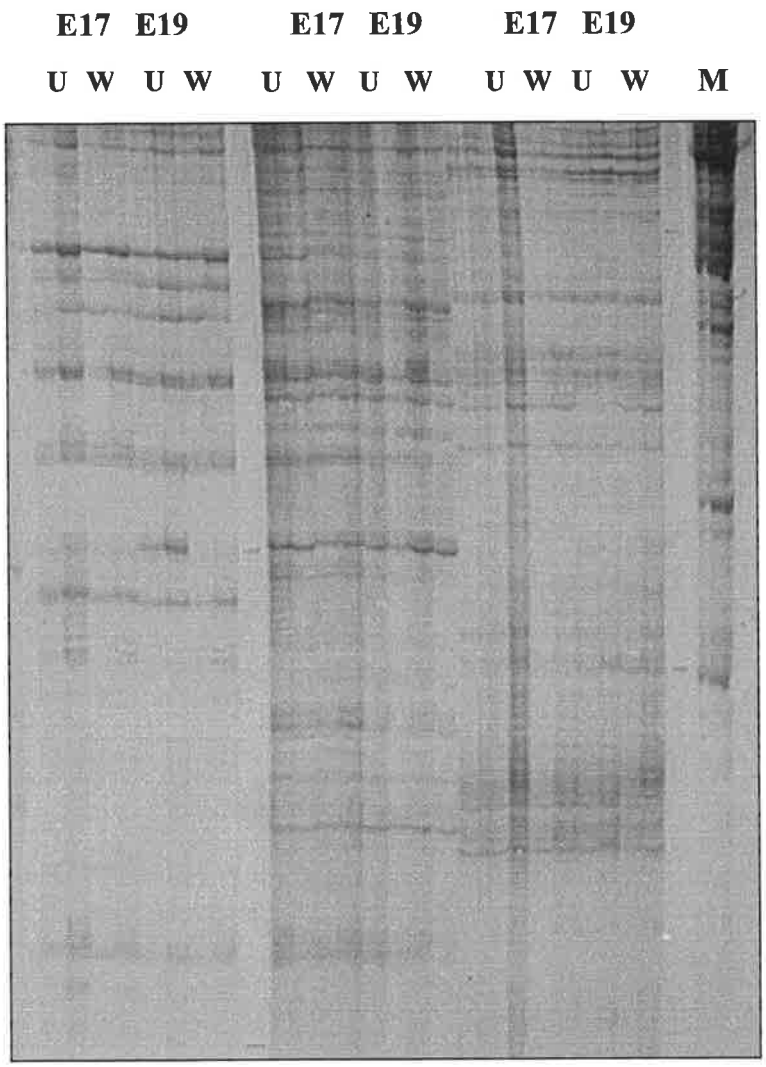

Figure 3.2 Silver-stained cDNA fragments detected after electrophoresis of differential display reactions on a 6% denaturing polyacrylamide gel.

One microgram of wounded E17 and E19 total skin RNA was reverse transcribed and PCR amplified with the $(T)_{11}XG$ and OPA-03 primers. The reactions were resolved by denaturing polyacrylamide gel electrophoresis (PAGE) and silver staining was used to visualise the DNA products. Duplicate lanes are labelled according to the tissue source of the mRNA as follows: E17, fetal E17 skin; E19, fetal E19 skin; W, wounded skin; U, unwounded skin; M, DNA markers. In this particular experiment, all skins were cultured for 30 minutes in DMEM + 10% FBS as described in section 2.2.3. However, in all subsequent experiments the skins were either harvested immediately after wounding at time zero or after 24 hours in culture (see section 3.3.2).

was incorporated into the amplified DNA. Increasing the ratio of unlabelled:labelled dATP reduced this background and gave a clearer, better-resolved and distinct banding pattern.

Taq polymerase

Taq polymerase was tested at concentrations of 1.25 and 2.5 Units per reaction, although no difference in banding pattern was found. Hence, 1.25U was used per reaction due to expense. Different thermostable DNA polymerases tested in DD-PCR under the same conditions and using the same cDNA templates produced variable banding patterns (data not shown). This is consistent with previous reports (Haag and Raman, 1994) and hence the same batch of polymerase was used for all samples to be compared using a given primer pair.

Input RNA and cDNA

Slight variations in the quality and quantity of RNA were found to result in variability in the banding pattern. To determine the amount of RNA needed to obtain the best results, 0.5 and 1μg of RNA template were used to produce first strand cDNA. One or 2μL of cDNA template was then added to the DD-PCR. The display patterns appeared similar regardless of the amount of input cDNA, however, more bands were visualised on the display gels when 1μg of total RNA was used in the RT (data not shown). A control RT reaction without added reverse transcriptase was always performed on each RNA sample to check for contaminating genomic DNA. Subsequent amplification using β-actin specific primers did not result in the detection of β-actin DNA, confirming the RNA samples were free from DNA and hence fingerprints generated in DD-PCR were RNA-dependent and not due to contaminating genomic DNA.

Thermal cycling conditions

To find the optimum thermal cycling conditions for this study, different annealing temperatures (40°C - 48°C) were examined for all the different 5' and 3' primer combinations being used. Good banding patterns were observed in some primer combinations at the higher temperatures, while other primers did not anneal to the template (data not shown). Since all primers did anneal to the cDNA and amplify a banding pattern at 40°C over 2 minutes, this was chosen as the optimum annealing condition to be used for all reactions.

^{33}P-dATP concentration

Finally, different amounts of [α-^{33}P]-dATP were evaluated to determine the optimal signal. The most cDNA transcripts were amplified (~50-150 bands per lane) when 4μCi of [α-^{33}P]-dATP was used per reaction, less transcripts were amplified with 3μCi and even less with 2μCi. The least background noise was also seen on the display when 4μCi of [α-^{33}P]-dATP was used, so this amount was added to all differential display reactions.

In summary, the optimised conditions for DD-PCR used 1μg total RNA for RT and 1μL of cDNA as a template in PCR containing 200μM dNTPs, 1.25U *Taq*, 4μCi [α-^{33}P]-dATP and 40°C as the annealing temperature.

3.3.2 Controls to improve the reproducibility of differential display

Differential display reactions were performed using RNA from 4 different categories of skin: E17 and E19 wounded skins at the time of wounding (t=0) and after 24 hours in culture (t=24h). These time points were chosen for comparison because after 24 hours in culture E17 wounds appear to be closing while E19 wounds remain open (see Chapter 2).

Three skins were pooled before RNA extraction, as opposed to using RNA from one skin sample, to minimise experimental variation (see Figure 3.3). Indeed, pooling skins before RNA extraction resulted in more reproducible DD-PCR patterns between the samples (data not shown).

Figure 3.4 is an example of a polyacrylamide gel showing duplicate DD-PCR reactions of each RNA sample, obtained with the $(T)_{11}XG$ and OPA-03 primers. Candidate transcripts were selected based on distinct upregulation or downregulation in a particular tissue compared to the other 3 conditions. As short primers were used, a low annealing temperature during PCR was required for priming. This low stringency PCR still created a few spurious bands that were not reproducibly amplified, and might have been a source of false positives. The selection of DNA bands for further analysis was, therefore, restricted to those uniformly seen in duplicate patterns of each RNA sample.

Indicated in Figure 3.4 are 8 bands that may represent differentially expressed genes. All candidate bands were given an identification number based on the corresponding primer combination used to generate the band and its relative position on the gel (e.g. 3XG1 corresponds to anchor primer $(T)_{11}XG$ and arbitrary primer OPA-03, and it is the highest molecular weight band selected from the gel as being differentially expressed). Band 3XG1 appears to be switched on in E17 skin after 24 hours in culture post-wounding, as it is not seen in the E17 time zero or the E19 samples. Band 3XG4 appears to be downregulated in E17 skin at both time points and in E19 skin 24 hours post-wounding, as it is only seen in E19 skin at time zero. The generally reproducible banding pattern and presence of candidate differentially displayed products on the gel indicated that DD-PCR might indeed be the first step towards identifying genes differentially expressed in response to wounding.

A banding pattern that differs to the RNA-directed fingerprints was observed in control reactions that contained no cDNA template. Control amplifications using β-actin specific primers, in the absence of reverse transcription, did not result in the detection of a β-actin

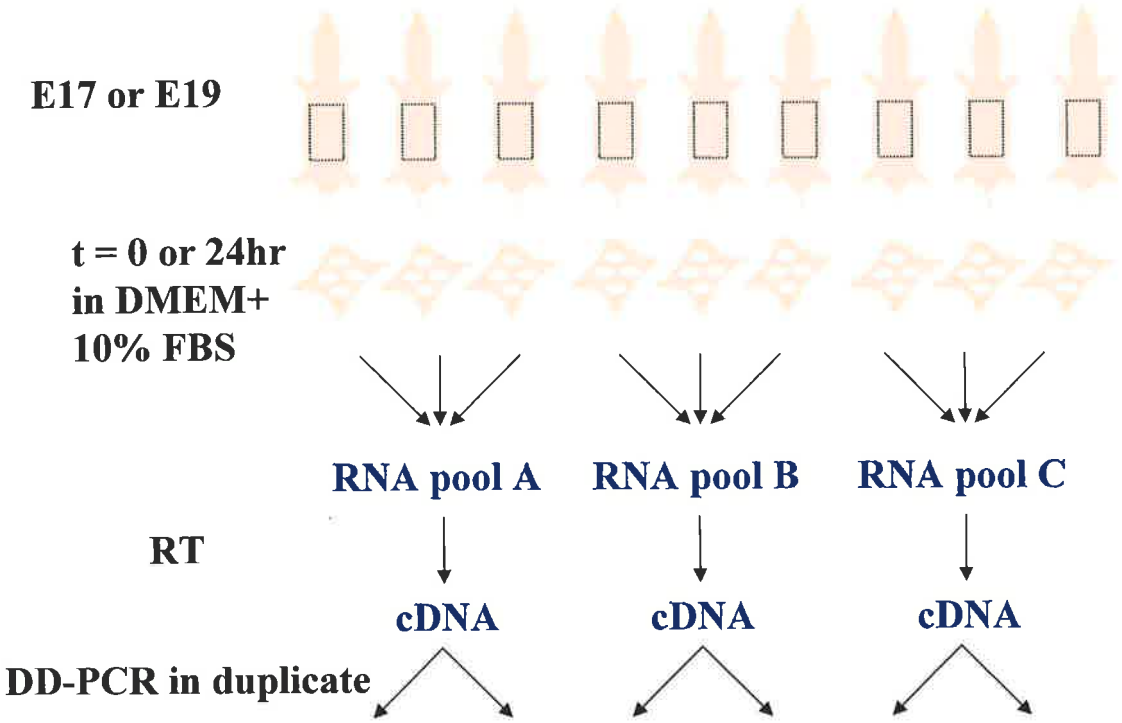

Figure 3.3 Improving DD-PCR reproducibility by pooling fetal rat skins.

Pooling 3 skins for extraction gave greater reproducibility in DD-PCR patterns between identically treated RNA preparations. Nine E17 and E19 skins were wounded and snap-frozen in liquid nitrogen at time zero and 9 skins of each age were wounded and cultured in serum-supplemented medium for 24 hours. From each condition, 3 pools of 3 skins were made and the total RNA was extracted from each pool. The RNA samples were reverse transcribed and then PCR amplified in duplicate to enhance reproducibility (see section 3.2.4).

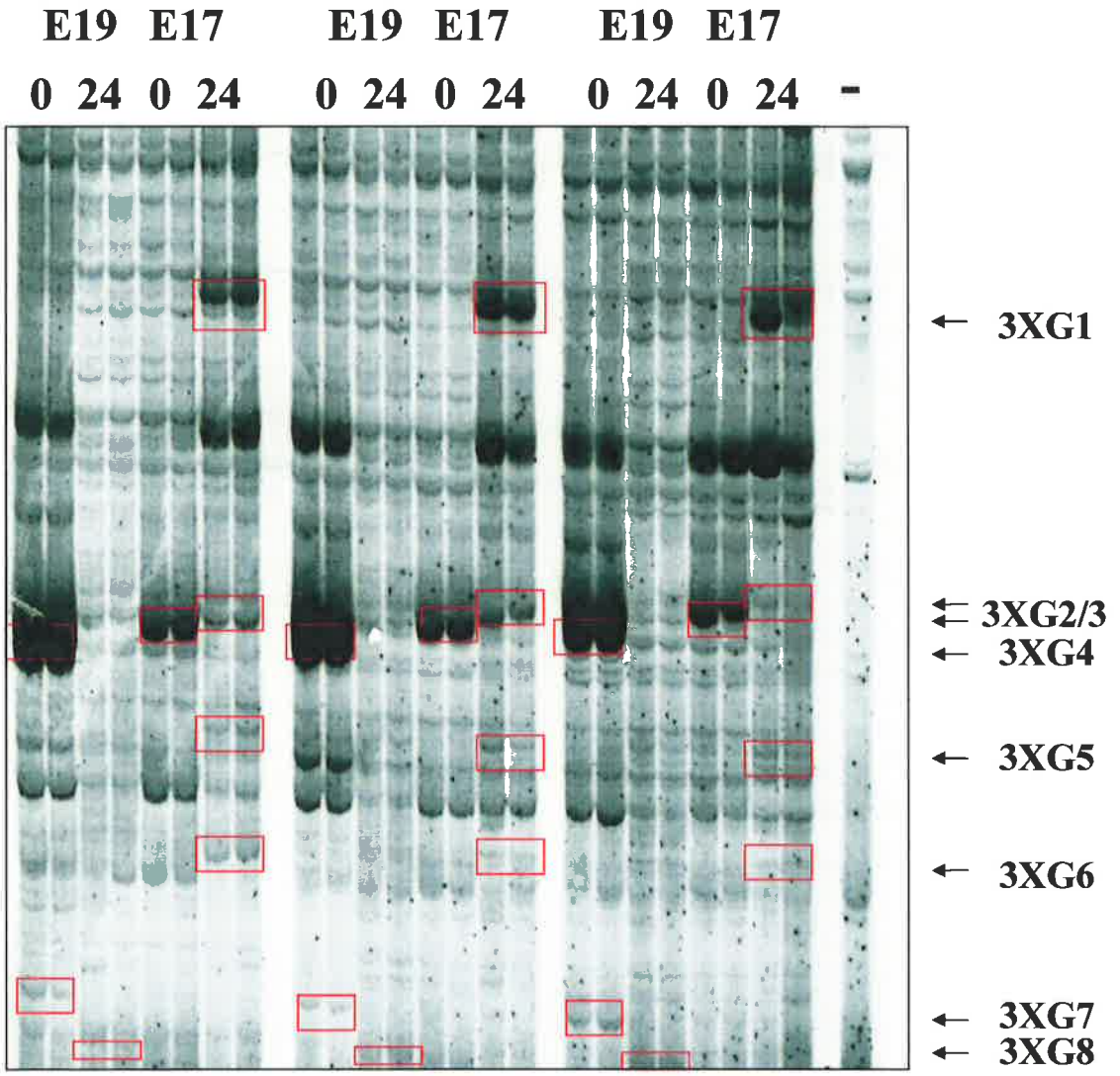

Figure 3.4 Polyacrylamide gel showing DD-PCR using optimised conditions.

One microgram of wounded E17 and E19 total skin RNA from t=0 and t=24 hours in culture was reverse transcribed and PCR amplified with $(T)_{11}XG$ and OPA-03 using the optimised conditions (200μM dNTPs, 4μCi [α-^{33}P]-dATP and 40°C as the annealing temperature, section 3.2.4). Duplicate lanes are labelled according to the tissue source of the mRNA as follows: E17, fetal E17 skin; E19, fetal E19 skin; 0, t=0 hours in culture; 24, t=24 hours in culture. Products that appear to be differentially expressed (designated 3XG1-8, corresponding to the primer combination and the relative position of each band on the gel) are boxed and indicated by arrows. The negative control reaction (-), which did not contain cDNA template, produced a banding pattern different to that of the skin samples.

transcript, excluding DNA contamination as the cause of banding. As an extra precaution, PCR mixes were treated with UV irradiation directly before adding the primers or template DNA, but this did not eliminate the spurious bands in the negative control. This indicated that the negative display pattern was not due to contaminating DNA in the PCR reagents but rather, self-extension and amplification of the arbitrary 10mer primers under the low annealing conditions.

Each of the 20 different 5' arbitrary 10mers were combined with 3 different 3' anchored primers, $(T)_{11}$XA, $(T)_{11}$XC and $(T)_{11}$XG, for a total of 60 DD-PCR reactions for each tissue category being compared. Figure 3.5 is another example of a polyacrylamide gel showing duplicate differential display reactions of each RNA sample, this time obtained with the $(T)_{11}$XC and OPA-02 primers. Bands that may represent differentially expressed genes are indicated. Both Figure 3.4 and 3.5 are good examples of gels displaying 50 – 150 bands per lane. From such gels, only the most clearly differentially expressed bands were selected for further study. However, the reactions of some primer combinations displayed very low signals with only a few bands per lane detected. Moreover, no differential expression between samples was seen in many of these reactions. For example, the 5'arbitrary primers OPA-05, -06, -07, and OPA-09 to –17, when combined with either of the 3'anchor primers, did not result in the detection of any differentially expressed bands (data not shown). In fact, of the 60 primer combinations that were tested in this differential display study, only 7 resulted in the detection of differentially expressed bands between samples. These primer combinations were OPA-02 / $(T)_{11}$XC, OPA-03 / $(T)_{11}$XC, OPA-04 / $(T)_{11}$XC, OPA-08 / $(T)_{11}$XC, OPA-18 / $(T)_{11}$XC, OPA-03 / $(T)_{11}$XG and OPA-03 / $(T)_{11}$XA. From these reactions, a total of 52 candidate products were identified as being differentially expressed in all triplicate RNA samples from the different tissue categories analysed (see Table 3.5). These were subsequently excised from their gels for further analysis.

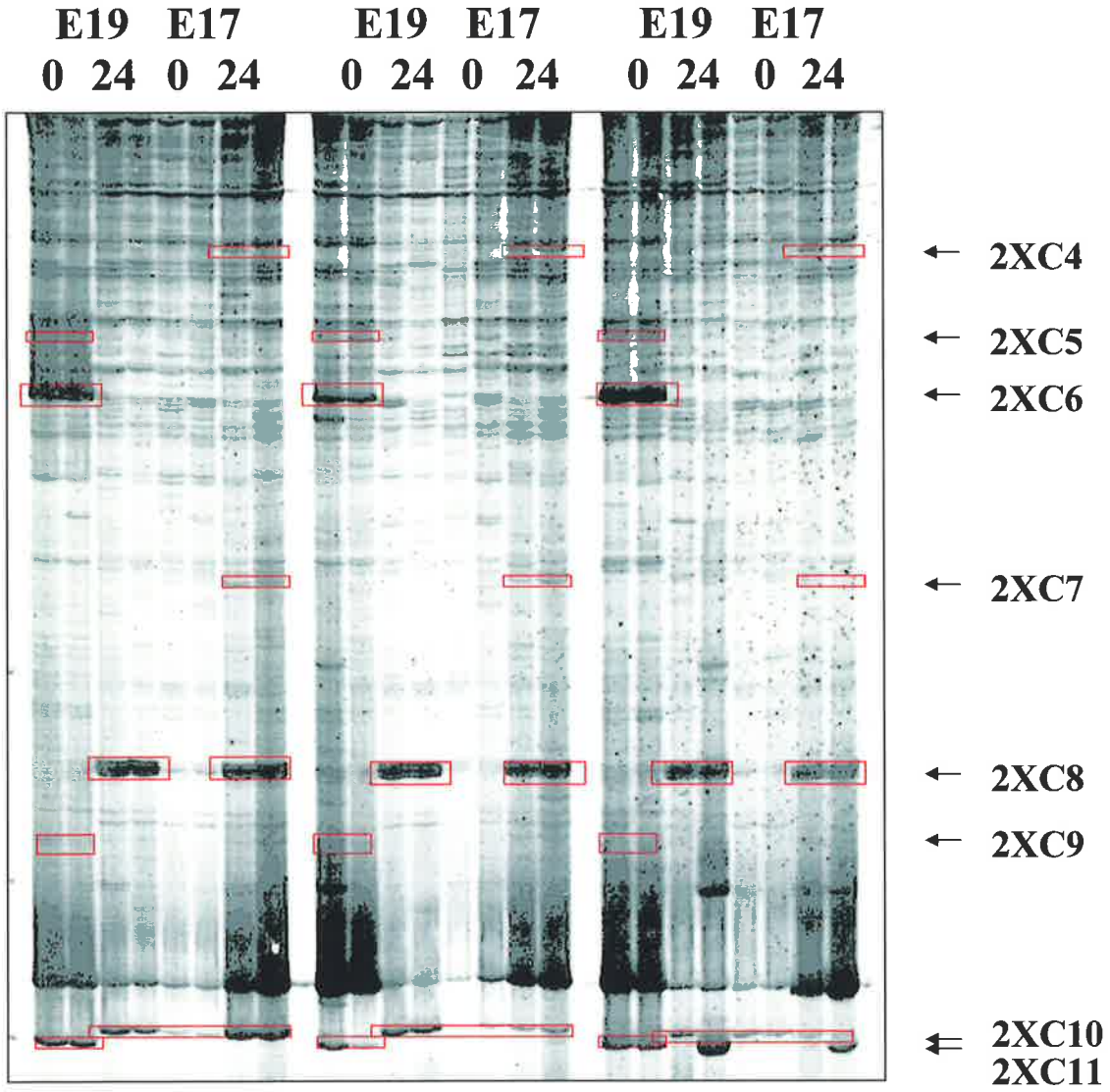

Figure 3.5 Polyacrylamide gel showing DD-PCR using OPA-02 and $(T)_{11}XC$.

One microgram of wounded E17 and E19 total skin RNA from t=0 and t=24 hours in culture was reverse transcribed and PCR amplified with $(T)_{11}XC$ and OPA-02 using the optimised conditions (200μM dNTPs, 4μCi [α-^{33}P]-dATP and 40°C as the annealing temperature, section 3.2.4). Duplicate lanes are labelled according to the tissue source of the mRNA as follows: E17, fetal E17 skin; E19, fetal E19 skin; 0, t=0 hours in culture; 24, t=24 hours in culture. Products that appear to be differentially expressed (designated 2XC4-11, corresponding to the primer combination and the relative position of each band on the gel) are boxed and indicated by arrows. Note that the differentially expressed products 2XC1-3 were of a higher molecular weight and are not shown.

Table 3.5 Comparative distribution of banding patterns representing categories of differential gene expression.

In each tissue column, "+" indicates a brighter band and "-" a dimmer band on the denaturing gel. A "+" thus means that the gene in question is more strongly expressed compared with conditions where a "-" appears. For instance, 13 transcripts appeared to be upregulated in fetal E17 skin 24 hours post-wounding compared with all 3 other conditions (fourth line from top).

Banding Patterns	E19 t=0	E19 t=24h	E17 t=0	E17 t=24h	No. of Bands
E19 t=0 upregulated	+	-	-	-	28
E19 t=24h upregulated	-	+	-	-	3
E17 t=0 upregulated	-	-	+	-	2
E17 t=24h upregulated	-	-	-	+	13
Both t=0 skin upregulated	+	-	+	-	1
Both t=24h skin upregulated	-	+	-	+	1
E17 skin upregulated	-	-	+	+	1
E19 t=0 downregulated	-	+	+	+	2
E17 t=24h downregulated	+	+	+	-	1
Total No. of Candidate Bands					52

3.3.3 Traditional method of recovery and reamplification of DD-PCR products

To recover the differentially expressed transcripts and identify the genes they represent, each band was excised and eluted from the gel in water (see section 3.2.6). In the present study, the DD-PCR products obtained were difficult to reamplify from the dried gel slices. Figure 3.6 shows an agarose gel of the eight 3XG bands that were excised from the polyacrylamide gel (see Figure 3.4) and reamplified under the initial DD-PCR conditions. Note that the negative control also produced a banding pattern on the denaturing gel but this differed from all other lanes. On the DD-PCR polyacrylamide gel shown in Figure 3.4 the 3XG bands resolved to different sizes, so after reamplification these bands should still be different lengths, with 3XG1 being the highest molecular weight and 3XG8 being the

lowest. However, Figure 3.6 shows that the 400 bp band seen in the negative control was also seen all lanes containing reamplified bands. This non-specific amplification was not unique to the OPA-03 and $(T)_{11}XG$ primer, as products were also seen in negative control reactions using other 5' and 3' DD-PCR primer combinations (see Figure 3.7). To determine if a different banding pattern is seen when genomic DNA is used as a template, 1μg of genomic DNA was added to the reamplification reaction. Figure 3.7 also shows that a different banding pattern was indeed seen when genomic DNA was included in the reamplification reaction. This indicated that the majority of false positive PCR products amplified in such negative controls do not appear in the reactions with added DNA template or they are, at least, under-represented in the presence of the competing DNA. In summary, this experiment implied that the short DD-PCR 10mers are self-priming, extending and amplifying at the low annealing temperatures used during DD-PCR, and the low amount of DNA eluted from a gel slice is not enough to compete with the extension of the 10mer primers during reamplification.

3.3.4 Modifications to the traditional recovery and reamplification of products

3.3.4.1 Strategies to increase the yield of eluted DNA

Different strategies were employed to reduce the primer extension effect observed during reamplification of DD-PCR products. Initially, to improve the yield of DNA recovered from the gel prior to reamplification, different elution and purification methods were tested. Elution in water was attempted overnight at 4°C and 37°C, as well as at 95°C for 15 minutes. Pooling many identical bands before and after elution was also performed to increase the amount of DNA recovered. Finally, phenol/chloroform extraction prior to ethanol precipitation was tested to increase DNA purity when pooling eluted products. None of these modifications improved reamplification.

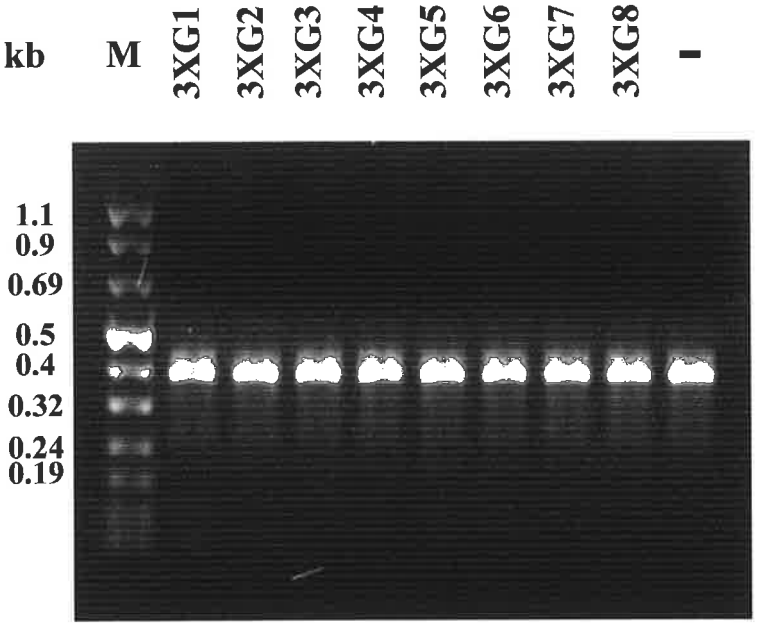

Figure 3.6 Agarose gel showing DD-PCR reamplification reactions.

Candidate DNA products from the OPA-03 and $(T)_{11}XG$ DD-PCR of wounded E17 and E19 skins at t=0 and t=24 hours post-wounding were excised from dried polyacrylamide gels, eluted in water and reamplified under the initial DD-PCR conditions (see section 3.2.6). These bands were first identified in Figure 3.4 and were designated 3XG1 to 3XG8 (as indicated above lanes). No DNA template was added to the negative control reaction (-), but a band of about 400 bp was still amplified. The sizes of the Boehringer Mannheim Molecular Weight Marker VIII (M) are indicated.

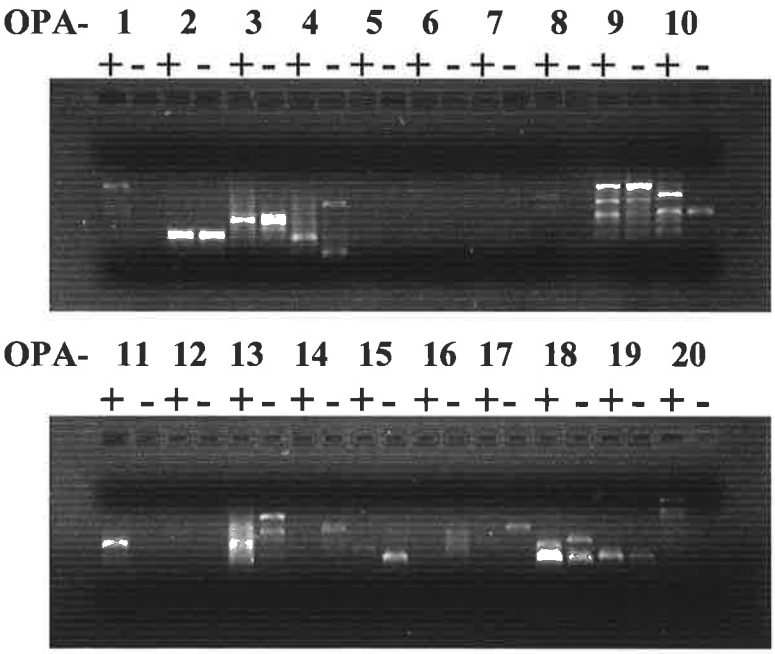

Figure 3.7 Agarose gel showing DD-PCR using the OPA-01 to –20 and T_{11}XA primers with either genomic DNA or no DNA template.

Lanes assigned a '+' contain 1μg DNA template, lanes assigned a '-' do not. OPA primers used in each + and - reaction are indicated above the corresponding lanes and were first shown in Table 3.2. All reactions were cycled as described in section 3.2.4.3. Mispriming of the 10mer primers in some reactions not containing DNA template generated banding artefacts (see reactions using primers OPA-2 to -4, OPA-9 and -10, and OPA-13 to -19).

3.3.4.2 Strategies to improve the specific reamplification of DD-PCR products

To increase the specificity of reamplification, two methods were examined. The first method, hotstart PCR, is expected to be more specific than standard PCR as the *Taq* polymerase used (HotStar, Qiagen) is only activated after a 15-minute incubation at 95°C. This should minimise any non-specific binding of the primers during PCR set-up. However, when HotStar *Taq* polymerase was used with the original cycling conditions modified to include the extra 15-minute incubation at 95°C, it provided no advantage over standard PCR using the DD-PCR 10mer primers (data not shown).

Secondly, a gradient PCR was performed to determine if a higher annealing temperature would increase the specificity of the DD-PCR primers to the template cDNA rather than themselves. Eight different reactions were set up in which the annealing temperatures varied between 42°C and 56°C and reactions either contained 1μL of cDNA template or no cDNA at all. Figure 3.8 shows that the primer extension products were not generated when the temperature was above 48°C, but neither were any template-derived products. Hence, no annealing occurred at the higher annealing temperatures.

An attempt was made to ligate the eluted DD-PCR products directly into the pGEM-T® vector, so that reamplification could proceed with more specific primers rather than the non-specific DD-PCR 10mer primers. The M13 sequencing primers anneal to flanking ends of the MCS in the pGEM-T® vector. Using these primers, a PCR product of 236 bp, corresponding to the MCS of the vector, is observed on agarose gels for clones lacking an insert. Clones containing an insert within the vector produce bands larger than 236 bp. Figure 3.9 shows the resulting agarose gel of the PCR. After an attempted ligation of an eluted band directly into the pGEM-T® vector, only a band corresponding to the MCS of the vector was amplified (lane marked '+', Figure 3.9). This result was seen in all 16 white transformants picked for screening, yet after a control insert (Qiagen) was ligated into the

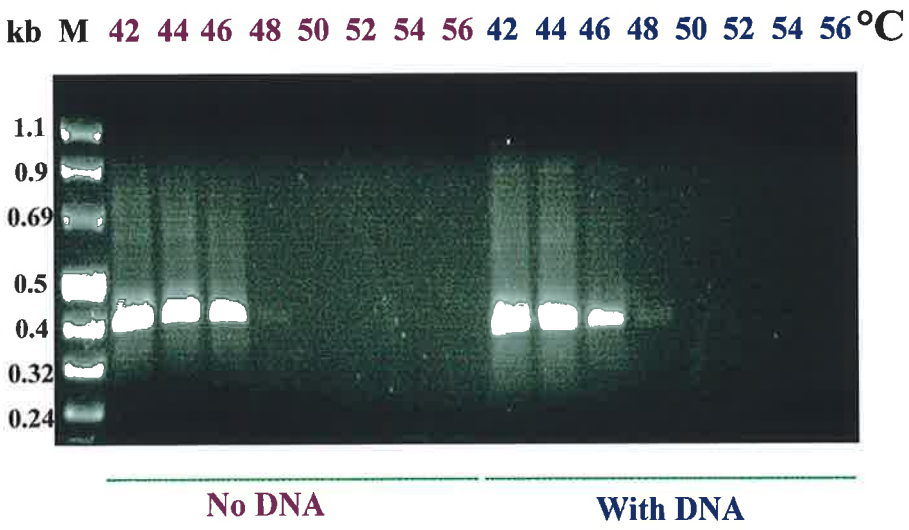

Figure 3.8 Agarose gel showing gradient DD-PCR using the OPA-03 and $(T)_{11}XG$ primers.

Indicated above corresponding lanes are increasing annealing temperatures without added cDNA template, and increasing annealing temperatures of reactions containing 1µL of cDNA. The sizes of Molecular Weight Marker VIII (M) are indicated.

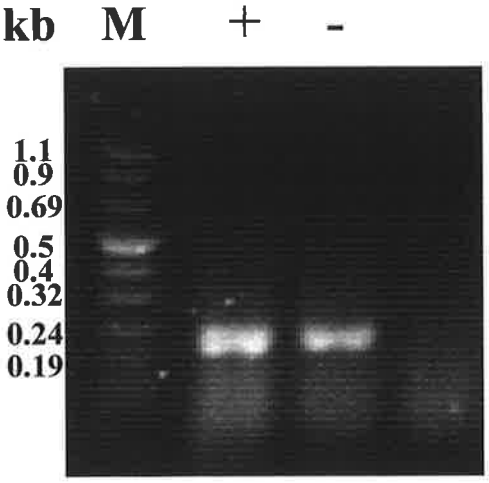

Figure 3.9 Agarose gel showing colony PCR screening of transformants.

DD-PCR products of interest were eluted from the gels (see section 3.2.6), directly ligated without prior reamplification into the pGEM-T® cloning vector and recombinant transformants were screened for by colony-PCR using the M13 primers (see section 3.2.8.2, 3.2.8.3 and 3.2.8.5 for cycling conditions). The lane marked '+' contained the ligation of a DD-PCR product into pGEM-T®. The lane marked '-' contained the vector self-ligation. No products larger than 236 bp, the size of the self-ligated vector, were seen, indicating ligation of the PCR product was not successful. The sizes of the Molecular Weight Marker VIII fragments (M) are indicated.

pGEM-T® vector, the appropriately sized fragment was amplified under the same conditions (data not shown). This demonstrated that the pGEM-T® vector and the cloning technique was effective but suggested that the small amount of DNA eluted from a gel slice was not enough for efficient ligation and transformation.

To try to increase the specificity of PCR amplification while reducing the inefficiency of background transformation, it was postulated that a PCR performed on the direct ligation using one M13 primer and one DD-PCR primer would increase the probability that only vector containing the DD-PCR insert would be amplified. A sequence alignment revealed a string of adenosine bases in the pGEM-T® vector that could anneal to the 3' DD-PCR primers, $(T)_{11}XY$, indicating that when paired with a M13 sequencing primer, these 3' anchored primers could amplify a region in the pGEM-T® vector and not the desired insert. Thus, the appropriate 5' DD-PCR primer had to be used instead. To test if the 5' arbitrary primer, OPA-03, could anneal to sites within the pGEM-T® vector, a PCR was performed on self-ligated vector using OPA-03 with each of the M13 primers. Figure 3.10 demonstrates that PCR products are amplified with both M13/OPA-03 combinations, thus, OPA-03 can anneal to a site(s) within the pGEM-T® vector. Clearly then, a PCR conducted on the DD-PCR product/pGEM-T® ligation could not be done with either the M13 sequencing or the DD-PCR primers.

To ensure the correct DD-PCR products were actually being reamplified during the second round of PCR, two clones of different molecular weight (~150 and 400 bp) were excised from a gel and eluted this time in 100μL of elution buffer instead of water. Two microlitres of the clones were reamplified under the original DD-PCR conditions using [α-^{33}P]-dATP then run in parallel with the original PCR on a polyacrylamide gel, rather than an agarose gel, for better resolution. Figure 3.11 shows the bands of interest are amplified much more in the second round than in the original DD-PCR, however, non-specific,

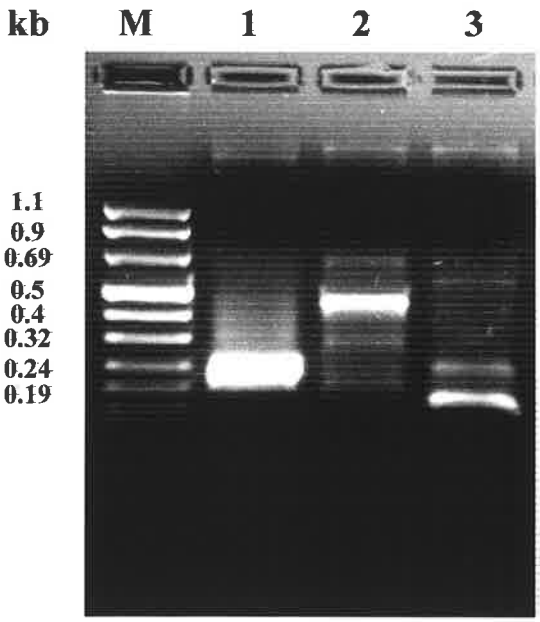

Figure 3.10 Agarose gel showing PCR amplification of pGEM-T® vector using USP and RSP with OPA-03.

Self-ligated p-GEM-T® vector (25ng) was PCR amplified using the M13 primers, USP and RSP (lane 1), USP and OPA-03 (lane 2) and RSP and OPA-03 (lane 3) using the initial DD-PCR cycling conditions (see section 3.2.4.3). Products are seen in all lanes, indicating that OPA-03 anneals to a site within the pGEM-T® vector. The sizes of the Molecular Weight Marker VIII fragments (M) are indicated.

primer-generated bands are also seen. After a second gel elution and third round of PCR to amplify the lower molecular weight band, many of these non-specific products have faded out. Yet, many primer products are still present after a third round of amplifying the higher molecular weight band. Therefore, several rounds of reamplification can not purify higher molecular weight DD-PCR products (≥ 400 bp) for cloning.

3.3.4.3 Specific reamplification of DD-PCR products using priming adapters

In another attempt to specifically reamplify DD-PCR products, two complementary adapter primers were synthesised that may be ligated to the 5' and 3' ends of DD-PCR products. One of the oligonucleotides was a 20mer with a phosphorylated 5' end (designated A20), while the other oligonucleotide was complementary to the 20mer but had a dephosphorylated 5' end and an extra thymine (T) as the 3' ultimate base (designated A21). Both oligonucleotides contained an internal *Sal I* (rare cutter) site for cloning. The strategy for specific reamplification is outlined in Figure 3.12. The two complementary primers were annealed together to form a duplex with a thymine overhang. The duplex can then be ligated to both ends of a DD-PCR transcript containing an adenosine (A) overhang. Self-ligation of the duplex should be inhibited as it is only phosphorylated at one end, at the 5' base opposite the thymine overhang. The ligation products can then be PCR amplified using the 21mer and then cloned into a vector for further analysis.

To determine if the A20/A21 duplex could ligate onto the ends of a DNA insert, a 250 bp PCR product (human BarX2) was provided by Guy Sanders as a positive control insert for the ligation reactions. Ligations using decreasing amounts of both hBarX2 insert and adapter duplex, and decreasing insert:adapter molar ratios of the two, were set up to determine the lowest amount of insert necessary for ligation to occur. Figure 3.13 shows that the initial ligations were successful using 2ng of PCR product with just 160pg of

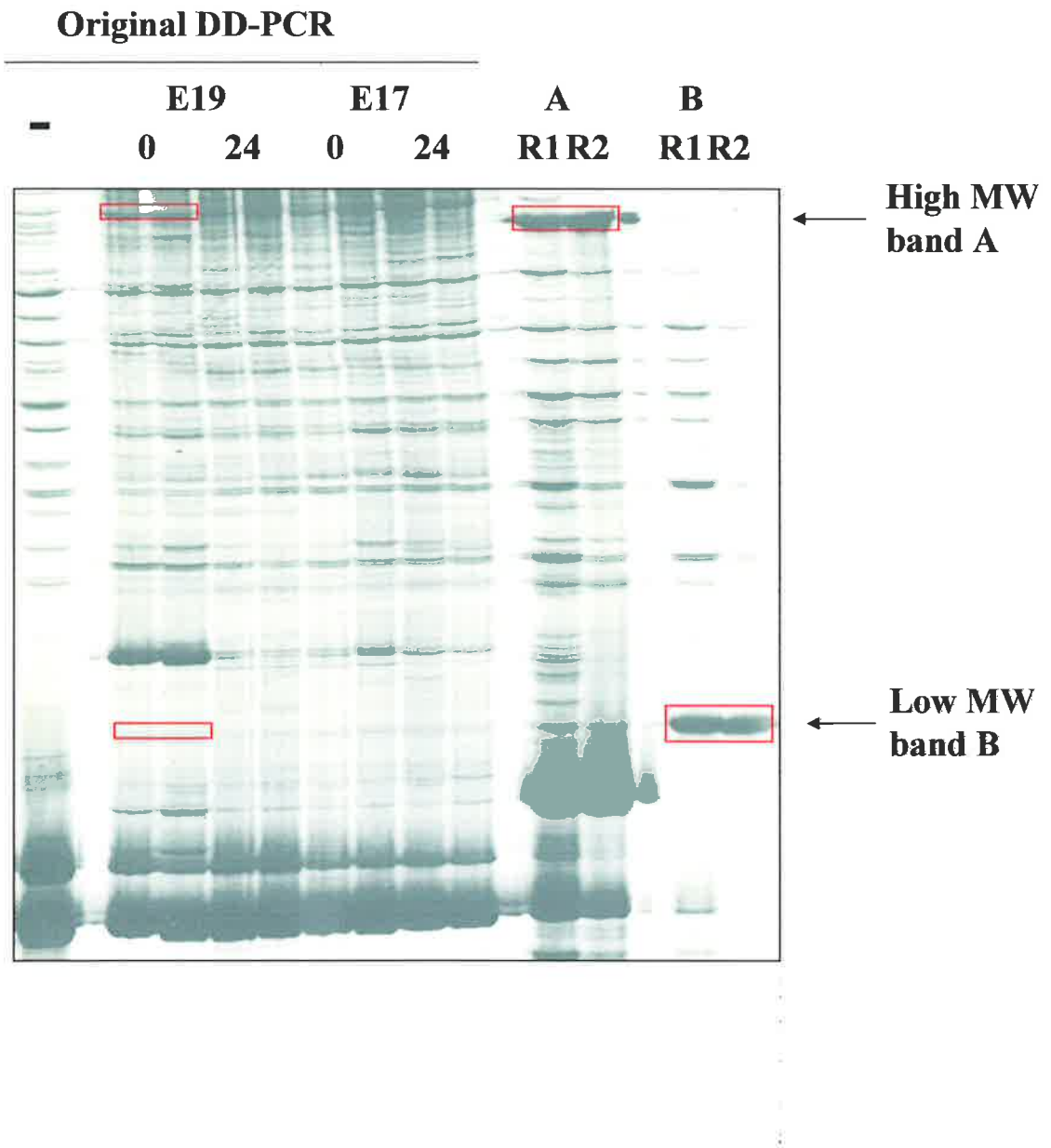

Figure 3.11 Polyacrylamide gel showing DD-PCR products after consecutive gel elution and reamplification.

The high molecular weight product, designated A, and lower molecular weight product, designated B, from the OPA-03 and $(T)_{11}XA$ DD-PCR of wounded E19 skins at t=0 (boxed) were excised, eluted in elution buffer and one fiftieth reamplified using the initial DD-PCR conditions (lanes marked R1, the first reamplification; see section 3.2.6). The resulting bands were then eluted and reamplified again (lanes marked R2, the second reamplification). The negative control reaction (-) did not contain eluted DNA template but a banding pattern was still amplified.

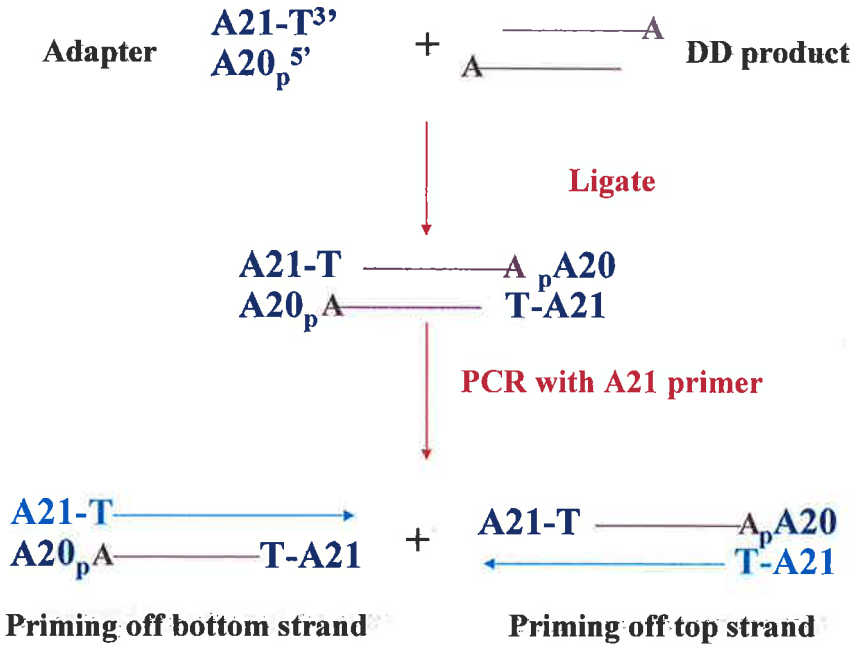

Figure 3.12 Flow diagram outlining specific reamplification of DD-PCR transcripts using priming adapters.

The top strand 21mer was synthesised with a dephosphorylated 5' end while the bottom 20mer oligonucleotide was synthesised then phosphorylated (p) at its 5' end. The primers anneal together to form a duplex with a 3' T-overhang to allow ligation to the 3' A-overhang of a PCR product. The ligated products can then be PCR amplified with the 21-mer, which primes off both strands, as described in section 3.2.7.

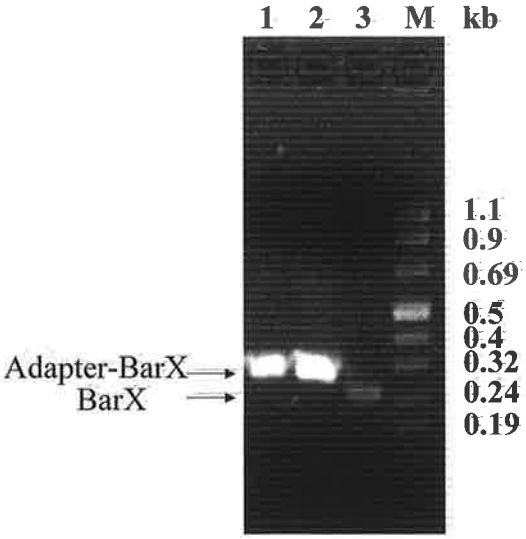

Figure 3.13 Agarose gel showing the PCR screening of human BarX2/adapter ligations.

Ligations of the hBarX2 PCR product to the A20/21 duplex and subsequent PCR using the A21 oligonucleotide were carried out as described in section 3.2.7.2 and 3.2.7.4, respectively. Lanes 1 and 2 contain the PCR amplified ligation reactions (2ng of hBarX2 combined with 160pg and 1.6ng of adapter, respectively, which equates to an insert:adapter molar ratio of 1:1 and 1:10, respectively). Lane 3 contains the purified 250 bp-hBarX2 PCR product only. The sizes of the Molecular Weight Marker VIII fragments (M) are indicated.

adapter duplex (insert:adapter molar ratio of 1:1). Therefore, smaller amounts of the human BarX2 transcript were ligated into the A20/A21 duplex. As demonstrated in Figure 3.14, as little as 2pg of the DNA fragment and 1.6pg of the adapter was required for successful ligation (lane 5). A smeared banding pattern was seen after PCR of the ligation without added BarX2 insert (lane 6), and correspondingly, there appeared to be some non-specific amplification in the PCR when an excess of adapter was added to the BarX2 ligation (insert:adapter molar ratio 1:10, lanes 1 and 3). This experiment indicated that although the adapter itself was capable of undergoing self-ligation and being amplified in the subsequent PCR, it was also capable of enabling the amplification of very small amounts of DNA.

As a result of this, an attempt was made to ligate the adapter duplex onto the ends of a DD-PCR product and amplify it. Two DD-PCR bands, designated 3XGhigh and 3XGlow (estimated sizes 500 bp and 200 bp, respectively) for their respective positions on the DD-PCR display gel, were eluted and precipitated as described in section 3.2.6, resuspended in 10µL of water, then 6µL of each were ligated into A20/A21. As a control for a higher molecular weight PCR product, a ligation was also set up combining the adapter with a 550 bp PCR product (pig collagen III, kindly donated by Nick Hatzriodas) as described in section 3.2.7.2 and 3.2.7.4. The ensuing PCR products were electrophoresed on an agarose gel as shown in Figure 3.15. The 550 bp collagen III product was amplified from both ligations, but non-specific binding was also evident by the presence of smaller molecular weight bands (lanes 5 and 6). The 200 bp and 300 bp bands amplified in the adapter self-ligation reaction (lane 2) were different to the smear of bands between 200 and 300 bp that were amplified in the same reaction in Figure 3.14 (lane 6). However, these two bands amplified in the adapter self-ligation in Figure 3.15 were also seen in the ligations containing the 3XG PCR products (compare lane 2 with lanes 3 and 4). Two products of different sizes were expected to be amplified due to the different sizes of the two 3XG

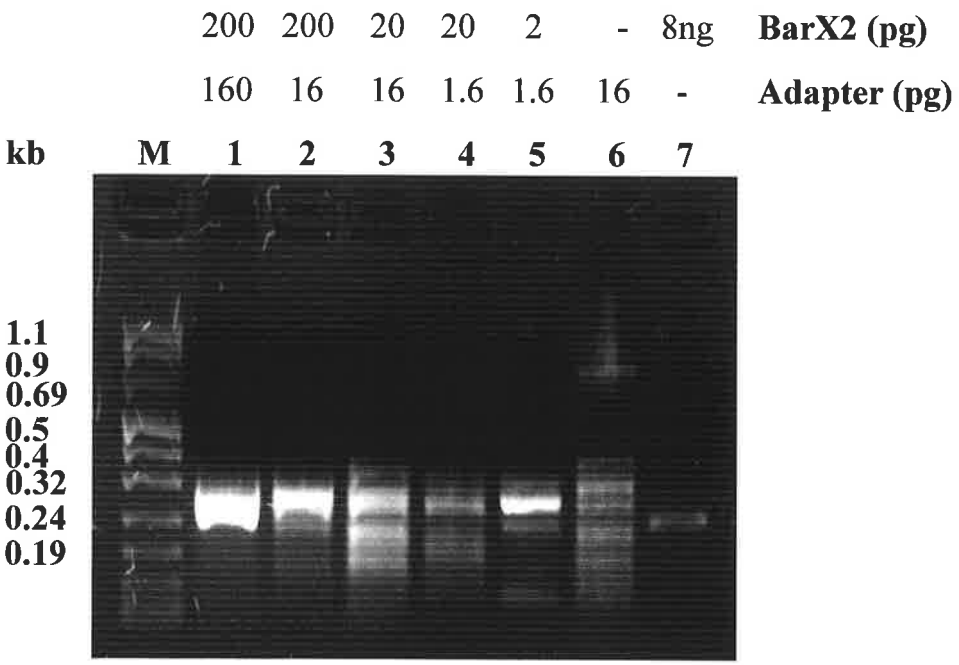

Figure 3.14 Agarose gel showing the PCR screening of ligations using decreasing amounts of human BarX2 and adapter.

Ligations of the hBarX2 PCR product to the A20/21 duplex and subsequent PCR using the A21 oligonucleotide were carried out as described in section 3.2.7.2 and 3.2.7.4. Lanes 1 to 5 contain the ligations of decreasing amounts of BarX2 PCR product with the adapter duplex. Lane 1: 200pg of BarX2 and 160pg of adapter (molar ratio 1:10); lane 2: 200pg BarX2 with 16pg adapter (molar ratio 1:1); lane 3: 20pg of BarX2 with 16pg adapter (molar ratio 1:10); lane 4: 20pg of BarX2 with 1.6pg of adapter (molar ratio 1:1); lane 5: 2pg of BarX2 with 1.6pg of adapter (molar ratio 1:10). Lane 6 is the resultant PCR of a ligation containing 16pg of the A20/A21 adapter only, and lane 7 contains 8ng of the purified 250 bp-hBarX2 PCR fragment only. The sizes of the Molecular weight Marker VIII fragments (M) are indicated.

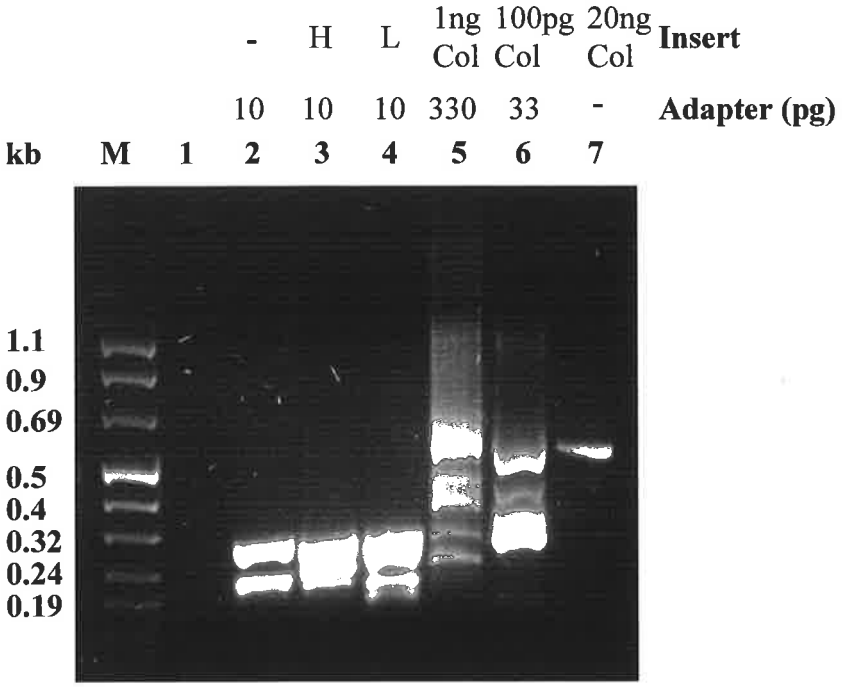

Figure 3.15 Agarose gel showing the PCR screening of DD-PCR product/adapter ligations.

Ligations of the 550 bp pig collagen III DNA fragment, the 3XGhigh DD-PCR product and the 3XGlow DD-PCR product to the A20/21 duplex and subsequent PCR using the A21 oligonucleotide were carried out as described in sections 3.2.7.2, 3.2.7.3 and 3.2.7.4, respectively. Lanes 2 to 6 contain the ligations of the different PCR products with the adapter duplex. Lane 1: PCR negative control (no DNA added); lane 2: PCR of a ligation containing 10pg of A20/A21 adapter only; lane 3: 3XGhigh product with 10pg adapter; lane 4: 3XGlow product with 10pg of adapter; lane 5: 1ng of collagen III with 330pg of adapter (insert:adapter molar ratio of 1:10); lane 6: 100pg of collagen III with 33pg of adapter (molar ratio 1:10). Lane 7 contains 20ng of the purified 550 bp-pig collagen III PCR fragment only. The sizes of the Molecular Weight Marker VIII fragments (M) are indicated.

bands. Failure to detect any specific amplified bands indicated that, as seen with the direct ligation into the pGEM-T® vector, there was insufficient eluted DD-PCR product to ligate with the adapter to prevent it from self-ligating and achieve successful amplification of the DD-PCR inserts.

3.3.5 Modified differential display using longer primers

The possibility that the lack of success in reamplification was due to the high number of low stringency PCR cycles with short 10mer oligonucleotides was investigated by modifying the primers and PCR conditions for DD-PCR based on the RNA arbitrarily primed PCR fingerprinting method (Welsh *et al.*, 1992). The long primers and high annealing temperatures of conventional PCR provide high specificity relative to DD-PCR. To allow for increased stringency, the 5' ends of the original DD-PCR primers were extended by ten nucleotides and a low annealing temperature (40°C) was used only for the first 5 PCR cycles. For the following PCR cycles, the annealing temperature was raised (55°C) so the longer length of the primers (20mers) would allow for more specific replication of products synthesised in the initial cycles.

Typical results of such reactions are shown in Figure 3.16, in which fetal rat skins at the time of wounding and after 24 hours of culture are compared using the 20mer primers. As seen on the display gel, the reactions were repeated with three different RNA samples from each group. The similar results obtained with the different RNA preparations indicate that the process of RNA extraction was not a major source of variability and internal errors between tubes were largely not evident. Another 5' primer, HindIIIOPA-03, was tested and the results were consistent (Figure 3.17). Many bands were produced under the selected PCR conditions with each pair of composite anchor and arbitrary primers. Although each anchor and arbitrary primer has the same 5' end, the banding pattern changed with different

combinations of the primers, which indicates that each pair has its own priming specificity (compare Figures 3.16 and 3.17). The negative control included for each primer combination, which contained no cDNA template in the DD-PCR, did not generate an artefactual banding pattern. This was evidence that the modified primers and cycling conditions provided enhanced specificity.

Figure 3.16 and 3.17 also show that from these two differential display reaction sets alone, a total of 11 candidate products were identified as being differentially expressed in all triplicate RNA samples from the different tissue categories analysed (2VG1-4 and 3VG1-7, see Table 3.6). These were subsequently excised from their gels for further verification. Band 2VG2 was particularly strong, and was specifically and repeatedly seen in the E17 t=24 hour post-wounding samples. Consequently, it was reamplified in a 50μL PCR mixture containing the corresponding HindIII primer pair with 40 high stringency cycles as described in sections 3.2.4.3 and 3.2.6. The reaction was then run on both an acrylamide gel and an agarose gel to check that the corresponding single band had amplified. Both gels showed that the specificity of DD-PCR did improve with the modified method, as only a single 300 bp band was reamplified (see Figure 3.16, lane 'R', band appears smeared presumably due to overloading of the gel, and Figure 3.18, lane 4). Furthermore, no spurious bands were produced in the negative control reaction (Figure 3.16 lane '-' and Figure 3.18 lane 2). This 300 bp band was chosen for further analysis of differential expression as described in Chapter 4 and 5.

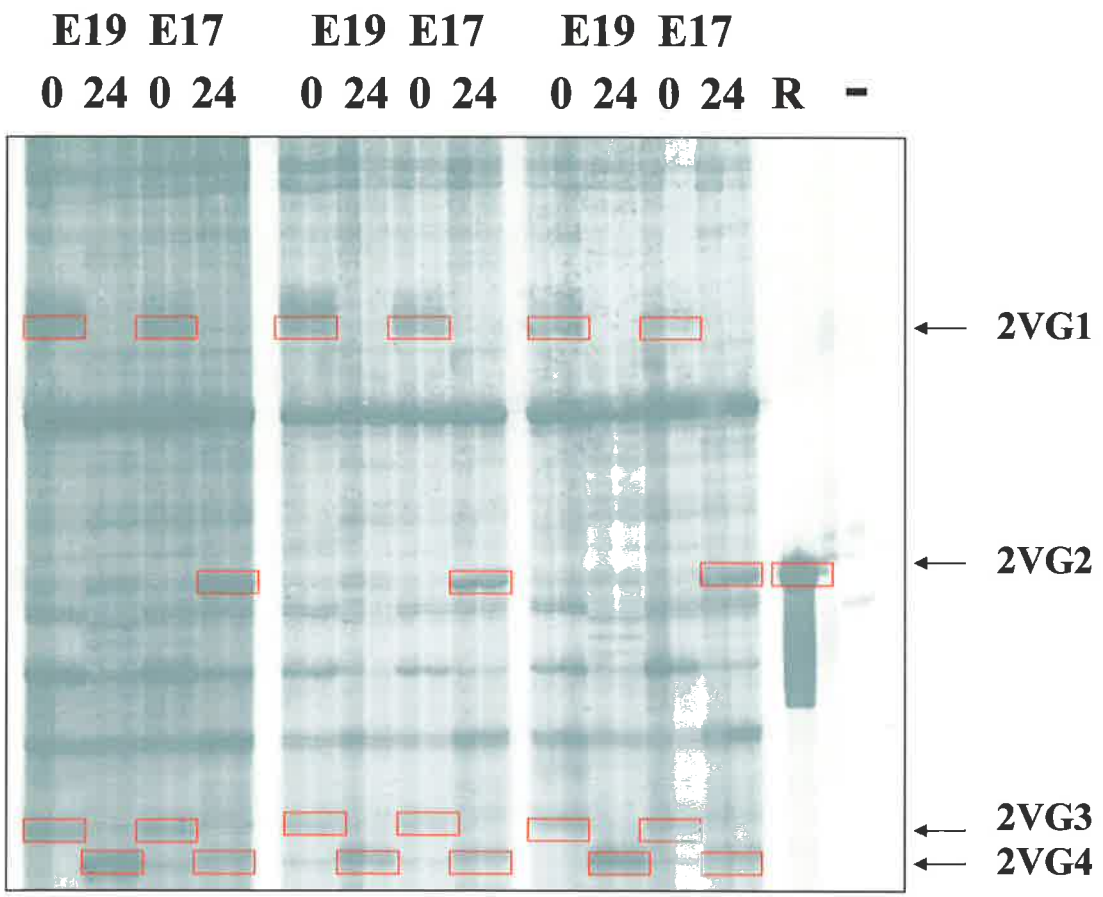

Figure 3.16 Polyacrylamide gel showing DD-PCR using HindIIIOPA-02 and HindIIIT_{11}VG.

Total skin RNA from wounded E17 or E19 fetal rats at t=0 or t=24 hours in culture was reverse transcribed and PCR amplified using *Taq* polymerase (Qiagen) with HindIII$(T)_{11}$VG and HindIIIOPA-02 under high stringency conditions (section 3.2.4.3). Products that appear to be differentially expressed (designated 2VG1-4, according to the primer combination and the relative position of each band on the gel) are boxed and indicated by arrows. The DD-PCR product that was expressed in E17 skin at 24 hours post-wounding and designated 2VG2 was excised, eluted and reamplified as described in section 3.2.6. A product corresponding to the eluted 2VG2 band (300 bp) was amplified (R). The negative control reaction (-) did not contain cDNA template.

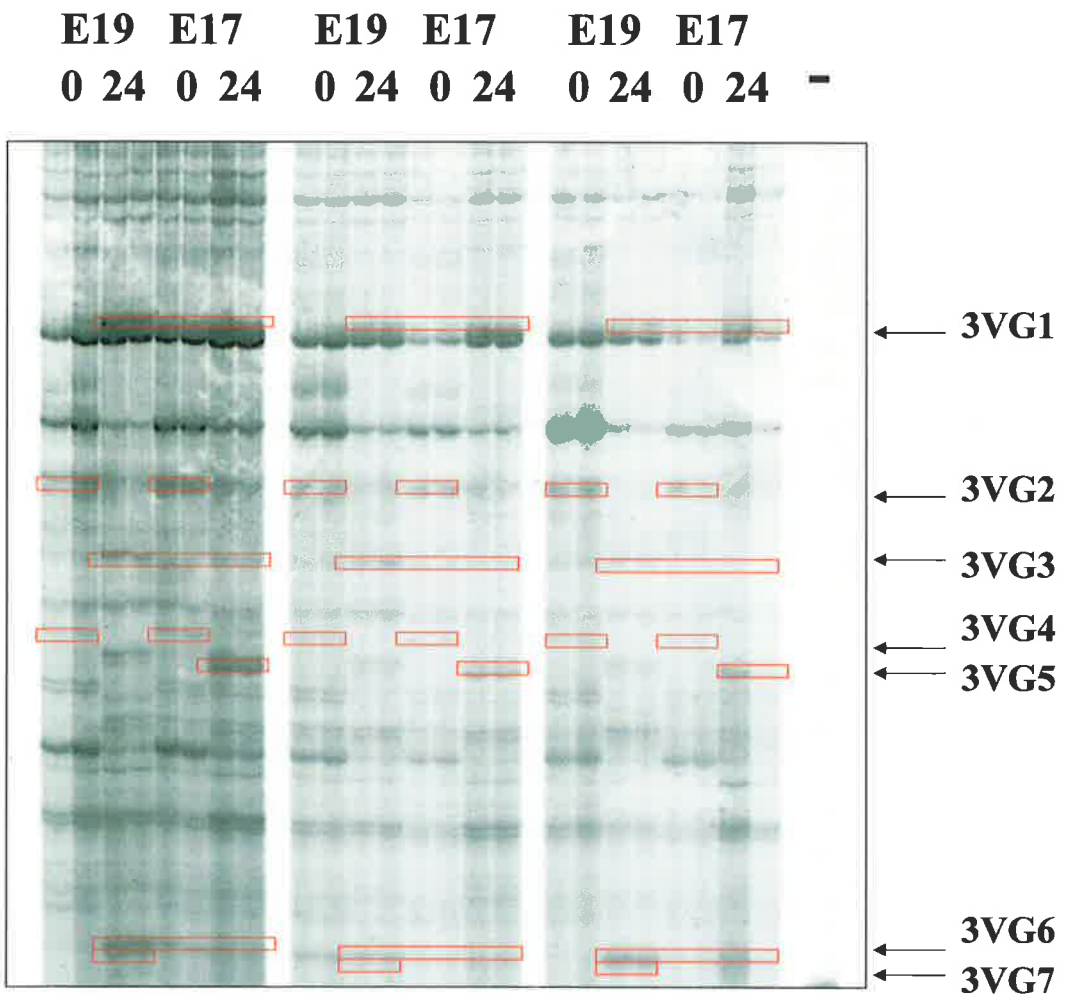

Figure 3.17 Polyacrylamide gel showing DD-PCR using HindIIIOPA-03 and HindIIIT_{11}VG.

Total skin RNA from wounded E17 or E19 fetal rats at t=0 or t=24 hours in culture was reverse transcribed and PCR amplified using *Taq* polymerase (Qiagen) with HindIII$(T)_{11}$VG and HindIIIOPA-03 under the high stringency cycling conditions (section 3.2.4.3). Products that appear to be differentially expressed (3VG1-7) are boxed and indicated by arrows. The negative control reaction (-) did not contain cDNA template.

Table 3.6 Comparative distribution of banding patterns representing categories of differential gene expression.

In each tissue column, "+" indicates a brighter band and "-" a dimmer band on the denaturing gel. A "+" thus means that the gene in question is more strongly expressed compared with conditions where a "-" appears. For instance, 2 transcripts appeared to be upregulated in fetal E17 skin 24 hours post-wounding compared with all 3 other conditions (second line from top).

Banding Patterns	E19 t=0	E19 t=24h	E17 t=0	E17 t=24h	No. of Bands
E19 t=24h upregulated	-	+	-	-	1
E17 t=24h upregulated	-	-	-	+	2
Both t=0 skin upregulated	+	-	+	-	4
Both t=24h skin upregulated	-	+	-	+	1
E19 t=0 downregulated	-	+	+	+	3
Total No. of Candidate Bands					11

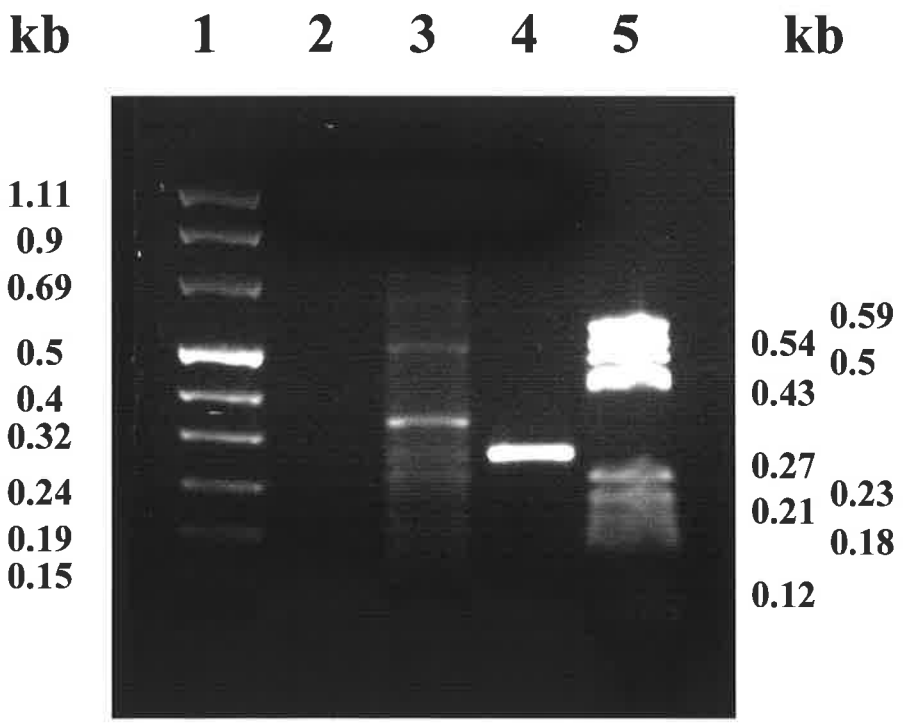

Figure 3.18 Agarose gel showing reamplification of the 2VG2 transcript using HindIIIOPA-02 and HindIIIT_{11}VG.

The 2VG2 product from the HindIII$(T)_{11}$XG and HindIIIOPA-02 DD-PCR of wounded E17 skins at t=24 hours post-wounding (see Figure 3.16) was excised, eluted and reamplified as described in section 3.2.4.3 and 3.2.6 (lane 4). Lane 2 contains the same DD-PCR without added DNA template (negative control). Lane 3 contains the DD-PCR that originally produced the 2VG2 DNA band, using cDNA reverse transcribed from E17 skin RNA as the template. Note that the DD-PCR banding pattern in lane 3 differs to the pattern seen on the polyacrylamide gel in Figure 3.16, due to the greater resolution of PAGE. The sizes of the Molecular Weight Marker VIII and the pBR322 *Hae I* digest (lanes 1 and 5, respectively) are indicated.

3.4 DISCUSSION

The introduction of molecular biology techniques to study wound repair has allowed the cellular events in healing wounds to be more sensitively quantified in relation to traditional techniques. *In situ* hybridisation studies using recombinant DNA probes and quantitative RT-PCR methods enable the mRNA levels of specific proteins, such as growth factors and ECM components, to be measured. Immunohistochemistry using antibodies enables expression of the various encoding proteins to also be qualitatively detected. The relatively novel method of DD-PCR is powerful for identifying genes exhibiting different patterns of expression between experimental samples. These differences may reflect developmental or tissue-specific regulation, may be induced (e.g. drug treatment, dietary or environmental changes) or they may be pre-determined by selection or genetic variation. In this study, the technique of DD-PCR was used to detect differences in gene expression between the processes of fetal E17 and E19 skin wound healing in the rat.

Although DD-PCR appears to be technically easy, the road from "band on a gel" to a positive clone can be difficult. The criticisms it has received include:

- high variability
- high false positive rate
- a questionable ability to identify both abundant and rare mRNAs (Ledakis *et al.*, 1998)
- the coding regions are generally not cloned making gene identification laborious
- much time and large amounts of RNA are required for cDNA verification.

An intensive study by Wan *et al.* (1996) comparing DD-PCR, ES and SH found the biggest disadvantage of DD-PCR to be the time consuming process of verifying a true positive and obtaining its coding region. However, they found many advantages of DD-PCR over ES and SH and listed these to be as followed:

- It requires less RNA and the amplified RNA can be used for verification analyses such as reverse Northern blot, further eliminating the need for large quantities of RNA
- It identifies both abundant and rare mRNAs in a sequence specific manner, as opposed to ES and SH which depend on message abundance
- It simultaneously identifies both upregulated and downregulated mRNA (unlike SH)
- It is relatively inexpensive to set up and execute (unlike ES)
- It provides quick assessment of results with a few gels allowing early re-evaluation of the experimental design
- The false positive rates are equal to or lower than those found with ES or SH
- The candidate genes corresponding to the 3' untranslated regions isolated from most DD-PCR experiments can be identified using DNA or EST databases.

In short, the authors concluded DD-PCR was the superior method for identifying differentially expressed genes. For these reasons, DD-PCR was the technique chosen to identify genes differentially expressed in wounded fetal rat skin.

3.4.1 Establishment of differential display sampling conditions

Since its initial description for screening mRNA differences between related cell populations (Liang and Pardee, 1992), numerous refinements of the DD-PCR protocol have been proposed. For RT in this study, only four 3' degenerate primers were used instead of all 12 possible primers (see Table 3.1). It is probable that the 12 possible 3' primers will recognise one-twelfth of the total mRNA population because there are 12 possible combinations of the last two 3' bases, omitting T as the penultimate base. However, it has been shown that the penultimate base from the 3' end of the $(T)_{11}XY$ primer exhibits considerable degeneracy during priming in the RT step (Liang *et al.*, 1993). Primarily, it is the last base from the 3' end that provides most of the specificity. Therefore, instead of

using all 12 possible 3' DD-PCR primers, only four degenerate primers that differ in the last base were used for RT and DD-PCR. By combining equal amounts of the three primers that differ in the penultimate base from the 3' end, the following primers were obtained: $(T)_{11}XA$, $(T)_{11}XC$, $(T)_{11}XG$ and $(T)_{11}XT$.

After RT and PCR, the DD-PCR products can be separated on agarose gels, denaturing or non-denaturing polyacrylamide gels. Agarose gels do not resolve the banding pattern as well as polyacrylamide gels and the sensitivity of ethidium bromide staining is quite low, so they are rarely used (Sokolov and Prockop, 1994). Non-denaturing gels have been reported to simplify the band complexity (Bauer *et al.*, 1993), but double-stranded DNA, incompletely annealed DNA and heteroduplexes for the same gene may be resolved as different bands on a non-denaturing gel (Liang and Pardee, 1995). For this reason, DD-PCR reactions were separated on denaturing polyacrylamide gels as described in the original protocol (Liang and Pardee, 1992).

In order to detect amplification products after PAGE, silver staining was first used in this study, according to the method of Doss (1996). This technique provides several advantages over the versions of DD-PCR that require the use of radioactive dNTPs for autoradiography, besides those relating to safety issues. Since radiolabelled compounds and X-ray film are not used, it is much less expensive. It is also simpler and faster, with direct detection of amplified fragments on the gel. In turn, the silver-stained bands can be excised directly from the gel and no careful alignment of an autoradiograph with the gel is required. Despite these previously described benefits, the silver staining method was not sensitive enough, nor was the banding pattern resolved enough, to detect transcripts that may be differentially expressed in wounded fetal rat skin.

To increase the sensitivity of detection, radioactive dNTPs were included in the PCR and the banding pattern was visualised by autoradiography. When a ^{32}P label was added to the PCR, the sensitivity increased but band resolution was still quite low. The identification

and isolation of a single cDNA, corresponding to a single differentially expressed gene, is easiest to perform when the bands are sharply defined. Only one band should be cut out of the gel, and not two bands that are similar in size and have not resolved well. The subsequent use of ^{33}P improved the resolution of the banding pattern.

For this investigation, many excisional wounds were made in each E17 and E19 skin biopsy to increase the wound response, and hence increase the chances of detecting differentially expressed genes. Novel immediate-early response genes that are differentially expressed after 30 minutes post-wounding were sought after first. However, culturing for just 30 minutes gave inconsistent patterns between related samples. Because the fetuses were on ice for different lengths of time after being removed from the uterus and prior to dissection, this might have impacted on their response to wounding. Alternatively, the weight of the rat fetuses, which correlates with stage of development, might have been slightly different, although care was taken to include weight-matched fetuses. A comparison of unwounded and wounded E17 and E19 skins fixed at 24 hours post-wounding was, therefore, expected to yield more consistent differences in expression, because by this time point E17 wounds are closing while E19 wounds remain open. Although differences in the expression profiles of E17 and E19 skin were seen that were presumed to be development-related, no major differences in gene expression were reproducibly detected between the respective unwounded and wounded skin samples. It was postulated that unwounded and wounded skins taken from a given aged fetus and cultured using the aforementioned model were too similar, as both samples being compared were dissected from the back of the rat fetuses and hence wounded to some extent. It was thought DD-PCR was not sensitive enough to detect the small differences in expression between the explant harbouring multiple excisional wounds and the explant that was left unwounded. Therefore, E17 skins wounded with several excisions fixed at the time of wounding and after 24 hours of culture were compared with wounded E19 skins at these time points.

When comparing these skin types, DD-PCR was expected to detect genes expressed in fetal rat skin to support normal housekeeping functions and embryonic development as well as tissue repair. The fraction of expressed genes corresponding to each of these categories should be different. Comparing the closely related mRNA combinations from E17 and E19 skin samples led to display gels with overall similar banding patterns. The mRNA species governing housekeeping type functions produced identical banding across the different samples analysed and these accounted for the majority of expressed genes. The differences seen in banding pattern between samples corresponded to the differences in gene expression. It was predicted that in addition to the expression of different genes in response to wounding, developmental events between the E17 and E19 fetus would also require a substantial subset of transcripts. Although an exhaustive screen of DD-PCR profiles was not conducted in this study, only one band was identified as being specific to E17 skin, indicative of a developmental difference (see Table 3.5). The other 62 differentially expressed bands identified were specific to the E17 and E19 tissues either at the time of wounding or after 24 hours of culture, and hence were all thought to be related to wounding (see Tables 3.5 and 3.6). Within this group, those DNA bands seen only in E17 skin at 24 hours post-wounding (or in all categories except this) were the transcripts of interest that were possibly related to the transition from scar-free to scar-forming wound repair. As described in Chapter 2, all skins were transferred to tissue culture for 24 hours upon wounding. Although E19 wounds do not heal at all using this model, the particular procedures described here were followed to support previous work by others who demonstrated the scar-free and scar-forming phenotypes after sufficient elapsed time in E17 and E19 fetal rat skin, respectively (Houghton *et al.*, 1995; Ihara *et al.*, 1990; Ihara and Motobayashi, 1992; Soo *et al.*, 2000).

3.4.2 Modifications of differential display

Differential display gels are renowned for their potential variability and uncertainty in interpretation. The procedural and experimental controls used in this study are emphasised to ensure that the observed alterations in gene expression have a high probability of representing true differences. This optimisation process was considered important as irreproducible display patterns can result in the isolation of false positive cDNA. Numerous experiments were also performed to achieve successful reamplification and cloning of DD-PCR products. Firstly, elution and purification protocols were modified to increase the amount of DNA recovered from gels. Secondly, different PCR and ligation conditions were tested to increase the specificity of reamplification. Finally, successful reamplification and cloning was only achieved after the original differential display primers were extended by 10 nucleotides and the cycling conditions were modified to increase the specificity of the PCR. The following discussion aims to demonstrate the importance of quality control for all parameters of DD-PCR and to highlight the difficulties inherent to DD-PCR that can be avoided when using the modified method.

In this analysis, the RT and PCR steps for all DD-PCR experiments used identical amounts of input RNA (1μg) and cDNA (1μL), respectively, to minimise spurious variations in band intensity. Furthermore, a total of 4 specimen groups (E17 t=0, E17 t=24h post-wounding, E19 t=0, E19 t=24h post-wounding) were compared, each divided into 3 sets of RNA samples. Three skins were pooled per RNA extraction to minimise sample variation. The extracted RNA samples were reverse transcribed and PCR amplified in duplicate, then electrophoresed in parallel lanes to avoid random errors. Efforts were also made to keep the level of genomic DNA contamination as low as possible to prevent false positive signals, as has been well documented in the past (Zhao *et al.*, 1995). A comparison of the overall pattern generated by DD-PCR illustrated the high reproducibility of the technique in this project. Only the bands differentially expressed in all 3 replicates were

selected for cloning and further analysis. The fact that such candidate bands were observed in all 3 replicates further suggested that the experiment was reproducible and that the clones identified are specifically upregulated or downregulated in the fetal wound healing process. Results like this demonstrated that DD-PCR could be successfully applied to identify genes differentially expressed in response to wounding.

When using the original DD-PCR protocol, artefact bands were amplified in negative control reactions that did not contain cDNA template. Other users of DD-PCR have reported similar observations of PCR products generated from non-reverse transcribed RNA (Mou *et al.*, 1994; Zhao *et al.*, 1995). One study has shown that the non-reproducible bands are not likely to be due to contaminating DNA as amplification using β-actin specific primers, in the absence of RT, did not result in the detection of a β-actin product (Mou *et al.*, 1994). Furthermore, in Welsh *et al.* (1992), the addition of denatured genomic DNA to the DD-PCR reaction almost completely abolished the RNA-dependent pattern and resulted in a largely uniform background smear, presumably due to promiscuous priming under the low stringency conditions used. In short, this banding artefact was found to be a common phenomenon in negative controls of DD-PCR. It was indicated by control experiments in this study to be the result of the non-specific self-priming and amplification of the arbitrary 10mers under the low annealing conditions of DD-PCR. These spurious bands hindered the reamplification of DD-PCR products after gel elution. Reamplification is necessary for further analysis of the bands, as the yield of DNA eluted from a single band is quite low. In this study, the low amount of DNA eluted from the gel was not enough to compete with the self-priming of the 10mer primers during reamplification.

Other researchers have also reported poor recovery of DD-PCR products from gels (Bhattacharjee *et al.*, 1997). Traditionally, a differentially expressed band is excised from the denaturing gel and the DNA is eluted from the gel slice in water then alcohol precipitated before reamplification (Liang *et al.*, 1993). However, Sanguinetti *et al.* (1994)

found that the recovery of bands from polyacrylamide gels could not be achieved in water but required the use of an elution buffer. Frost and Guggenheim (1999) followed this up to show that elution of excised gel slices in water adversely affected the ability of the eluted DNA to act as a template for PCR reamplification due to depurination. In contrast, when eluted in a solvent designed to minimise depurination, the same DNA fragment was reamplified in high yield. Since no bands were recovered in the initial experiments by eluting in water, elution of DNA from gel slices was done in an elution buffer (see section 3.2.6), but this was still not effective in enabling reamplification.

Previous studies have indicated that the urea in denaturing gels is a strong inhibitor of PCR (Konecny and Redinbaugh, 1997). Although fixing polyacrylamide gels should prevent urea contamination of the gel eluate, it was thought that further purification might increase the concentration of candidate DNA bands and minimise the primer artefacts seen after reamplification. Phenol/chloroform extraction before ethanol precipitation of the eluted DNA did not encourage specific amplification of the DNA of interest, as the yield of DNA recovered from the gel was further reduced. Elimination of the precipitation step and direct amplification of eluted DNA has previously been possible using gene specific primers at urea concentrations less than 0.35M (Raju *et al.*, 1995). This bypasses the problem of poor DNA recovery that is associated with precipitation and possible contamination due to handling. When using non-specific DD-PCR primers to reamplify the eluted transcripts, however, inadequate amounts of reamplified products were obtained under the conditions described here. It was thought that the urea concentration may still be too high and hence inhibitory to the second PCR, yet even when it was estimated that the concentration of urea was diluted to approximately 0.014M, the eluted templates did not reamplify and the primer self-extension products were still seen. This contrasts with the work of Bhattacharjee *et al.* (1997), who successfully reamplified several DD-PCR templates at urea concentrations as

high as 0.07M, and suggests that the reamplification efficiencies of DD-PCR products are template-dependent so each reamplification needs to be optimised for urea.

To increase the specificity of DD-PCR using the DD-PCR 10mer primers, the two different methods of hotstart PCR and gradient PCR were tested. Hotstart PCR, which was expected to minimise the amplification of non-specific products, proved to have no advantage over standard PCR using the DD-PCR 10mers. Gradient PCR was performed to determine if a higher annealing temperature would increase the specificity of the DD-PCR primers to the template cDNA rather than themselves. Others have previously reported that raising the annealing temperature from 40°C to 48°C can eliminate the contaminating background, thus resulting in the specific reamplification of a distinct cDNA product (Gery and Lavi, 1997). In this study the primers could not anneal at the higher temperatures needed to reduce background, so the DNA of interest could not be specifically reamplified.

To ensure the correct DD-PCR products were actually being reamplified during the second round of PCR, two DD-PCR products of different molecular weight were reamplified and run in parallel with the original PCR on a polyacrylamide gel, rather than an agarose gel, for better resolution. Although the bands of interest were amplified in the second round of DD-PCR, many non-specific bands were also seen as before. A second gel elution and third round of PCR resulted in an increased yield of the lower molecular weight band and most of the non-specific products did not reamplify. In contrast, after a third round of PCR to amplify the higher molecular weight band, many primer-derived products were still present. Higher molecular weight bands do not elute out of gels as readily as lower molecular weight bands, meaning the recovery of DNA may be decreased. Additionally, the higher molecular weight bands may not amplify as efficiently due to their length and hence the increased likelihood of depurination during elution from the gel. Nevertheless, this result suggested it might be possible to clone low molecular weight bands that are purified after several rounds of gel elution and reamplification.

Reeves *et al.* (1995) reported similar problems when trying to reamplify gel-purified cDNA. Like the current study, the authors made particular reference to the poor yields of reamplified DNA and the generation of non-specific amplification products due to the use of short arbitrary primers and high PCR cycle numbers. They described a novel technique, ligation linked PCR, whereby cDNA extracted from a DD-PCR gel was first transiently ligated into a TA cloning vector and then directly PCR-amplified using a poly (dT) primer and a T7 promoter primer that anneals to the MCS of the vector. They demonstrated that transient ligation into the TA vector and the use of specific primers for PCR resulted in increased yield of the cDNA of interest. When this was attempted in the current study, the small amount of DNA eluted from a gel slice, by all of the different methods tested above, was not sufficient for ligation before reamplification. Furthermore, a similar ligation to small oligonucleotide adapters, synthesised to specifically reamplify the cDNA of interest, was not successful due to low yields after elution.

Since the inception of DD-PCR, numerous efforts have been made to improve primer design in order to enhance the sampling of differentially expressed genes and to allow the isolation of more relevant genes (Graf *et al.*, 1997; Rohrwild *et al.*, 1995). After failing to successfully reamplify any candidate genes using the original protocol, the PCR conditions were modified and longer primers were used instead of the 10mers to increase the specificity and reproducibility of the method. It was postulated that when 20mers are used, a low annealing temperature of 40°C is required only in the first few cycles to achieve arbitrary priming. Under these conditions, the primers behave in a similar way to the short 10mers of the original protocol, priming synthesis of sequences that are complementary to their 3' ends and allowing minor mispairing with the cDNA template. The resulting products of this first step have the primer sequences introduced at both ends so subsequent high stringency PCR cycles (55°C – 65°C for annealing) favour perfect matches with the longer primers.

Such a strategy was first described by Welsh *et al.* (1992), who used just one arbitrary 20mer in both RT and the two-step PCR that was consequently termed Arbitrarily Primed PCR. The method has since been modified to include a longer (T-rich)-3'-primer for the first strand cDNA synthesis that is then coupled with the longer arbitrary primer for PCR. Authors using this modified method have reported significant improvements in DD-PCR reproducibility, specificity and sensitivity, as well as subsequent band reamplification and sequencing (Linskens *et al.*, 1995; Zhao *et al.*, 1995).

The use of long sequence-specific primers, originally designed for RT-PCR analysis of various genes, as a 5' arbitrary primer in DD-PCR has also been published (Jurecic *et al.*, 1996). Alignment of the nucleotide sequences of these long primers and the resulting DD-PCR clones showed that 8-10 nucleotides at the 3' end of the primer were perfectly matched, whereas the 5' end showed a high degree of degeneracy with 6-8 mismatches. The authors found that amplification with the long, sequence-specific primers targeted genes arbitrarily in their study, but they did not rule out the possibility that such primers carrying common sequence motifs may target particular classes or families of genes when used for DD-PCR.

The inclusion of restriction sites or other modifications such as biotinylated primers could also be useful later in cloning and sequencing. The presence of a *HindIII* restriction site at the 5' end of the primer sequences designed in this thesis was to facilitate cloning of the DD-PCR products. Brenz Verca *et al.* (1998) lengthened DD-PCR primers by adding about half of the T7 and half of the Sp6 RNA polymerase promoter onto the 5' terminus of the traditional oligo-dT primer and arbitrary primer, respectively. They also designed universal reamplification primers that harbour the complete cognate promoter sequences to prime within these constant regions so that the reamplified cDNA contained functional polymerase promoters. This in turn allowed direct generation of sense and antisense

riboprobes for hybridisation analysis and direct sequencing of the reamplified cDNA without prior cloning.

Inspired by these improvements, the primer strategy developed here aimed to facilitate reamplification, analysis and cloning of the cDNA fragments. Differential gene expression in the wounded skin of the E17 and E19 fetus was demonstrated using the longer arbitrary primers, HindIIIOPA-2 and HindIIIOPA-3. Comparison of the overall band patterns illustrates the high reproducibility of the DD-PCR results in the particular groups. Using a particular primer combination, the higher annealing temperature also reduced the number of PCR products seen per lane to about 100. These are representative of expressed genes in normal and wounded tissues. It has been claimed that DD-PCR has the potential to visualise almost all expressed genes in a cell by using multiple primer pair combinations (Bauer *et al.*, 1993). The main factor limiting the number of detectable expressed genes in this study was the small number of primer combinations used, which was only two in the final protocol. Nevertheless, it is unlikely that the entire mRNA population can be screened by DD-PCR, as such a calculation is based on the assumption that individual bands equate to individual genes and estimates of the number of genes screened are derived by multiplying the number of bands per display gel by the number of gels (Ledakis *et al.*, 1998). Furthermore, some bands that appear to be single bands on a display gel may actually contain many different transcripts of the same size, or on the other hand, two or more bands that are different sizes may be different lengths of the same gene.

Using the two longer arbitrary primers, 13 transcripts showed reproducible differential expression patterns among the different developmental stages and culture conditions in this study. These were designated 2VG1-4 and 3VG1-7, after the primer combination used for each DD-PCR. The utilisation of long primers and a higher annealing temperature in the optimised protocol significantly improved not just the reproducibility and sensitivity of DD-PCR in this study, but also facilitated the specific reamplification and isolation of candidate

differentially expressed bands. To demonstrate this, one band, 2VG2, was chosen for further analysis. Reamplification of this band revealed a single DNA transcript of the expected size. These minor modifications made the method more powerful, reliable and practical.

In summary, physiological research suggests that early fetal wounds contain intrinsic factors that provide the organism with a mechanism for scar-free healing (Longaker *et al.*, 1994a; Lorenz *et al.*, 1992; Morykwas *et al.*, 1991b). The results shown here are consistent with this hypothesis, given that an altered pattern of gene expression was detected in healing E17 skin 24 hours post-wounding compared to E17 skin at the time of wounding and non-healing E19 skin. The following chapter describes the isolation, sequencing and identification of the 2VG2 gene that is differentially upregulated in healing E17 skin 24 hours post-wounding.

Chapter Four

Identification of the Differentially Expressed Gene in Fetal Wounds and its Predicted Protein Product

4 Identification of the Differentially Expressed Gene in Fetal Wounds and its Predicted Protein Product

4.1 INTRODUCTION

To better understand the molecular control of fetal wound healing, differential display (DD) was used to identify new genes that may be up or down regulated during repair. Martin *et al.* (1998) recently described the DD technique as being essentially bipartite, consisting of

i) RT-PCR and electrophoresis, and

ii) Gene identification and verification

During DD-PCR, mRNA species present in one sample but not the other, or present at different levels, should generate bands that vary in intensity between the samples. These bands represent gene sequences that are only putative candidates for differential expression, as the inherent vagaries of DD-PCR give a fairly high rate of false positives. The previous chapter describes how improved primers and PCR conditions were employed to reduce the likelihood of selecting false positive transcripts and facilitate the specific reamplification of candidate bands. However, as Martin *et al.* (1998) suggested, DD-PCR products must be screened to verify that expression differences do indeed exist.

Northern blot analysis, using the reamplified cDNA as a probe, is the standard procedure for confirming that a cDNA band differentially expressed on a display gel does represent a true difference. A common experience is to either obtain no signal, owing to the low abundance of the gene, or to find a false positive due to the presence of more than one cDNA species in the single gel band. Most DD-PCR products obtained after purification from the polyacrylamide gel and reamplification contain a significant proportion of contaminating DNA sequences, even after gel purification of the reamplified product. The

major sources of contamination include DNA present in the total RNA used for cDNA synthesis, undetectable bands present alongside candidate bands in display gels, and accidental co-purification of neighbouring bands. The levels of non-specific cDNA can be further increased during reamplification, and in some cases these co-migrating species may even amplify with greater efficiency than the cDNA of interest. This phenomenon clearly precludes the direct use of the reamplified product as a probe for either Northern blot analysis or for the screening of libraries to obtain the full-length sequence.

Another problem inherent to DD-PCR analysis is the nature of the amplified cDNA fragments. Differentially expressed bands typically range from about 100 bp to 500 bp in length. Usually this DNA is in the 3' untranslated region (UTR), giving no sequence information about the nature of the respective protein. Traditionally, the full-length transcript is obtained from cDNA libraries by hybridisation with radioisotope-labelled probes. This is a relatively labour intensive and tedious procedure. In addition, the cDNA is rarely full-length (Wang *et al.*, 1997). Rapid amplification of cDNA ends (RACE), on the other hand, is a PCR-based technique used to facilitate the cloning of full-length 5' and 3' cDNA ends after the partial cDNA sequence has been obtained by other methods. Using RACE, it is possible to obtain the full-length cDNA relatively quickly without constructing and screening cDNA libraries.

In this project, DD-PCR was performed on RNA isolated from embryonic day 17 (E17) and E19 wounded skins at the time of wounding (t=0) and at 24 hours after injury (t=24h). One 300 nucleotide (nt) fragment, designated 2VG2, showed specific upregulation in E17 fetal rat skin 24 hours post-wounding by DD-PCR (see Chapter 3). The current chapter describes how the steps of gene identification and verification were improved by applying previously published techniques in a novel manner. In summary, the aims of the work described in this chapter were:

i) To use dot blot hybridisation to isolate the correct 300 bp 2VG2 cDNA from the different transcripts that may have reamplified from the DD-PCR gel slice and confirm its differential expression in wounded E17 skin;

ii) To determine the correct size of the 2VG2 transcript and its time of induction in cultured E17 skin after wounding by using Northern blot analysis; and

iii) To identify the sequence of the full size 2VG2 cDNA using 5' RACE.

By predicting the sequence of the corresponding 2VG2 protein, it may be possible to draw conclusions as to the role of the 2VG2 gene product in fetal rat skin.

4.2 MATERIALS AND METHODS

4.2.1 Molecular reagents

Unless otherwise stated, the general laboratory chemicals and molecular reagents used were the same as those described in Chapter 3. Additionally, restriction endonucleases such as *HindIII* were obtained from GeneWorks Ltd. (Adelaide, SA, Australia) and Promega (Sydney, NSW, Australia) and ELONGASE™ Enzyme Mix was purchased from Gibco BRL Life Technologies Inc. (Grand Island, NY, USA). HyBond™-N nylon hybridisation transfer membrane and Sephadex G50 spin columns were purchased from Amersham Pharmacia Biotech (Castle Hill, NSW, Australia) and ULTRAhyb™ Ultrasensitive Hybridisation Buffer was obtained from Ambion, Inc. (Austin, TX, USA). Kits used in this chapter included the Strip-EZ™ DNA kit (Ambion, Inc.), the Plasmid Mini kit (Qiagen, Clifton Hill, VIC., Australia), the ThermoSequenase Radiolabelled Terminator Cycle Sequencing kit (Amersham Pharmacia Biotech), the 5' RACE System Version 2.0 and 3' RACE System for rapid amplification of cDNA ends and the Concert™ Rapid Gel Extraction system (Gibco BRL Life Technologies).

4.2.2 Oligonucleotides

The RT-PCR primers were designed to hybridise to the 2VG2 DD-PCR clone just inside of the anchor primer site at each end (see Table 4.1). The 5' and 3' RACE gene specific primers were designed to hybridise to either the original 300 bp DD product, 2VG2, or to sequences arising from RACE reactions that extended this clone (see Tables 4.2 and 4.3, respectively). All primers were analysed for the absence of any obvious hairpin structures and stable primer-dimers using the Oligo 4.0 software package (National Biosciences, Inc., Plymouth, MN, USA) and then synthesised by Gibco BRL Life

Technologies. The Abridged Anchor Primer (AAP), Abridged Universal Amplification Primer (AUAP) and the Adapter Primer (AP) were purchased as part of the 5' RACE System Version 2.0 and 3' RACE System kits.

4.2.3 Retrieval and cloning of the 300 bp 2VG2 differential display product

The DNA band designated 2VG2, which successfully reamplified after purification from the DD-PCR gel (see Figure 3.18), was purified using the BresaSpin® purification kit according to the manufacturer's instructions. The purified 2VG2 insert was ligated into the pGEM-T® cloning vector and colony PCR was employed to screen for insert-containing transformants as described in section 3.2.8.

4.2.4 Dot blot hybridisation

Dot blot hybridisation was the method used to eliminate false positive DNA sequences from the purified DD-PCR bands, so that only clones corresponding to the regulated genes identified by differential display were selected. Sixteen clones were analysed from the 2VG2 / pGEM-T® ligation. Three microlitres of each colony PCR was mixed with 3µL 0.4M NaOH, incubated at 37°C for 15 minutes and placed on ice. Hybridisation arrays were prepared by spotting duplicate HyBond™-N nylon membranes with 2µL of each denatured colony PCR fragment in a 1cm x 1cm grid format. The DNA was cross-linked at 125mJ in a GS Gene Linker™ UV Chamber (program C-L, Bio-Rad, Richmond, CA, USA).

Membrane arrays were dipped in milliQ water, then 5 x standard saline citrate (SSC) for 5 minutes (Sambrook *et al.*, 1989). Membranes were incubated for 2 – 4 hours in roller bottles containing 10mL of prehybridisation solution (5 x SSC / 5 x Denhardt's / 0.5% sodium dodecyl sulphate (SDS)) per 100cm^2 of membrane at 42°C in a rotating hybridisation oven (Ratek Instruments, Boronia, VIC., Australia). Replicate arrays were

hybridised in parallel with ^{32}P-labelled differential display reactions using template RNA from either the E19 or E17 wounded t=24h skin specimens (see section 4.2.5). Briefly, the purified radioactive PCR products were heat-denatured at 100°C for 5 minutes and quickly snap-cooled on ice. Each denatured probe was then added to the prehybridisation solution. The nylon membranes were incubated in the resulting hybridisation buffers at 42°C overnight. After hybridisation, the membranes were washed twice for 15 minutes in 100mL of 2 x SSC / 0.1% SDS at room temperature. For more stringent conditions, the membranes were washed twice more for 20 minutes at 42°C in 0.5 x SSC / 0.1% SDS, then for 20 minutes in 0.1 x SSC / 0.1% SDS first at 42°C then at 65°C. Blots were exposed to X-ray XOMAT AR film overnight at -70°C with an intensifying screen.

4.2.5 Synthesis of DD-PCR probe

^{32}P-labelled DD-PCR probes for dot blot were prepared using the HindIIIOPA-2 and HindIII$(T)_{11}$VG primers that were used in the original DD-PCR that gave rise to the DNA band of interest, 2VG2. The reverse transcription reactions from E19 and E17 wounded t=24h skin specimens were used as templates for the synthesis of each probe. Differential display reactions were set up essentially as described in section 3.2.4.3 except 20μCi [α-^{32}P]-dATP (3000Ci/mmol) was used instead of 4μCi [α-^{33}P]-dATP.

One microlitre of each DD-PCR probe was added to 3mL of scintillation fluid for counting before purification and the remainder was purified using the BresaSpin® kit according to the manufacturer's instructions. The purified probes were solubilised in 50μL of TE (10mM Tris, 1mM EDTA, pH 8). One microlitre of each probe was added to 3mL of scintillation fluid for counting after purification, while the remainder was stored at -20°C until required for dot blot hybridisation. The scintillation vials containing unpurified and purified probes were counted on a 1900TR Liquid Scintillation Analyzer (Canberra-Packard

Pty. Ltd., Mount Waverly, VIC., Australia), set for 1 minute of ^{32}P, in order to determine the percentage incorporation of ^{32}P into each probe and to ensure that the radioactive counts of the E19 and E17 probes were comparable.

4.2.6 Rapid small scale preparation of DNA (Miniprep)

Plasmid DNA was prepared for both DNA sequencing and labelled DNA probe generation (section 4.2.7 and 4.2.10). Briefly, 3mL of LB broth (1% bactotryptone / 0.5% bacto yeast extract / 1% NaCl (w/v) pH 7) containing ampicillin (100µg/mL) was inoculated with a single transformant colony and incubated at 37°C overnight with agitation. Cell cultures were transferred to 1.5mL tubes and centrifuged at 13000*g* on a microfuge for 30 seconds. Plasmid DNA was then prepared from bacterial pellets using the Plasmid Mini kit following the manufacturer's protocol and resuspended in 10µL of TE. Insert sizes were confirmed either by digestion with *HindIII* restriction endonuclease or PCR using M13 primers (see Table 3.4) and electrophoresis on a 1.5% agarose gel. Miniprep DNA was stored at -20°C until required.

4.2.7 2VG2 gene identification

DNA sequencing was performed first on 2VG2 clones that were confirmed to be differentially expressed in E17 wounds by dot blot analysis (see section 4.2.4), and later on RACE products to identify the full-length of the gene represented by 2VG2 (see sections 4.2.12 and 4.2.13). DNA sequencing was carried out by the dideoxynucleotide chain termination method using the ThermoSequenase Radiolabelled Terminator Cycle Sequencing kit, according to the manufacturer's instructions. All clones were sequenced bidirectionally using the M13 forward and reverse primers. Complete sequence contigs were compiled by aligning overlapping regions of the forward and reverse sequences of each

clone using the Basic Logical Alignment Search Tool (BLAST) algorithm via the world wide web (www) and hence checking for sequence errors. The forward and reverse sequences of every clone were less than 600 bp and completely overlapped. All sequences obtained, including the final deduced 2VG2 sequence, were queried against the National Centre for Biotechnology Information (NCBI) databases using BLAST server programs (BlastN and BlastX versions 2.0.8, www.ncbi.nlm.nih.gov/BLAST/) (Altschul *et al.*, 1990).

4.2.8 Verification of 2VG2 expression differences using RT-PCR

The 2VG2 sense and antisense primers (see Table 4.1) were used to determine if the 2VG2 gene fragment could be detected in both unwounded and wounded E17 and E19 skins at t=0 and t=24h post-wounding by standard RT-PCR (8 skin categories in total). The RT reaction was done essentially as described for DD-PCR but using oligo-$d(T)_{11}$ instead of the anchored 3' primer (see section 3.2.4.2). After cDNA synthesis, 1µL of each RT was added to a 19µL PCR mixture containing 1 x PCR buffer, 1 x Q-Solution (proprietary solution supplied by Qiagen), 1.5mM $MgCl_2$, 200µM dNTP mix, 1µM or 0.5µM 2VG2 sense and antisense primers and 1.25 Units (U) *Taq* DNA polymerase (Qiagen). The reactions were cycled in a Corbett Research thermal cycler (model PC-960, Mortlake, NSW, Australia) using the following parameters: 1 cycle of 94°C for 1 minute, 30 or 40 cycles of 94°C for 30 seconds, 62°C for 1 minute, 72°C for 1 minute, and then a final extension of 72°C for 5 minutes. To ensure that there was no DNA contamination in the original RNA preparations, a RT-PCR without reverse transcriptase was performed. The RT-PCR products were separated on 2% agarose/TBE gels stained with ethidium bromide as described in section 3.2.5.1.

Table 4.1 Sequence of 2VG2-specific primers used for RT-PCR of fetal rat skin RNA

These primers correspond to the cDNA sequence of clone 2VG2 (expected product size 300bp). Both primers are shown 5' to 3'.

2VG2-specific primers:	
2VG2 sense	TTGGTGTTGTATGTTTGTTG
2VG2 antisense	CTCCAGAAGTTTATTTAGGA

4.2.9 RNA gels for Northern blot analysis

For Northern blot analysis, samples of total RNA were resolved by electrophoresis on 1.5% agarose gels containing 2.2M formaldehyde and 1 x (N-morpholino) propanesulphonic acid (MOPS) buffer. RNA samples (10µg/lane) from adult rat lung and fetal E17 and E19 skins (see section 3.2.4.1) were prepared for electrophoresis as followed:

5.3µL RNA + DEPC-treated water

3.67µL formaldehyde (37%, pH 4.5)

10µL deionised formamide

1µL 10 x MOPS buffer (0.2M MOPS / 50mM sodium acetate / 10mM EDTA (pH 7))

RNA samples were incubated at 65°C for 15 minutes to denature and snap-cooled on ice. Three microlitres of 10 x gel loading buffer (50% glycerol / 1mM EDTA (pH 8) / 0.25% bromophenol blue / 0.25% xylene cyanol FF) and 1µL of ethidium bromide (10µg/µL) was added to RNA before loading onto gels. Northern gels were run at 60V in 1 x MOPS until the bromophenol blue dye had reached the bottom of the gel. Following electrophoresis, the position of the ribosomal bands was established and the amount of RNA for each preparation was roughly equivalent on the gel as judged by UV transillumination. Prior to blotting, the gels were washed once in DEPC-treated water then twice in 20 x SSC, each for 15 minutes with gentle agitation. RNA was blotted to HyBond™-N nylon

membranes using downward transfer (Chomczynski, 1992) with 20 x SSC as the buffer, then fixed at 30mJ in a GS Gene Linker™ UV Chamber.

4.2.10 Synthesis of 2VG2 DNA probe

A double-stranded DNA probe was synthesised for Northern blot analysis. The 2VG2 clone was radiolabelled to 2-8 x 10^7 cpm using the Strip-EZ™ DNA kit. Briefly, 9µL of linearised DNA (25ng) was denatured at 95°C for 5 minutes then snap-frozen in liquid nitrogen. The primer extension mix (1 x Decamer solution, 1 x Buffer – dATP/dCTP, 1 x modified dCTP, 50µCi [α-^{32}P]-dATP, 1U exonuclease-free Klenow) was prepared and added to the denatured DNA in a final volume of 25µL. The reaction was allowed to proceed at 37°C for 10 minutes then stopped by the addition of 1µL of 0.5M EDTA. After diluting to 50µL with milliQ water, 1µL of the 2VG2 probe was added to 3mL of scintillation fluid for counting before purification. A Sephadex G50 spin column was used to separate incorporated from unincorporated radioactive nucleotide in the remaining probe according to the manufacturer's instructions. One microlitre of the purified probe was added to 3mL of scintillation fluid and both scintillation vials containing unpurified and purified probe were counted on a 1900TR Liquid Scintillation Analyser, set for 1 minute of ^{32}P, in order to determine the percentage incorporation of ^{32}P. The probe was stored at -20°C for up to one week until required for Northern blot hybridisation.

4.2.11 Northern blot hybridisation

RNA membranes were pre-hybridised in roller bottles containing 10mL of ULTRAhyb™ Buffer per 100cm^2 of membrane for 2 – 4 hours at 42°C in a rotating hybridisation oven. Each membrane was hybridised with the ^{32}P-labelled 2VG2 clone (see section 4.2.10), then equal RNA loading was controlled for by stripping each membrane

using the Strip-EZ™ DNA kit and reprobing with a ^{32}P-labelled β-actin oligonucleotide. Briefly, the probes were heat-denatured at 100°C for 5 minutes and quickly snap-cooled on ice. Each denatured probe was added to the ULTRAhyb™ and the nylon membranes were incubated in the resulting hybridisation buffer at 42°C overnight. The membranes were then washed twice for 15 minutes in 100mL of 2 x SSC/ 0.1% SDS at room temperature and twice for 20 minutes at 42°C in 0.5 x SSC/ 0.1% SDS. For more stringent conditions, the membranes were washed twice more for 20 minutes at 42°C in 0.1 x SSC/ 0.1% SDS, then once for 20 minutes at 65°C in 0.1 x SSC/ 0.1% SDS. Blots were exposed to X-ray XOMAT AR film from 3 hours to 3 days at -70°C with an intensifying screen. All experiments were performed three times with comparable results.

4.2.12 5' Rapid amplification of cDNA ends (5' RACE PCR)

5' RACE PCR was carried out using the 5' RACE System Version 2.0, according to the manufacturer's instructions. Briefly, first strand cDNA synthesis was performed with 1μg of total RNA from E17 t=18h wounded skin specimens (see sections 2.2.3 and 3.2.4.1) using 0.1μM of a gene specific primer (one of the three different GSP-1, see Table 4.2). RNA was degraded with an RNase mix and first strand cDNA was purified through a GlassMAX® Spin Cartridge (Gibco BRL Life Technologies). A homopolymeric tail was then added to the 3' end of the cDNA using terminal deoxynucleotidyl transferase and dCTP. The dC-tailed cDNA was PCR amplified with *Taq* polymerase (Qiagen) using AAP (see Table 4.2A) and 0.4μM of a nested gene specific primer (one of the three different GSP-2, see Table 4.2) using the following cycling parameters: 94°C for 2 minutes, 35 cycles of 94°C for 1 minute, 55-63°C for 30 seconds, 72°C for 2 minutes and 72°C final extension for 10 minutes.

Table 4.2 Sequence of the 5' RACE Primers

The two abridged primers supplied with the kit are shown in (A). The GSP-1 primers used in each first strand cDNA synthesis, the GSP-2 primers used in each PCR of dC-tailed cDNA, and the GSP-3 primers used in each nested amplification of three sequential 5' RACE experiments (B-D) are shown. All primers are read 5' to 3' and I represents inosine.

(A) 5' RACE Abridged Primers:	
AAP	GGCCACGCGTCGACTAGTACGGGIIGGGIIGGGIIG
AUAP	GGCCACGCGTCGACTAGTAC

(B) Gene Specific Primers used in First 5' RACE:	
1GSP-1	TCGCTGCTTTGCTGTTGGTC
1GSP-2	AGACCCCAGGCTTTCTCTTT
1GSP-3	CCCCTGAGATTGTCCATTGG

(C) Gene Specific Primers used in Second 5' RACE:	
2GSP-1	AGCTTTTGAAATACTGAGTT
2GSP-2	CCTATGGAAATACTTCTTGC
2GSP-3	TTAACCTTAAATACAGCGTG

(D) Gene Specific Primers used in Third 5' RACE:	
3GSP-1	CCCTGGCACCTGAGGATCAC
3GSP-2	TCCTCGAGAACCCTGACCCA
3GSP-3	GGGTCTAGGTTCACCACAGC

If no product was amplified or, on the other hand, if many products were amplified in the 5' RACE, the primary PCR product(s) was diluted and reamplified using AUAP (see Table 4.2A) and 0.2μM of another nested gene specific primer (one of the three different

GSP-3, see Table 4.2) using the cycling conditions above. An aliquot of each amplified sample was analysed by 1.5% agarose gel electrophoresis with ethidium bromide staining (see section 3.2.5.1). The 5' RACE products were then purified using BresaSpin® kit and cloned into the pGEM-T® vector as described in sections 3.2.8.2 and 3.2.8.3. Positive clones were identified by colony PCR (see section 3.2.8.5) and mini-prep DNA of 2-3 positive clones was prepared (see section 4.2.6) for DNA sequencing (see section 4.2.7).

After the third consecutive 5' RACE reaction yielded only small RACE products (< 25 bp) using this method, the protocol was modified to allow the synthesis of cDNA transcripts with high GC content. It is known that poly (dC) tracks present in GC rich cDNA can serve as effective priming sites for AAP, the deoxyinosine-containing primer. PCR of such a template then results in truncated products. Therefore, the manufacturer's alternative protocol for 5' RACE of GC-rich cDNA was followed for 5' RACE with the 3GSP primers (see Table 4.2D). In addition, the volume and temperature of the reverse transcription reaction was increased to avoid problems with 5' RACE due to secondary structure of the target mRNA and ELONGASE™ Enzyme Mix was used in the PCR to increase the chances of amplifying longer products. The cycling conditions for this modified 5' RACE PCR were: 94°C for 1 minute, 40 cycles of 94°C for 1 minute, 63°C for 30 seconds, 68°C for 2 minutes and 68°C final extension for 10 minutes.

4.2.13 3' Rapid amplification of cDNA ends (3' RACE PCR)

3' RACE PCR was first attempted using the 3' RACE System for rapid amplification of cDNA ends, according to the manufacturer's instructions. Briefly, first strand cDNA synthesis was performed with 1µg of total RNA from E17 t=18h wounded skin specimens (see sections 2.2.3 and 3.2.4.1) using 0.5µM of the 3' RACE AP (see Table 4.3A). RNA was degraded with RNase H and amplification was performed with *Taq* polymerase

(Qiagen) using 0.2μM AUAP (see Table 4.3A) and 0.2μM of a gene specific primer (3' GSP-1, see Table 4.3B) under the cycling conditions described for 5' RACE. In an attempt to generate a specific amplification product, the primary PCR product(s) was diluted and reamplified using 0.2μM of a second gene specific primer, (3' NEST-1, see Table 4.3B) and AUAP. Since more than one product was still being amplified, a third nested GSP (3' NEST-2, see Table 4.3B) was designed for the specific amplification of the diluted products. The products from this final PCR were gel purified using the Concert™ Rapid Gel Extraction system and cloned into the pGEM-T® vector as described in section 3.2.8.2 and 3.2.8.3. Positive clones were identified by colony PCR (see section 3.2.8.5) and mini-prep DNA of 2-3 positive clones was prepared (see section 4.2.6) for DNA sequencing (see section 4.2.7).

Table 4.3 Sequence of the 3' RACE Primers

The two primers supplied with the kit are shown in (A). The GSP-1 primer used in the first amplification and the nested primers used in each subsequent amplification are shown in (B). All primers are read 5' to 3'.

(A) 3' RACE Primers:	
AP	GGCCACGCGTCGACTAGTACTTTTTTTTTTTTTTTT
AUAP	GGCCACGCGTCGACTAGTAC

(B) Gene Specific Primers used in First 3' RACE:	
3' GSP-1	TTTTACTCTTTCTCTGCCCC
3' NEST-1	GTCAGGGCAAAGCAGCAGCA
3' NEST-2	GTGATGACCCCTTTCTGTGC

Sequencing of these clones did not result in the identification of true 2VG2 extension products and instead, unrelated transcripts had amplified in the 3' RACE reactions.

Therefore, the temperature of the reverse transcription reaction was increased in case secondary structure in the target mRNA was inhibiting its transcription and ELONGASE™ Enzyme Mix was used in the PCR to increase the chances of amplifying longer products. The cycling parameters were as described above for the GC-rich cDNA 5' RACE protocol.

4.2.14 Primer extension analysis

To map the transcription initiation site of the 2VG2 mRNA, primer extension was performed according to Sambrook *et al.* (1989), with minor modifications. Firstly, 50pmol of the 3GSP-1 and 3GSP-3 primers were labelled with 10pmol (30μCi) [γ-^{33}P]-ATP using 20U of *FPLC*pure™ T4 polynucleotide kinase in 1 x One-Phor-All *PLUS* buffer. The labelling reaction was incubated at 37°C for 30 minutes then 2.5μL of EDTA (0.5M) was added to stop the reaction. Unincorporated [γ-^{33}P]-ATP was removed by standard phenol/chloroform extraction and ethanol/sodium acetate precipitation and the pellets were resuspended in 10μL of DEPC-treated water. Ten micrograms of total RNA, from either E17 t=18h wounded skin or yeast as a control (Ambion Inc.), was added to each primer and the mixtures were precipitated with ethanol/sodium acetate at -80°C for 30 minutes. After drying, the pellets were resuspended in 10μL of 1 x First Strand Buffer (SuperScript™II kit, Gibco BRL Life Technologies), heated at 85°C for 10 minutes, snap-cooled on ice for 2 minutes, then incubated at 42°C for 2 hours. A further 2μL each of DEPC-treated water, 5 x First Strand Buffer and 0.1M DTT, and 1μL each of 10mM dNTPs and SuperScript™II reverse transcriptase was added to the annealed primer/template mixtures and the reactions were incubated for another hour at 37°C. The nucleic acids were again ethanol precipitated and resuspended in 5μL of formyl loading buffer (section 3.2.4.3). The DNA/RNA hybrids were denatured by incubating at 95°C for 5 minutes then resolved on a 6% denaturing polyacrylamide gel until the bromophenol blue had reached the bottom of the gel (see

section 3.2.5.2). The gels were fixed, dried, taped down in autoradiographic cassettes with intensifying screens and exposed to BioMax X-ray film overnight as described in section 3.2.4.3. Bromophenol blue and xylene cyanol dye migration were used as markers of product sizes.

4.3 RESULTS

4.3.1 Retrieval and cloning of the 2VG2 differential display product

The reamplified 2VG2 clone identified by DD-PCR in Chapter 3 was purified and ligated into the pGEM-T® vector and transformed into *E.coli* cells. PCR screening of colonies showed that one transformant had an insert of approximately 570 bp, but it was later found to be a false positive in the ensuing dot blot analysis (Figure 4.1 lane 13 and Figure 4.2 dot in second column and third row). All other white transformants selected contained a gene insert 300 bp in length (see Figure 4.1), however, it was still not known if all clones had the same nucleotide sequence.

To circumvent the isolation of unwanted sequences that are not differentially expressed, duplicate dot blots of the colony PCR products were set up on nylon membranes in an ordered grid. One blot was probed with a DD reaction using E17 RNA and the other with a DD reaction using RNA from E19 skin, both cultured for 24 hours post-wounding. These reactions employed the HindIIIOPA-2 and HindIII$(T)_{11}$VG primers that originally gave rise to the 2VG2 product, and the reactions were labelled to high specific activity (see section 4.2.5). The dot blot hybridisations were performed using conditions that parallel Northern blotting, in that hybridisation and washing buffers, incubation times and temperatures were all the same. Figure 4.2 shows two clones, circled in red, that appear to be expressed in E17 skin after 24 hours post-wounding but not in E19 skin at this time point. The DNA from each of these clones were sequenced, aligned to each other using BLAST (data not shown), and found to be identical. Although the other clones displayed stronger signals on the E17 blot than the E19 blot, they were not expected to be as highly differentially expressed as the clones circled in red. Indeed, the cDNA sequences of these clones differed to that of the clones circled in red, hence, their specific expression was not studied further. The dot blot data indicate that despite the high specificity of the reamplification protocol, more than one

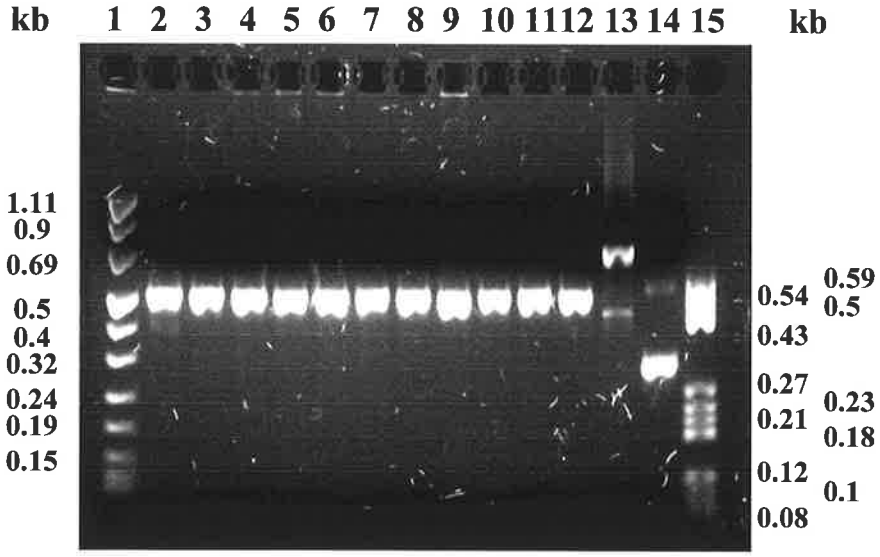

Figure 4.1 Colony PCR of 2VG2-pGEM-T transformants.

The reamplified 2VG2 product was cloned into pGEM-T® and transformed into JM109 cells as described in section 3.2.8.2 and 3.2.8.3. PCR confirmed that white colonies were positive transformants. Most bands appear to be ~550 bp corresponding to the 300 bp 2VG2 insert plus the 236 bp sequence of the pGEM-T® multiple cloning site (MCS, lanes 2-12). One band was approximately 800 bp, corresponding to an insert size of 570 bp, and was later found to be a false positive transformant during the dot blot analysis. PCR performed on blue colonies amplified only the 236 bp band corresponding to the MCS (lane 14). The sizes of the Boehringer Mannheim Molecular Weight Marker VIII and the pBR322 *Hae I* digest (lanes 1 and 15, respectively) are indicated.

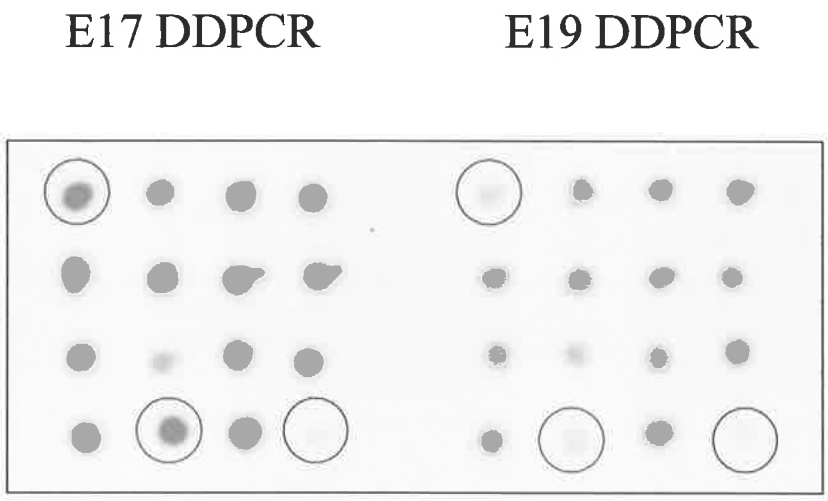

Figure 4.2 Dot Blot of 2VG2 colony PCR products.

The two membranes shown are replicates loaded with equal amounts of identical PCR clones. The left membrane was hybridised with a labelled DD reaction using RNA from E17 skin 24h post-wounding. The right membrane was hybridised with a labelled DD reaction using RNA from E19 skin 24h post-wounding. Clones circled in red represent cDNA transcripts differentially expressed in E17 but not E19 skin 24h post-wounding. The negative control, a colony PCR product generated from a blue pGEM-T colony containing no insert, is circled in blue on each blot. All other clones that generated signals on both blots were not studied further.

DNA population was reamplified from the DD-PCR gel slice as a 300 bp band.

The nucleotide sequence of the differentially expressed 2VG2 clone is shown in Figure 4.3. It was found to be flanked at both ends by the sequence of the 3' anchor primer used, HindIII$(T)_{11}$VG. Therefore, the sequence contains a poly (A) track that was present in the primer used to synthesise the first strand cDNA and this may represent a bonafide poly (A) tail. In addition, the mRNA contains an internal poly (T) track that was also recognised by the 3' anchor oligonucleotide during DD-PCR to prime in the reverse orientation. A canonical polyadenylation signal (AATAAA) was also located upstream of the putative poly (A) tail, further suggesting that the 2VG2 fragment corresponds to the 3' end of the mRNA.

NCBI database analysis of the rat 2VG2 cDNA fragment revealed it to have high nucleotide identity with numerous rat expressed sequence tags (EST) from various organs. Such organs included the ovary (99% identity with accession numbers AI176315 and AI011757), lung (99% identity with accession number AI710030), embryo (99% identity with accession number AW915223), ventricle (96% identity with accession number BF420182), placenta (96% identity with accession number AI237852) and thalamus (92% identity with accession number AW521135).

4.3.2 Confirmation of differential expression by RT-PCR

To confirm and extend the differential display and dot blot results on the relative expression of the 2VG2 gene in fetal rat skin, a series of verification experiments were performed. Firstly, the sequence information shown in Figure 4.3 was used to design two 2VG2-specific primers for RT-PCR. These primers were used to amplify 2VG2 gene transcripts in RNA from the following 8 specimens: E17 and E19 wounded and unwounded skin at the time of excision (t=0) and after 24 hours in culture (t=24h). Note that all of the skin samples were excised from the back of the rat fetuses and are, therefore, wounded to some degree. Thus, in this chapter wounded skin refers to skin that has been dissected from

Figure 4.3 Nucleotide sequence of the 2VG2 DD-PCR clone.

The 300 bp sequence was obtained from DD-PCR as described above. The sequence of the 3' anchor primer used, HindIII$(T)_{11}$VG, is shown in bold type, while a canonical polyadenylation signal is underlined. The red arrows indicate the binding sites of the 2VG2-specific primers shown in Table 4.1.

the back of the rat and wounded several more times with a 19G needle, whereas unwounded skin refers to skin that has been dissected from the rat but not wounded further. Reaction conditions were as described in section 4.2.8 and enough RNA was present to support amplification of a specific message.

Initially, 40 cycles of PCR were performed to allow for amplification of rare transcripts. Using these primers, 2VG2 mRNA expression was observed in all fetal rat skin types (see Figure 4.4A). None of the negative control reactions, in which the reverse transcriptase was omitted, amplified a PCR product, indicating amplification was supported only by RNA and not contaminating chromosomal DNA (data not shown). Thus, the 2VG2 band that was observed in the DD-PCR experiments to be upregulated in fetal E17 skin at 24 hours post-wounding is expressed in the other skin samples, but possibly at a lower abundance.

The concentration of primers was subsequently reduced from 1μM to 0.5μM and the number of PCR cycles was reduced in order to try and observe an induction pattern of the 2VG2 product in the fetal rat skin samples. The minimum number of PCR cycles needed to detect the 2VG2 product under these conditions was still relatively high at 30 (see Figure 4.4B), with a lower cycle number not supporting amplification of the 2VG2 product in any of the samples and a higher cycle number showing a lower degree of 2VG2 induction (data not shown). At 30 PCR cycles, amplification of the transcript was greatest only in the E17 t=24h samples, with fainter bands seen in the E19 t=24h samples and the rat lung RNA (see Figure 4.4B). A control β-actin RT-PCR using identical conditions (30 cycles and 0.5μM primers) showed uniform amplification, suggesting no significant change in expression of this housekeeping gene in all samples (see Figure 4.4C).

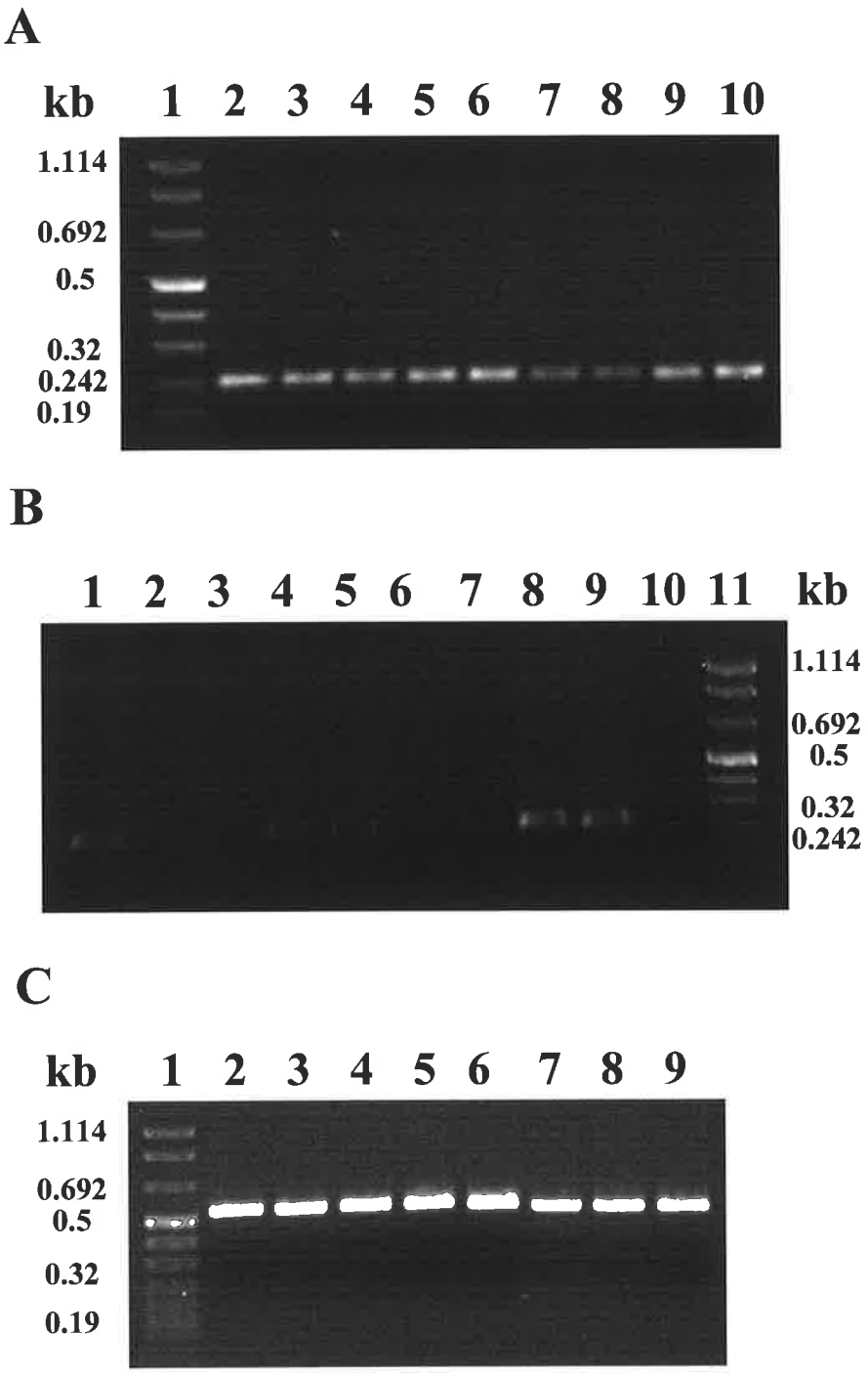

Figure 4.4 RT-PCR analysis of rat 2VG2 expression in fetal skin.

Specific 5' and 3' primers were designed from the original 300nt rat 2VG2 fragment isolated from DD-PCR. (A) 40-cycle RT-PCR was performed as described in section 4.2.8 using 1μM of each 2VG2-specific primer and RNA isolated from rat lung (lane 2), unwounded and wounded E17 rat skin at t=0 (lanes 3 and 4) and at t=24h (lanes 5 and 6), unwounded and wounded E19 skin at t=0 (lanes 7 and 8) and at t=24h (lanes 9 and 10), respectively. (B) 30-cycle RT-PCR was performed as described in section 4.2.8 using 0.5μM of each 2VG2-specific primer and RNA isolated from rat lung (lane 1), unwounded and wounded E19 skin at t=0 (lanes 2 and 3) and at t=24h (lanes 4 and 5), unwounded and wounded E17 skin at t=0 (lanes 6 and 7) and at t=24h (lanes 8 and 9), respectively. Lane 10 contains the negative control, the RT-PCR without added template. (C) 30-cycle RT-PCR was performed as described in section 4.2.8 using 0.5μM of β-actin specific primers on RNA isolated from unwounded and wounded E19 skin at t=0 (lanes 2 and 3) and at t=24h (lanes 4 and 5), unwounded and wounded E17 skin at t=0 (lanes 6 and 7) and at t=24h (lanes 8 and 9), respectively. The sizes of the Molecular Weight Marker VIII (lane 1 in A and C and lane 11 in B) are indicated.

4.3.3 Confirmation of differential expression by Northern-blot analysis

Although the preliminary results in Figure 4.4 indicated that RT-PCR could be used to demonstrate that the 2VG2 transcript is differentially expressed in fetal rat skin, there was insufficient time to optimise the protocol for a more thorough investigation. Additionally, RT-PCR does not enable the full size of the mRNA transcript to be determined. Therefore, the validity of the DD-PCR and dot blot hybridisation results was confirmed by the more established technique of Northern blotting. The 300bp 2VG2 DD-PCR fragment was labelled with ^{32}P to high specific activity and used to probe Northern blots containing 10μg total RNA from unwounded and wounded E17 and E19 skins at time zero and after 24 hours in culture (see section 4.2.10 and 4.2.11). Lung tissue was included as a positive control since 2VG2 was found to have 99% homology to a rat lung EST (see section 4.3.1). Figure 4.5A shows that a single 3 kb transcript is detected in the lung RNA, in unwounded E17 skin and more faintly in wounded E17 explants after 24 hours in culture. The 2VG2 transcript is not seen in the time zero or in the E19 skin specimens. To control for RNA loading, the blot was stripped and reprobed with a β-actin probe (see Figure 4.5B). This blot, together with the original ethidium-stained gel (see Figure 4.5C), shows nearly uniform loading of RNA across all lanes except lanes 9 and 10, which show that less RNA from the E19 t=24h skins was loaded. Nevertheless, this experiment was repeated with triplicate RNA samples (unwounded and wounded skins from three different E17 and E19 rat fetuses were cultured) and all of the results support the DD-PCR observations that the gene corresponding to 2VG2 is upregulated in cultured E17 skin explants.

In order to determine if 2VG2 gene expression is specifically upregulated in cultured E17 skin explants, the wounding experiments were repeated using whole cultured fetuses. Briefly, multiple wounds (approximately 9-12 wounds) were made in the dorsal skin of E17 fetuses using a 19G needle and the whole fetuses were cultured in serum-supplemented medium for up to 24 hours. The skin surrounding the wounds (approximately 1 x 1 cm) was

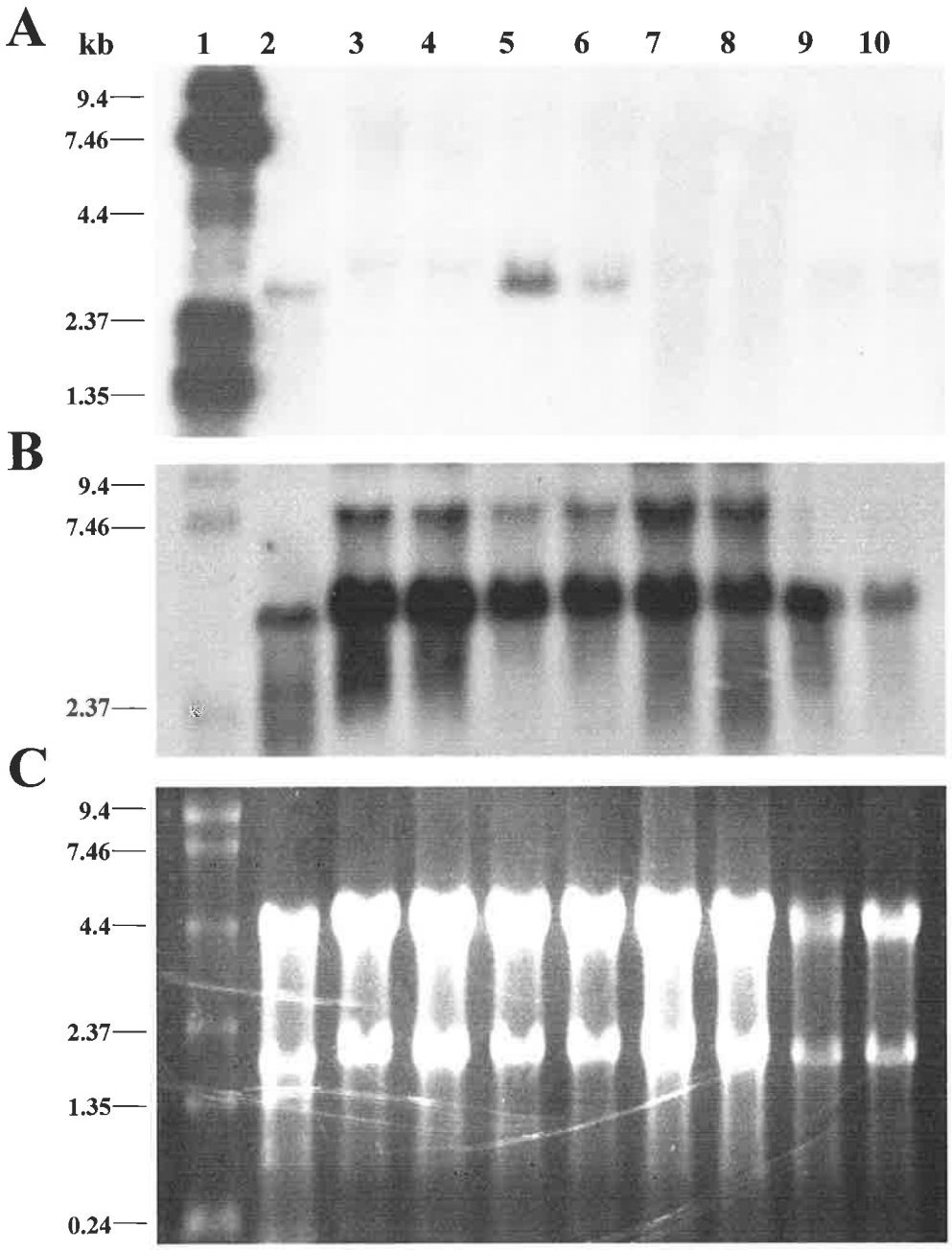

Figure 4.5 Northern blot analysis of 2VG2 expression in fetal rat skin.

Each lane of a 1.5% agarose / 2.2M formaldehyde gel was loaded with 10μg of total RNA as follows: rat lung (lane 2), unwounded and wounded E17 rat skin at t=0 (lanes 3 and 4), unwounded and wounded E17 rat skin at t=24h (lanes 5 and 6), unwounded and wounded E19 skin at t=0 (lanes 7 and 8) and unwounded and wounded E19 at t=24h (lanes 9 and 10). (A) The RNA was blotted onto a HyBond™ filter and hybridised to the double-stranded 300bp 2VG2 fragment. The filter was washed at low stringency (20 minutes at 42°C in 0.5 x SSC/ 0.1% SDS) and then exposed to X-ray film for 3 days (see section 4.2.11). (B) The blot was stripped, reprobed with a β-actin probe as an RNA loading control, washed at high stringency (20 minutes at 65°C in 0.1 x SSC/ 0.1% SDS) and then exposed to X-ray film for 3 hours (see section 4.2.11). (C) The loading was also verified before transfer onto HyBond™ membrane by ethidium bromide staining. The sizes of the RNA markers (Gibco BRL) in lane 1 are indicated to the left of the blots.

not dissected from the fetuses until after the given time in culture, when it was transferred to RNAlater™ (Ambion, Inc.) until RNA extraction. As a control, several unwounded fetuses were cultured for the same times before a 1 x 1 cm section of skin was also dissected from the back of each. No 2VG2 gene expression was detected in either unwounded or wounded skin taken from cultured whole E17 fetuses by Northern analysis (data not shown), although a low level basal expression can not be ruled out given the previous RT-PCR results shown in Figure 4.4. In any case, this indicates that upregulation of 2VG2 gene expression is restricted to cultured E17 skin explants.

4.3.4 Time course of induction

Figure 4.5A shows that a stronger signal for the 2VG2 transcript was seen in the unwounded E17 skin compared to the wounded skin after 24 hours in culture. It was thought that the E17 explant harbouring multiple punch wounds might have an intensified wound response and upregulate the 2VG2 transcript at earlier time points compared to the unwounded explant. In turn, gene expression might be returning to basal levels in the wounded E17 specimen at around 24 hours post-wounding. Therefore, to determine the time course of the induction of 2VG2 mRNA expression in E17 skin, RNA was isolated from wounded and unwounded E17 skin explants cultured for various times. The resulting Northern blots, probed with the original 300bp DD-PCR product, show that in wounded E17 skin the 3 kb 2VG2 mRNA is upregulated after just 4 hours, and expression levels appear to fall after about 24 hours of culture (see Figure 4.6A). However, less RNA from the wounded t=24h sample was loaded on this gel (see Figure 4.6B and C). This analysis was repeated with RNA from triplicate samples (skins from three different wounded E17 rat fetuses were cultured for each time point) and all blots showed that a strong signal is still observed at least 18 hours post-wounding but mRNA expression levels fall by 24 hours (data not shown).

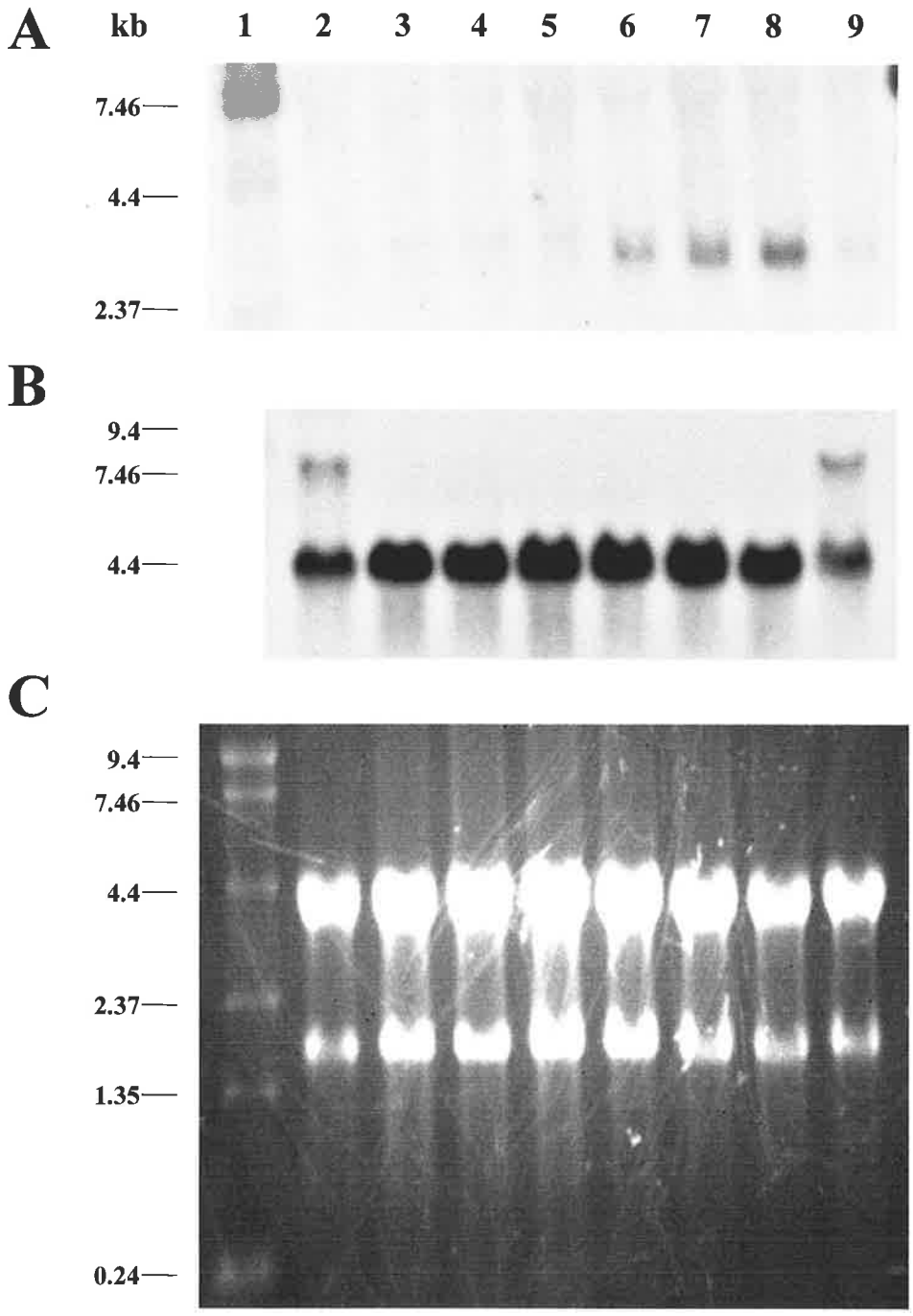

Figure 4.6 Time course of 2VG2 gene expression in wounded E17 rat skin explants.

Each lane of a 1.5% agarose / 2.2M formaldehyde gel was loaded with 10μg of total RNA from wounded E17 skin cultured for the following time points: t=0 (lane 2), t=0.5h (lane 3), t=1h (lane 4), t=2h (lane 5), t=4h (lane 6), t=6h (lane 7), t=12h (lane 8) and t=24h (lane 9). The RNA was blotted onto a HyBond™ filter and hybridised to the double-stranded 300bp 2VG2 fragment (A). The blot was stripped and reprobed with a β-actin probe as an RNA loading control (B). The loading was also verified before transfer onto HyBond™ membrane by ethidium bromide staining (C). The sizes of the RNA markers (Gibco BRL) in lane 1 are indicated to the left of the blots.

In unwounded E17 skin, that is, time-cultured explants that were not wounded further with a 19G needle, the 2VG2 transcript is detectable from 12 hours onwards (Figure 4.7A). Probing with the ^{32}P-labelled β-actin oligonucleotide and ethidium bromide staining of the gel revealed that less RNA from the unwounded E17 explants at t=12, 18 and 24h was loaded (see Figure 4.7B and C). Despite the reduced amount of RNA, the 2VG2 transcript is only seen in these samples, indicating that it is not upregulated in unwounded E17 explants until after 12 hours of culture and expression is still seen after 24 hours (see Figure 4.7A). Taken together, the results in Figures 4.6 and 4.7 support the notion that maximising the volume of wounded tissue accelerates 2VG2 gene induction.

Despite not detecting the 2VG2 transcript in the t=0 and t=24h skin samples taken from the E19 rat fetus by Northern blot analysis, the same time course of 2VG2 mRNA expression study was conducted on E19 skin to determine if it is induced at an earlier stage of culture. However, the transcript was not observed on Northern blots using total RNA from either unwounded or wounded E19 rat skin explants cultured for any of the other time points tested (see Figure 4.8).

4.3.5 Full cloning and identification of the rat 2VG2 mRNA

As a first step toward determining the protein encoded by the 2VG2 gene, the 5' end of the rat 2VG2 cDNA was cloned by three successive 5' RACE experiments performed on E17 t=18h post-wounding RNA. RNA isolated from E17 rat skin at 18 hours post-wounding was chosen for the RACE experiments because Northern blot analysis indicated that the 2VG2 transcript is expressed at the highest levels at this time point (data not shown).

The first 5' RACE, which consisted of the RT, first PCR and nested PCR using the 1GSP primers (see Table 4.2B), produced a distinct product 542 bp in length (see Figure 4.9A). This PCR product was purified, cloned and sequenced. When aligned and extended onto the original 300 bp sequence of the DD-PCR clone, the sequence of 2VG2 was 842 nt

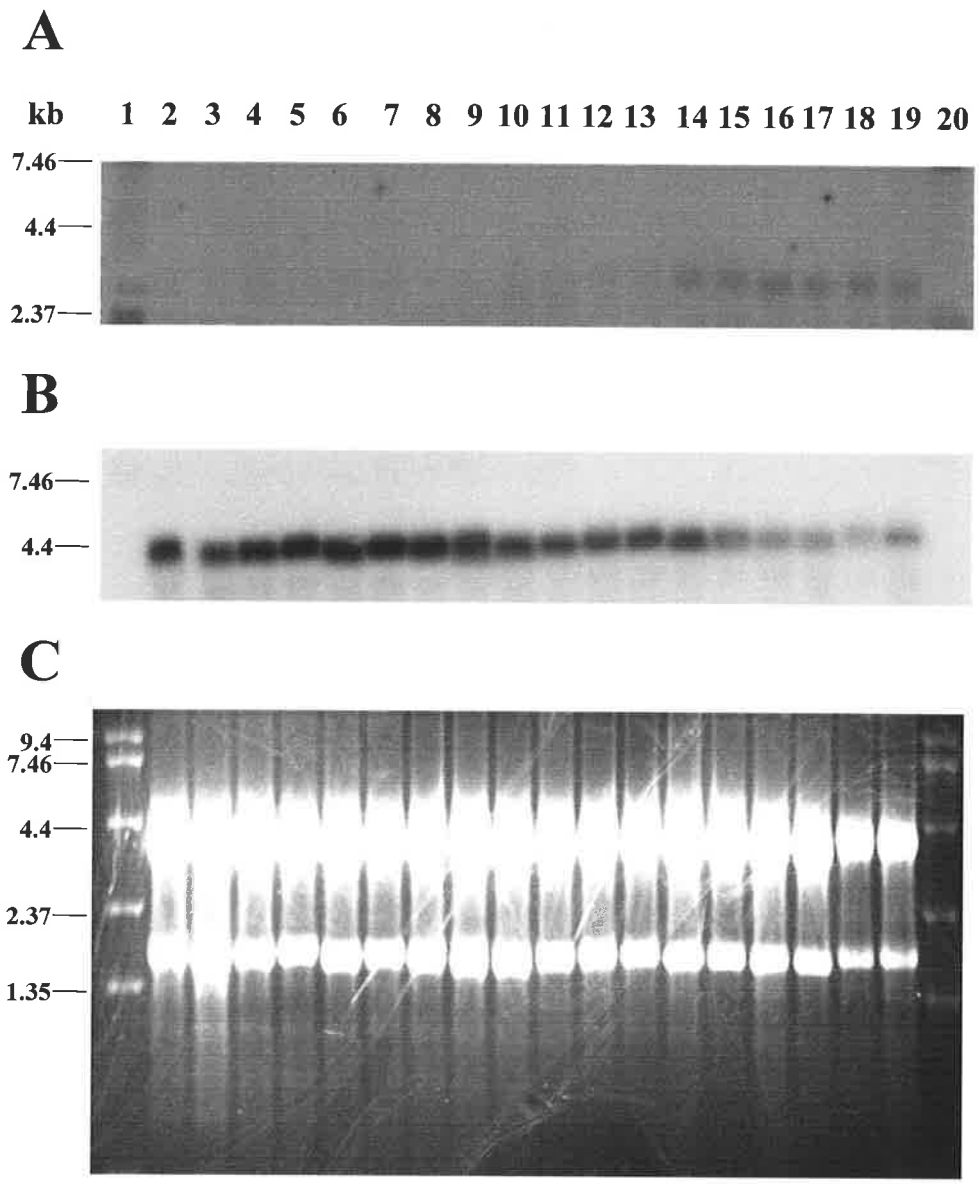

Figure 4.7 Time course of 2VG2 gene expression in unwounded E17 rat skin explants.

The 1.5% agarose / 2.2M formaldehyde gel contains duplicate RNA preparations, that is, two unwounded skins from different E17 fetuses processed separately at each time point. Each lane was loaded with 10μg of total RNA from unwounded E17 skin explants cultured for the following time points: t=0 (lanes 2 and 3), t=0.5h (lanes 4 and 5), t=1h (lanes 6 and 7), t=2h (lanes 8 and 9), t=4h (lanes 10 and 11), t=6h (lanes 12 and 13), t=12h (lanes 14 and 15), t=18h (lanes 16 and 17) and t=24h (lanes 18 and 19). The RNA was blotted onto a HyBond™ filter and hybridised to the double-stranded 300bp 2VG2 fragment (A). The blot was stripped and reprobed with a β-actin probe as an RNA loading control (B). The loading was also verified before transfer onto HyBond™ membrane by ethidium bromide staining (C). The sizes of the RNA markers (Gibco BRL) in lanes 1 and 20 are indicated to the left of the blots.

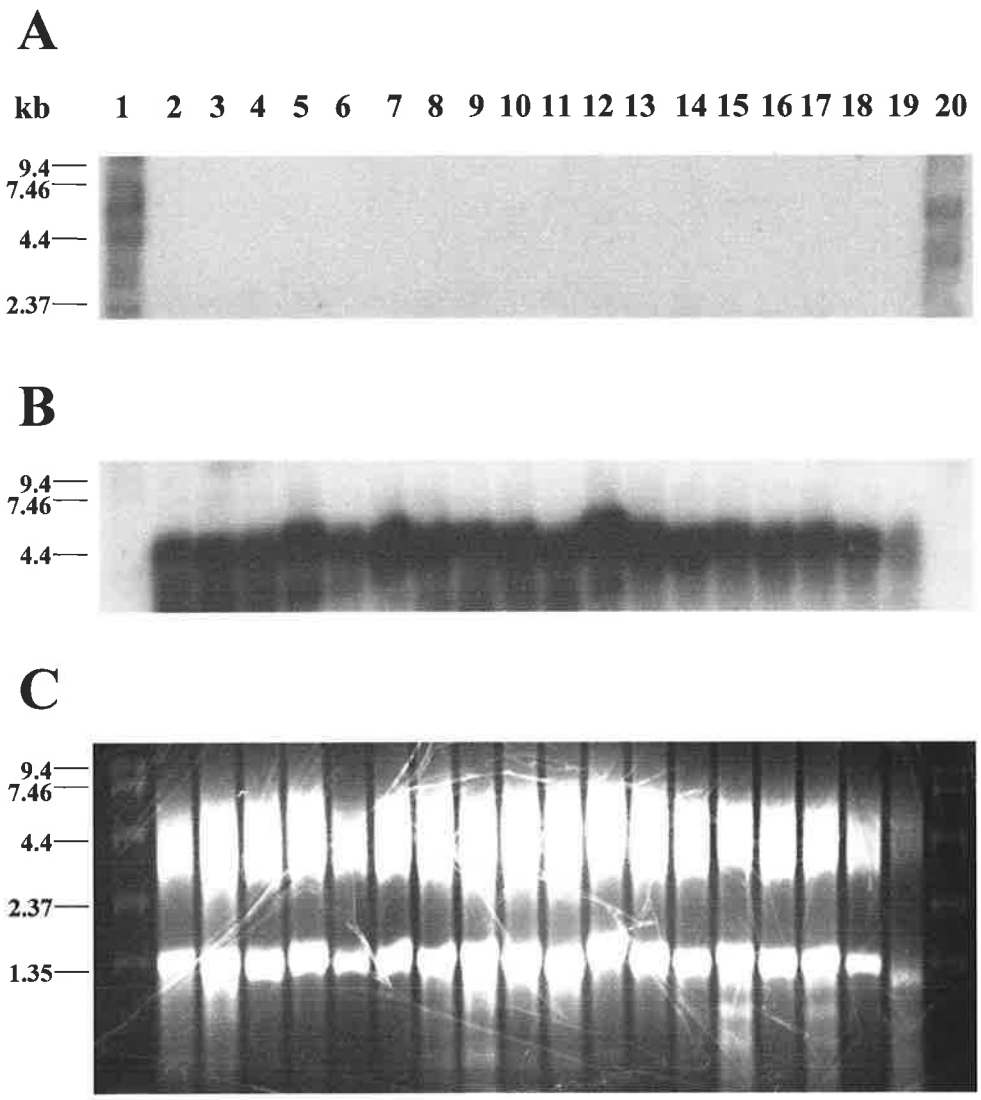

Figure 4.8 Time course of 2VG2 gene expression in E19 rat skin explants.

Each lane of a 1.5% agarose / 2.2M formaldehyde gel was loaded with 10μg of total RNA from wounded and unwounded E19 skin explants, respectively, cultured for the following time points: t=0 (lanes 2 and 3), t=0.5h (lanes 4 and 5), t=1h (lanes 6 and 7), t=2h (lanes 8 and 9), t=4h (lanes 10 and 11), t=6h (lanes 12 and 13), t=12h (lanes 14 and 15), t=18h (lanes 16 and 17) and t=24h (lanes 18 and 19). The RNA was blotted onto a HyBond™ filter and hybridised to the double-stranded 300bp 2VG2 fragment (A). The blot was stripped and reprobed with a β-actin probe as an RNA loading control (B). The loading was also verified before transfer onto HyBond™ membrane by ethidium bromide staining (C). The sizes of the RNA markers (Gibco BRL) in lanes 1 and 20 are indicated to the left of the blots.

in length. Database analysis showed that this resulting sequence had 99% nucleotide identity to a full-length EST identified in rat ovary (accession number AI011757.1, 683 nt in length). This sequence also showed 95% nucleotide identity to part of a Sugano mouse liver cDNA clone (accession number AI315857, 421 nt in length, aligned at position 344 to 405 nt). The 5' region of the Sugano mouse liver clone in turn shows similarity to the cDNA encoding human low affinity immunoglobulin gamma Fc receptor III-B (hIgG FcγRIII-B).

New gene-specific primers were designed to align with the 5' end of this longer clone (2GSP, see Table 4.2C) and another 5' RACE was performed on RNA from E17 t=18h wounded skin. A 550 bp PCR product was purified, cloned and sequenced (see Figure 4.9B). After alignment and extension to the previous sequences, the total length of the 2VG2 clone was then 1.153 kb. The 5' end of this extended sequence showed 88% nucleotide identity to the same Sugano mouse liver clone described above (aligned at position 19 to 419 nt).

A third 5' RACE, using the 3GSP primers (see Table 4.2D), was performed to extend the 2VG2 clone but only a product of about 200 bp was obtained, which equated to just 25 nt of new sequence information (see Figure 4.9C, lane 3). Since the 5' end of the 2VG2 clone was not able to be extended any further using E17 t=18h post-wounding RNA as the template, 5' RACE was repeated with rat lung RNA, because the original 2VG2 DD-PCR product has high nucleotide sequence identity to a rat lung EST (see section 4.3.1). However, a product of approximately the same size (~ 230 bp) was obtained from rat lung RNA when using the 3GSP primers (see Figure 4.9C, lane 2), indicating that either the 5' end of the message had been reached or that amplification of the full-length product was being inhibited.

In order to try and amplify a longer 5' RACE product, the ELONGASE™ Enzyme Mix was used for the PCR. In addition to the parent enzyme, this mix also contains a proof-reading enzyme to enable it to amplify long DNA templates (Barnes, 1994; Cheng *et al.*,

1994). However, a 200 bp product was amplified again (see Figure 4.9D). To ensure that secondary structure within the target mRNA was not causing the amplification of truncated 5' RACE products, the volume and temperature of the RT reaction was increased. Furthermore, an alternative 5' RACE protocol that is suitable for the amplification of GC-rich cDNA was also followed, in case this was inhibiting the amplification of full-length products (5' RACE System Version 2.0; Frohman *et al.*, 1988). Under these modified conditions no 5' RACE products were amplified. Therefore, all of these different strategies resulted in the amplification of the same 5' RACE PCR product, indicating that the 5' end had possibly been reached.

As a final confirmation, a primer extension assay was performed on E17 t=18h post-wounding RNA to try to map the 2VG2 transcription initiation site. The first experiment used the 3GSP-3 primer but resulted in too many background bands (≤ 200 bp) on the gel image and it was difficult to determine specific cDNA products from background (data not shown). Since this is usually due to the primer hybridising to other RNA species in the sample or inefficient extension by reverse transcriptase, the experiment was repeated using higher annealing and extension temperatures to reduce RNA secondary structure and improve primer specificity. When this did not work another primer, 3GSP-1, was used and yeast RNA (Ambion Inc.) was utilised as a negative control template. No bands were seen in the yeast control, which confirmed the specificity of the primer, but many background bands of up to about 200 bp in size were still seen in the E17 t=18h post-wounding RNA sample (data not shown). It is possible that the length of the 5' end of the 2VG2 clone predicted from the 5' RACE experiments was correct, but despite several attempts at primer extension this could not be confirmed.

As the resulting 2VG2 nucleotide sequence was still only 1.178 kb, approximately 1.8 kb of further sequence information was expected to be obtained by 3' RACE, based on the transcript size of 3 kb (see Figures 4.5 – 4.7). The first attempt at 3' RACE resulted in the

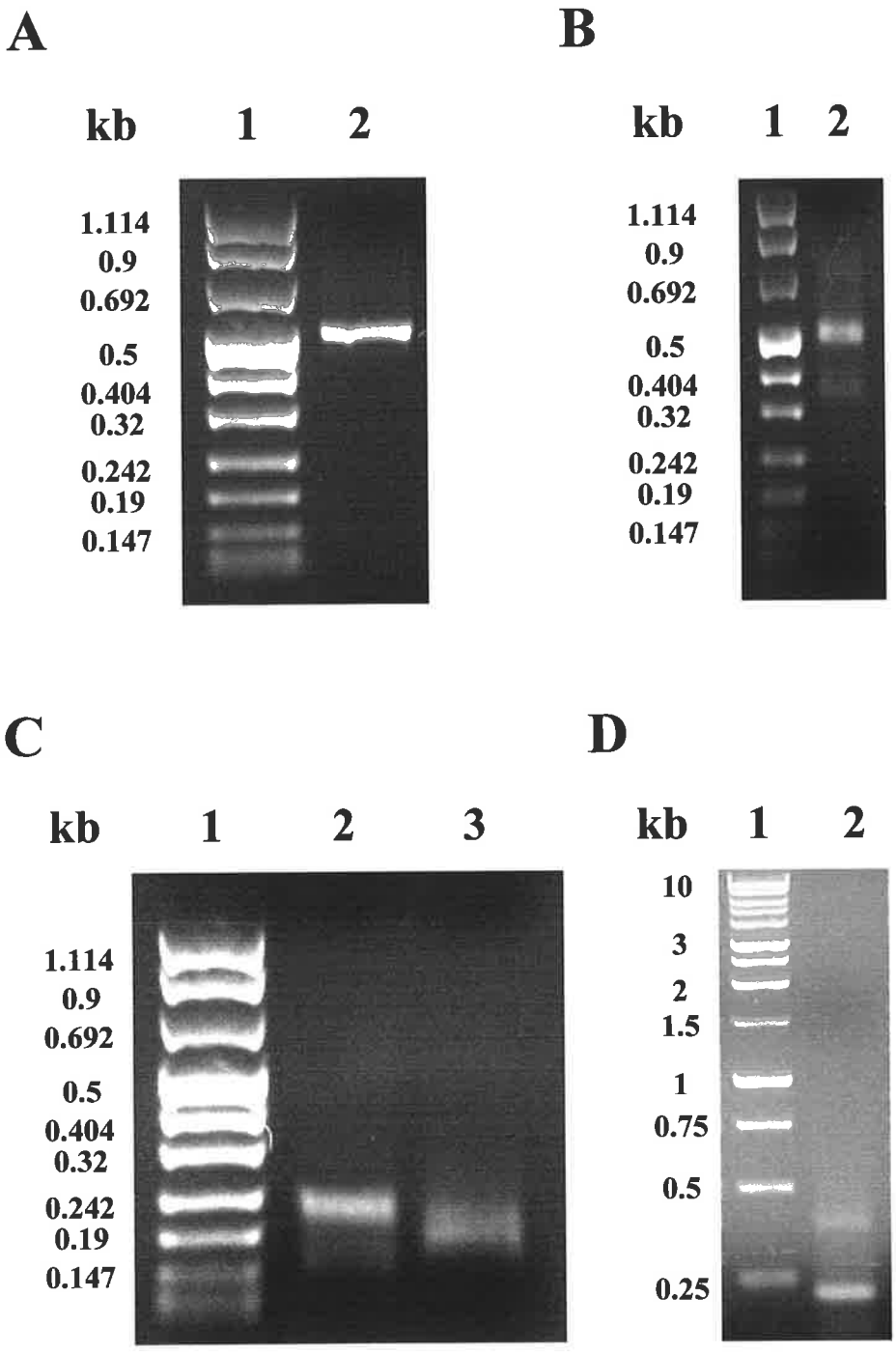

Figure 4.9 Agarose gels showing cDNA obtained by 5' RACE.

5' RACE was performed on total RNA from E17 skin at t=18h post-wounding as described in section 4.2.12 with either *Taq* polymerase (Qiagen, gels A-C) or ELONGASE™ (Gibco BRL Life Technologies, gel D), and the 1GSP primers (A), the 2GSP primers (B) or the 3GSP primers (C and D). Lane 1 of gels A-C contains Molecular Weight Marker VIII and lane 1 of gel D contains the 1 kb DNA Ladder (Promega, sizes indicated at the left of gels). Lane 2 of gel A contains the first 5' RACE product that extends from the original 2VG2 DD product. Lane 2 of gel B contains the second 5' RACE product, which extends from the first product. Lane 3 of gel C and lane 2 of gel D contain the third 5' RACE product, which extends from the second product. Lane 2 of gel C contains the 5' RACE product of the 3GSP primers using rat lung RNA as the template.

amplification of a 700 bp product, yet after cloning and sequencing, none of the positive transformants selected had overlapping sequence identity with the 2VG2 clone (data not shown). Moreover, the 3' RACE products only contained the sequence of the adapter primer (AP, see Table 4.3A) and not the nested GSPs (see Table 4.3B), indicating that they were unrelated PCR products.

Like the modification to 5' RACE, the temperature for the RT step of 3' RACE was increased to prevent the formation of possible secondary structure in the target mRNA that may inhibit its specific amplification. After RT using the AP primer, the first PCR using the AUAP and 3' GSP-1 primers, and then the nested PCR using AUAP and 3' NEST-1 primers, the reaction products generally appeared as a smear but distinct 1.5 kb and 750 bp bands were also seen (Figure 4.10 lane 2). A seconded nested PCR reaction using the 3' NEST-2 primer with AUAP again resulted in the amplification of the 1.5 kb and 750 bp bands but the heterogeneous smear was not eliminated (Figure 4.10 lane 3). Despite not being able to generate a single 3' RACE product, the products obtained were purified, cloned and successfully sequenced. However, none of the 3' RACE products showed overlapping sequence identity with the 2VG2 clone (data not shown). As before, all products were found to have the AP and AUAP primer sequences at each end and not the gene-specific or nested primers, hence they were the result of internal mispriming by the supplied 3' RACE primers. Therefore, the AP primer could not be used for the amplification of the 3' end of the 2VG2 cDNA and the 3' RACE procedure was halted.

The resulting 1.178 kb 2VG2 nucleotide sequence is shown in Figure 4.11. This region contains a single long open reading frame (ORF) beginning with an ATG start codon at nucleotide 30 and terminating with a TGA stop codon at nucleotide 777. The ORF predicts a protein of 249 amino acids. Although only 398 bp of sequence information from the 3' UTR has been obtained, Northern blot analysis data reveals a transcript size of about 3 kb (see section 4.3.3), which together with the predicted coding region suggests that the 3' UTR

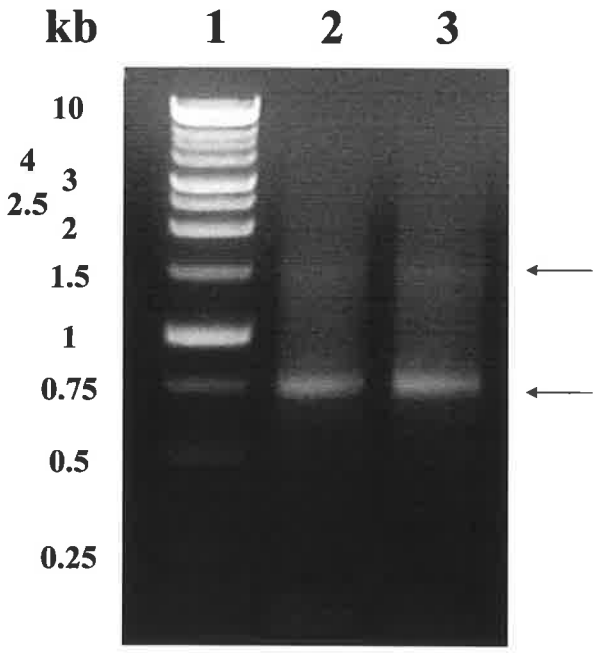

Figure 4.10 Agarose gel showing cDNA obtained by 3' RACE.

3' RACE was performed on total RNA from E17 skin at t=18h post-wounding as described in section 4.2.13 with ELONGASE™ Enzyme Mix (Gibco BRL Life Technologies). In an attempt to generate a specific amplification product, the primary PCR products were reamplified using the 3' NEST-1 and AUAP primers (lane 2). Since more than one product was still being amplified, a third PCR was performed on these products using the 3' NEST-2 and AUAP primers (lane 3). Lane 1 contains the 1 kb DNA Ladder (Promega, sizes indicated at the left of gel).

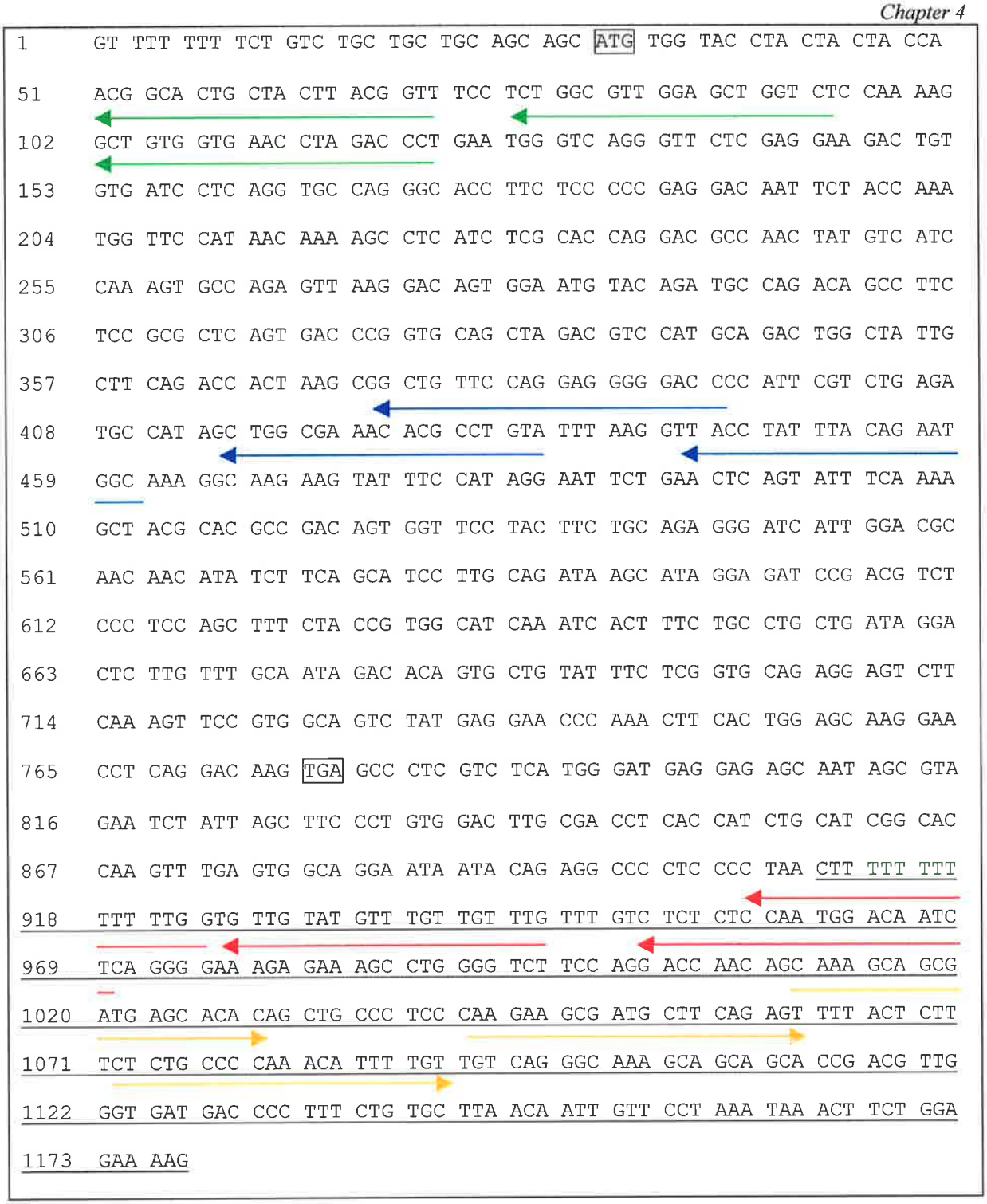

Figure 4.11 Nucleotide sequence of the 2VG2 cDNA.

The 1.178 kb sequence was obtained from 5' RACE. Only the sense strand is shown and nucleotide numbering is at the left. The potential start codon and stop codons are boxed. The 300 bp region representing the original DD-PCR fragment is underlined to show its downstream location on the mRNA. The arrows indicate the binding sites and directions of the gene specific primers designed for RACE. In ascending order, red arrows indicate the sites of the primers used in the first 5' RACE, 1GSP-1, 1GSP-2 and 1GSP-3, blue arrows indicate the sites of the primers used in the second 5' RACE, 2GSP-1, 2GSP-2 and 2GSP-3, while green arrows indicate the sites of the primers used in the third 5' RACE, 3GSP-1, 3GSP-2 and 3GSP-3. In descending order, the orange arrows indicate the sequence of the gene specific primers used in 3' RACE, 3' GSP-1, 3' NEST-1 and 3' NEST-2.

is about 1.8 kb in length.

NCBI database searches using BlastN and Gap alignments using WebAngis GCG (www.angis.org) have revealed the final 2VG2 nucleotide sequence to have 70% and 69% identity globally to the 887 bp cDNA for human IgG FcγRIII-A and RIII-B, respectively. After gaps are introduced to optimise homology, 72% identity is observed between the coding region of 2VG2 and both of the human low affinity Fcγ receptors (see Table 4.4), while 39% and 42% identity is seen between the 3' UTR of 2VG2 and human FcγRIII-A and III-B, respectively. Interestingly, a family of at least eight IgG FcγRIII isoforms exist in the rat (designated FcγRIIIA-H; Farber *et al.*, 1993; Farber and Sears, 1991), but the full length mRNA for 2VG2 only shows 52% global identity to the representative 1318 bp rat FcγRIII-C mRNA, with 59% identity in the coding regions (see Table 4.4) and 41% identity in the 3' UTR after gaps are introduced. The ORF for 2VG2 also shows 60%, 69% and 65% nucleotide identity to murine, bovine and porcine FcγRIII mRNA, respectively. The 2VG2 mRNA shows less identity to the other human and rat Fc receptors (FcRs), namely IgG FcγRII, RI and IgE FcεRIα (see Table 4.4).

4.3.6 Structural features of the deduced amino acid sequence

The nucleotide sequence of 2VG2 was translated using the EditSeq™ program (DNASTAR Inc., Madison, WI, USA) and found to encode a 249-amino acid polypeptide (see Figure 4.12). The predicted protein is relatively rich in serine (11.2%), leucine (11.6%) and valine (6.8%), as measured by frequency of amino acid residues, with a calculated molecular mass of about 28.2 kDa and pI of 8.49 (ProtParam tool, ExPASy molecular biology www server, au.expasy.org/tools/protparam.html) (Appel *et al.*, 1994). There are at least 3 potential *O*-linked glycosylation sites (NetOGlyc 2.0 www server, www.cbs.dtu.dk/services/NetOGlyc/) (Hansen *et al.*, 1995, 1997 and 1998) and 3 possible

N-linked glycosylation sites in the predicted protein (motif search using Prosite v99.07 www server, au.expasy.org/prosite/) (Bairoch *et al.*, 1997; Hofmann *et al.*, 1999), which would increase its mass to ~ 40 kDa after glycosylation if one assumes an additional 2.5 kDa per site.

Table 4.4 2VG2 mRNA shows considerable nucleotide identity with FcR cDNAs.

The coding region of the 2VG2 mRNA (nucleotide 30 – 777) was aligned with the cDNA sequence of each of the following FcRs using the GAP algorithm (WebAngis GCG). Indicated are the European Molecular Biology Laboratory (EMBL) database accession numbers for each receptor cDNA sequence, the length of the FcR cDNA and the percent identity between the coding nucleotide sequence of 2VG2 and the given FcR.

Accession # (EMBL)	Name of Receptor	Length of cDNA (bp)	% nt ID with coding region of 2VG2
X52645	Human IgG FcγRIII-A	887	72
X16863	Human IgG FcγRIII-B	887	72
M64368	Rat IgG FcγRIII-C	1318	59
M31932	Human IgG FcγRII-A	2372	55
U87560	Human IgG FcγRII-B	930	54
X17652	Human IgG FcγRII-C	1433	54
X73371	Rat IgG FcγRII	1448	53
X14356	Human IgG FcγRI	1321	50
X06948	Human IgE FcεRIα	1198	51
M17153	Rat IgE FcεRIα form 1	1036	48
M21623	Rat IgE FcεRIα form 2	983	46

Figure 4.13 shows the result of a hydropathy analysis of the predicted protein as determined using the ProtScale Prediction algorithm (via the ExPASy www server, au.expasy.org/cgi-bin/protscale.pl), according to the method of Kyte and Doolittle (1982). Two stretches of very highly hydrophobic sequences are seen, with one at the NH_2-terminus

```
1     MWYLLLPTALLLTVSSGVGAGLQKAVVNLDPEWVRVLEEDCVILRCQGTFSPEDNSTKWF

61    HNKSLISHQDANYVIQSARVKDSGMYRCQTAFSALSDPVQLDVHADWLLLQTTKRLFQEG

121   DPIRLRCHSWRNTPVFKVTYLQNGKGKKYFHRNSELSISKATHADSGSYFCRGIIGRNNI

181   SSASLQISIGDPTSPSSFLPWHQITFCLLIGLLFAIDTVLYFSVQRSLQSSVAVYEEPKL

241   HWSKEPQDK
```

Figure 4.12 Deduced amino acid sequence of the 2VG2 protein.

The predicted amino acid sequence of the ORF is shown is single letter code and amino acid numbering is at the left. The putative signal sequence at the NH_2 terminus and the transmembrane domain near the COOH terminus are double underlined (determined using the SMART v3.1 www server and the HMMTOP Prediction v1.1 www server). The potential *N*-linked glycosylation sites (NXS/TX) and *O*-linked glycosylation sites (S or T with a nearby P) are underlined and cysteine residues predicted to form disulfide bonds are boxed (determined using the NetOGlyc 2.0 and Prosite v99.07 www servers).

and the other at the COOH-terminus (also shown double underlined in Figure 4.12). The first 18 residues of the predicted protein score higher than 2.0 on the hydropathy scale and are expected to make up a signal sequence (SMART v3.1 www server, smart.embl-heidelberg.de/) (Ponting *et al.*, 1999; Schultz *et al.*, 1998 and 2000). The signal cleavage site is predicted to be between amino acid positions 20 and 21 (ValGlyAla – GlyLeu, SignalP v2.0 www server, www.cbs.dtu.dk/services/SignalP-2.0/) (Nielsen *et al.*, 1997).

Following the signal peptide in the predicted extracellular domain are two tandem homology segments that exhibit sequence similarity to members of the IgG superfamily (residues 39-90 and 120-173, Pfam database of alignments and HMMs, www.sanger.ac.uk/Pfam/) (Williams and Barclay, 1988). As indicated in Figure 4.12, the extracellular domain contains four cysteine residues that are most likely paired in immunoglobulin-like disulfide bonds (Cys-46 with Cys-88 and Cys-127 with Cys-171), on the basis of homology to other immunoglobulin (Ig) superfamily protein structures, particularly the FcγRs (Peltz *et al.*, 1989; Scallon *et al.*, 1989; Simmons and Seed, 1988; Zeger *et al.*, 1990). In addition, other cysteine residues exist both in the extracellular and in the transmembrane domains that could also form disulfide-bonds.

The hydrophobicity of the second region is higher than the NH_2-terminal hydrophobic region and is predicted to span amino acids 204 – 224 (predictions of transmembrane helices in proteins performed using ExPASy proteomics tools (au.expasy.org/tools/) including HMMTOP version 1.1 (Tusnady and Simon, 1998; von Heijne, 1992), TMHMM version 2.0 (Centre for Biological Sequence Analysis), the TMAP program (Persson and Argos, 1994 and 1996) and the TMpred algorithm (Hofmann and Stoffel, 1992) see Figure 4.13). This hydrophobic region is flanked by two hydrophilic regions, an arrangement that is similar to transmembrane domains of other known membrane proteins (Kyte and Doolittle, 1982; Wang *et al.*, 1996). Thus, the 25-amino acid hydrophilic region at the COOH-terminus of the protein encoded by 2VG2 is predicted to be a cytoplasmic tail.

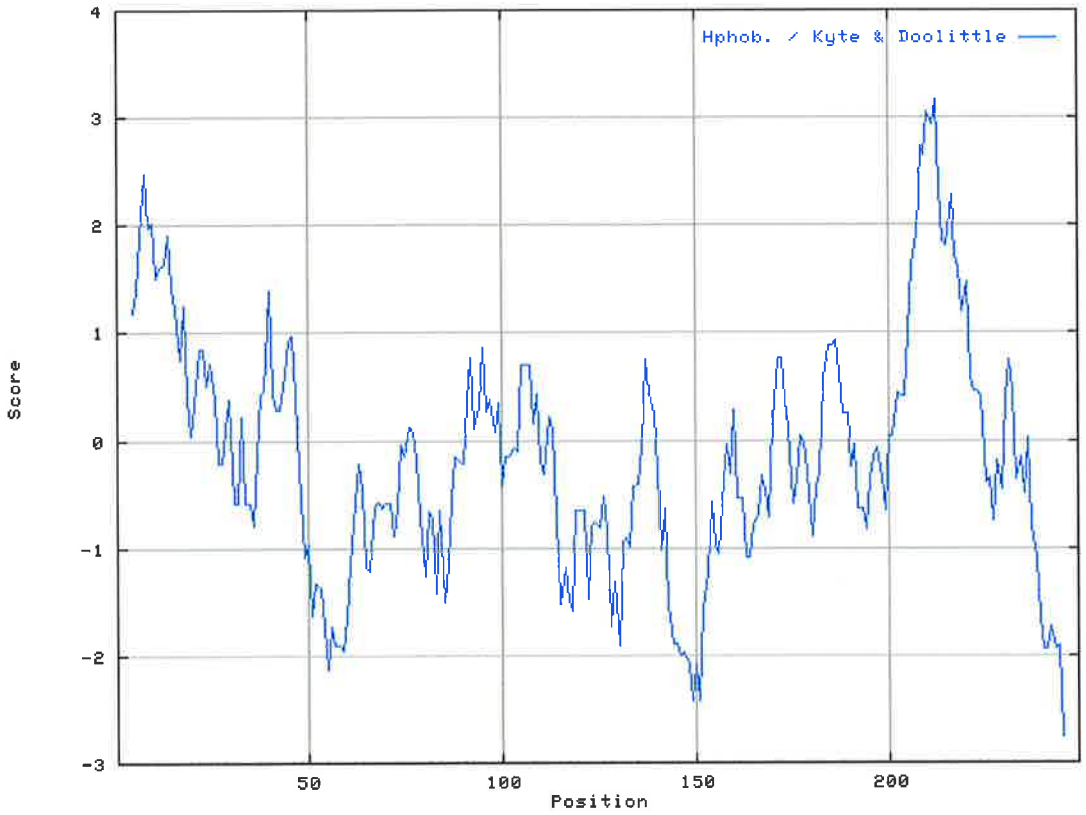

Figure 4.13 Hydropathy plot of the predicted amino acid sequence of 2VG2.

Hydrophobic regions that tend to be buried inside the molecule or inside other hydrophobic environments such as membranes appear above the centre-line, while values below the line denote hydrophilic regions that may be exposed on the outside of the molecule. The plot was produced in ProtScale (using the www ExPASy server) under a window of 9 amino acids according to the method of Kyte and Doolittle (1982). One hydrophobic region (residues methionine 1 to alanine 20) resembles a typical signal peptide (SMART v3.1 and SignalP v2.0 www servers) and the other (residues phenylalanine 204 to phenylalanine 224) may function as a transmembrane domain (HMMTOP v1.1; Tusnady and Simon, 1998; von Heijne, 1992).

4.3.7 Comparison of the 2VG2 protein with rat and human FcRs

A SwissProt database (NCBI) search revealed that the 2VG2 protein had strong identity to various FcR sequences. Table 4.5 summarises the amino acid identity between 2VG2 and the human and rat FcR sequences in the SwissProt database. The predicted protein had 61% amino acid identity globally with the 254 amino acid human low affinity IgG FcγRIII-A (or CD16-A), found on natural killer (NK) cells and 60% identity with the 233 amino acid human low affinity IgG FcγRIII-B (or CD16-B) found on polymorphonuclear leukocytes (PMNs). In contrast to the two human class III receptors, rat FcγRIII is defined by a family of highly homologous class III isoforms. Interestingly, all rat isoforms are homologues of human FcγRIII-A and no rat homologues of human FcγRIII-B have been found (Farber and Sears, 1991; Zeger *et al.*, 1990). As seen above with the nucleotide sequences, the predicted 2VG2 protein shows less identity to the rat Fcγ class III receptors, for example, the 267 amino acid rat low affinity IgG FcγRIII-C (46% global amino acid identity). Table 4.5 also lists the amino acid identity between the signal sequences, the extracellular regions, the transmembrane domains and the cytoplasmic regions of human and rat FcγRIII and those predicted for 2VG2. Figure 4.14 shows the global alignment of the predicted 2VG2 sequence to human IgG FcγRIII-A and the representative rat counterpart. In addition to FcγRIII, the predicted amino acid sequence of 2VG2 has considerable amino acid identity to other human and rat FcRs (Table 4.5). Moreover, 2VG2 shares considerable amino acid identity with mouse, bovine and porcine IgG FcγRIII, mouse, bovine and guinea pig RII and mouse IgG FcγRI and IgE FcεRIα (data not shown).

Figure 4.15 shows a phylogenetic tree relating 2VG2 to the known human and rat members of the IgG and IgE FcR family. The predicted 2VG2 protein groups close to the human class III receptors but far from the other FcR members (<50% similarity). It seems reasonable, therefore, to assume that the 2VG2 protein cloned here is a previously

```
1    M- - - - - - - - - - - - - - - WYLLLPTALLLTVS  2VG2
1    M- - - - - - - - - - - - - - - WQLLLPTALLLLVS  Human FcγRIII-A
1    MTLETQMFQNAHSGSQWLLPPLTMLLLFAF  Rat FcγRIII-C

16   SGV-GAGLQKAVVNLDPEWVRVLEEDCVIL  2VG2
16   AGMRTEDLPKAVVFLEPQWYRVLEKDSVTL  Human FcγRIII-A
31   ADRQTANLPKAVVKRDPPWIQVLKEDTVTL  Rat FcγRIII-C

45   RCQGTFSPEDNSTKWFHNKSLISHQDANYV  2VG2
46   KCQGAYSPEDNSTQWFHNESLISSQASSYF  Human FcγRIII-A
61   TCEGTHNPGNSSTQWFHNQSSTWGQVQASY  Rat FcγRIII-C

75   IQSARVKDSGMYRCQTAFSALSDPVQLDVH  2VG2
76   IDAATVDDSGEYRCQTNLSTLSDPVQLEVH  Human FcγRIII-A
91   TFKATVNDSGEYRCRMAHTSLSDPVHLEVI  Rat FcγRIII-C

105  ADWLLLQTTKRLFQEGDPIRLRCHSWRNTP  2VG2
106  IGWLLLQAPRWVFKEEDPIHLRCHSWKNTA  Human FcγRIII-A
121  SDWLLLQTPQLVFEEGETITLRCHSWKNKQ  Rat FcγRIII-C

135  VFKVTYLQNGKGKKYFHRNSELSISKATHA  2VG2
136  LHKVTYLQNGKGRKYFHHNSDFYIPKATLK  Human FcγRIII-A
151  LTKVLLFQNGKPVRYYYQSSNFSIPKANHS  Rat FcγRIII-C

165  DSGSYFCRGIIGRNNISSASLQISIGD- - -  2VG2
166  DSGSYFCRGLFGSKNVSSETVNITITQGLA  Human FcγRIII-A
181  HSGNYYCKAYLGRTMHVSKPVTITVQGSAT  Rat FcγRIII-C

192  -PTSPSSFLPWHQITFCLLIGLLFAIDTVL  2VG2
196  VSTISSFFPPGYQVSFCLVMVLLFAVDTGL  Human FcγRIII-A
211  ASTSS- - -LVWFHAAFCLVMCLLFAVDTGL  Rat FcγRIII-C

221  YFSVQRSLQSSVAVYEEP-KLHWSKEPQDK  2VG2
226  YFSVKTNIRSSTRDWKDH-KFKWRKDPQDK  Human FcγRIII-A
238  YFCVRRNLQTSGEDWRKSLSVGKYKAPQDK  Rat FcγRIII-C
```

Figure 4.14 Sequence comparison of the predicted 2VG2 protein with rat and human IgG FcγRIII.

Alignment performed using the Clustal method (Thompson *et al.*, 1994) on the MegAlign™ program (DNASTAR, Inc). The single letter amino acid code is used, amino acid numbering is at the left and residues identical in at least two of the three sequences are shaded with solid bright yellow. Dashes signify the gaps introduced to optimise identical amino acid alignment.

Table 4.5 The predicted 2VG2 protein shows considerable amino acid identity with the FcRs.

The predicted 249-amino acid sequence of 2VG2 was aligned with the protein sequence of each of the following FcRs using the GAP algorithm (WebAngis GCG). Indicated are the SwissProt database accession numbers for each receptor, the length of the FcR amino acid sequence and the percent identity between the amino acid sequence of 2VG2 and the given FcR. *The amino acid identity between the signal (or leader, L) sequence, extracellular domain (EC), transmembrane domain (TM) and cytoplasmic region (C) of 2VG2 and the class III receptors are given.

Accession # (SwissProt)	Name of Receptor	Length of protein (aa)	% aa identity with 2VG2 protein
P08637	Human IgG FcγRIII-A	254	61 (L-78, EC-61; TM-67; C-36)*
O75015	Human IgG FcγRIII-B	233	60 (L-78; EC-58; TM-67)*
P27645	Rat IgG FcγRIII-C	267	46 (L-27; EC-47; TM-62; C-35)*
P12318	Human IgG FcγRII-A	317	40
P31994	Human IgG FcγRII-B	310	38
P31995	Human IgG FcγRII-C	323	38
Q63203	Rat IgG FcγRII	285	40
P12314	Human IgG FcγRI	374	39
P12319	Human IgE FcεRIα	257	38
P12371	Rat IgE FcεRIα form 1	245	37
P12840	Rat IgE FcεRIα form 2	157	38

unreported member of the FcR family that diverged early during evolution from the FcγRIII subfamily. Whether or not the sequence divergence is simply due to the species difference is questionable. The phylogenetic analysis suggests that the predicted 2VG2 protein in rat is more similar to the human forms of FcγRIII than the previously isolated rat FcγRIII isoforms, which share on average 50% amino acid identity to human FcγRIII-A (GAP comparison, WebAngis GCG). The representative rat FcγRIII-C isoform is positioned in the

same group with rat FcγRII and by proceeding another node back it is seen that these rat isoforms are grouped with the human class II receptors. This indicates that the rat class III isoforms may not be true homologues of human FcγRIII. However, the phylogenetic tree shown in Figure 4.15 was constructed solely on the global amino acid identities between the proteins, with no consideration given to the motifs that are conserved in the FcγRIII and FcεRIα subfamilies. Furthermore, protein expression and function studies must be conducted before it can be determined if rat 2VG2 encodes a true and functional FcγRIII protein.

Close comparison found that 2VG2 displays interesting homology to the transmembrane domains of 8 FcRs: human, rat, mouse, bovine and porcine FcγRIII, and the FcεRIα subunit of human, rat and mouse high affinity IgE-binding receptors (see Figure 4.16A). The unique eight amino acid sequence, LFAVDTGL, is highly conserved in the transmembrane domains of all of the Fcγ class III receptors and Fcε class I receptors. In the protein encoded by 2VG2, the hydrophobic valine residue is conservatively replaced with the similarly sized isoleucine, while the small glycine residue is replaced with valine. Despite not being identical in the 2VG2 protein, the amino acid differences in the transmembrane motif are relatively conservative and consistent with the predicted hydrophobic nature of the transmembrane domain (see Figure 4.13). Additionally and perhaps importantly, the charged aspartic acid residue conspicuously situated within the membrane-spanning segment of FcγRIII and FcεRIα is conserved in the 2VG2 sequence.

The cytoplasmic sequence of 2VG2 also exhibits some identity to the corresponding FcγRIII sequence from each of these species (Figure 4.16B). In particular, the four COOH-terminal amino acids, PQDK, are conserved in the human, rat and mouse class III receptors as well as 2VG2. The cytoplasmic domain of human FcγRIII-B is not included in this comparison as it is only four amino acids long and bears the glycosyl phosphatidylinositol

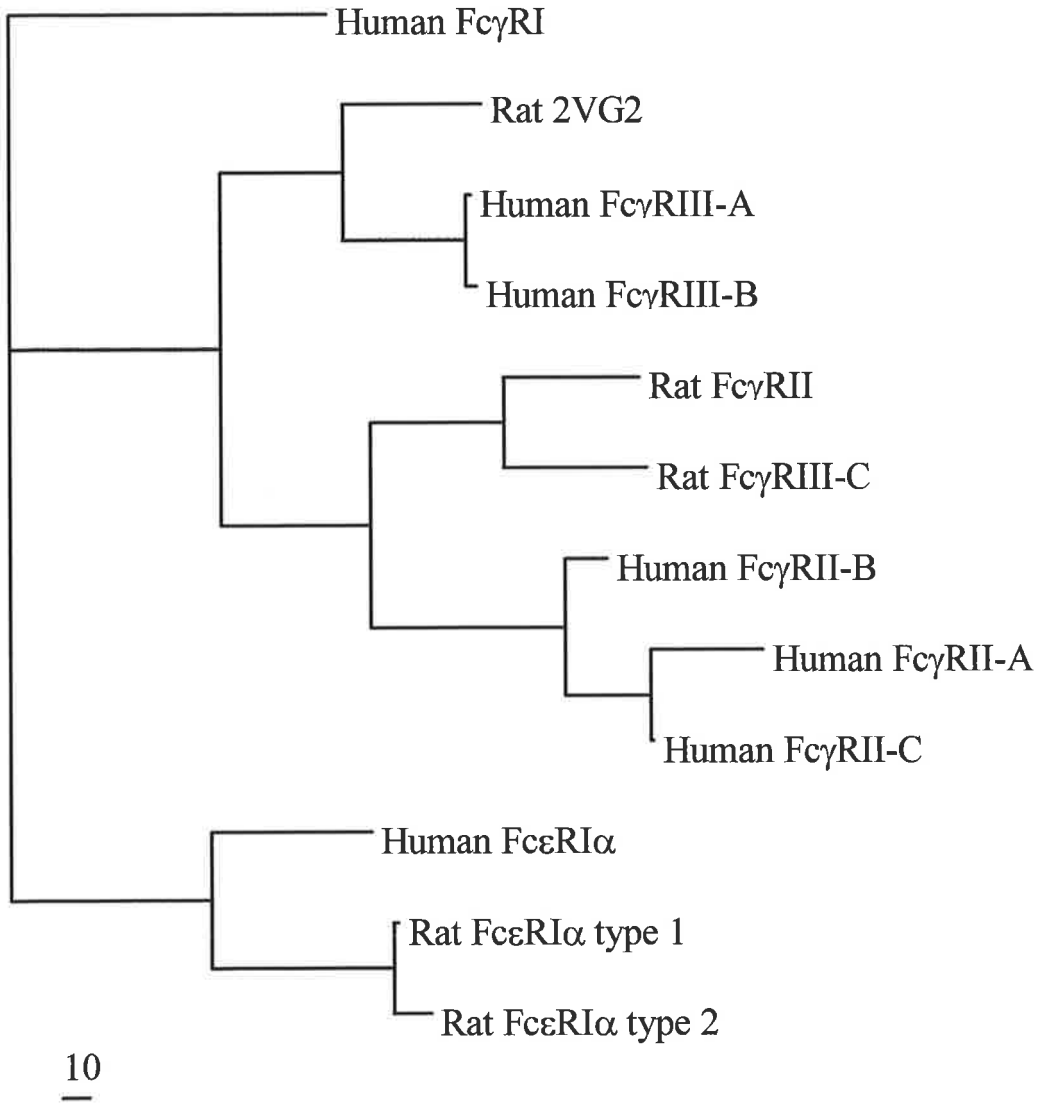

Figure 4.15 Phylogenetic tree relating the predicted 2VG2 protein to members of the human and rat FcR family.

A distance-based phylogenetic tree (Swofford, 1999) was constructed by comparing the amino acid sequences of the FcRs and the predicted 2VG2 protein using the neighbour-joining method in the TreeView program (Saitou and Nei, 1987). The sequence of human FcγRI was used as an outgroup because it has the longest uninterupted branch length and hence the greatest general dissimilarity to the other members. To determine the number of amino acid differences (D) between any two proteins within the tree the equation [D = (S/L)*10] is used, where S (mm) is defined as the sum of the horizontal lines joining the two proteins and L (mm) the length of the 10 bar (Bar: 10 amino acid differences). The tree reveals four main groups of the receptors that are more similar in amino acid sequence to each other than to members of other groups.

phospholipid (GPI-PL) linkage that anchors FcγRIII-B to PMNs (Peltz *et al.*, 1989; Simmons and Seed, 1988). Since 2VG2 is predicted to have a longer cytoplasmic domain more similar to that of FcγRIII-A than FcγRIII-B, it is more likely to be anchored by means of a polypeptide transmembrane domain.

Finally, the predicted cytoplasmic region of 2VG2 also contains a possible peptide-binding Src homology 2 (SH2) domain in YEEP (see Figure 4.16B). The motif phosphotyrosine-hydrophilic-hydrophilic-proline is reportedly recognised by SH2 domains from the protein Abl (Songyang *et al.*, 1993).

A

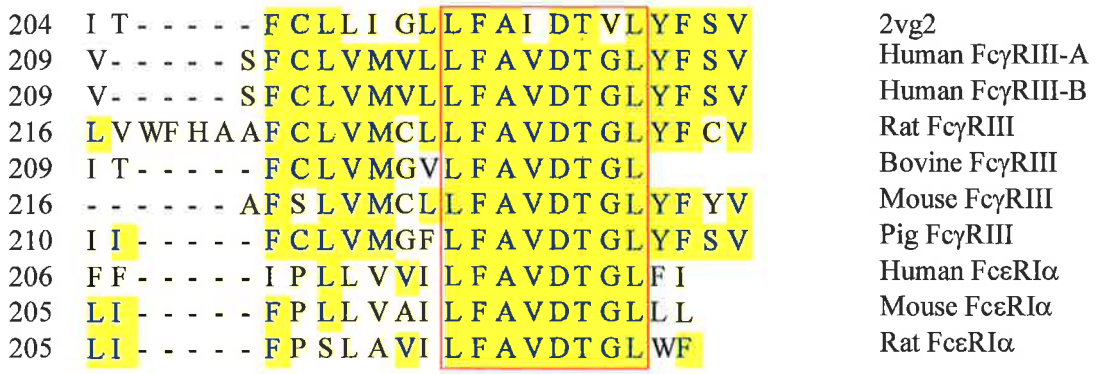

B

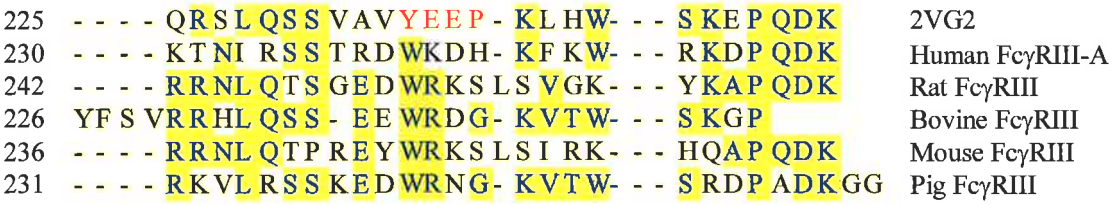

Figure 4.16 Amino acid comparison of the transmembrane (A) and cytoplasmic (B) domains of rat 2VG2 with other FcRs.

The amino acid sequence of each FcγRIII and FcεRIα was aligned using the Clustal method on the MegAlign™ program. The single letter amino acid code is used, amino acid numbering is at the left and residues identical to the consensus sequences are shaded with solid bright yellow. The 8-amino acid motif that is highly conserved in the FcγRIII and FcεRIα transmembrane domains from all species is boxed in red. The amino acid residues of the predicted SH2 domain in the cytoplasmic region of 2VG2 are coloured in red.

4.4 DISCUSSION

4.4.1 Retrieval of the true differentially expressed 2VG2 cDNA

Although differential display has appeared to represent a significant advance in molecular biology methods, there have been numerous reports documenting problems with the technique (see Chapter 3 for a discussion). An additional criticism has come from the frequent inability to confirm the original gene expression profile seen by DD-PCR (Miele *et al.*, 1998). Clones derived from DD-PCR that fail to replicate the original displayed profile are often not the original candidate transcript, but instead are contaminating, co-migrating sequences. For this reason direct Northern blot analysis using impure probes, such as those that result when DD bands are reamplified with the original DD primers and directly labelled without prior cloning, should be avoided. Some groups have reported a modification of the single-strand conformation polymorphism (SSCP) protocol to purify the excised DD-PCR candidate from potential co-migrating cDNA species before reamplification and cloning (Miele *et al.*, 1998; Zhao *et al.*, 1996). However, most techniques that have been described for the efficient elimination of contaminating sequences are, like the present study, based on the selection by hybridisation of the PCR product of interest after cloning in a plasmid.

Callard *et al.* (1994) described the set up of a single dot blot containing several independent plasmid clones that is hybridised to a probe made from the band originally isolated from the gel. After autoradiography, the plasmid clones that contained the insert corresponding to the differentially expressed band strongly hybridised to the probe whereas negative clones containing inserts originating from the contaminating DNA did not give a signal above background. Cloning the DNA of interest before applying it to the dot blot removed RT-PCR-related false positive sequences that may have been produced during the reamplification reaction. A drawback of this method is that it assumed that the probe itself

contained just one cDNA species, the DD-PCR product of interest. It is quite possible that the probe could be heterogeneous as co-migrating fragments of DNA may be excised from the gel along with the candidate DD-PCR product. Such heterogeneous probes can lead to the inaccurate classification of DD bands as false positives (Martin *et al.*, 1998).

Mou and co-workers (1994) also used dot blotting to simultaneously verify the differential expression of many cDNA fragments recovered from DD-PCR. Similar to the technique used in this study, duplicate dot blots containing many reamplified DD transcripts were screened with cDNA probes made from the two RNA samples being compared. However, in the investigation by Mou *et al.* (1994), each DNA fragment isolated from differential display was reamplified and directly used for dot blot analysis without band separation or prior cloning. Therefore, each clone may not have been homogeneous and contaminating cDNA sequences were not completely eliminated.

In short, both of these previously published dot blot procedures may not always be conclusive. Hence, the principles of both methods were combined and modified in this study to produce a more accurate and sensitive approach. Briefly, probes made from the original DD reactions being compared, using E17 and E19 skin RNA as the template, were utilised here to screen duplicate blots consisting of the reamplified and cloned bands of interest. The method presented here confirmed that the gene represented by the DD-PCR product, 2VG2, is differentially expressed in E17 fetal rat skin at 24h post-wounding. The dot blot screening also permitted the simultaneous analysis of all transformant clones identified and, in doing so, efficiently eliminated contaminating sequences prior to the execution of RNA studies. This improvement is likely to reduce the incidence of selecting false positives, so they will no longer be thought of as inherent to the DD-PCR technique. By accurately identifying positives from false positive clones, this assay provides clear advantages over using Northern blot alone in terms of time, effort and amount of RNA required per gene assayed. However, dot blot arrays do not provide information about

transcript size that can be used to verify hybridisation to the correct mRNA, or quantify relative RNA expression levels between the cell populations being compared (Martin *et al.*, 1998). Therefore, reduced cycle RT-PCR and Northern blot were used to further validate the dot blot results.

The sensitive methods of reduced cycle RT-PCR (Soo *et al.*, 1999) and limiting RNA-dilution RT-PCR (Darden *et al.*, 2000) are often used to verify and quantify differential gene expression patterns between cell populations. One benefit of RT-PCR is that it uses less RNA than is often readily available. Since only very low amounts of RNA can be extracted from the small fetal rat skin explants, reduced cycle RT-PCR was initially performed in this investigation.

The reduced cycle RT-PCR technique is based on the principle that if two samples of RNA contain differing concentrations of a specific message, the sample with the higher concentration will support amplification of that message over less PCR cycles. For each sample, one can determine a discrete end-point, the lowest number of PCR cycles at which amplification of the target RNA is detected. The differing cycle number end-points are inversely proportional to the quantities of the specific message in the two samples, with the higher concentration sample requiring less PCR cycles to amplify that message. The process is dependent on the efficiency of amplification, thus, the samples must be amplified in the same PCR machine, at the same time and under identical conditions. Preliminary RT-PCR data in this study indicated relative upregulation of the 2VG2 gene in the E17 t=24h post-wounding skin samples, however, protocol optimisation was proving to be quite time consuming. Therefore, the more traditional method of Northern blot analysis was used instead to confirm the DD-PCR results.

No 2VG2 mRNA expression could be detected in fetal rat skin immediately after wounding (t=0), or in E19 skin over the 24-hour period after wounding, by Northern blot. In contrast, elevated levels of the 3 kb 2VG2 mRNA were seen in E17 skin explants after 24

hours in culture, which agreed with the DD-PCR and dot blot hybridisation result. Despite seeing 2VG2 expression in both the unwounded and the wounded E17 skin explants after 24 hours in culture, no expression of 2VG2 mRNA was detected by Northern blot analysis in unwounded or wounded E17 skin that was excised after the whole fetus was cultured for 24 hours. The fact that no 2VG2 expression was detected by Northern blot in fetal rat skin when the whole fetus is cultured indicates that 2VG2 expression is only upregulated in cultured E17 skin explants. This result was unexpected because it was thought that if 2VG2 is upregulated in wounded epidermal cells of the excised E17 skin, it should also be upregulated in the wounded epidermis of the whole cultured fetus, especially since this cell layer is still directly exposed to the surrounding serum-supplemented medium. However, it is possible that when the skin is dissected off the back of the rat fetus, 2VG2 mRNA expression might be stimulated in the wounded dermal and/or basal epidermal cells after a given time in serum-supplemented culture. Therefore, it might not be upregulated in the wounded skin of the whole fetus in culture because the underlying dermal and basal epidermal cells are not wounded to the same extent as the explanted skin. Furthermore, these deeper cell layers are not directly exposed to the rich culture medium environment, hence, 2VG2 expression might also be dependent on the serum response of these cells.

Although the zero and 24 hour time-points chosen for the initial DD-PCR study were somewhat arbitrary, it was predicted that they would show interesting differences in gene expression that might lead to the histological and morphological differences observed between E17 and E19 wounds during the healing process (see Chapter 2). The observation of 2VG2 differential expression at these time-points by DD-PCR and subsequent confirmation by Northern blot both support this prediction. However, instead of using DD-PCR to further characterise 2VG2 gene expression over more frequent time intervals post-wounding, only Northern blotting was used due to its greater accuracy and reliability. The results showed that 2VG2 mRNA is not upregulated in E19 rat skin at any of the time points

tested. In contrast, the 2VG2 transcript is induced in wounded E17 skin explants after just 4 hours of culture and expression levels fall after about 24 hours of culture. Interestingly, the 2VG2 transcript is not upregulated in unwounded E17 explants until after 12 hours of culture and expression is still seen after 24 hours in culture. The fact that 2VG2 expression is detected in both wounded and unwounded E17 skin explants by Northern blot analysis supports the notion that 2VG2 is upregulated in cultured skin after dissection from the back of the E17 rat fetus. The accelerated 2VG2 gene expression in wounded E17 skin explants compared to unwounded explants supports the idea that maximising the volume of wounded tissue quickens the wound response. Taken together, the Northern blot results presented in this chapter provide preliminary evidence of 2VG2 involvement in the E17 fetal skin wound response *in vitro*.

Differential display is widely recognised as being biased towards the 3' end of the message. This notion is supported in this study since DNA sequencing of the 300 bp 2VG2 clone that was identified by dot blot to be the true candidate revealed that the 3' anchored primer, HindIII$(T)_{11}$VG, was used for both sense and antisense cDNA synthesis. The HindIIIOPA-02 primer sequence was not recognised in the 2VG2 clone and did not take part in its amplification. Furthermore, a canonical polyadenylation signal was located within 30 bases upstream of the putative poly (A) tail in the 2VG2 clone, as is seen in most eukaryotic mRNAs (Wickens, 1990). There was also limited 3' sequence information available from the database searches, as 2VG2 showed little homology to known genes but high nucleotide identity to many ESTs of unknown function. Therefore, the full-length sequence of the gene represented by 2VG2 had to be determined for its accurate identification.

The most common methods to obtain the full-length gene represented by a DD-PCR product are cDNA library screening using the differential display product as a probe, cDNA walking or RACE-PCR. The 2VG2 product recovered by differential display was extended by 5' RACE because the other two methods were expected to be more time consuming,

particularly if a fetal rat skin cDNA library was to be made. While the RACE technique is theoretically simple, it does have some limitations. Important information on tissue-specific changes in the 5' ends of mRNAs that arise from alternate splicing and promoter usage is not readily obtained from the existing RACE methods. Additionally, the 5' ends mapped by RACE often do not correspond to the actual transcription start sites, since premature termination of reverse transcription results in size heterogeneity of the RACE products and the shortest or most abundant DNA products are preferentially amplified. Secondary structure present in the message, such as a hairpin-loop, is a common cause of premature termination of reverse transcription resulting in truncated 5' or 3' RACE products. Indeed, it is believed that the 1.178 kb cDNA obtained here by three independent and consecutive 5' RACE experiments is not the full-length sequence for 2VG2. The Northern blot data indicate that the transcript is approximately 3 kb in size, thus, secondary structure present within the mRNA could have prevented its full recovery. Attempts to modify the 5' and 3' RACE protocol to reduce the likelihood of secondary structure were unsuccessful in retrieving additional sequence information for the 2VG2 transcript. However, sequencing of the 1.178 kb cDNA revealed an ORF beginning with an ATG start codon at nucleotide 30 and terminating with a TGA stop codon at nucleotide 777. Since only 398 bp of sequence information from the 3' UTR could be obtained, the discrepancy between the cDNA length retrieved by RACE and the size identified by the Northern analyses is most likely due to a strong secondary structure in the 3' region of the mRNA. In turn, this implies that the poly A signal found at nucleotide 1159 is internal and that another poly A signal(s) might also exist further downstream.

4.4.2 Identification of the protein encoded by 2VG2

The predicted protein product of 2VG2 is 249 amino acids in length and contains multiple motifs: a typical signal sequence of 20 amino acids at the NH_2-terminus, a long

extracellular domain with multiple potential glycosylation sites, a transmembrane domain predicted to be at least 20 amino acids in length near the COOH-terminus and a 25-amino acid cytoplasmic tail. There are also two tandem homology segments that are similar to Ig-like domains within the extracellular region. These features suggest that the differentially expressed gene encodes a membrane-bound glycoprotein involved in cellular interaction and immune recognition.

Results from database searches and amino acid alignments indicate that the protein encoded by 2VG2 may be a novel rat FcR. Receptors for the Fc portion of immunoglobulins (FcRs) play an important role in immune defence. The FcRs are differentially expressed on all leukocytes and bind immune complexes or antibody ligands to initiate specific immune functions associated with tumour and viral immunity, inflammation and allergy, depending on the receptor structure and the expressing cell type (reviewed in Raghavan and Bjorkman (1996) and Ravetch and Kinet (1991)).

FcRs are defined by their specificity for Ig isotypes. The receptors for IgG (FcγR) have been grouped into three major classes according to primary structure homology, cell-type specific expression, ligand-binding affinity, and putative function (Raghavan and Bjorkman, 1996; Ravetch and Kinet, 1991). Class I receptors, or FcγRI, are high affinity receptors for monomeric IgG expressed on activated monocytes, PMNs and macrophages. Class II receptors, or FcγRII, are low affinity receptors expressed on lymphocytes, macrophages, monocytes, PMNs, natural killer (NK) cells and non-haematopoietic cells such as epithelial and endothelial cells (Groger *et al.*, 1996; Lyden *et al.*, 2001; Metes *et al.*, 1998; Stuart *et al.*, 1989). Class III receptors, or FcγRIII, are also low affinity receptors for monomeric IgG and are expressed on PMNs, NK cells, activated endothelial cells, placental trophoblasts and glomerular mesangial cells (Farber *et al.*, 1993; Morcos *et al.*, 1994; Nishikiori *et al.*, 1993; Santiago *et al.*, 1989; Tuijnman *et al.*, 1992a). The receptor for IgE (FcεR) shares similarity

to FcγRIII in its transmembrane domain, is expressed primarily on mast cells and basophils and mediates a variety of allergic and inflammatory responses.

The α chains, which are the Ig-binding portions of FcγRI, FcγRII, FcγRIII (also known as CD64, CD32 and CD16 in humans, respectively) and FcεRI are type I transmembrane proteins containing, like the predicted protein encoded by 2VG2, an extracellular region with two or more Ig-like domains arranged in tandem. The assignment of the FcRs to the Ig gene superfamily was recently confirmed by Sondermann *et al.* (1999 and 2000). All FcR Ig domains are speculated to have originated from a common ancestor, an ancient single-domain receptor that acquired a second domain by gene duplication. Further divergent development of the two-domain receptor resulted in the present diversity, including FcγRI, which acquired a third domain (Qiu *et al.*, 1990).

Genomic and cDNA clones have been characterised for all three classes of human and mouse FcγRs, but the rat FcγRs have only just recently been characterised (Farber and Sears, 1991). Chromosome *in situ* hybridisation and analysis of mouse-human hybrids have placed the genes for FcγRI, RII, RIII and FcεRIα on the long arm of human chromosome 1, bands q23-24 (Qiu *et al.*, 1990). In particular, the FcγRIII genes are tightly linked to FcγRII and each other (Peltz *et al.*, 1989). This region of chromosome 1 is syntenic in the mouse for these and other markers. Molecular cloning of the genes encoding the Fcγ and the Fcε receptors has also revealed that the α subunits of many FcRs are found in multiple forms (Brooks *et al.*, 1989; Ravetch and Perussia, 1989). For instance, two FcγRIII genes, FcγRIII-A and B, have been identified in humans. Both human FcγRIII isoforms are polymorphic, with FcγRIII-A being biallelic and FcγRIII-B triallelic (Bux *et al.*, 1997; Koene *et al.*, 1997 and 1998; Ravetch and Perussia, 1989).

Molecular characterisation of the human FcγRIII-A and B genes has revealed that the promoter regions display distinct tissue-specific transcriptional activities (Gessner *et al.*,

1995). FcγRIII-A is primarily found on NK cells, but it is also expressed on macrophages, mast cells, placental trophoblasts (Nishikiori *et al.*, 1993) and some non-haemopoietic cells such as glomerular mesangial cells (Morcos *et al.*, 1994; Santiago *et al.*, 1989) and activated endothelial cells (Tuijnman *et al.*, 1992a), while FcγRIII-B is mainly expressed on PMNs. Therefore, they are commonly referred to as NK cell-FcγRIII and PMN-FcγRIII, respectively. The FcγRIII-A isoform encodes a protein that is resistant to phosphatidylinositol-specific phospholipase C (PI-PLC) digestion, whereas FcγRIII-B is susceptible to PI-PLC treatment (Ravetch and Perussia, 1989; Scallon *et al.*, 1989). A serine is found at position 203 in FcγRIII-B, which determines the attachment of a GPI-anchor structure, while in FcγRIII-A a phenylalanine is found at this position. A stop codon in FcγRIII-B is converted to CGA in FcγRIII-A, which codes for arginine at position 234, thereby creating an open reading frame for 21 amino acids that form the cytoplasmic domain of FcγRIII-A.

Functionally, FcγRIII-A differs from FcγRIII-B by triggering the killing of antibody-coated target cells. Although both isoforms bind IgG-coated cells, polypeptide-anchored FcγRIII-A is also able to mediate phagocytosis of such target cells when it is co-expressed with the FcεRIγ subunit. Under similar conditions FcγRIII-B is not able to induce antibody-dependent cell-mediated cytotoxicity (ADCC) or phagocytosis (Nagarajan *et al.*, 1995). Instead, it has been postulated that GPI-linked FcγRIII may serve as a trap for immune complexes that do not activate PMNs. Consistent with this is the observation that cross-linking of FcγRIII-B with immune complexes does not induce a rise in intracellular calcium and phosphoinositide hydrolysis, whereas cross-linking of FcγRIII-A on NK cells does induce calcium immobilisation and hydrolysis of membrane phosphoinositides (Ravetch and Kinet, 1991).

The 2VG2 protein shares greatest overall amino acid identity with human IgG FcγRIII, particularly with the A isoform as the predicted protein also contains a 25 amino acid-long cytoplasmic tail. Phylogenetic analysis suggests early divergence of the 2VG2 protein from the class III receptors. The sequence divergence is interesting since eight highly homologous (94 - 99% global amino acid identity) class III receptor isoforms have been previously reported in the rat (Farber *et al.*, 1993; Farber and Sears, 1991; Zeger *et al.*, 1990), but 2VG2 shares only 46% global amino acid identity to the representative rat FcγRIII-C. All of the rat isoforms contain the polypeptide membrane linkage and, to date, no GPI-linked isoforms have been identified in the rat. Furthermore, the previously identified rat IgG FcγRIII isoforms have even less global amino acid identity with human FcγRIII-A (~ 50% global amino acid identity) than 2VG2 does, and the phylogenetic tree analysis has positioned them in the same group as the rat and human class II receptors. However, the phylogenetic tree was constructed solely on the global amino acid identities between the proteins. The transmembrane motifs that are conserved in the FcγRIII and FcεRIα subfamilies, as well as potential motifs found only in 2VG2 but not in the class III receptors, were not taken into account.

Interestingly, the 2VG2 mRNA was shown in this chapter to be about 3 kb in size. In contrast, the FcγRIII transcripts recognised by Northern blot in the rat are between 1.4 and 1.6 kb in size, while mouse FcγRIII and human FcγRIII-A mRNA are 1.4 kb and 2.2 kb, respectively (Peltz *et al.*, 1989; Zeger *et al.*, 1990). Moreover, only one 2VG2 transcript is identified in fetal rat skin by Northern analysis. This is consistent with reports of one mouse FcγRIII and human FcγRIII-A transcript, but contrasts the many FcγRIII transcripts previously identified in the rat using a single FcγRIII probe (Farber *et al.*, 1993; Farber and Sears, 1991; Zeger *et al.*, 1990). Therefore, the Northern blot data support the notion that 2VG2 is not another rat FcγRIII homologue but rather a novel member of the FcR family.

Efficient cell surface expression of the FcγRIII isoforms in rodents and FcγRIII-A in humans requires co-expression of the FcεRIγ chain or the homologous CD3ζ chain of the human T cell receptor (TCR) complex (Farber and Sears, 1991; Hibbs *et al.*, 1989; Lanier *et al.*, 1989). The transmembrane form of FcγRIII is non-covalently associated with the γ chain in most species and the ζ chain in humans, thus forming a homo- or heterodimer complex. In contrast, human FcγRIII-B is expressed on the cell surface without other subunits (Ravetch and Kinet, 1991). The γ chain and ζ chain share a common cytoplasmic signal transduction motif termed ITAM (immunoreceptor tyrosine-based activation motif), that consists of two YXXL boxes separated by seven amino acids (Lynch, 2000). No tyrosine motifs are located in the cytoplasmic domain of NK cell-FcγRIII, therefore, the association of the α chain of the receptor with the γ chain of FcεRI and/or the ζ chain of the TCR-CD3 complex is necessary for signal transduction mediated by tyrosine kinases. For example, the ADCC response occurs when transmembrane Fcγ class III receptors on effector cells are cross-linked by binding to the IgG molecules that are present on the sensitised target cell, inducing activation of Src family protein tyrosine kinases (PTKs). These PTKs phosphorylate tyrosine residues in the ITAMs located on the γ or ζ chains, causing their association with other PTKs and a biochemical cascade that results in effector cell activation and release of the cytotoxic granules that mediate the ADCC reaction (Lynch, 2000; Raghavan and Bjorkman, 1996). Protein tyrosine phosphorylation is also likely to play an important role in the phagocytic signal initiated by FcγRIII-associated subunits (Nagarajan *et al.*, 1995; Suzuki *et al.*, 2000).

In contrast, the predicted cytoplasmic domain of 2VG2 contains a possible tyrosine-containing SH2 domain (Tyr-Glu-Glu-Pro). Src homology 2 domains are found in a variety of signalling proteins and bind phosphotyrosine-containing peptide sequences. As such they provide tyrosine phosphorylation-dependent and sequence-specific contacts for assembly of

receptor signalling complexes. This indicates that if the 2VG2 protein is, in fact, a functional FcR, its association with other subunits containing the ITAM motif may not be necessary for signal transduction, as it contains its own phosphotyrosine binding domain. Site-directed mutagenesis of the tyrosine residue in the SH2 domain of the protein encoded by 2VG2 could show whether it is essential to 2VG2 function. Similarly, human FcγRII-A contains an ITAM motif within its cytoplasmic tail that is critically involved in the delivery of its phagocytic signal (Van den Herik-Oudijk *et al.*, 1995a and b). Furthermore, human FcγRII-A does not require any subunits for cell surface expression. Therefore, cell surface expression studies, such as COS cell transfection analysis and Ig-coated cell rosetting assays, could be performed to determine firstly if the 2VG2 protein is expressed on the cell surface and if so, if its expression is augmented by co-expression of other subunits. In turn, this would indicate whether or not the 2VG2 protein associates with other subunits to form heteroprotein complexes.

An eight-amino acid transmembrane motif that is evolutionarily conserved in the Fcγ class III receptors and FcεRIα, Leu-Phe-Ala-Val-Asp-Thr-Gly-Leu, is thought to contribute to the heteroprotein subunit interactions of these receptors (Farber and Sears, 1991). Interestingly, this sequence is not completely conserved in 2VG2. However, the amino acid differences between the two transmembrane motifs are conservative, suggesting that interactions between 2VG2 and other subunits may still occur. Moreover, the aspartic acid residue situated directly within the membrane-spanning segment of FcγRIII and FcεRIα is conserved in the 2VG2 sequence. This residue is believed to be involved in the interactions that occur between the transmembrane regions of FcγRIII and the FcεRIγ chain (Farber *et al.*, 1993; Farber and Sears, 1991). Similarly, the anomalous placement of the charged aspartic acid residue in the predominantly hydrophobic transmembrane domain predicted for 2VG2 implies a possible interaction with an accessory molecule. Farber and Sears (1991)

have described a model of the potential heteroprotein interactions between the transmembrane regions of rat FcγRIII and rat FcεRIγ that predicts neutralising electrostatic interactions occur between the following conserved negative and positive charged amino acid pairs:

1) the carboxyl of Asp_{234} in FcγRIII and the ε-amino of Lys_{29} in FcεRIγ; and

2) the imidazole of His_{220} in FcγRIII and the carboxyl of Asp_{11} in FcεRIγ (see Figure 4.17, purple residues).

Given the conservation of these sequences, this model is predicted to apply to the intramembrane heteroprotein complexes formed between FcγRIII (or FcεRIα) and FcεRIγ polypeptides from all species. The exception is that in the human FcγRIII and rat 2VG2 sequences His_{220} is replaced by glutamine (see Figure 4.17, purple residues), but this residue could also make polar contacts with Asp_{11} in FcεRIγ. This further supports the idea that interactions between 2VG2 and other subunits, such as FcεRIγ, may occur.

The predicted cytoplasmic sequence of 2VG2 also exhibits some identity to the amino acid sequence of FcγRIII. In particular, the four COOH-terminal amino acids, Pro-Gln-Asp-Lys, are conserved in the human, rat and mouse class III receptors as well as 2VG2. Since these FcγRIII isoforms are mainly expressed on NK cells, this COOH-terminal sequence, as well as the transmembrane motif discussed above, is believed to be directly involved in the signal transducing mechanism that triggers antibody-dependent NK-cell-mediated cytotoxicity and phagocytosis (Ravetch and Kinet, 1991; Zeger *et al.*, 1990). Likewise, the conservation of this sequence in the 2VG2 protein also suggests a possible involvement in ADCC and the lysis of target cells. Finally, it must be noted that the number and distribution of charged amino acids in human FcγRIII-A and the protein encoded by 2VG2 differ. However, further discussion of their significance to the structure, function and interactions of the 2VG2 protein would be speculative at this stage.

4.4.3 FcRs and their interactions with immunoglobulins: Evidence for 2VG2 being a homologue receptor

A structure-based sequence alignment by Sondermann *et al.* (1999) has provided support for a similar structure and Ig-like domain arrangement in all FcRs. Figure 4.17 shows the residues contributing with their side chains to interdomain contact in human FcγRIII as coloured in blue, namely Asp_{41}, Gln_{112}, His_{129} and Trp_{131}. The corresponding amino acid residues in human FcγRI, FcγRII and FcγRIα are all conserved, except Asp_{41} is conservatively replaced with glutamic acid in FcγRI and FcεRIα. The conservation of these amino acid residues in the protein encoded by 2VG2 suggests that they also contribute to interdomain contact and hence, that 2VG2 has a similar domain arrangement to the FcRs.

In each of the FcRs, it is the second extracellular domain that is responsible for the direct binding of Ig, with the first domain making an as yet undefined contribution to maintain optimal binding affinity. Mutagenesis studies and the subsequent localisation of Ig-binding regions in domain 2 of FcεRI, FcγRII and FcγRIII have identified common regions of these receptors that are involved in the interaction with their Ig ligands. The three regions involved in the binding of IgG by FcγRII and FcγRIII and in the binding of IgE by FcεRI are the BC, C'E and FG loops between the β-strands of the second domain (see Figure 4.18). The CC' loop of FcεRI and FcγRIII also contributes to Ig binding in both of these receptors, however, it does not appear to be involved in FcγRII (Hulett *et al.*, 1995 and 1999; Sondermann *et al.*, 1999). The two NH_2-terminal domains of FcγRI are closely related to the FcγRII/III domains and probably bind similarly to the Fc fragment of IgG. However, the third domain of FcγRI lacks the signature sequences conserved in the first two domains and it still unclear exactly how it enhances the binding affinity of FcγRI to IgG (Sondermann *et al.*, 1999). The binding site on IgG for all the FcγRs involves the hinge

```
1     M- - - - - - - - - - - - - - - - WYLLLPTALLLTVS   2VG2
1     M- - - - - - - - - - - - - - - - WQLLLPTALLLLVS   Human FcγRIII-A
1     MTLETQMF QNAHSGSQWLLPPLTMLLLFAF   Rat FcγRIII-C

16    SGV- GAGLQKAVVNLDPEWVRVLEEDCVIL   2VG2
16    AGMRTEDLPKAVVFLEPQWYRVLEKDSVTL   Human FcγRIII-A
31    ADRQTANLPKAVVKRDPPWI QVLKEDTVTL   Rat FcγRIII-C

45    RCQGTFSPEDNSTKWFHNKSLISHQDANYV   2VG2
46    KCQGAYSPEDNSTQWFHNESLISSQASSYF   Human FcγRIII-A
61    TCEGTHNPGNSSTQWFHNQSSTWGQVQASY   Rat FcγRIII-C

75    IQSARVKDSGMYRCQTAFSALSDPVQLDVH   2VG2
76    IDAATVDDSGEYRCQTNLSTLSDPVQLEVH   Human FcγRIII-A
91    TFKATVNDSGEYRCRMAHTSLSDPVHLEVI   Rat FcγRIII-C

105   ADWLLLQTTKRLFQEGDPIRLRCHSWRNTP   2VG2
106   IGWLLLQAPRWVFKEEDPIHLRCHSWKNTA   Human FcγRIII-A
121   SDWLLLQTPQLVFEEGETITLRCHSWKNKQ   Rat FcγRIII-C

135   VFKVTYLQNGKGKKYFHRNSELSISKATHA   2VG2
136   LHKVTYLQNGKGRKYFHHNSDFYIPKATLK   Human FcγRIII-A
151   LTKVLLFQNGKPVRYYYQSSNFSIPKANHS   Rat FcγRIII-C

165   DSGSYFCRGIIGRNNISSSASLQISIGD- - -   2VG2
166   DSGSYFCRGLFGSKNVSSETVNITITQGLA   Human FcγRIII-A
181   HSGNYYCKAYLGRTMHVSKPVTITVQGSAT   Rat FcγRIII-C

192   - PTSPSSFLPWHQITFCLLIGLLFAIDTVL   2VG2
196   VSTISSFFPPGYQVSFCLVMVLLFAVDTGL   Human FcγRIII-A
211   ASTSS- - - LVWFHAAFCLVMCLLFAVDTGL   Rat FcγRIII-C

221   YFSVQRSLQSSVAVYEEP- KLHWSKEPQDK   2VG2
226   YFSVKTNI RSSTRDWKDH- KFKWRKDPQDK   Human FcγRIII-A
238   YFCVRRNLQTSGEDWRKSLSVGKYKAPQDK   Rat FcγRIII-C
```

Figure 4.17 Sequence alignment indicating amino acids involved in interdomain contact and complex formation.

The amino acid residues of FcγRIII and 2VG2 that are potentially involved in heteroprotein contacts with FcεRIγ are coloured purple. The residues that may contribute to interdomain contact are coloured blue. Residues in human FcγRIII that are conserved in 2VG2 and appear to be the primary amino acids involved in complex formation with human Fc1 are underlined. The green asparagine residue is a potential *N*-glycosylation site located close to the binding region of the human FcγRIII-hFc1 complex. Red residues are those believed to bind the hinge peptide region of hFc1 (Sondermann *et al.*, 2000).

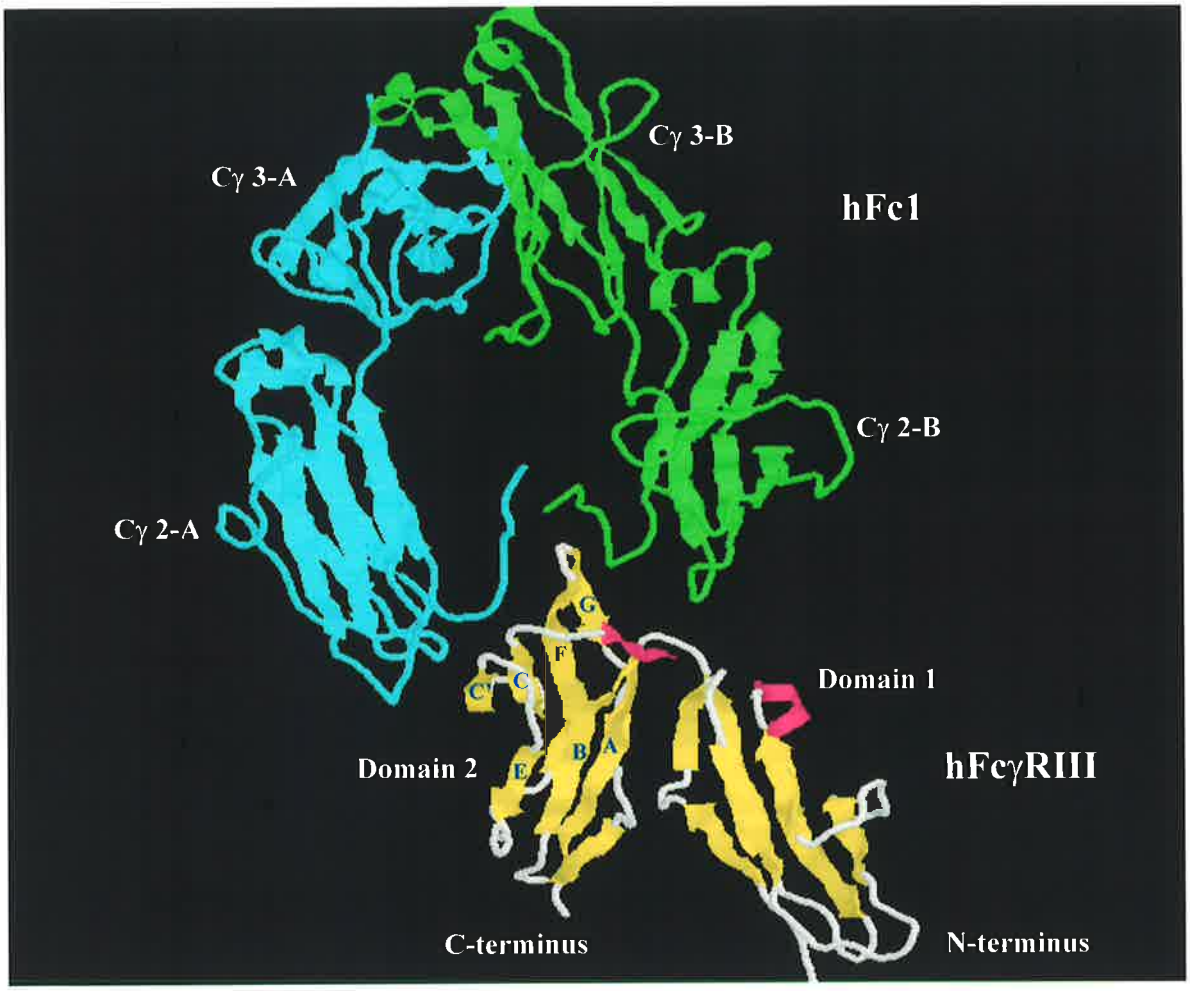

Figure 4.18 The overall structure of the soluble hFcγRIII-hFc1 complex.

Stereo ribbon representation with the dimer axis of the human Fc fragment of IgG1 (hFc1, light blue and green) orientated vertically. Figure was adapted from the hFcγRIII-hFc1 complex in the Protein Data Bank (accession code le4k). The β-strands of hFcγRIII are coloured yellow and those of domain 2 are labelled to highlight the loop regions implicated in IgG binding (BC, CC', C'E and FG).

and the hinge-proximal portion of the Cγ2 domain. The binding site for FcεRIα is at an analogous location on the IgE molecule, the Cε2-Cε3 interface. FcγRI, FcγRIII and FcεRI all have a 1:1 receptor-Ig stoichiometry (FcγRII has a 2:1 receptor-Ig stoichiometry), which suggests asymmetry in the Fc regions of receptor-bound Igs, such that one receptor binding site on the Fc homodimer is inaccessible (Raghavan and Bjorkman, 1996).

The elucidation of the molecular basis of FcR-Ig interactions is fundamental for understanding the mechanisms by which these receptors mediate biological functions such as activation of inflammatory cells, induction of cytokine release and destruction of pathogens (Hulett *et al.*, 1995). High-resolution crystal structures of the adhesion molecule-like receptors in complex with their Fc ligands have provided a more complex understanding of FcR-Ig interactions. From these crystal structure studies, a common model has recently been proposed that can describe the principal FcR interactions within the various complexes (Sondermann *et al.*, 2000). The primary binding motif in all FcR-Ig complexes appears to be the proline sandwich. In this arrangement, two tryptophans are conserved in all FcRs and the proline occurs in all IgG forms and IgE. In human FcγRIII, it is Trp_{108} and Trp_{131} that tightly encage Pro_{329} of the human Fc fragment of IgG1 (hFc1, see Figure 4.17, conserved residues are underlined). These tryptophan residues are conserved in the protein encoded by 2VG2, suggesting that they may also contribute to formation of the proline sandwich motif with Ig. Additional FcγRIII contact points that are also conserved in 2VG2 are the two lysine residues and the threonine (at positions 138, 149 and 140 in human FcγRIII, respectively, underlined in Figure 4.17) that interact with Asp_{265}, Glu_{269} and the NAG1 carbohydrate residue of human Fc1, respectively. Crystal structure studies have also revealed that one potential *N*-glycosylation site in human FcγRIII, Asn_{180}, is located close to the binding region of the FcγRIII-hFc1 complex (see Figure 4.17, green residue) (Sondermann *et al.*, 2000). This potential *N*-glycosylation site is also conserved in 2VG2.

Although the asparagine side chain points away from the binding site, a larger carbohydrate moiety in the FcγRIII is thought to influence the affinity to IgG.

The other central recognition site in FcR-Ig complexes is the hinge peptide of Ig. More sequence variation exists in this contact region and this is thought to be the reason for the differing affinities in the FcR-Ig pairs. For instance, Gly_{236} and Gly_{237} of the Cγ2-B domain hinge peptide are bound in the narrow channel between His_{137}, His_{153} and Lys_{138} in human FcγRIII (see Figure 4.17, red residues). Lys_{138} is conserved in human FcγRII but Val_{137} and Leu_{153} replace the histidine residues (Sondermann *et al.*, 2000). Likewise, lysine is conserved in 2VG2 but the histidine residues are replaced by phenylalanine and arginine, respectively (see Figure 4.17, red residues). One could postulate that the exchange of histidine for phenylalanine could create a small hydrophobic patch that may allow a tighter contact of receptor and hinge peptide. Yet, the substitution of the second histidine for the larger arginine side chain may have the opposite effect and reduce the affinity of 2VG2 for IgG. Nevertheless, the amino acid residues thought to be the primary sites of FcR-Ig contact are generally conserved in the 2VG2 protein, indicating that it may interact with ligands such as IgG.

4.4.4 Potential role of the 2VG2 gene product in fetal skin wound healing

The physiological function of the protein encoded by 2VG2 is not yet known, however, the specific upregulation of its mRNA following E17 but not E19 fetal skin wounding suggests that it is associated with wound closure in E17 skin. Another line of evidence supporting this idea comes indirectly from what is known about the functions of the related FcRs. Effector responses mediated by FcγRs include phagocytosis and endocytosis for immune complex clearance, ADCC for antitumour and antibacterial immunity and the release of cytokines for inflammation and immune regulation. For instance, FcγRIII-A

cross-linking to IgG results in transcriptional activation and release of specific cytokines like IL-6, IFN-γ and TNF (Morcos *et al.*, 1994; Ravetch and Kinet, 1991), that may be linked to the inflammatory response during adult wound repair. However, 2VG2 expression is not predicted to be linked to inflammation, as there is only a sparse inflammatory response during fetal wound repair and, in any case, the organ culture model used in this wound healing study eliminates the process of inflammation.

Instead, the FcR-related 2VG2 protein could be involved in the clearance of debris and damaged cells in the fetal wound for efficient, scar-free healing. The PMNs responsible for phagocytosis during early post-natal wound repair are largely absent from fetal wounds and inflammatory cells are not expected to be present in the organ culture model. Therefore, the 2VG2 protein might be expressed on other cells of non-haematopoietic origin in the fetal wound site that may be able to switch to a phagocytic state. The cellular localisation of 2VG2 has not yet been elucidated, but *in situ* hybridisation and immunohistochemical analyses will determine if the cell types that express 2VG2 mRNA and protein are also those known to be involved in wound healing, namely the cells of the epidermis and dermis.

As discussed in section 4.4.1, since 2VG2 upregulation appears to be restricted to cultured E17 skin explants, it is more likely that dermal cells, which include endothelial cells, fibroblasts and muscle cell precursors, are the candidate 2VG2-expressing cells. Indeed, dermal microvascular endothelial cells of normal human skin express FcγRII-A (Groger *et al.*, 1996) and FcγRIII-A has been found on activated endothelial cells (Tuijnman *et al.*, 1992a) and glomerular mesangial cells (Morcos *et al.*, 1994; Santiago *et al.*, 1989). In fact, expression of FcγRIII-A on human endothelial cells correlates with endothelial activation found in immunopathological and inflammatory conditions (Tuijnman *et al.*, 1992a). Since the E17 dermis is still developing and the cells in healing E17 dermal tissue may represent a more "activated cell type" as opposed to quiescent, unwounded dermal

tissue, one might speculate that they are more amenable to revert to a phagocytic phenotype and this change may require 2VG2 expression. This is supported by data showing that certain endothelial cells are capable of receptor-mediated endocytosis and phagocytosis (Dini *et al.*, 1995 and 2000; Emura *et al.*, 1992; Falasca *et al.*, 1993; Hamill *et al.*, 1986; Knolle and Gerken, 2000; Matsumoto *et al.*, 2000; Steffan *et al.*, 1986; van Velthuysen *et al.*, 1994; Vora and Karasek, 1994).

There are several indirect lines of evidence that support a participation of 2VG2 in phagocytosis or receptor-mediated endocytosis. Firstly, the GPI-anchored FcγRIII-B does not deliver a phagocytic signal whereas the polypeptide-anchored FcγRIII-A that is co-expressed with the γ subunit can deliver a signal for phagocytosis (Nagarajan *et al.*, 1995). The predicted amino acid sequence of 2VG2 has more identity to human FcγRIII-A than FcγRIII-B and like the former, contains a polypeptide anchor. Secondly, the polypeptide-anchored FcγRIII requires co-expression of the ITAM-containing γ subunit to mediate phagocytosis, whereas FcγRII-A contains a functionally critical ITAM motif within its own cytoplasmic domain that is believed to be directly involved in signalling phagocytosis (Van den Herik-Oudijk *et al.*, 1995a and b). Once the ITAM tyrosines are phosphorylated, the ITAM creates sites for the assembly of Src homology 2 (SH2) domains. From this point, the Src family of tyrosine kinases are differentially involved in FcγR signalling and certain kinases are able to fully transduce phagocytic signalling (Suzuki *et al.*, 2000). Although not an ITAM motif, the cytoplasmic tail of 2VG2 does contain a possible phosphotyrosine-binding SH2 domain that might also be capable of initiating a phagocytic signal. Thirdly, it has previously been shown that when transfected into mouse fibroblasts, human FcγRII-A mediates phagocytosis of sensitised erythrocytes (Tuijnman *et al.*, 1992b). This indicates that fibroblasts, including those that may be present in E17 dermis, possess the basic

machinery for ingestion and are capable of phagocytosis, provided that they are equipped with the appropriate receptor.

Other hints that the 2VG2 protein may be involved in the clearance of damaged cells come from the finding that, in addition to its role in ADCC, the related human FcγRIII-A is also directly involved in the killing of some virus-infected cells and tumour cells, independent of antibody binding. The presence of a putative FcγRIII-A ligand on appropriate target cells was recently demonstrated by the use of a FcγRIII-A-Ig fusion protein (Mandelboim *et al.*, 1999). A similar ligand for the 2VG2 protein may also be expressed on certain cells in response to stresses like wounding, to mediate their clearance for scarless fetal repair. The relative absence of B lymphocytes in the fetal wound site further supports the notion that the ligand for the predicted 2VG2 receptor is not an antibody. The nature of such a ligand for 2VG2 remains unknown, but it may be one or several of the known Ig superfamily members ubiquitously expressed on cells, since the FcγRIII ligand in ADCC is the Fc portion of Ig.

It is also important to note that a single transcript of similar size (3 kb) was also detected in rat lung by Northern analysis using the radiolabelled 300bp 2VG2 DD-PCR fragment. Given that ESTs showing high identity to the original 2VG2 DD-PCR fragment were identified in other tissues, it would be interesting to determine if these tissues also express the 2VG2 transcript and if its expression is linked to other physiological or developmental processes in the rat.

In summary, this study demonstrates the specific upregulation of the novel rat gene, denoted 2VG2, in cultured E17 skin from 4 hours to 24 hours post-wounding. Only basal levels of 2VG2 mRNA expression are seen in cultured E19 skin wounds. The differential expression of the 3 kb 2VG2 transcript during the early phases of repair in the organ culture model suggests that it is associated with wound closure in E17 fetal rat skin. Additionally,

the 5' sequence information of the gene represented by 2VG2 was obtained by 5' RACE. NCBI database analysis revealed that this transcript and its predicted protein sequence share the highest identity with the nucleotide and amino acid sequences of human FcγRIII-A, respectively. Although 2VG2 may appear to be a rat homologue of human FcγRIII-A at the overall amino acid level, it only shares about 46% amino acid identity with the previously identified and highly homologous rat class III isoforms. Furthermore, the eight-amino acid transmembrane motif characteristic of the FcγRIII and FcεRIα subfamilies is not completely conserved in the predicted 2VG2 protein. However, the amino acid residues that contribute to the interdomain contacts in FcRs, as well as those residues believed to be involved in FcR-Ig complex formation, are all conserved in the protein encoded by 2VG2. Therefore, it is likely that the sequence cloned here encodes a novel rat protein related to the IgG FcγRIII subfamily. Future protein expression and function studies would ultimately determine if rat 2VG2 encodes a novel and functional Fcγ receptor involved in the E17 wound response.

Chapter Five

General Discussion

5 General Discussion

Tissue repair in the mammalian fetus is fundamentally different to that seen in the post-natal animal. In the adult, wound repair is divided into the following well-characterised, overlapping, phases: haemostasis, inflammation, cell proliferation and wound contraction, and tissue remodeling (Clark, 1996b). This typically results in fibrosis and scar tissue formation. Scarring is a clinical problem of major importance that affects all organ systems through a multitude of diseases. This is because scar tissue never quite regains the strength of normal tissue and can disrupt the function and growth of an organ, and with regard to skin, its cosmetic appearance. Thus, the primary therapeutic objective of study in the area of wound healing, particularly with respect to fibrotic diseases, is to decrease or prevent scar formation. The most dramatic observation in modern wound healing research, therefore, is that most mammalian fetal wounds up to a certain point in gestation heal rapidly, with no acute inflammation, minimal cell proliferation and minimal or absent scar formation (Adzick and Longaker, 1992; Burrington, 1971; Dostal and Gamelli, 1993; Harrison and Adzick, 1991; Krummel *et al.*, 1987; Nodder and Martin, 1997; Rowlatt, 1979; Siebert *et al.*, 1990).

So in evolutionary terms, it appears that adult wounds are optimised for speed of healing under adverse, non-sterile conditions and the result is an excessive inflammatory infiltrate. The potential fetal regenerative response in adult wounds may be overrun by an inflammation-induced growth factor surplus leading to scar formation. Since the remarkable ability of the fetus to heal without scarring remains poorly understood, fetal wound healing studies are necessary to determine what accounts for scarring and how scar formation can be prevented (Adzick and Lorenz, 1994). This may lead to new treatment modalities to correct or prevent pathologic healing processes, like keloids, hypertrophic scars, burn contractures and hepatic and pulmonary fibrosis in children and adults (Adzick and Longaker, 1992). On

the other hand, defining the unique characteristics of fetal wound repair could also facilitate attempts to solve the anticipated wound healing problems of human fetal surgery (Olutoye and Cohen, 1996).

Many possible mechanisms associated with differential fetal wound healing have already been extensively investigated. For instance, although the sterile, intrauterine fetal environment may be a contributing factor to the final outcome, it is commonly recognised now that the unique fetal healing properties are not linked to its environment, but are intrinsic to the fetal tissue itself (Armstrong and Ferguson, 1995; Ihara and Motobayashi, 1992; Longaker *et al.*, 1994a; Martin and Lewis, 1992). Furthermore, fetal tissues and wounds have distinct growth factor ratios and the composition of the extracellular matrix (ECM) differs compared to adult wounds (Stern *et al.*, 1992; Whitby and Ferguson, 1991a, b and c). A transition from fetal to adult repair is also known to occur late in gestation (Longaker *et al.*, 1990b and 1992a; Longaker and Adzick, 1991; Lorenz *et al.*, 1993b), yet the intrinsic molecular factors that regulate this transition are far from fully determined. Numerous studies have found the late gestation transition from scarless healing to healing with scar formation correlates with gestational age-related changes in the growth factor response to wounding (Coleman *et al.*, 1998; Lin *et al.*, 1995; Martin *et al.*, 1993; Nath *et al.*, 1994a; Nodder and Martin, 1997; Soo *et al.*, 2000; Sullivan *et al.*, 1995b; Whitby and Ferguson, 1991a), the composition of the ECM (Longaker *et al.*, 1990b; Lovvorn, III *et al.*, 1999), the existence of myofibroblasts (Cass *et al.*, 1997c; Estes *et al.*, 1994) and the ability of the fetus to generate an inflammatory response (Armstrong and Ferguson, 1995; Cowin *et al.*, 1998; McCallion and Ferguson, 1996). Despite these exciting results, the overall clinical experience with growth factors and other mediators to improve post-natal wound healing has been discouraging. This supports the notion that the interactions occurring during fetal wound repair are more complex.

Extensive work in certain amphibians has demonstrated that, in contrast to mammals, they can almost flawlessly replace an amputated limb by substituting regeneration for repair (D'Jamoos *et al.*, 1998; Stocum, 1998). The developmental processes occurring during limb regeneration, including cell division, migration and differentiation, also occur during limb development of vertebrate embryos (Brockes, 1997; Tassava *et al.*, 1996) and many of the same ECM components are expressed, such as hyaluronate, fibronectin, laminin and tenascin (Ffrench-Constant and Hynes, 1989; Tassava *et al.*, 1996). Amphibian limb regeneration is also marked by the induction of homeobox gene expression (Brockes, 1997; Brown and Brockes, 1991; Reginelli *et al.*, 1995). Similarly, high levels of homeobox proteins, which are believed to be master developmental regulators, have been observed in early fetal tissues (Mackenzie *et al.*, 1991; Reginelli *et al.*, 1995). Hence, the cellular and molecular mechanisms functioning during limb regeneration very likely follow those involved in embryonic limb formation. In turn, it is possible that the genes expressed during amphibian limb regeneration are also expressed during regenerative fetal wound healing (Stocum, 1998). Indeed, the involvement of differentially expressed homeobox transcription factors has already been implicated in the control of mammalian scarless fetal wound repair (Brockes, 1997; Stelnicki *et al.*, 1998).

All in all, the studies discussed above led to the current hypothesis that novel proteins exist in fetal tissues that play a regulatory role in the fetal wound healing process. Therefore, the investigations reported in this project sought to identify other genes specifically expressed in fetal skin in age- and time-dependent manners during wound healing. Hence, the aims of the project were:

i) To establish a modified organ culture model based on that of Belford (1997) and confirm that the healing of multiple wounds occurs in embryonic day 17 (E17) but not in E19 rat skin;

ii) To quantify the healing of multiple wounds in E17 rat skin;

iii) To set up the differential display polymerase chain reaction (DD-PCR) protocol as a tool for comparing the gene expression profiles of E17 and E19 rat skin wounds; and

iv) To isolate, identify and characterise key genes that are differentially expressed during the E17 to E19 transition in wound healing.

In the second chapter of this thesis, an organ culture model of fetal wound repair was established. Multiple excisional wounds created in E17 fetal rat skins were shown to heal by movement of the epidermis over the wound margins and dermal contraction, as evidenced by histological analysis and wound area calculations, respectively. Although the E17 and E19 skin explants were wounded to a similar extent, the epithelial and dermal response to wounding that was mounted in E17 skin was not seen in E19 skin. This study clearly showed a difference in the wound response of skin taken from the E17 and E19 fetus and supports previous findings that a developmental transition in the mechanism of wound reepithelialisation and wound contraction occurs late in gestation. The *in vitro* transition in the wound response is also consistent with previous work that demonstrates the scar-free and scar-forming phenotypes are seen upon wounding E17 and E19 fetal rat skin, respectively (Houghton *et al.*, 1995; Ihara *et al.*, 1990; Ihara and Motobayashi, 1992; Soo *et al.*, 2000). Hence, the organ culture system provides a good model for investigating the transition in fetal rat skin wound healing.

Although elucidating the repair mechanism of the multiple wounds created in E17 skin was not an aim of this project, previous work in our laboratory has found actin polymerisation and condensation occurs in the epithelium of E17 rat skin wounds, indicating that it is causing the wounds to close (Allison Cowin, personal communication). This supports the actin cable purse-string mechanism of wound closure observed in other species including the fetal chick and mouse (Martin and Lewis, 1992; McCluskey *et al.*, 1993; McCluskey and Martin, 1995). No actin cables have been detected in the epithelial margins of the non-closing E19 rat wounds, although actin filaments are seen at the dermal wound

margin. These data suggest that a component of the fetal to adult transition in the mechanism of repair is a loss in the ability of the fetal epidermal cell to respond to wounding by migrating over the mesenchyme according to a substrate-independent purse-string mechanism. Recent studies have demonstrated that wound healing in *Drosophila* also involves actin recruitment to the wound margins and contraction of a newly-formed, supracellular purse-string (Kiehart *et al.*, 2000), which parallels observations in fetal vertebrate tissues. Additionally, experimental wound healing in cichlid fish appears to be fast and proceed centripetally from the wound margins (Quilhac and Sire, 1998 and 1999), similar to embryonic wound healing in mammals (McCluskey and Martin, 1995). Both of these observations have established *Drosophila* and cichlid fish as other candidate systems for the investigation of fetal-like wound repair. Therefore, the purse-string mechanism of wound closure *in vitro* fits the *in vivo* observations of wound healing in embryonic chick and mouse, as well as *Drosophila* and cichlid fish, and hence, further validates the use of the skin culture model for studying fetal excisional wound repair.

A major aim of the current study was to use DD-PCR to show that, in addition to their distinct wound responses, E17 and E19 fetal rat skin wounds also have distinct gene expression profiles. A common problem found by many researchers is that DD-PCR fingerprint patterns are not reproducible between experiments. For this reason DD-PCR has mainly been used to compare the regulation of genes in closely related cell populations, such as isolated cell lines maintained in tissue culture. Only recently have workers successfully used whole tissue systems comprising more than one major cell type in DD-PCR to study the differential expression of genes (Chen *et al.*, 1997; Darden *et al.*, 2000; Keshav *et al.*, 1997; Malhotra *et al.*, 1999; Soo *et al.*, 1999; Suzuki *et al.*, 1999; Utans *et al.*, 1994; Wang *et al.*, 1996). A limitation of using complex tissue systems is that differences in total expression levels of a certain gene could be the result of variation in cellular composition rather than actually reflecting transcriptional or translational regulation. This is particularly

true during wound repair due to the migration and proliferation of various cell types. As only minor changes in the cellular composition of skin can occur *in vitro*, this was another reason why an organ culture model was used to compare the E17 and E19 response to wounding.

For the DD-PCR comparison in this study, skins were harvested from E17 and E19 rats immediately after wounding or after 24 hours of culture. This time point was chosen because multiple wounds in E17 rat skin begin to close after 24 hours in culture, whereas wounds in E19 skin do not. Skin isolated in this way is primarily comprised of epidermal and dermal cells, with the latter including fibroblasts, endothelial cells and muscle cell precursors. Circulating inflammatory cells are not likely to be present, given that the dorsal skin explants are dissected off the fetuses and extensively washed in medium during the wounding process, prior to culturing. When using DD-PCR as a tool for the analysis of differential gene expression in such complex tissues and processes, the variety of mRNA populations present might lead to an increased number of false positives, or alternatively, to an under-representation of low abundance mRNA species within the PCR products. Chapter 3 of this thesis describes the numerous refinements made to the DD-PCR protocol to circumvent these drawbacks. The most important modification was the use of longer arbitrary primers and higher annealing temperatures during PCR compared to conventional DD-PCR protocols. This increased the specificity of the primer-DNA interaction, which resulted in a more reproducible banding pattern and greater success in the reamplification of candidate cDNA bands. The results of these DD-PCR experiments were consistent with the hypothesis that, in addition to their different responses to wounding, a different pattern of gene expression is detected in E17 and E19 fetal rat skin wounds.

A shortcoming of the DD-PCR work described here is that only a relatively small number of transcripts were identified by DD-PCR as being differentially expressed. This was unexpected as the multiple developmental and wound healing processes occurring

simultaneously in the skin culture model suggest the differential expression of numerous genes. One limitation of the current study was that only a small number of primer combinations were used, which would partly explain the low number of differentially expressed bands. It is also possible that instead of being differentially expressed at the transcriptional level, more genes could be regulated at the level of translation during wound healing, with further regulation of their encoding proteins also markedly distinguishing the E17 response to injury from the E19 response. Alternatively, it is possible that many transcripts were not identified because they are so rare that they are below the threshold sensitivity of DD-PCR. Indeed, Trenkle *et al.* (1998) reported the differential expression of a rare gene on cDNA arrays probed with RNA arbitrarily primed PCR (RAP-PCR) fingerprints, even though the gene was not abundant enough to be visualised on the original RAP-PCR fingerprint gel.

The final goal of this project, which was to isolate key genes, confirm their differential expression during the E17 to E19 transition in wound healing and then determine their identity, was addressed in Chapter 4. The cDNA bands differentially expressed only in E17 skin samples at 24 hours post-wounding were the transcripts of particular interest, due to their possible link to the scar-free fetal phenotype. Therefore, this project focussed on the identification and characterisation of one such candidate band that was revealed by DD-PCR to be strongly induced in E17 skin at 24 hours post-wounding but not in E19 skin. This gene was designated 2VG2 for the purpose of this study.

Ideally, the method for cloning specifically expressed transcripts should enable their efficient isolation and then identification of their full-length sequences in the shortest time and at the lowest cost possible (Wang *et al.*, 1997). The modified approach for isolating candidate clones outlined in this project is relatively simple, fast and applicable for use with limited tissue resources. The use of dot blot hybridisation for the initial screening of interesting bands makes it possible to evaluate large numbers of candidate clones

simultaneously. The method that was developed here successfully identified the clone of interest from other contaminating sequences. In doing so, the dot blot also confirmed the preferential upregulation of the transcript in E17 and not E19 fetal skin wounds. Many more animals and reagents would be required if this selection process used Northern blot alone.

A drawback of dot blot arrays is that they do not provide information about transcript size or quantify relative RNA expression levels between the cell populations being compared (Martin *et al.*, 1998). Therefore, Northern blot analysis was used to further analyse the expression of the gene represented by 2VG2. Consistent with the DD-PCR results, no 2VG2 mRNA expression was detected in fetal rat skin immediately after wounding (t=0) or in E19 skin over the 24 hour period after wounding by Northern blotting. In contrast, elevated levels of the 3 kb 2VG2 mRNA were seen in wounded E17 skin explants after just 4 hours of culture and expression levels were shown to fall after about 24 hours of culture. These successful verifications are evidence that carefully performed DD-PCR experiments can yield accurate data. It is important to note that RT-PCR revealed 2VG2 to be present in E19 as well as E17 skin, indicating that basal expression of 2VG2 mRNA occurs in both skins but upregulation of the gene is specific to cultured E17 explants.

The upregulation of the 2VG2 transcript during the early phases of repair in the organ culture model also provides preliminary evidence of a role for 2VG2 in the wound response of E17 fetal rat skin. The expression profiles of 2VG2 at 24 hours or more post-wounding were not assessed and it is possible that E19 skin wounds do upregulate this gene at later time points. Importantly then, the results presented so far can only suggest that it is the differential expression of the 2VG2 transcript, rather than its presence, that may be crucial to the different wound responses seen in the E17 and E19 fetuses. This has previously been demonstrated for many ECM components and growth factors, the most notable being TGFβ1, which is selectively upregulated in adult but not fetal wounds, and hence, believed to contribute to fibrotic wound repair (Longaker *et al.*, 1989b and 1990b; Sullivan *et al.*,

1995b; Whitby *et al.*, 1991; Whitby and Ferguson, 1991a, b and c). To determine if the role of 2VG2 in healing is specifically associated with the wound closure observed in E17 skin *in vitro*, antisense oligonucleotides targeted to 2VG2 could be tested to see if they can effectively block the closure of excisional wounds in culture. Alternatively, since 2VG2 is predicted to encode a transmembrane protein, antibody blockade could also be used to try to inhibit excisional wound closure.

The use of 5' RACE to obtain potentially full-length cDNA transcripts clearly facilitates the characterisation of identified DD-PCR clones. The 5' RACE and PCR-based cloning strategy described here was carried out in considerably less time than it would take using traditional methods, such as cDNA library construction and screening. Moreover, it allowed the predicted full-length open reading frame of the 2VG2 transcript to be successfully obtained. Conceptual translation of the 2VG2 transcript revealed a 249 amino acid protein with multiple motifs characteristic of a membrane-bound glycoprotein. Database searches and amino acid alignments indicate that the protein encoded by 2VG2 may be a novel rat receptor for the Fc portion of immunoglobulins (FcRs).

In particular, rat 2VG2 has the most identity (61%) with human immunoglobulin G (IgG) FcγRIII-A and only 46% amino acid identity to the rat FcγRIII isoforms. However, it is not expected to be a true homologue of FcγRIII-A, as the eight-amino acid transmembrane motif characteristic of the FcγRIII and FcεRIα subfamilies is not completely conserved in the predicted 2VG2 protein. The unique tissue distribution and inducibility of 2VG2 further supports this notion. The 2VG2 transcript is expressed in fetal rat skin and its levels appear to be increased in response to wounding. In contrast, the FcγRs are primarily expressed on leukocytes, although some class II and III receptors have been found on non-haematopoietic cells (Groger *et al.*, 1996; Lyden *et al.*, 2001; Morcos *et al.*, 1994; Nishikiori *et al.*, 1993; Santiago *et al.*, 1989; Stuart *et al.*, 1989; Tuijnman *et al.*, 1992a), and are involved in

immune defence. They bind immune complexes or antibody ligands to initiate specific immune functions associated with tumour and viral immunity, inflammation and allergy, depending on the receptor structure and the expressing cell type (reviewed in Raghavan and Bjorkman (1996) and Ravetch and Kinet (1991)). Nevertheless, the amino acid residues that contribute to the interdomain contacts in FcRs, as well as those residues believed to be involved in FcR-Ig complex formation, are all conserved in the protein encoded by 2VG2. Therefore, it is likely that the sequence cloned here encodes a novel rat protein related to the IgG FcγRIII subfamily.

Future protein expression and function studies would ultimately determine if rat 2VG2 encodes a novel and functional FcγR. For instance, COS cell transfection analysis and Ig-coated cell rosetting assays could be performed to determine firstly if the 2VG2 protein is expressed on the cell surface and if so, if its expression is augmented by co-expression of other subunits. Northern analyses could also be performed to determine if the wounded rat tissue that express 2VG2 co-express other subunit transcripts such as FcεRIγ or CD3ζ. Together, these data would indicate whether or not the 2VG2 protein associates with other subunits to form heteroprotein complexes. To assay for the ligand binding specificity of 2VG2, transfectants could then be tested for their ability to bind and rosette sheep red blood cells coated with monoclonal antibodies of different rat and human IgG subclasses.

If 2VG2 is confirmed to encode a new FcγRIII-related polypeptide, it will be necessary to address its functional and physiological significance in the rat, as the other eight class III isoforms that exist in the rat are far more highly conserved at the amino acid level. The rat class III receptor isoforms are thought to have different IgG-binding specificities for different rat IgG isotypes, so the expression of 2VG2 may increase the antibody-binding capacity of FcγRIII-bearing cells in the rat even more. Additionally, the DNA database searches conducted in this study have yielded many rat expressed sequence tags (ESTs) with

very high identity to the rat 2VG2 DD-PCR product. These sequences are likely to code for the same protein since the ESTs also share very high identity to each other. Judging from the many different origins of the ESTs, it is possible that the 2VG2 gene is expressed in a variety of organs. Future work should, therefore, focus on determining the cellular localisation of the 2VG2 mRNA in the fetal wound site, and in other organs, by *in situ* hybridisation. This would elucidate whether or not 2VG2 mRNA is expressed in cells primarily of haematopoietic origin like the other known FcRs, or if it is expressed in non-haematopoietic cells such as the epidermal and dermal cells known to be involved in fetal wound healing.

Moreover, it is unknown whether or not the 2VG2 protein level or its post-translational modification correlate with the changes that are seen in 2VG2 mRNA expression in E17 fetal rat skin wounds. This question could be addressed by raising an antiserum to determine 2VG2 protein abundance in E17 fetal rat skin wounds and unwounded controls by immunohistochemistry. The time course of mRNA expression could also be taken into account to determine the time-dependent expression of the 2VG2 protein during wound healing processes in the E17 fetus.

A specific role for the FcRs in wound healing has not yet been described, but comparison of the known functions of some FcRs with facts known about fetal wound healing allows a mechanism to be suggested by which FcγR-related 2VG2 may affect this physiological process. Classically, the FcRs are key mediators of various immune response processes, including phagocytosis and endocytosis for immune complex clearance, antibody-dependent cell-mediated cytotoxicity (ADCC) for antitumour and antibacterial immunity and the release of cytokines for inflammation and immune regulation that may serve to regulate wound healing events. The expression of 2VG2 is not expected to be linked to inflammation, as a key difference between scarless repair and scar formation is the relative absence of inflammation and proinflammatory cytokines in fetal wound healing

(Nodder and Martin, 1997). In any case, the organ culture model used in this wound healing study eliminates the process of inflammation. Therefore, the 2VG2 protein is more likely to be involved in the clearance of debris and damaged cells in the fetal wound for efficient, scar-free healing. Evidence supporting this role for 2VG2 is indirect and speculative, but nonetheless, still worthy of mention.

Briefly, it is already known that FcγRIII-A can be expressed on human endothelial cells, and this expression correlates with endothelial activation found in immunopathological conditions (Tuijnman *et al.*, 1992a). Similarly, such activated cells in the developing E17 dermis might also be stimulated to express FcγR-related 2VG2 in response to wounding. Since certain endothelial cells are capable of phagocytosis and receptor-mediated endocytosis (Dini *et al.*, 1995 and 2000; Emura *et al.*, 1992; Falasca *et al.*, 1993; Hamill *et al.*, 1986; Knolle and Gerken, 2000; Matsumoto *et al.*, 2000; Steffan *et al.*, 1986; van Velthuysen *et al.*, 1994; Vora and Karasek, 1994), the expression of 2VG2 might also stimulate these activated E17 dermal cells to revert to a phagocytic phenotype, given the absence of phagocytic polymorphonuclear leukocytes in the developing fetus. The presence of the polypeptide anchor, particularly the four conserved COOH-terminal amino acids, Pro-Gln-Asp-Lys, and the Src homology 2 phosphotyrosine-binding domain in the cytoplasmic tail of 2VG2, further suggest that 2VG2 might be capable of initiating a phagocytic signal (Ravetch and Kinet, 1991; Suzuki *et al.*, 2000; Zeger *et al.*, 1990). Once the ligand for 2VG2 has been discovered, a phagocytosis assay or the micropipette technique for observing phagocytosis at the single cell level (Nagarajan *et al.*, 1995) could be used to determine if 2VG2 is capable of mediating phagocytosis.

The relative absence of B lymphocytes in the fetal wound site, particularly in the organ culture model used in this study, suggests that the ligand for the predicted 2VG2 receptor is not an antibody. This is quite possible as, in addition to its role in ADCC, the related human

FcγRIII-A is also directly involved in the lysis of some virus-infected cells and tumour cells independent of antibody binding. Indeed, the presence of a putative FcγRIII-A ligand on appropriate target cells was recently demonstrated by the use of a FcγRIII-A-Ig fusion protein (Mandelboim *et al.*, 1999). A similar ligand for the 2VG2 protein may also be expressed on damaged cells to mediate their phagocytosis and clean up the fetal wound for scarless repair. The nature of such a ligand for 2VG2 remains unknown, but it may be one or several of the known Ig superfamily members ubiquitously expressed on cells, since the FcγRIII-A ligand in ADCC is the Fc portion of Ig. In short, future studies on the expression of 2VG2 during development and the wounding response, as well as functional studies on its interactions with other protein subunits and ligands, should help clarify the question of its role in fetal excisional wound closure. Confirmation of the hypothesis that the protein encoded by 2VG2 is a novel FcγR involved in the clearance of debris and damaged cells during scarless wound repair could lead to novel strategies for more efficient healing of post-natal wounds.

It is in no way claimed in this study that 2VG2 is the primary factor involved in E17 wound closure. The process is complex and the interaction of many gene products is expected to contribute to the effect. Greater knowledge of gene regulation in fetal skin wounds is important for understanding the molecular basis of scarless wound healing. The future of research in this area lies partly in the development of more sensitive techniques for detecting differential expression. At the commencement of this project, subtractive hybridisation, electronic subtraction and DD-PCR were all common methods for identifying differentially expressed genes, but DD-PCR was considered to be the more superior technique (Wan *et al.*, 1996). Despite its wide application in studying differential gene expression in various disease states and biological systems, there were no other fetal wound healing studies reporting the use of DD-PCR at this time. In fact, only recently has DD-

PCR been used to identify new genes that are differentially expressed during post-natal wound repair.

In the first instance, this technique was used to isolate genes regulated by TGFβ1 in cultured keratinocytes, in order to gain insight into the mechanisms of TGFβ1 action in skin (Munz *et al.*, 1997; Werner *et al.*, 2000). TGFβ1 was chosen because of its strong induction during adult wound repair (Frank *et al.*, 1996). Together, the results of these studies led to the hypothesis that wound-derived growth factors like TGFβ1 induce the expression of p11, but suppress keratin 15, after skin injury. Hence, both of these studies identified potential repair-related peptides not previously known to be involved in post-natal wound healing.

DD-PCR has also been directly performed on wounds in the post-natal mouse and rat to search for genes that are regulated by skin injury (Munz *et al.*, 1999; Soo *et al.*, 1999). Both of these studies identified a gene that is significantly upregulated at 12 hours post-wounding. Additionally, immunohistochemistry showed significant induction of their cognate protein products during wound healing. Evidence suggested that the differentially expressed gene identified in the mouse, skeletal muscle nascent polypeptide-associated complex, is involved in modulating muscular repair processes after wounding (Munz *et al.*, 1999). In contrast, the gene identified in the rat was novel and, therefore, it was predicted to be associated with fibroblast proliferation during wound healing, as its marked upregulation correlates with the inflammatory and early granulation tissue phases of repair (Soo *et al.*, 1999).

Only very recently have other reports been published on the study of scarless fetal wound repair by DD-PCR (Darden *et al.*, 2000; Li *et al.*, 2000). In contrast to the present *in vitro* rat model that compared the healing of excisional wounds, both of these studies used an *in vivo* model that compared the healing of incisional wounds between E21 fetal and adult rabbits. It is likely that the authors looked at incisional wounds because they are known to heal without scarring in the early fetal rabbit, unlike excisional wounds that do not

close in this species *in utero* (Haynes *et al.*, 1989; Krummel *et al.*, 1989; Somasundaram and Prathap, 1970). Unwounded and wounded skin from the fetal and adult rabbit was harvested at 12 hours post-wounding for the DD-PCR comparison. The differentially expressed genes identified in the first study included a chaperonin-like transcript that was downregulated in fetal wounds, and a glycophorin-like transcript, 28S rRNA and four other unknown sequences that were all upregulated in fetal wounds (Darden *et al.*, 2000). The second study identified the E-prostanoid (EP4) receptor for prostaglandin E_2 (PGE_2) as being preferentially induced in wounded fetal rabbit skin. Like the project described in this thesis, only the differential expression of genes during fetal and adult wound healing was investigated in both of these studies. The expression of the proteins encoded by the identified genes, or their putative function during wound healing, was not determined. However, both authors postulated on the possible roles of these proteins during wound healing. For instance, as chaperonins mediate the folding of denatured proteins such as actin to their functional state, the authors hypothesised that the chaperonin-like transcript isolated in the first study might help fold α-smooth muscle actin to form stress fibres during myofibroblast formation in scarring wounds. Therefore, the downregulation of the chaperonin-like transcript seen in fetal rabbit skin wounds was speculated to inhibit myofibroblast formation, which is consistent with the absence of myofibroblasts in scar-free wound healing. The authors of the second study suggested that PGE_2 might be involved in the differential cellular responses and in the regulation of intracellular signal transduction during fetal wound repair, through its binding to the upregulated EP4 receptor. Although both of these functional postulations are conjecture, the DD-PCR investigations did identify potential repair-related genes that were not previously known to play a role in fetal wound healing. The studies also support the idea that fetal wound healing is complex, with still many unknown genetic and biochemical mechanisms contributing to the result.

Complementary DNA microarray technology is another RNA fingerprinting method representing a new generation of approaches to isolate and characterise differentially expressed genes. Although classical DD-PCR remains a powerful technique for studying altered gene expression, arrays containing thousands of cDNA clones from various tissues, stages of development and disease states are now available that permit the simultaneous evaluation of both up- and down-regulated genes in control and treated samples (Alizadeh and Staudt, 2000; Bowtell, 1999; Pennie, 2000; Trenkle *et al.*, 1998). Although some cDNA microarray analyses have been conducted on cultured fibroblasts (Iyer *et al.*, 1999; Shelton *et al.*, 1999) and skin wounds (Tsou *et al.*, 2000) to investigate differential gene expression during post-natal repair processes, no fetal wound healing studies using microarrays have been reported to date. This technology is currently underway in our laboratory to improve on the work done here with DD-PCR so that, when combined with other novel proteomic tools, a more complete picture of the differences occurring during the E17 to E19 transition in wound healing will emerge.

In conclusion, this study describes the successful isolation and identification of a novel rat gene. The gene was demonstrated to be differentially expressed in E17 fetal rat skin explants using an *in vitro* model of excisional wound closure and DD-PCR. Northern blot analysis confirmed the specific upregulation of the gene in E17 rat skin in response to wounding. In contrast, the gene was not upregulated in E19 rat skin, indicating that its function may assist E17 fetal skin wound closure. The full-length open reading frame of the gene was obtained by 5' RACE and database analysis revealed the translated protein product to have high identity to human FcγRIII-A, but to be distinct from all known rat FcγRIII isoforms. To date, no other FcγR has been implicated in fetal wound healing but their role in immune defence suggests that the FcγRIII-related gene may be involved in clearing the

fetal wound for efficient, scarless repair. Finally, these results demonstrate that RNA fingerprinting methods like DD-PCR can provide powerful insight into the molecular mechanisms of fetal wound healing by both large-scale gene screening and identification of novel genes associated with repair. Information so obtained on gene regulation during fetal skin wound repair could allow us to orchestrate the expression of a variety of genes that control the wound cellular milieu. In this way, we might be able to modulate the normal scar-forming response currently seen in post-natal wounds to the scar-free response seen in fetal wounds.

References

References

Abatangelo, G., Martelli, M., and Vecchia, P. (1983). Healing of hyaluronic acid-enriched wounds: Histological observations. *J Surg Res* **35**: 410-416.

Abraham, J. A. and Klagsbrun, M. (1996). Modulation of wound repair by members of the fibroblast growth factor family. *In* "The Molecular and Cellular Biology of Wound Repair" (R. A. F. Clark, Ed.), pp. 195-248, Plenum Press, New York.

Adolph, V. R., DiSanto, S. K., Bleacher, J. C., Dillon, P. W., and Krummel, T. M. (1993). The potential role of the lymphocyte in fetal wound healing. *J Pediatr Surg* **28**: 1316-1320.

Adzick, N. S., Harrison, M. R., Glick, P. L., Beckstead, J. H., Villa, R. L., Scheuenstuhl, H., and Goodson, W. H. 3. (1985a). Comparison of fetal, newborn, and adult wound healing by histologic, enzyme-histochemical, and hydroxyproline determinations. *J Pediatr Surg* **20**: 315-319.

Adzick, N. S. and Longaker, M. T. (1991). Animal models for the study of fetal tissue repair. *J Surg Res* **51**: 216-222.

Adzick, N. S. and Longaker, M. T. (1992). Scarless fetal healing. Therapeutic implications. *Ann Surg* **215**: 3-7.

Adzick, N. S. and Lorenz, H. P. (1994). Cells, matrix, growth factors, and the surgeon. The biology of scarless fetal wound repair. *Ann Surg* **220**: 10-18.

Adzick, N. S., Outwater, K. M., Harrison, M. R., Davies, P., Glick, P. L., deLorimier, A. A., and Reid, L. M. (1985b). Correction of congenital diaphragmatic hernia *in utero*. IV. An early gestational fetal lamb model for pulmonary vascular morphometric analysis. *J Pediatr Surg* **20**: 673-680.

Agren, M. S. (1999). Matrix metalloproteinases (MMPs) are required for re-epithelialization of cutaneous wounds. *Arch Dermatol Res* **291**: 583-590.

Airola, K., Ahonen, M., Johansson, N., Heikkilä, P., Kere, J., Kähäri, V. M., and Saarialho-Kere, U. K. (1998). Human TIMP-3 is expressed during fetal development, hair growth cycle, and cancer progression. *J Histochem Cytochem* **46**: 437-447.

Alaish, S. M., Bettinger, D. A., Olutoye, O. O., Gould, L. J., Yager, D. R., Davis, A., Crossland, M. C., Diegelmann, R. F., and Cohen, I. K. (1995). Comparison of the polyvinyl alcohol sponge and expanded polytetrafluoroethylene subcutaneous implants as models to evaluate wound healing potential in human beings. *Wound Rep Reg* **3**: 292-298.

Alaish, S. M., Yager, D., Diegelmann, R. F., and Cohen, I. K. (1994). Biology of fetal wound healing: Hyaluronate receptor expression in fetal fibroblasts. *J Pediatr Surg* **29**: 1040-1043.

Alizadeh, A. A. and Staudt, L. M. (2000). Genomic-scale gene expression profiling of normal and malignant

immune cells. *Curr Opin Immunol* **12**: 219-225.

Altschul, S. F., Gish, W., Miller, W., Myers, E. W., and Lipman, D. J. (1990). Basic local alignment search tool. *J Mol Biol* **215**: 403-410.

Appel, R. D., Bairoch, A., and Hochstrasser, D. F. (1994). A new generation of information retrieval tools for biologists: the example of the ExPASy WWW server. *Trends Biochem Sci* **19**: 258-260.

Armstrong, J. R. and Ferguson, M. W. (1995). Ontogeny of the skin and the transition from scar-free to scarring phenotype during wound healing in the pouch young of a marsupial, *Monodelphis domestica. Dev Biol* **169**: 242-260.

Arnold, F., Jia, C., He, C., Cherry, G. W., Dphil, O., Carbow, B., Meyer-Ingold, W., Bader, D., and West, D. C. (1995). Hyaluronan, heterogeneity, and healing: The effects of ultrapure hyaluronan of defined molecular size on the repair of full -thickness pig skin wounds. *Wound Rep Reg* **3**: 299-310.

Arumugam, S., Jang, Y. C., Chen-Jensen, C., Gibran, N. S., and Isik, F. F. (1999). Temporal activity of plasminogen activators and matrix metalloproteinases during cutaneous wound repair. *Surgery* **125**: 587-593.

Austyn, J. M. and Gordon, S. (1981). F4/80, a monoclonal antibody directed specifically against the mouse macrophage. *Eur J Immunol* **11**: 805-815.

Axel, R., Feigelson, P., and Schutz, G. (1976). Analysis of the complexity and diversity of mRNA from chicken liver and oviduct. *Cell* **7**: 247-254.

Bairoch, A., Bucher, P., and Hofmann, K. (1997). The PROSITE database, its status in 1997. *Nucleic Acids Res* **25**: 217-221.

Barnes, W. M. (1994). PCR amplification of up to 35-kb DNA with high fidelity and high yield from lambda bacteriophage templates. *Proc Natl Acad Sci USA* **91**: 2216-2220.

Battelino, T., Miralles, F., Krzisnik, C., Scharfmann, R., and Czernichow, P. (2000). TGF-β activates genes identified by differential mRNA display in pancreatic rudiments. *Pflugers Arch* **439**: R26-R28.

Bauer, D., Muller, H., Reich, J., Riedel, H., Ahrenkiel, V., Warthoe, P., and Strauss, M. (1993). Identification of differentially expressed mRNA species by an improved display technique (DDRT-PCR). *Nucleic Acids Res* **21**: 4272-4280.

Bauer, E. A., Cooper, T. W., Huang, J. S., Altman, J., and Deuel, T. F. (1985). Stimulation of *in vitro* human skin collagenase expression by platelet-derived growth factor. *Proc Natl Acad Sci USA* **82**: 4132-4136.

Belford, D. A. (1997). The mechanism of excisional fetal wound repair *in vitro* is responsive to growth factors. *Endocrinology* **138**: 3987-3996.

Bennett, N. T. and Schultz, G. S. (1993). Growth factors and wound healing: Part II. Role in normal and

chronic wound healing. *Am J Surg* **166**: 74-81.

Bhattacharjee, A., Rutherford, M.S., Abrahamsen, M.S., Lappi, V.R. and Schook, L.B. (1997). Refinements in re-amplification and cloning of DDRT-PCR products. *Biotechniques* **22**: 1048-1051.

Bishop, J. O., Morton, J. G., Rosbash, M., and Richardson, M. (1974). Three abundance classes in HeLa cell messenger RNA. *Nature* **250**: 199-204.

Blewett, C. J., Cilley, R. E., Ehrlich, H. P., Blackburn, J. H., II, Dillon, P. W., and Krummel, T. M. (1997). Regenerative healing of incisional wounds in midgestational murine hearts in organ culture. *J Thorac Cardiovasc Surg* **113**: 880-885.

Blewett, C. J., Cilley, R. E., Ehrlich, H. P., Dillon, P. W., Blackburn, J. H. 2., and Krummel, T. M. (1995). Regenerative healing of incisional wounds in murine fetal lungs maintained in organ culture. *J Pediatr Surg* **30**: 945-948.

Border, W. A., Noble, N. A., Yamamoto, T., Harper, J. R., Yamaguchi, Y., Pierschbacher, M. D., and Ruoslahti, E. (1992). Natural inhibitor of transforming growth factor-β protects against scarring in experimental kidney disease. *Nature* **360**: 361-364.

Border, W. A., Okuda, S., Languino, L. R., Sporn, M. B., and Ruoslahti, E. (1990). Suppression of experimental glomerulonephritis by antiserum against transforming growth factor beta 1. *Nature* **346**: 371-374.

Bowtell, D. D. (1999). Options available - from start to finish - for obtaining expression data by microarray. *Nat Genet* **21**: 25-32.

Brenz Verca, M. S., Brenz, V. S., Rusconi, S., and Dreyer, J. L. (1998). Modification of primer design facilitates the use of differential display. *Biotechniques* **24**: 374-380.

Brock, J., Midwinter, K., Lewis, J., and Martin, P. (1996). Healing of incisional wounds in the embryonic chick wing bud: Characterization of the actin purse-string and demonstration of a requirement for Rho activation. *J Cell Biol* **135**: 1097-1107.

Brockes, J. P. (1997). Amphibian limb regeneration: Rebuilding a complex structure. *Science* **276**: 81-87.

Broker, B. J., Chakrabarti, R., Blynman, T., Roesler, J., Wang, M. B., and Srivatsan, E. S. (1999). Comparison of growth factor expression in fetal and adult fibroblasts: a preliminary report. *Arch Otolaryngol Head Neck Surg* **125**: 676-680.

Broker, B. J. and Reiter, D. (1994). Fetal wound healing. *Otolaryngol Head Neck Surg* **110**: 547-549.

Brooks, D. G., Qiu, W. Q., Luster, A. D., and Ravetch, J. V. (1989). Structure and expression of human IgG FcRII(CD32). Functional heterogeneity is encoded by the alternatively spliced products of multiple genes. *J Exp Med* **170**: 1369-1385.

Brown, G. L., Curtsinger, L., Brightwell, J. R., Ackerman, D. M., Tobin, G. R., Polk, H. C., George-Nascimento, C., Valenzuela, P., and Schultz, G. S. (1986). Enhancement of epidermal regeneration by biosynthetic epidermal growth factor. *J Exp Med* **163**: 1319-1324.

Brown, R. and Brockes, J. P. (1991). Identification and expression of a regeneration-specific homeobox gene in the newt limb blastema. *Development* **111**: 489-496.

Bucala, R., Spiegel, L. A., Chesney, J., Hogan, M., and Cerami, A. (1994). Circulating fibrocytes define a new leukocyte subpopulation that mediates tissue repair. *Mol Med* **1**: 71-81.

Bullard, K. M., Cass, D. L., Banda, M. J., and Adzick, N. S. (1997). Transforming growth factor beta-1 decreases interstitial collagenase in healing human fetal skin. *J Pediatr Surg* **32**: 1023-1027.

Burd, D. A., Greco, R. M., Regauer, S., Longaker, M. T., Siebert, J. W., and Garg, H. G. (1991). Hyaluronan and wound healing: A new perspective. *Br J Plast Surg* **44**: 579-584.

Burd, D. A., Longaker, M. T., Adzick, N. S., Compton, C. C., Harrison, M. R., Siebert, J. W., and Ehrlich, H. P. (1990b). Fetal wound healing: an in vitro explant model. *J Pediatr Surg* **25**: 898-901.

Burd, D. A., Longaker, M. T., Adzick, N. S., Harrison, M. R., and Ehrlich, H. P. (1990a). Fetal wound healing in a large animal model: the deposition of collagen is confirmed. *Br J Plast Surg* **43**: 571-577.

Burd, D. A., Siebert, J. W., Ehrlich, H. P., and Garg, H. G. (1989). Human skin and post-burn scar hyaluronan: demonstration of the association with collagen and other proteins. *Matrix* **9**: 322-327.

Burkitt, H. G., Young, B., and Heath, J. W. (1993). Skin. *In* "Wheater's Functional Histology: A text and colour atlas" (B. Young, H. G. Burkitt, and J. W. Heath, Eds.), pp. 153-169, Churchill Livingstone Inc, New York.

Burrington, J. D. (1971). Wound healing in the fetal lamb. *J Pediatr Surg* **6**: 523-528.

Bux, J., Stein, E. L., Bierling, P., Fromont, P., Clay, M., Stroncek, D., and Santoso, S. (1997). Characterization of a new alloantigen (SH) on the human neutrophil Fc gamma receptor IIIb. *Blood* **89**: 1027-1034.

Callard, D., Lescure, B., and Mazzolini, L. (1994). A method for the elimination of false positives generated by the mRNA differential display technique. *Biotechniques* **16**: 1096-3.

Canady, J. W., Landas, S. K., Morris, H., and Thompson, S. A. (1994). *In utero* cleft palate repair in the ovine model. *Cleft Palate Craniofac J* **31**: 37-44.

Cass, D. L., Bullard, K. M., Sylvester, K. G., Yang, E. Y., Longaker, M. T., and Adzick, N. S. (1997b). Wound size and gestational age modulate scar formation in fetal wound repair. *J Pediatr Surg* **32**: 411-415.

Cass, D. L., Bullard, K. M., Sylvester, K. G., Yang, E. Y., Sheppard, D., Herlyn, M., and Adzick, N. S. (1998). Epidermal integrin expression is upregulated rapidly in human fetal wound repair. *J Pediatr Surg* **33**: 312-316.

Cass, D. L., Meuli, M., and Adzick, N. S. (1997a). Scar wars: Implications of fetal wound healing for the pediatric burn patient. *Pediatr Surg Int* **12**: 484-489.

Cass, D. L., Sylvester, K. G., Yang, E. Y., Crombleholme, T. M., and Adzick, N. S. (1997c). Myofibroblast persistence in fetal sheep wounds is associated with scar formation. *J Pediatr Surg* **32**: 1017-1021.

Castilla, A., Prieto, J., and Fausto, N. (1991). Transforming growth factors beta 1 and alpha in chronic liver disease. Effects of interferon alfa therapy. *N Engl J Med* **324**: 933-940.

Cavani, A., Zambruno, G., Marconi, A., Manca, V., Marchetti, M., and Giannetti, A. (1993). Distinctive integrin expression in the newly forming epidermis during wound healing in humans. *J Invest Dermatol* **101**: 600-604.

Chamberlain, J., Shah, M., and Ferguson, M. W. J. (1995). The effects of suramin on healing adult rodent dermal wounds. *J Anat* **186**: 87-96.

Chang, J., Longaker, M. T., Lorenz, H. P., Roberts, A. B., Harrison, M. R., Adzick, N. S., and Banda, M. J. (1993). Fetal and adult sheep fibroblast TGF-β gene expression *in vitro*: Effects of hypoxia and gestational age. *Surg Forum* **44**: 720-722.

Chen, W., Hardy, P., and Wilce, P. A. (1997). Differential expression of mitochondrial NADH dehydrogenase in ethanol-treated rat brain: Revealed by differential display. *Alcohol Clin Exp Res* **21**: 1053-1056.

Cheng, C. Y., Martin, D. E., Leggett, C. G., Reece, M. C., and Reese, A. C. (1988). Fibronectin enhances healing of excised wounds in rats. *Acta Dermatol* **124**: 221-225.

Cheng, S., Fockler, C., Barnes, W. M., and Higuchi, R. (1994). Effective amplification of long targets from cloned inserts and human genomic DNA. *Proc Natl Acad Sci USA* **91**: 5695-5699.

Chesney, J. and Bucala, R. (1997). Peripheral blood fibrocytes: Novel fibroblast-like cells that present antigen and mediate tissue repair. *Biochem Soc Trans* **25**: 520-524.

Chin, J. R., Murphy, G., and Werb, Z. (1985). Stromelysin, a connective tissue-degrading metalloendopeptidase secreted by stimulated rabbit synovial fibroblasts in parallel with collagenase. Biosynthesis, isolation, characterization, and substrates. *J Biol Chem* **260**: 12367-12376.

Choi, B. M., Kwak, H. J., Jun, C. D., Park, S. D., Kim, K. Y., Kim, H. R., and Chung, H. T. (1996). Control of scarring in adult wounds using antisense transforming growth factor-β1 oligodeoxynucleotides. *Immunol Cell Biol* **74**: 144-150.

Chomczynski, P. (1992). One-hour downward alkaline capillary transfer for blotting of DNA and RNA. *Anal Biochem* **201**: 134-139.

Chopra, V., Blewett, C. J., Ehrlich, H. P., and Krummel, T. M. (1997). Transition from fetal to adult repair occurring in mouse forelimbs maintained in organ culture. *Wound Rep Reg* **5**: 47-51.

Cimino, G. D., Metchette, K., Isaacs, S. T., and Zhu, Y. S. (1990). More false-positive problems. *Nature* **345**: 773-774.

Clark, R. A. F. (1993). Regulation of fibroplasia in cutaneous wound repair. *Am J Med Sci* **306**: 42-48.

Clark, R. A. F. (1996b). "The Molecular and Cellular Biology of Wound Repair," Plenum Press, New York.

Clark, R. A. F. (1996a). Wound Repair; Overview and general considerations. *In* "The Molecular and Cellular Biology of Wound Repair" (R. A. F. Clark, Ed.), pp. 3-50, Plenum Press, New York.

Clark, R. A. F., LAnigan, J. M., DellaPella, P., Manseau, E., Dvorak, H. F., and Colvin, R. B. (1982). Fibronectin and fibrin provide a provisional matrix for epidermal cell migration during wound reepithelialization. *J Invest Dermatol* **79**: 264-269.

Cohen, I. K. and Mast, B. A. (1990). Models of wound healing. *J Trauma* **30**: S149-S155.

Cohen, S. (1983). The epidermal growth factor (EGF). [Review]. *Cancer* **51**: 1787-1791.

Coleman, C., Tuan, T. L., Buckley, S., Anderson, K. D., and Warburton, D. (1998). Contractility, transforming growth factor-β, and plasmin in fetal skin fibroblasts: Role in scarless wound healing. *Pediatr Res* **43**: 403-409.

Connor, T. B., Jr., Roberts, A. B., Sporn, M. B., Danielpour, D., Dart, L. L., Michels, R. G., de Bustros, S., Enger, C., Kato, H., and Lansing, M. (1989). Correlation of fibrosis and transforming growth factor-beta type 2 levels in the eye. *J Clin Invest* **83** : 1661-1666.

Corbett, S. A. and Schwarzbauer, J. E. (1999). Requirements for α5β1 integrin-mediated retraction of fibronectin-fibrin matrices. *J Biol Chem* **274**: 20943-20948.

Cowin, A. J., Brosnan, M. P., Holmes, T. M., and Ferguson, M. W. J. (1998). Endogenous inflammatory response to dermal wound healing in the fetal and adult mouse. *Dev Dyn* **212**: 385-393.

Cullen, B., Silcock, D., Brown, L. J., Gosiewska, A., and Geesin, J. C. (1997). The differential regulation and secretion of proteinases from fetal and neonatal fibroblasts by growth factors. *Int J Biochem Cell Biol* **29**: 241-250.

Culty, M., Miyake, K., Kincade, P. W., Sikorski, E., Butcher, E. C., and Underhill, C. (1990). The hyaluronate receptor is a member of the CD44 (H-CAM) family of cell surface glycoproteins [published erratum appears in J Cell Biol 1991 Feb; 112(3): 513]. *J Cell Biol* **111**: 2765-2774.

D'Jamoos, C. A., McMahon, G., and Tsonis, P. A. (1998). Fibroblast growth factor receptors regulate the ability for hindlimb regeneration in xenopus laevis. *Wound Rep Reg* **6**: 388-397.

Dahl, L., Hopwood, J. J., Laurent, U. B. G., Lilja, K., and Tengblad, A. (1983). The concentration of hyaluronate in amniotic fluid. *Biochem Med* **30**: 280-283.

Darden, D. L., Hu, F. Z., Ehrlich, M. D., Gorry, M. C., Dressman, D., Li, H. S., Whitcomb, D. C., Hebda, P. A., Dohar, J. E., and Ehrlich, G. D. (2000). RNA differential display of scarless wound healing in fetal rabbit indicates downregulation of a CCT chaperonin subunit and upregulation of a glycophorin-like gene transcript. *J Pediatr Surg* **35**: 406-419.

Decker, M., Chiu, E. S., Dollbaum, C., Moiin, A., Hall, J., Spendlove, R., Longaker, M. T., and Stern, R. (1989). Hyaluronic acid-stimulating activity in sera from the bovine fetus and from breast cancer patients. *Cancer Res* **49**: 3499-3505.

DeLozier, J., Nanney, L. B., Hagan, K., and Rees, R. S. (1987). Epidermal growth factor enhances fetal epithelization. *Surg Forum* **38**: 623-626.

Dennis, P. A. and Rifkin, D. B. (1991). Cellular activation of latent transforming growth factor beta requires binding to the cation-independent mannose 6- phosphate/insulin-like growth factor type II receptor. *Proc Natl Acad Sci USA* **88**: 580-584.

DePalma, R. L., Krummel, T. M., Durham, L. A. 3., Michna, B. A., Thomas, B. L., Nelson, J. M., and Diegelmann, R. F. (1989). Characterization and quantitation of wound matrix in the fetal rabbit. *Matrix* **9**: 224-231.

DePalma, R. L., Krummel, T. M., Nelson, J. M., Durham, L. A., Michna, B. A., Diegelmann, R. F., and Cohen, I. K. (1987). Fetal wound matrix is composed of proteoglycan rather than collagen. *Surg Forum* **38**: 626-628.

Desmouliere, A., Geinoz, A., Gabbiani, F., and Gabbiani, G. (1993). Transforming growth factor-beta 1 induces alpha-smooth muscle actin expression in granulation tissue myofibroblasts and in quiescent and growing cultured fibroblasts. *J Cell Biol* **122**: 103-111.

Dillon, P. W., Keefer, K., Blackburn, J. H., Houghton, P. E., and Krummel, T. M. (1994). The extracellular matrix of the fetal wound: Hyaluronic acid controls lymphocyte adhesion. *J Surg Res* **57**: 170-173.

Dini, L. (2000). Recognizing death: Liver phagocytosis of apoptotic cells. *Eur J Histochem* **44**: 217-227.

Dini, L., Lentini, A., Diez, G. D., Rocha, M., Falasca, L., Serafino, L., and Vidal-Vanaclocha, F. (1995). Phagocytosis of apoptotic bodies by liver endothelial cells. *J Cell Sci* **108**: 967-973.

Ditesheim, J. A., Delozier, J. B., Rees, R. S., Broadley, K., Davidson, J. M., and Nanney, L. B. (1989). Covered fetal excisional wounds heal by tissue regeneration. *Surg Forum* **40**: 615-617.

Dohar, J. E., Klein, E. C., Betsch, J. L., and Hebda, P. A. (1998). Fetal airway wound repair - A new frontier. *Arch Otolaryngol Head Neck Surg* **124**: 25-29.

Doillon, C. J., Dunn, M. G., Bender, E., and Silver, F. H. (1985). Collagen fiber formation in repair tissue: development of strength and toughness. *Collag & Relat Res* **5**: 481-492.

Doss, R. P. (1996). Differential display without radioactivity - A modified procedure. *Biotechniques* **21**: 408-

410.

Dostal, G. H. and Gamelli, R. L. (1993). Fetal wound healing. *Surg Gynecol Obstet* **176**: 299-306.

Durham, L. A. 3., Krummel, T. M., Cawthorn, J. W., Thomas, B. L., and Diegelmann, R. F. (1989). Analysis of transforming growth factor beta receptor binding in embryonic, fetal, and adult rabbit fibroblasts. *J Pediatr Surg* **24**: 784-788.

Ehrlich, H. P. (1988). Wound closure: evidence of cooperation between fibroblasts and collagen matrix. [Review]. *Eye* **2**: 149-157.

Ehrlich, H. P., Blewett, C., Krummel, T. M., and Cutroneo, K. R. (1996). Inhibition of wound closure by transforming growth factor-β and dexamethasone in a fetal mouse limb organ culture model. *Wound Rep Reg* **4**: 482-488.

Ehrlich, H. P., Keefer, K. A., Myers, R. L., and Passaniti, A. (1999). Vanadate and the absence of myofibroblasts in wound contraction. *Arch Surg* **134**: 494-501.

Ehrlich, H. P. and Krummel, T. M. (1996). Regulation of wound healing from a connective tissue perspective. *Wound Rep Reg* **4**: 203-210.

Ellis, I., Grey, A. M., Schor, A. M., and Schor, S. L. (1992). Antagonistic effects of TGF-β1 and MSF on fibroblast migration and hyaluronic acid synthesis: Possible implications for dermal wound healing. *J Cell Sci* **102**: 447-456.

Ellis, I. R. and Schor, S. L. (1996). Differential effects of TGF-β1 on hyaluronan synthesis by fetal and adult skin fibroblasts: Implications for cell migration and wound healing. *Exp Cell Res* **228**: 326-333.

Eming, S. A., Whitsitt, J. S., He, L., Krieg, T., Morgan, J. R., and Davidson, J. M. (1999). Particle-mediated gene transfer of PDGF isoforms promotes wound repair. *J Invest Dermatol* **112**: 297-302.

Emura, S., Masuko, S., and Sunaga, T. (1992). Heterogeneity of rabbit aortic endothelial cells, with special reference to phagocytosis. *Angiology* **43**: 599-605.

Eschelbach, A., Hunziker, A., and Klimaschewski, L. (1998). Differential display PCR reveals induction of immediate early genes by vasoactive intestinal peptide in PC12 cells. *Ann NY Acad Sci* **865**: 181-188.

Estes, J. M., Adzick, N. S., Harrison, M. R., Longaker, M. T., and Stern, R. (1993). Hyaluronate metabolism undergoes an ontogenic transition during fetal development: Implications for scar-free wound healing. *J Pediatr Surg* **28**: 1227-1231.

Estes, J. M., Vande Berg, J. S., Adzick, N. S., MacGillivray, T. E., Desmoulière, A., and Gabbiani, G. (1994). Phenotypic and functional features of myofibroblasts in sheep fetal wounds. *Differentiation* **56**: 173-182.

Estes, J. M., Whitby, D. J., Lorenz, H. P., Longaker, M. T., Szabo, Z., Adzick, N. S., and Harrison, M. R.

(1992a). Endoscopic creation and repair of fetal cleft lip. *Plast Reconstr Surg* **90**: 743-746.

Estes, J. M., Whitby, D. J., Lorenz, H. P., Longaker, M. T., Szabo, Z., Adzick, N. S., and Harrison, M. R. (1992b). Endoscopic creation and repair of fetal cleft lip - Discussion. *Plast Reconstr Surg* **90**: 747-749.

Etzioni, A. (1999). Integrins - The glue of life. *Lancet* **353**: 341-343.

Falasca, G. F., Ramachandrula, A., Kelley, K. A., O'Connor, C. R., and Reginato, A. J. (1993). Superoxide anion production and phagocytosis of crystals by cultured endothelial cells. *Arthritis Rheum* **36**: 105-116.

Farber, D. L., Giorda, R., Nettleton, M. Y., Trucco, M., Kochan, J. P., and Sears, D. W. (1993). Rat class III Fc gamma receptor isoforms differ in IgG subclass-binding specificity and fail to associate productively with rat CD3 zeta. *J Immunol* **150**: 4364-4375.

Farber, D. L. and Sears, D. W. (1991). Rat CD16 is defined by a family of class III Fc gamma receptors requiring co-expression of heteroprotein subunits. *J Immunol* **146**: 4352-4361.

Ferguson, M. W. J., Whitby, D. J., Shah, M., Armstrong, J., Siebert, J. W., and Longaker, M. T. (1996). Scar formation: The spectral nature of fetal and adult wound repair. *Plast Reconstr Surg* **97**: 854-860.

Fessler, L. I., Duncan, K. G., Fessler, J. H., Salo, T., and Tryggvason, K. (1984). Characterization of the procollagen IV cleavage products produced by a specific tumor collagenase. *J Biol Chem* **259**: 9783-9789.

Ffrench-Constant, C. and Hynes, R. O. (1989). Alternative splicing of fibronectin is temporally and spatially regulated in the chicken embryo. *Development* **106**: 375-388.

Filsell, W., Rudman, S., Jenkins, G., and Green, M. R. (1999). Coordinate upregulation of tenascin C expression with degree of photodamage in human skin. *Br J Dermatol* **140**: 592-599.

Fisher, C., Gilbertson-Beadling, S., Powers, E. A., Petzold, G., Poorman, R., and Mitchell, M. A. (1994). Interstitial collagenase is required for angiogenesis *in vitro*. *Dev Biol* **162**: 499-510.

Flake, A. W., Harrison, M. R., Adzick, N. S., and Zanjani, E. D. (1986). Transplantation of fetal hematopoietic stem cells *in utero*: the creation of hematopoietic chimeras. *Science* **233**: 776-778.

Fleischmajer, R., Perlish, J. S., Burgeson, R. E., Shaikh-Bahai, F., and Timpl, R. (1990). Type I and type III collagen interactions during fibrillogenesis. *Ann NY Acad Sci* **580**: 161-175.

Frank, S., Hubner, G., Breier, G., Longaker, M. T., Greenhalgh, D. G., and Werner, S. (1995). Regulation of vascular endothelial growth factor expression in cultured keratinocytes. Implications for normal and impaired wound healing. *J Biol Chem* **270**: 12607-12613.

Frank, S., Madlener, M., Pfeilschifter, J., and Werner, S. (1998). Induction of inducible nitric oxide synthase and its corresponding tetrahydrobiopterin-cofactor-synthesizing enzyme GTP-cyclohydrolase I during cutaneous wound repair. *J Invest Dermatol* **111**: 1058-1064.

Frank, S., Madlener, M., and Werner, S. (1996). Transforming growth factors β1, β2, and β3 and their receptors are differentially regulated during normal and impaired wound healing. *J Biol Chem* **271**: 10188-10193.

Frank, S., Munz, B., and Werner, S. (1997). The human homologue of a bovine non-selenium glutathione peroxidase is a novel keratinocyte growth factor-regulated gene. *Oncogene* **14**: 915-921.

Franklin, J. D. and Lynch, J. B. (1979). Effects of topical applications of epidermal growth factor on wound healing. *Plastic & Reconstructive Surgery* **64**: 766-770.

Franklin, T. J., Gregory, H., and Morris, W. P. (1986). Acceleration of wound healing by recombinant human urogastrone (epidermal growth factor). *J Lab Clin Med* **108**: 103-108.

Frantz, F. W., Bettinger, D. A., Haynes, J. H., Johnson, D. E., Harvey, K. M., Dalton, H. P., Yager, D. R., Diegelmann, R. F., and Cohen, I. K. (1993). Biology of fetal repair: the presence of bacteria in fetal wounds induces an adult-like healing response. *J Pediatr Surg* **28**: 428-433.

Frantz, F. W., Diegelmann, R. F., Mast, B. A., and Cohen, I. K. (1992). Biology of fetal wound healing: collagen biosynthesis during dermal repair. *J Pediatr Surg* **27**: 945-948.

Franz, O., Röder, T., and Gewecke, M. (1998). Analysis of differential gene expression in the central nervous system of *Schistocerca gregaria* by differential display PCR. *J Comp Physiol [A]* **182**: 627-633.

Freund, R. M., Siebert, J. W., Cabrera, R. C., Longaker, M. T., Eidelman, Y., Adzick, N. S., and Garg, H. G. (1993). Serial quantitation of hyaluronan and sulfated glycosaminoglycans in fetal sheep skin. *Biochem Mol Biol Int* **29**: 773-783.

Frohman, M. A., Dush, M. K., and Martin, G. R. (1988). Rapid production of full-length cDNAs from rare transcripts: amplification using a single gene-specific oligonucleotide primer. *Proc Natl Acad Sci USA* **85**: 8998-9002.

Frost, M. R. and Guggenheim, J. A. (1999). Prevention of depurination during elution facilitates the reamplification of DNA from differential display gels. *Nucleic Acids Res* **27**: e6.

Gallivan, E. K., Crombleholme, T. M., and Moriarty, K. P. (1996). Effect of fetal serum on fibroblast pericellular matrix formation. *J Surg Res* **64**: 128-131.

Gallivan, K., Alman, B. A., Moriarty, K. P., Pajerski, M. E., O'Donnell, C., and Crombleholme, T. M. (1997). Differential collagen I gene expression in fetal fibroblasts. *J Pediatr Surg* **32**: 1033-1036.

Gallo, R., Kim, C., Kokenyesi, R., Adzick, N. S., and Bernfield, M. (1996). Syndecans-1 and -4 are induced during wound repair of neonatal but not fetal skin. *J Invest Dermatol* **107**: 676-683.

Gardner, H., Broberg, A., Pozzi, A., Laato, M., and Heino, J. (1999). Absence of integrin α1β1 in the mouse causes loss of feedback regulation of collagen synthesis in normal and wounded dermis. *J Cell Sci* **112**: 263-

272.

Gery, S. and Lavi, S. (1997). Purification and cloning of differential display products. *Biotechniques* **23**: 198-200, 202.

Gessner, J. E., Grussenmeyer, T., Kolanus, W., and Schmidt, R. E. (1995). The human low affinity immunoglobulin G Fc receptor III-A and III-B genes. Molecular characterization of the promoter regions. *J Biol Chem* **270**: 1350-1361.

Glanville, R. W. (1982). A comparison of models for the macromolecular structure of interstitial and basement membrane collagens. *Arzneimittel-Forschung* **32**: 1353-1357.

Goodson, W. H., III and Hunt, T. K. (1982). Development of a new miniature method for the study of wound healing in human subjects. *J Surg Res* **33**: 394-401.

Gould, L. J., Yager, D. R., Cohen, I. K., and Diegelmann, R. F. (1997). *In vitro* analysis of fetal fibroblast collagenolytic activity. *Wound Rep Reg* **5**: 151-158.

Graf, D., Fisher, A. G., and Merkenschlager, M. (1997). Rational primer design greatly improves differential display PCR (DD-PCR). *Nucleic Acids Res* **25**: 2239-2240.

Greenhalgh, D. G., Sprugel, K. H., Murray, M. J., and Ross, R. (1990). PDGF and FGF stimulate wound healing in the genetically diabetic mouse. *Am J Pathol* **136**: 1235-1246.

Greenwald, D. P., Gottlieb, L. J., Mass, D. P., Shumway, S. M., and Temaner, M. (1992). Full-thickness skin wound explants in tissue culture: A mechanical evaluation of healing. *Plast Reconstr Surg* **90**: 289-294.

Greiling, D. and Clark, R. A. F. (1997). Fibronectin provides a conduit for fibroblast transmigration from collagenous stroma into fibrin clot provisional matrix. *J Cell Sci* **110**: 861-870.

Grinnell, F. (1994). Fibroblasts, myofibroblasts, and wound contraction. *J Cell Biol* **124**: 401-404.

Groger, M., Sarmay, G., Fiebiger, E., Wolff, K., and Petzelbauer, P. (1996). Dermal microvascular endothelial cells express CD32 receptors *in vivo* and *in vitro*. *J Immunol* **156**: 1549-1556.

Gross, J., Farinelli, W., Sadow, P., Anderson, R., and Bruns, R. (1995). On the mechanism of skin wound "contraction': A granulation tissue "knockout" with a normal phenotype. *Proc Natl Acad Sci USA* **92**: 5982-5986.

Grotendorst, G. R., Martin, G. R., Pencev, D., Sodek, J., and Harvey, A. K. (1985). Stimulation of granulation tissue formation by platelet-derived growth factor in normal and diabetic rats. *J Clin Invest* **76**: 2323-2329.

Guo, L. F., Degenstein, L., and Fuchs, E. (1996). Keratinocyte growth factor is required for hair development but not for wound healing. *Genes Dev* **10**: 165-175.

Haag, E. and Raman, V. (1994). Effects of primer choice and source of *Taq* DNA polymerase on the banding patterns of differential display RT-PCR. *Biotechniques* **17**: 226-228.

Hallock, G. G., Rice, D. C., and McClure, H. M. (1987). *In utero* lip repair in the rhesus monkey: An update. *Plast Reconstr Surg* **80**: 855-858.

Hamill, R. J., Vann, J. M., and Proctor, R. A. (1986). Phagocytosis of *Staphylococcus aureus* by cultured bovine aortic endothelial cells: Model for postadherence events in endovascular infections. *Infect Immun* **54**: 833-836.

Hansen, J. E., Lund, O., Engelbrecht, J., Bohr, H., Nielsen, J. O., and Hansen, J. E. (1995). Prediction of O-glycosylation of mammalian proteins: Specificity patterns of UDP-GalNAc: Polypeptide N-acetylgalactosaminyltransferase. *Biochem J* **308**: 801-813.

Hansen, J. E., Lund, O., Rapacki, K., and Brunak, S. (1997). O-GLYCBASE version 2.0: A revised database of O-glycosylated proteins. *Nucleic Acids Res* **25**: 278-282.

Hansen, J. E., Lund, O., Tolstrup, N., Gooley, A. A., Williams, K. L., and Brunak, S. (1998). NetOglyc: Prediction of mucin type O-glycosylation sites based on sequence context and surface accessibility. *Glycoconj J* **15**: 115-130.

Harris, M. C., Mennuti, M. T., Kline, J. A., and Polin, R. A. (1988). Amniotic fluid fibronectin concentrations with advancing gestational age. *Obstet Gynecol* **72**: 593-595.

Harrison, M. R. and Adzick, N. S. (1991). The fetus as a patient. Surgical considerations. *Ann Surg* **213**: 279-291.

Haynes, J. H., Johnson, D. E., Mast, B. A., Diegelmann, R. F., Salzberg, D. A., Cohen, I. K., and Krummel, T. M. (1994). Platelet-derived growth factor induces fetal wound fibrosis. *J Pediatr Surg* **29**: 1405-1408.

Haynes, J. H., Krummel, T. M., Schatzki, P. F., Dunn, J. D., Flood, L. C., Cohen, I. K., and Diegelmann, R. F. (1989). Histology of the open fetal rabbit wound. *Surg Forum* **40**: 558-560.

Haynes, J. H., Mast, B. A., Krummel, T. M., Cohen, I. K., and Diegelmann, R. F. (1995). Exposure to amniotic fluid inhibits closure of open wounds in the fetal rabbit. *Wound Rep Reg* **3**: 467-472.

Hellstrom, S. and Laurent, C. (1987). Hyaluronan and healing of tympanic membrane perforations: An experimental study. *Acta Otolaryngol (Stockh)* **442**: 54-61.

Hennessey, P. J., Black, C. T., and Andrassy, R. J. (1990a). EGF increases short-term type I collagen accumulation during wound healing in diabetic rats. *J Pediatr Surg* **25**: 893-897.

Hennessey, P. J., Black, C. T., and Andrassy, R. J. (1990b). Epidermal growth factor and insulin act synergistically during diabetic healing. *Arch Surg* **125**: 926-929.

Hibbs, M. L., Selvaraj, P., Carpen, O., Springer, T. A., Kuster, H., Jouvin, M. H., and Kinet, J. P. (1989). Mechanisms for regulating expression of membrane isoforms of Fc gamma RIII (CD16). *Science* **246**: 1608-1611.

Hill, D. J., Strain, A. J., Elstow, S. F., Swenne, I., and Milner, R. D. (1986). Bi-functional action of transforming growth factor-beta on DNA synthesis in early passage human fetal fibroblasts. *J Cell Physiol* **128**: 322-328.

Hodivala-Dilke, K. M., DiPersio, C. M., Kreidberg, J. A., and Hynes, R. O. (1998). Novel roles for α3β 1 integrin as a regulator of cytoskeletal assembly and as a trans-dominant inhibitor of integrin receptor function in mouse keratinocytes. *J Cell Biol* **142**: 1357-1369.

Hofmann, K., Bucher, P., Falquet, L., and Bairoch, A. (1999). The PROSITE database, its status in 1999. *Nucleic Acids Res* **27**: 215-219.

Hofmann, K. and Stoffel, W. (1992). PROFILEGRAPH: An interactive graphical tool for protein sequence analysis. *Comput Appl Biosci* **8**: 331-337.

Holbrook, K. A. (1991). Structure and function of the developing human skin. *In* "Physiology, Biochemistry and Molecular Biology of the Skin" (L. A. Goldsmith, Ed.), pp. 63-110, Oxford University Press, New York.

Houghton, P. E., Keefer, K. A., and Krummel, T. M. (1995). The role of transforming growth factor-β in the conversion from "scarless" healing to healing with scar formation. *Wound Rep Reg* **3**: 229-236.

Hsu, D. K., Donohue, P. J., Alberts, G. F., and Winkles, J. A. (1993). Fibroblast growth factor-1 induces phosphofructokinase, fatty acid synthase and Ca(2+)-ATPase mRNA expression in NIH 3T3 cells. *Biochem Biophys Res Commun* **197**: 1483-1491.

Hudson, L. G. and McCawley, L. J. (1998). Contributions of the epidermal growth factor receptor to keratinocyte motility. *Microsc Res Tech* **43**: 444-455.

Hulett, M. D., Brinkworth, R. I., McKenzie, I. F., and Hogarth, P. M. (1999). Fine structure analysis of interaction of FcepsilonRI with IgE. *J Biol Chem* **274**: 13345-13352.

Hulett, M. D., Witort, E., Brinkworth, R. I., McKenzie, I. F., and Hogarth, P. M. (1995). Multiple regions of human Fc gamma RII (CD32) contribute to the binding of IgG. *J Biol Chem* **270**: 21188-21194.

Hunt, T. K., Twomey, P., Zederfeldt, B., and Dunphy, J. E. (1967). Respiratory gas tensions and pH in healing wounds. *Am J Surg* **114**: 302-307.

Hynes, R. (1985). Molecular biology of fibronectin. [Review]. *Annu Rev Cell Biol* **1**: 67-90.

Ihara, S. and Motobayashi, Y. (1992). Wound closure in foetal rat skin. *Development* **114**: 573-582.

Ihara, S., Motobayashi, Y., Nagao, E., and Kistler, A. (1990). Ontogenetic transition of wound healing pattern

in rat skin occurring at the fetal stage. *Development* **110**: 671-680.

International Human Genome Sequencing Consortium (2001). Initial sequencing and analysis of the human genome. *Nature* **409**: 860-921.

Iocono, J. A., Ehrlich, H. P., Keefer, K. A., and Krummel, T. M. (1998a). Hyaluronan induces scarless repair in mouse limb organ culture. *J Pediatr Surg* **33**: 564-567.

Iocono, J. A., Krummel, T. M., Keefer, K. A., Allison, G. M., and Ehrlich, H. P. (1998b). Repeated additons of hyaluronan alters granulation tissue deposition in sponge implants in mice. *Wound Rep Reg* **6**: 442-448.

Ishai-Michaeli, R., Eldor, A., and Vlodavsky, I. (1990). Heparanase activity expressed by platelets, neutrophils, and lymphoma cells releases active fibroblast growth factor from extracellular matrix. *Cell Regul* **1**: 833-842.

Iyer, V. R., Eisen, M. B., Ross, D. T., Schuler, G., Moore, T., Lee, J. C., Trent, J. M., Staudt, L. M., Hudson, J., Jr., Boguski, M. S., Lashkari, D., Shalon, D., Botstein, D., and Brown, P. O. (1999). The transcriptional program in the response of human fibroblasts to serum. *Science* **283**: 83-87.

Jennings, R. W., Adzick, N. S., Longaker, M. T., Duncan, B. W., Scheuenstuhl, H., and Hunt, T. K. (1991). Ontogeny of fetal sheep polymorphonuclear leukocyte phagocytosis. *J Pediatr Surg* **26**: 853-855.

Jonsson, K., Jensen, J. A., Goodson, W. H. 3., Scheuenstuhl, H., West, J., Hopf, H. W., and Hunt, T. K. (1991). Tissue oxygenation, anemia, and perfusion in relation to wound healing in surgical patients. *Ann Surg* **214**: 605-613.

Jurecic, R., Nguyen, T., and Belmont, J. W. (1996). Differential mRNA display using anchored oligo-dT and long sequence-specific primers as arbitrary primers. *Trends Genet* **12**: 502-504.

Jyung, R. W., Mustoe, T. A., Busby, W. H., and Clemmons, D. R. (1994). Increased wound-breaking strength induced by insulin-like growth factor I in combination with insulin-like growth factor binding protein-1. *Surgery* **115**: 233-239.

Kahari, V. M. and Saarialho-Kere, U. (1997). Matrix metalloproteinases in skin. *Exp Dermatol* **6**: 199-213.

Keshav, S., McKnight, A. J., Arora, R., and Gordon, S. (1997). Cloning of intestinal phospholipase A2 from intestinal epithelial RNA by differential display PCR. *Cell Prolif* **30**: 369-383.

Kiehart, D. P., Galbraith, C. G., Edwards, K. A., Rickoll, W. L., and Montague, R. A. (2000). Multiple forces contribute to cell sheet morphogenesis for dorsal closure in *Drosophila*. *J Cell Biol* **149**: 471-490.

Kim, C. W., Goldberger, O. A., Gallo, R. L., and Bernfield, M. (1994). Members of the syndecan family of heparan sulfate protoglycans are expressed in distinct cell-, tissue-,and development-specific patterns. *Mol Biol Cell* **5**: 797-805.

Klein, C. E., Steinmayer, T., Mattes, J. M., Kaufmann, R., and Weber, L. (1990). Integrins of normal human

epidermis: Differential expression, synthesis and molecular structure. *Br J Dermatol* **123**: 171-178.

Klein, S. A., Bond, S. J., Gupta, S. C., Yacoub, O. A., and Anderson, G. L. (1999). Angiogenesis inhibitor TNP-470 inhibits murine cutaneous wound healing. *J Surg Res* **82**: 268-274.

Knolle, P. A. and Gerken, G. (2000). Local control of the immune response in the liver. *Immunol Rev* **174: 21-34.**: 21-34.

Knox, P., Crooks, S., Scaife, M. C., and Patel, S. (1987). Role of plasminogen, plasmin, and plasminogen activators in the migration of fibroblasts into plasma clots. *J Cell Physiol* **132**: 501-508.

Koene, H. R., Kleijer, M., Algra, J., Roos, D., dem Borne, A. E., and de Haas, M. (1997). Fc gammaRIIIa-158V/F polymorphism influences the binding of IgG by natural killer cell Fc gammaRIIIa, independently of the Fc gammaRIIIa-48L/R/H phenotype. *Blood* **90**: 1109-1114.

Koene, H. R., Kleijer, M., Roos, D., de Haas, M., and dem Borne, A. E. (1998). Fc gamma RIIIB gene duplication: Evidence for presence and expression of three distinct Fc gamma RIIIB genes in NA(1+,2+)SH(+) individuals. *Blood* **91**: 673-679.

Kojima, S., Nara, K., and Rifkin, D. B. (1993). Requirement for transglutaminase in the activation of latent transforming growth factor-beta in bovine endothelial cells. *J Cell Biol* **121**: 439-448.

Konecny, P. and Redinbaugh, M. G. (1997). Amplification of differentially displayed PCR products isolated from untreated denaturing polyacrylamide gels. *Biotechniques* **22**: 240-2, 244.

Koopman, E., Blok, L. J., Brinkmann, A. O., Helmerhorst, H. J. M., and Huikeshoven, F. J. M. (1999). Differential gene expression in progesterone-sensitive and progesterone-insensitive endometrial carcinoma cells. *Eur J Obstet Gynecol Reprod Biol* **82**: 135-138.

Krummel, T. M., Ehrlich, H. P., Nelson, J. M., Michna, B. A., Thomas, B. L., Haynes, J. H., Cohen, I. K., and Diegelmann, R. F. (1989). Fetal wounds do not contract *in utero*. *Surg Forum* **40**: 613-614.

Krummel, T. M., Ehrlich, H. P., Nelson, J. M., Michna, B. A., Thomas, B. L., Haynes, J. H., Cohen, I. K., and Diegelmann, R. F. (1993). *In vitro* and *in vivo* analysis of the inability of fetal rabbit wounds to contract. *Wound Rep Reg* **1**: 15-21.

Krummel, T. M., Michna, B. A., Thomas, B. L., Sporn, M. B., Nelson, J. M., Salzberg, A. M., Cohen, I. K., and Diegelmann, R. F. (1988). Transforming growth factor beta (TGF-β) induces fibrosis in a fetal wound model. *J Pediatr Surg* **23** : 647-652.

Krummel, T. M., Nelson, J. M., Diegelmann, R. F., Lindblad, W. J., Salzberg, A. M., Greenfield, L. J., and Cohen, I. K. (1987). Fetal response to injury in the rabbit. *J Pediatr Surg* **22**: 640-644.

Kujawa, M. J., Pechak, D. G., Fiszman, M. Y., and Caplan, A. I. (1986). Hyaluronic acid bonded to cell culture surfaces inhibits the program of myogenesis. *Dev Biol* **113**: 10-16.

Kujawa, M. J. and Tepperman, K. (1983). Culturing chick muscle cells on glycosaminoglycan substrates: Attachment and differentiation. *Dev Biol* **99**: 277-286.

Kyte, J. and Doolittle, R. F. (1982). A simple method for displaying the hydropathic character of a protein. *J Mol Biol* **157**: 105-132.

Lanier, L. L., Yu, G., and Phillips, J. H. (1989). Co-association of CD3 zeta with a receptor (CD16) for IgG Fc on human natural killer cells. *Nature* **342**: 803-805.

Lanning, D. A., Diegelmann, R. F., Yager, D. R., Wallace, M. L., Bagwell, C. E., and Haynes, J. H. (2000). Myofibroblast induction with transforming growth factor-β_1 and -β_3 in cutaneous fetal excisional wounds. *J Pediatr Surg* **35**: 183-187.

Lanning, D. A., Nwomeh, B. C., Montante, S. J., Yager, D. R., Diegelmann, R. F., and Haynes, J. H. (1999). TGF-β1 alters the healing of cutaneous fetal excisional wounds. *J Pediatr Surg* **34**: 695-700.

Latijnhouwers, M. A. H. E., Pfundt, R., De Jongh, G. J., and Schalkwijk, J. (1998). Tenascin-C expression in human epidermal keratinocytes is regulated by inflammatory cytokines and a stress response pathway. *Matrix Biol* **17**: 305-316.

Lawrence, W. T., Sporn, M. B., Gorschboth, C., Norton, J. A., and Grotendorst, G. R. (1985). The reversal of an adriamycin induced healing impairment with chemoattractants and growth factors. *Ann Surg* **203**: 142-147.

Lazarus, G. S., Cooper, D. M., Knighton, D. R., Margolis, D. J., Pecoraro, R. E., Rodeheaver, G., and Robson, M. C. (1994). Definitions and guidelines for assessment of wounds and evaluation of healing. *Arch Dermatol* **130**: 489-493.

Ledakis, P., Tanimura, H., and Fojo, T. (1998). Limitations of differential display. *Biochem Biophys Res Commun* **251**: 653-656.

Lee, N. J., Wang, S. J., Durairaj, K. K., Srivatsan, E. S., and Wang, M. B. (2000). Increased expression of transforming growth factor-β1, acidic fibroblast growth factor, and basic fibroblast growth factor in fetal versus adult fibroblast cell lines. *Laryngoscope* **110**: 616-619.

LeGrand, E. K., Senter, L. H., Gamelli, R. L., and Kiorpes, T. C. (1993). Evaluation of PDGF-BB, PDGF-AA, bFGF, IL-1, and EGF dose responses in polyvinyl alcohol sponge implants assessed by a rapid histologic method. *Growth Factors* **8**: 315-329.

Leibovich, S. J. and Ross, R. (1975). The role of the macrophage in wound repair. *Am J Pathol* **78**: 71-100.

Levenson, S. M., Geever, E. F., Crowley, L. V., Oates, J. F., Berard, C. W., and Rosen, H. (1968). The healing of rat skin wounds. *Ann Surg* **161**: 293-308.

Li, H. S., Hebda, P. A., Kelly, L. A., Ehrlich, G. D., Whitcomb, D. C., and Dohar, J. E. (2000). Up-regulation of prostaglandin EP4 receptor messenger RNA in fetal rabbit skin wound. *Arch Otolaryngol Head Neck Surg*

126: 1337-1343.

Liang, P., Averboukh, L., Keyomarsi, K., Sager, R., and Pardee, A. B. (1992). Differential display and cloning of messenger RNAs from human breast cancer versus mammary epithelial cells. *Cancer Res* **52**: 6966-6968.

Liang, P., Averboukh, L., and Pardee, A. B. (1993). Distribution and cloning of eukaryotic mRNAs by means of differential display: refinements and optimization. *Nucleic Acids Res* **21**: 3269-3275.

Liang, P., Averboukh, L., Zhu, W., and Pardee, A. B. (1994). Ras activation of genes: Mob-1 as a model. *Proc Natl Acad Sci USA* **91**: 12515-12519.

Liang, P. and Pardee, A. B. (1992). Differential display of eukaryotic messenger RNA by means of the polymerase chain reaction. *Science* **257**: 967-971.

Liang, P. and Pardee, A. B. (1995). Recent advances in differential display. *Curr Opin Immunol* **7**: 274-280.

Liechty, K. W., Adzick, N. S., and Crombleholme, T. M. (2000a). Diminished interleukin 6 (IL-6) production during scarless human fetal wound repair. *Cytokine* **12**: 671-676.

Liechty, K. W., Crombleholme, T. M., Cass, D. L., Martin, B., and Adzick, N. S. (1998). Diminished interleukin-8 (IL-8) production in the fetal wound healing response. *J Surg Res* **77**: 80-84.

Liechty, K. W., Kim, H. B., Adzick, N. S., and Crombleholme, T. M. (2000b). Fetal wound repair results in scar formation in interleukin-10-deficient mice in a syngeneic murine model of scarless fetal wound repair. *J Pediatr Surg* **35**: 866-872.

Lin, R. Y., Sullivan, K. M., Argenta, P. A., Lorenz, H. P., and Adzick, N. S. (1994). Scarless human fetal skin repair is intrinsic to the fetal fibroblast and occurs in the absence of an inflammatory response. *In situ* hybridization and immunohistochemical studies. *Wound Rep Reg* **2**: 297-305.

Lin, R. Y., Sullivan, K. M., Argenta, P. A., Meuli, M., Lorenz, H. P., and Adzick, N. S. (1995). Exogenous transforming growth factor-beta amplifies its own expression and induces scar formation in a model of human fetal skin repair. *Ann Surg* **222**: 146-154.

Linskens, M. H., Feng, J., Andrews, W. H., Enlow, B. E., Saati, S. M., Tonkin, L. A., Funk, W. D., and Villeponteau, B. (1995). Cataloging altered gene expression in young and senescent cells using enhanced differential display. *Nucleic Acids Res* **23**: 3244-3251.

Liu, Y. E., Wang, M., greene, J., Su, J., Ullrich, S., Li, H., Sheng, S., Alexander, P., Sang, Q. X. A., and Shi, Y. E. (2000). Preparation and characterization of recombinant tissue inhibitor of metalloproteinase 4 (TIMP-4). *J Biol Chem* **272**: 20479-20483.

Longaker, M. T. and Adzick, N. S. (1991). The biology of fetal wound healing: A review. *Plast Reconstr Surg* **87**: 788-798.

Longaker, M. T., Adzick, N. S., Hall, J. L., Stair, S. E., Crombleholme, T. M., Duncan, B. W., Bradley, S. M., Harrison, M. R., and Stern, R. (1990a). Studies in fetal wound healing, VII. Fetal wound healing may be modulated by hyaluronic acid stimulating activity in amniotic fluid. *J Pediatr Surg* **25**: 430-433.

Longaker, M. T., Bouhana, K. S., Harrison, M. R., Danielpour, D., Roberts, A. B., and Banda, M. J. (1994b). Wound healing in the fetus: Possible role for inflammatory macrophages and transforming growth factor-β isoforms. *Wound Rep Reg* **2**: 104-112.

Longaker, M. T., Bouhana, K. S., Roberts, A. B., Harrison, M. R., Adzick, N. S., and Banda, M. J. (1991b). Regulation of fetal wound healing. *Surg Forum* **42**: 654-655.

Longaker, M. T., Burd, D. A., Gown, A. M., Yen, T. S., Jennings, R. W., Duncan, B. W., Harrison, M. R., and Adzick, N. S. (1991a). Midgestational excisional fetal lamb wounds contract *in utero*. *J Pediatr Surg* **26**: 942-948.

Longaker, M. T., Chiu, E. S., Adzick, N. S., Stern, M., Harrison, M. R., and Stern, R. (1991c). Studies in fetal wound healing. V. A prolonged presence of hyaluronic acid characterizes fetal wound fluid. *Ann Surg* **213**: 292-296.

Longaker, M. T., Chiu, E. S., Harrison, M. R., Crombleholme, T. M., Langer, J. C., Duncan, BW, Adzick, N. S., Verrier, E. D., and Stern, R. (1989c). Studies in fetal wound healing. IV. Hyaluronic acid-stimulating activity distinguishes fetal wound fluid from adult wound fluid. *Ann Surg* **210**: 667-672.

Longaker, M. T., Harrison, M. R., Crombleholme, T. M., Langer, J. C., Decker, M., Verrier, E. D., Spendlove, R., and Stern, R. (1989a). Studies in fetal wound healing: I. A factor in fetal serum that stimulates deposition of hyaluronic acid. *J Pediatr Surg* **24**: 789-792.

Longaker, M. T., Moelleken, B. R., Cheng, J. C., Jennings, R. W., Adzick, N. S., Mintorovich, J., Levinsohn, D. G., Gordon, L., Harrison, M. R., and Simmons, D. J. (1992a). Fetal fracture healing in a lamb model. *Plast Reconstr Surg* **90**: 161-171.

Longaker, M. T., Stern, M., Lorenz, P., Whitby, D. J., Dodson, T. B., Harrison, M. R., Adzick, N. S., and Kaban, L. B. (1992b). A model for fetal cleft lip repair in lambs. *Plast Reconstr Surg* **90**: 750-756.

Longaker, M. T., Whitby, D. J., Adzick, N. S., Crombleholme, T. M., Langer, J. C., Duncan, B. W., Bradley, S. M., Stern, R., Ferguson, M. W., and Harrison, M. R. (1990b). Studies in fetal wound healing, VI. Second and early third trimester fetal wounds demonstrate rapid collagen deposition without scar formation. *J Pediatr Surg* **25**: 63-68.

Longaker, M. T., Whitby, D. J., Adzick, N. S., Kaban, L. B., and Harrison, M. R. (1991e). Fetal surgery for cleft lip: A plea for caution. *Plast Reconstr Surg* **88**: 1087-1092.

Longaker, M. T., Whitby, D. J., Ferguson, M. W., Harrison, M. R., Crombleholme, T. M., Langer, J. C., Cochrum, K. C., Verrier, E. D., and Stern, R. (1989b). Studies in fetal wound healing: III. Early deposition of

fibronectin distinguishes fetal from adult wound healing. *J Pediatr Surg* **24**: 799-805.

Longaker, M. T., Whitby, D. J., Ferguson, M. W. J., Lorenz, H. P., Harrison, M. R., and Adzick, N. S. (1994a). Adult skin wounds in the fetal environment heal with scar formation. *Ann Surg* **219**: 65-72.

Longaker, M. T., Whitby, D. J., Jennings, R. W., Duncan, B. W., Ferguson, M. W., Harrison, M. R., and Adzick, N. S. (1991d). Fetal diaphragmatic wounds heal with scar formation. *J Surg Res* **50**: 375-385.

Lorenz, H. P., Chang, J., Longaker, M. T., and Banda, M. J. (1993a). Transforming growth factors β1 and β2 synergistically increase gene expression of collagen types I and III in fetal but not adult fibroblasts. *Surg Forum* **44**: 723-725.

Lorenz, H. P., Lin, R. Y., Longaker, M. T., Whitby, D. J., and Adzick, N. S. (1995). The fetal fibroblast: The effector cell of scarless fetal skin repair. *Plast Reconstr Surg* **96** : 1251-1259.

Lorenz, H. P., Longaker, M. T., Perkocha, L. A., Jennings, R. W., Harrison, M. R., and Adzick, N. S. (1992). Scarless wound repair: A human fetal skin model. *Development* **114**: 253-259.

Lorenz, H. P., Whitby, D. J., Longaker, M. T., and Adzick, N. S. (1993b). Fetal wound healing: The ontogeny of scar formation in the non-human primate. *Ann Surg* **217**: 391-396.

Lovvorn, H. N., III, Cass, D. L., Sylvester, K. G., Yang, E. Y., Crombleholme, T. M., Adzick, N. S., and Savani, R. C. (1998). Hyaluronan receptor expression increases in fetal excisional skin wounds and correlates with fibroplasia. *J Pediatr Surg* **33**: 1062-1069.

Lovvorn, H. N., III, Cheung, D. T., Nimni, M. E., Perelman, N., Estes, J. M., and Adzick, N. S. (1999). Relative distribution and crosslinking of collagen distinguish fetal from adult sheep wound repair. *J Pediatr Surg* **34**: 218-223.

Lyden, T. W., Robinson, J. M., Tridandapani, S., Teillaud, J. L., Garber, S. A., Osborne, J. M., Frey, J., Budde, P., and Anderson, C. L. (2001). The Fc receptor for IgG expressed in the villus endothelium of human placenta is Fc gamma RIIb2. *J Immunol* **166**: 3882-3889.

Lynch, R. G. (2000). Regulatory roles for FcgammaRIII (CD16) and FcgammaRII (CD32) in the development of T- and B-lineage lymphoid cells. *J Leukoc Biol* **67**: 279-284.

Mackenzie, A., Leeming, G. L., Jowett, A. K., Ferguson, M. W., and Sharpe, P. T. (1991). The homeobox gene Hox 7.1 has specific regional and temporal expression patterns during early murine craniofacial embryogenesis, especially tooth development *in vivo* and *in vitro*. *Development* **111**: 269-285.

Mackie, E. J., Halfter, W., and Liverani, D. (1988). Induction of tenascin in healing wounds. *J Cell Biol* **107**: 2757-2767.

Madden, J. W. and Peacock, E. E., Jr. (1968). Studies on the biology of collagen during wound healing. I. Rate of collagen synthesis and deposition in cutaneous wounds of the rat. *Surgery* **64**: 288-294.

Madlener, M., Mauch, C., Conca, W., Brauchle, M., Parks, W. C., and Werner, S. (1996). Regulation of the expression of stromelysin-2 by growth factors in keratinocytes: implications for normal and impaired wound healing. *Biochem J* **320**: 659-664.

Madlener, M., Parks, W. C., and Werner, S. (1998). Matrix metalloproteinases (MMPs) and their physiological inhibitors (TIMPs) are differentially expressed during excisional skin wound repair. *Exp Cell Res* **242**: 201-210.

Malhotra, K., Luehrsen, K. R., Costello, L. L., Raich, T. J., Sim, K., Foltz, L., Davidson, S., Xu, H., Chen, A., Yamanishi, D. T., Lindemann, G. W., Cain, C. A., Madlansacay, M. R., Hashima, S. M., Pham, T. L., Mahoney, W., and Schueler, P. A. (1999). Identification of differentially expressed mRNAs in human fetal liver across gestation. *Nucleic Acids Res* **27**: 839-847.

Mandelboim, O., Malik, P., Davis, D. M., Jo, C. H., Boyson, J. E., and Strominger, J. L. (1999). Human CD16 as a lysis receptor mediating direct natural killer cell cytotoxicity. *Proc Natl Acad Sci USA* **96**: 5640-5644.

Martin, K. J., Kwan, C.-P., O'Hare, M. J., Pardee, A. B., and Sager, R. (1998). Identification and verification of differential display cDNAs using gene-specific primers and hybridization arrays. *Biotechniques* **24**: 1018-1026.

Martin, P. (1997). Wound healing – Aiming for perfect skin regeneration. *Science* **276**: 75-81.

Martin, P., Dickson, M. C., Millan, F. A., and Akhurst, R. J. (1993). Rapid induction and clearance of TGFβ1 is an early response to wounding in the mouse embryo. *Dev Genet* **14**: 225-238.

Martin, P. and Lewis, J. (1992). Actin cables and epidermal movement in embryonic wound healing. *Nature* **360**: 179-183.

Martin, P., Nobes, C., McCluskey, J., and Lewis, J. (1994). Repair of excisional wounds in the embryo. [Review]. *Eye* **8**: 155-160.

Martin, P. and Nobes, C. D. (1992). An early molecular component of the wound healing response in rat embryos - Induction of c-*fos* protein in cells at the epidermal wound margin. *Mech Dev* **38**: 209-216.

Mashima, H., Yamada, S., Tajima, T., Seno, M., Yamada, H., Takeda, J., and Kojima, I. (1999). Genes expressed during the differentiation of pancreatic AR42J cells into insulin-secreting cells. *Diabetes* **48**: 304-309.

Mast, B. A. (1992). The Skin. *In* "Wound Healing Biochemical and Clinical Aspects" (I. K. Cohen, R. F. Diegelmann, and W. J. Lindblad, Eds.), pp. 344-355, W.B. Saunders Company, Philadelphia.

Mast, B. A., Diegelmann, R. F., Krummel, T. M., and Cohen, I. K. (1992a). Scarless wound healing in the mammalian fetus. *Surg Gynecol Obstet* **174**: 441-451.

Mast, B. A., Frantz, F. W., Diegelmann, R. F., Krummel, T. M., and Cohen, I. K. (1995). Hyaluronic acid degradation products induce neovascularization and fibroplasia in fetal rabbit wounds. *Wound Rep Reg* **3**: 66-

72.

Mast, B. A., Haynes, J. H., Krummel, T. M., Cohen, I. K., and Diegelmann, R. F. (1997). Ultrastructural analysis of fetal rabbit wounds. *Wound Rep Reg* **5**: 243-248.

Mast, B. A., Haynes, J. H., Krummel, T. M., Diegelmann, R. F., and Cohen, I. K. (1992b). *In vivo* degradation of fetal wound hyaluronic acid results in increased fibroplasia, collagen deposition, and neovascularization. *Plast Reconstr Surg* **89**: 503-509.

Matrisian, L. M. (1990). Metalloproteinases and their inhibitors in matrix remodeling. [Review]. *Trends Genet* **6**: 121-125.

Matrisian, L. M. and Hogan, B. L. M. (1990). Growth factor-regulated proteases and extracellular matrix remodeling during mammalian development. *In* "Current Topics in Developmental Biology." pp. 219-259, Academic Press Inc, New York.

Matsumoto, K., Sano, H., Nagai, R., Suzuki, H., Kodama, T., Yoshida, M., Ueda, S., Smedsrod, B., and Horiuchi, S. (2000). Endocytic uptake of advanced glycation end products by mouse liver sinusoidal endothelial cells is mediated by a scavenger receptor distinct from the macrophage scavenger receptor class A. *Biochem J* **352**: 233-240.

McCallion, R. L. and Ferguson, M. W. J. (1996). Fetal wound healing and the development of antiscarring therapies for adult wound healing. *In* "The Molecular and Cellular Biology of Wound Repair" (R. A. F. Clark, Ed.), pp. 561-600, Plenum press, New York.

McClelland, M., Mathieu-Daude, F., and Welsh, J. (1995). RNA fingerprinting and differential display using arbitrarily primed PCR. *Trends Genet* **11**: 242-246.

McCluskey, J., Hopkinson-Woolley, J., Luke, B., and Martin, P. (1993). A study of wound healing in the E11.5 mouse embryo by light and electron microscopy. *Tissue Cell* **25**: 173-181.

McCluskey, J. and Martin, P. (1995). Analysis of the tissue movements of embryonic wound healing-DiI Studies in the limb bud stage mouse embryo. *Dev Biol* **170**: 102-114.

McGee, G. S., Davidson, J. M., Buckley, A., Sommer, A., Woodward, S. C., Aquino, A. M., Barbour, R., and Demetriou, A. A. (1988). Recombinant basic fibroblast growth factor accelerates wound healing. *J Surg Res* **45**: 145-153.

McGrath, J. A. and Eady, R. A. J. (1997). Heparan sulphate proteoglycan and wound healing in skin. *J Pathol* **183**: 251-252.

McNeil, H. and Jensen, P. J. (1990). A high-affinity receptor for urokinase plasminogen activator on human keratinocytes: characterization and potential modulation during migration. *Cell Regul* **1**: 843-852.

Metes, D., Ernst, L. K., Chambers, W. H., Sulica, A., Herberman, R. B., and Morel, P. A. (1998). Expression

of functional CD32 molecules on human NK cells is determined by an allelic polymorphism of the FcgammaRIIC gene. *Blood* **91**: 2369-2380.

Meuli, M., Lorenz, H. P., Hedrick, M. H., Sullivan, K. M., Harrison, M. R., and Adzick, N. S. (1995). Scar formation in the fetal alimentary tract. *J Pediatr Surg* **30**: 392-395.

Miele, G., MacRae, L., McBride, D., Manson, J., and Clinton, M. (1998). Elimination of false positives generated through PCR reamplification of differential display cDNA. *Biotechniques* **25**: 138-144.

Mignatti, P. and Rifkin, D. B. (1993). Biology and biochemistry of proteinases in tumor invasion. [Review]. *Physiol Rev* **73**: 161-195.

Morcos, M., Hansch, G. M., Schonermark, M., Ellwanger, S., Harle, M., and Heckl-Ostreicher, B. (1994). Human glomerular mesangial cells express CD16 and may be stimulated via this receptor. *Kidney Int* **46**: 1627-1634.

Moriarty, K. P., Crombleholme, T. M., Gallivan, K., and O'Donnell, C. (1996). Hyaluronic acid-dependent pericellular matrices in fetal fibroblasts: Implication for scar-free wound repair. *Wound Rep Reg* **4**: 346-352.

Morris, L., Graham, C. F., and Gordon, S. (1991). Macrophages in haemopoietic and other tissues of the developing mouse detected by the monoclonal antibody F4/80. *Development* **112** : 517-526.

Morykwas, M. J., Ditesheim, J. A., Ledbetter, M. S., Crook, E., White, W. L., Jennings, D. A., and Argenta, L. C. (1991b). *Monodelphis domesticus*: A model for early developmental wound healing. *Ann Plast Surg* **27**: 327-331.

Morykwas, M. J., Ledbetter, M. S., Ditesheim, J. A., White, W. L., Vander Ark, A. D., and Argenta, L. C. (1991a). Cellular inflammation of fetal excisional wounds: Effects of amniotic fluid exclusion. *Inflammation* **15**: 173-180.

Mou, L., Miller, H., Li, J., Wang, E., and Chalifour, L. (1994). Improvements to the differential display method for gene analysis. *Biochem Biophys Res Commun* **199**: 564-569.

Mulvihill, S. J., Stone, M. M., Fonkalsrud, E. W., and Debas, H. T. (1986). Trophic effect of amniotic fluid on fetal gastrointestinal development. *J Surg Res* **40**: 291-296.

Munz, B., Gerke, V., Gillitzer, R., and Werner, S. (1997). Differential expression of the calpactin I subunits annexin II and p11 in cultured keratinocytes and during wound repair. *J Invest Dermatol* **108**: 307-312.

Munz, B., Wiedmann, M., Lochmuller, H., and Werner, S. (1999). Cloning of novel injury-regulated genes. Implications for an important role of the muscle-specific protein skNAC in muscle repair. *J Biol Chem* **274**: 13305-13310.

Murata, H., Zhou, L., Ochoa, S., Hasan, A., Badiavas, E., and Falanga, V. (1997). TGF-β3 stimulates and regulates collagen synthesis through TGF-β1-dependent and independent mechanisms. *J Invest Dermatol* **108**:

258-262.

Murphy, G., Atkinson, S., Ward, R., Gavrilovic, J., and Reynolds, J. J. (1992). The role of plasminogen activators in the regulation of connective tissue metalloproteinases. *Ann N Y Acad Sci* **667**: 1-12.

Murphy, G., Cockett, M. I., Ward, R. V., and Docherty, A. J. P. (1991). Matrix metalloproteinase degradation of elastin, type IV collagen and proteoglycan. *Biochem J* **277**: 277-279.

Murray, J. C. and Pinnell, S. R. (1992). Keloids and Excessive Dermal Scarring. *In* "Wound Healing Biochemical and Clinical Aspects" (I. K. Cohen, R. F. Diegelmann, and W. J. Lindblad, Eds.), pp. 500-509, W.B. Saunders Company, Philadelphia.

Mustoe, T. A., Pierce, G. F., Thomason, A., Gramates, P., Sporn, M. B., and Deuel, T. F. (1987). Accelerated healing of incisional wounds in rats induced by transforming growth factor-β. *Science* **237**: 1333-1336.

Mutsaers, S. E., Bishop, J. E., McGrouther, G., and Laurent, G. J. (1997). Mechanisms of tissue repair: From wound healing to fibrosis. *Int J Biochem Cell Biol* **29**: 5-17.

Nagarajan, S., Chesla, S., Cobern, L., Anderson, P., Zhu, C., and Selvaraj, P. (1995). Ligand binding and phagocytosis by CD16 (Fc gamma receptor III) isoforms. Phagocytic signaling by associated zeta and gamma subunits in Chinese hamster ovary cells. *J Biol Chem* **270**: 25762-25770.

Nakada, M., Nakada, K., Kitagawa, H., Kawaguchi, F., Hoson, M., Wakisaka, M., Kashimura, T., Ohkawa, I., Sato, Y., and Furuta, T. (1998). Efficacy of exogenous fibronectin in wound healing in malnourished rats. *J Pediatr Surg* **33**: 1699-1702.

Nath, R. K., LaRegina, M., Markham, H., Ksander, G. A., and Weeks, P. M. (1994a). The expression of transforming growth factor type beta in fetal and adult rabbit skin wounds. *J Pediatr Surg* **29**: 416-421.

Nath, R. K., Parks, W. C., Mackinnon, S. E., Hunter, D. A., Markham, H., and Weeks, P. M. (1994b). The regulation of collagen in fetal skin wounds: mRNA localization and analysis. *J Pediatr Surg* **29**: 855-862.

Nelson, J. M., Krummel, T. M., Haynes, J. H., Flood, L. C., Sauer, L., Flake, A. W., and Harrison, M. R. (1990). Operative techniques in the fetal rabbit. *J Invest Surg* **3**: 393-398.

Nielsen, H., Engelbrecht, J., Brunak, S., and von Heijne, G. (1997). Identification of prokaryotic and eukaryotic signal peptides and prediction of their cleavage sites. *Protein Engin* **10**: 1-6.

Nimni, M. E. (1997). Polypeptide growth factors: targeted delivery systems. *Biomaterials* **18**: 1201-1225.

Nishikiori, N., Koyama, M., Kikuchi, T., Kimura, T., Ozaki, M., Harada, S., Saji, F., and Tanizawa, O. (1993). Membrane-spanning Fc gamma receptor III isoform expressed on human placental trophoblasts. *Am J Reprod Immunol* **29**: 17-25.

Nissen, N. N., Polverini, P. J., Koch, A. E., Volin, M. V., Gamelli, R. L., and DiPietro, L. A. (1998). Vascular

endothelial growth factor mediates angiogenic activity during the proliferative phase of wound healing. *Am J Pathol* **152**: 1445-1452.

Nobes, C. D. and Hall, A. (1995). Rho, rac, and cdc42 GTPases regulate the assembly of multimolecular focal complexes associated with actin stress fibers, lamellipodia, and filopodia. *Cell* **81**: 53-62.

Nobes, C. D. and Hall, A. (1999). Rho GTPases control polarity, protrusion, and adhesion during cell movement. *J Cell Biol* **144**: 1235-1244.

Nodder, S. and Martin, P. (1997). Wound healing in embryos: A review. *Anat Embryol (Berl)* **195**: 215-228.

Nwomeh, B. C., Liang, H. X., Cohen, I. K., and Yager, D. R. (1999). MMP-8 is the predominant collagenase in healing wounds and nonhealing ulcers. *J Surg Res* **81**: 189-195.

Nwomeh, B. C., Liang, H. X., Diegelmann, R. F., Cohen, I. K., and Yager, D. R. (1998). Dynamics of the matrix metalloproteinases MMP-I and MMP-8 in acute open human dermal wounds. *Wound Rep Reg* **6**: 127-134.

Odland, G. F. (1991). Structure of the skin. *In* "Physiology, Biochemistry and Molecular Biology of the Skin" (L. A. Goldsmith, Ed.), pp. 3-62, Oxford University Press, New York.

Olutoye, O. O., Alaish, S. M., Carr, M. E., Jr., Paik, M. Y., Yager, D. R., Cohen, I. K., and Diegelmann, R. F. (1995). Aggregatory characteristics and expression of the collagen adhesion receptor in fetal porcine platelets. *J Pediatr Surg* **30**: 1649-1653.

Olutoye, O. O., Barone, E. J., Yager, D. R., Uchida, T., Cohen, I. K., and Diegelmann, R. F. (1997). Hyaluronic acid inhibits fetal platelet function: Implications in scarless healing. *J Pediatr Surg* **32**: 1037-1040.

Olutoye, O. O. and Cohen, I. K. (1996). Fetal wound healing: an overview. *Wound Rep Reg* **4**: 66-74.

Olutoye, O. O., Yager, D. R., Cohen, I. K., and Diegelmann, R. F. (1996). Lower cytokine release by fetal porcine platelets: A possible explanation for reduced inflammation after fetal wounding. *J Pediatr Surg* **31**: 91-95.

Orlandini, M., Marconcini, L., Ferruzzi, R., and Oliviero, S. (1996). Identification of a *c-fos*-induced gene that is related to the platelet-derived growth factor vascular endothelial growth factor family. *Proc Natl Acad Sci USA* **93**: 11675-11680.

Ortega, S., Ittmann, M., Tsang, S. H., Ehrlich, M., and Basilico, C. (1998). Neuronal defects and delayed wound healing in mice lacking fibroblast growth factor 2. *Proc Natl Acad Sci USA* **95**: 5672-5677.

Overall, C. M., Wrana, J. L., and Sodek, J. (1989). Independent regulation of collagenase, 72-kDa progelatinase, and metalloendoproteinase inhibitor expression in human fibroblasts by transforming growth factor-beta. *J Biol Chem* **264**: 1860-1869.

Overall, C. M., Wrana, J. L., and Sodek, J. (1991). Transcriptional and post-transcriptional regulation of 72-kDa gelatinase/type IV collagenase by transforming growth factor-beta 1 in human fibroblasts. Comparisons with collagenase and tissue inhibitor of matrix metalloproteinase gene expression. *J Biol Chem* **266**: 14064-14071.

Parrelli, J. M., Meisler, N., and Cutroneo, K. R. (1997). Abrogation of the fibrotic effect of transforming growth factor- β in dermal wound healing. *Wound Rep Reg* **5**: 136-140.

Peltonen, J., Kahari, L., Jaakkola, S., Kahari, V. M., Varga, J., Uitto, J., and Jimenez, S. A. (1990). Evaluation of transforming growth factor beta and type I procollagen gene expression in fibrotic skin diseases by *in situ* hybridization. *J Invest Dermatol* **94**: 365-371.

Peltz, G. A., Grundy, H. O., Lebo, R. V., Yssel, H., Barsh, G. S., and Moore, K. W. (1989). Human Fc gamma RIII: Cloning, expression, and identification of the chromosomal locus of two Fc receptors for IgG. *Proc Natl Acad Sci USA* **86**: 1013-1017.

Pennie, W. D. (2000). Use of cDNA microarrays to probe and understand the toxicological consequences of altered gene expression. *Toxicol Lett* **112-113**: 473-477.

Persson, B. and Argos, P. (1994). Prediction of transmembrane segments in proteins utilising multiple sequence alignments. *J Mol Biol* **237**: 182-192.

Persson, B. and Argos, P. (1996). Topology prediction of membrane proteins. *Protein Sci* **5**: 363-371.

Pierce, G. F., Mustoe, T. A., Lingelbach, J., Masakowski, V. R., Gramates, P., and Deuel, T. F. (1989b). Transforming growth factor β reverses the glucocorticoid-induced wound-healing deficit in rats: Possible regulation in macrophages by platelet-derived growth factor. *Proc Natl Acad Sci USA* **86**: 2229-2233.

Pierce, G. F., Mustoe, T. A., Lingelbach, J., Masakowski, V. R., Griffin, G. L., Senior, R. M., and Deuel, T. F. (1989a). Platelet-derived growth factor and transforming growth factor-β enhance tissue repair activities by unique mechanisms. *J Cell Biol* **109**: 429-440.

Pierce, G. F., Tarpley, J. E., Yanagihara, D., Mustoe, T. A., Fox, G. M., and Thomason, A. (1992). Platelet-derived growth factor (BB homodimer), transforming growth factor-β1, and basic fibroblast growth factor in dermal wound healing. *Am J Pathol* **140**: 1375-1388.

Piscatelli, S. J., Michaels, B. M., Gregory, P., Jennings, R. W., Longaker, M. T., Harrison, M. R., and Siebert, J. W. (1994). Fetal fibroblast contraction of collagen matrices *in vitro*: The effects of epidermal growth factor and transforming growth factor-beta. *Ann Plast Surg* **33**: 38-45.

Ponting, C. P., Schultz, J., Milpetz, F., and Bork, P. (1999). SMART: Identification and annotation of domains from signalling and extracellular protein sequences. *Nucleic Acids Res* **27**: 229-232.

Pritchard, J. A (1993). The morphological and functional development of the fetus. *In* "Williams Obstetrics"

(P. C. MacDonald, N. F. Gant, K. J. Leveno, and L. C. Gilstrap, Eds.), pp. 165-207, Appleton and Lange, Conneticut.

Qiu, W. Q., de Bruin, D., Brownstein, B. H., Pearse, R., and Ravetch, J. V. (1990). Organization of the human and mouse low-affinity Fc gamma R genes: Duplication and recombination. *Science* **248**: 732-735.

Quilhac, A. and Sire, J. Y. (1998). Restoration of the subepidermal tissues and scale regeneration after wounding a cichlid fish, *Hemicromis bimaculatus*. *J Exp Zool* **281**: 305-327.

Quilhac, A. and Sire, J. Y. (1999). Spreading, proliferation, and differentiation of the epidermis after wounding a cichlid fish, *Hemichromis bimaculatus*. *Anat Rec* **254**: 435-451.

Raghavan, M. and Bjorkman, P. J. (1996). Fc receptors and their interactions with immunoglobulins. *Annu Rev Cell Dev Biol* **12**: 181-220.

Raines, E. W. and Ross, R. (1992). Compartmentalization of PDGF on extracellular binding sites dependent on exon-6-encoded sequences. *J Cell Biol* **116**: 533-543.

Raju, R., Hoppe, B.L., Navaneetham, D. and Conti-Fine, B.M. (1995). Rapid method for the elution and analysis of PCR products seperated on high resolution acrylamide gels. *Biotechniques* **18**: 33-35.

Ravetch, J. V. and Kinet, J. P. (1991). Fc receptors. *Annu Rev Immunol* **9: 457-92.**: 457-492.

Ravetch, J. V. and Perussia, B. (1989). Alternative membrane forms of Fc gamma RIII(CD16) on human natural killer cells and neutrophils. Cell type-specific expression of two genes that differ in single nucleotide substitutions. *J Exp Med* **170**: 481-497.

Redlich, M., Cooperman, H., Yakovlev, H., Feferman, R., and Shoshan, S. (1998). Exogenous non-crosslinked collagen enhances granulation tissue formation in dermal excision wounds in guinea pigs. *Matrix Biol* **17**: 667-671.

Reeves, S. A., Rubio, M. P., and Louis, D. N. (1995). General method for PCR amplification and direct sequencing of mRNA differential display products. *Biotechniques* **18**: 18-20.

Reginelli, A. D., Wang, Y. Q., Sassoon, D., and Muneoka, K. (1995). Digit tip regeneration correlates with regions of Msx1 (Hox 7) expression in fetal and newborn mice. *Development* **121**: 1065-1076.

Riches, D. W. (1996). Macrophage involvement in wound repair, remodeling, and fibrosis. *In* "The Molecular and Cellular Biology of Wound Repair" (R. A. F. Clark, Ed.), pp. 95-141, Plenum Press, New York.

Ridley, A. J. and Hall, A. (1992). The small GTP-binding protein rho regulates the assembly of focal adhesions and actin stress fibers in response to growth factors. *Cell* **70**: 389-399.

Ridley, A. J., Paterson, H. F., Johnston, C. L., Diekmann, D., and Hall, A. (1992). The small GTP-binding protein rac regulates growth factor-induced membrane ruffling. *Cell* **70**: 401-410.

Rifkin, D. B. and Moscatelli, D. (1989). Recent developments in the cell biology of basic fibroblast growth factor. [Review]. *J Cell Biol* **109**: 1-6.

Rittenberg, T., Longaker, M. T., Adzick, N. S., and Ehrlich, H. P. (1991). Sheep amniotic fluid has a protein factor which stimulates human fibroblast populated collagen lattice contraction. *J Cell Physiol* **149**: 444-450.

Rivera-Marrero, C. A., Burroughs, M. A., Masse, R. A., Vannberg, F. O., Leimbach, D. L., Roman, J., and Murtagh, J. J., Jr. (1998). Identification of genes differentially expressed in *Mycobacterium tuberculosis* by differential display PCR. *Microb Pathog* **25**: 307-316.

Roberts, A. B. and Sporn, M. B. (1992). Mechanistic interrelationships between two superfamilies: The steroid/retinoid receptors and transforming growth factor-β. *Cancer Surv* **14**: 205-220.

Rohrwild, M., Alpan, R. S., Liang, P., and Pardee, A. B. (1995). Inosine-containing primers for mRNA differential display. *Trends Genet* **11**: 300.

Rowlatt, U. (1979). Intrauterine wound healing in a 20 week human fetus. *Virchows Archiv A, Patholog Anat & Hist* **381**: 353-361.

Ryoo, H. M., Hoffmann, H. M., Beumer, T., Frenkel, B., Towler, D. A., Stein, G. S., Stein, J. L., van Wijnen, A. J., and Lian, J. B. (1997). Stage-specific expression of Dlx-5 during osteoblast differentiation: Involvement in regulation of osteocalcin gene expression. *Mol Endocrinol* **11**: 1681-1694.

Saarialho-Kere, U. K., Chang, E. S., Welgus, H. G., and Parks, W. C. (1992). Distinct localization of collagenase and tissue inhibitor of metalloproteinases expression in wound healing associated with ulcerative pyogenic granuloma. *J Clin Invest* **90**: 1952-1957.

Saitou, N. and Nei, M. (1987). The neighbor-joining method: A new method for reconstructing phylogenetic trees. *Mol Biol Evol* **4**: 406-425.

Salo, T., Makela, M., Kylmaniemi, M., Autio-Harmainem, H., and Larjava, H. (1994). Expression of matrix metalloproteinase-2 and -9 during early human wound healing. *Lab Invest* **70**: 176-182.

Sambrook, J., Fritsch, E. F, and Maniatis, T. (1989). "Molecular Cloning: A Laboratory Manual," Cold Spring Harbor Laboratory Press, New York.

Sancho, M. A., Juliá, V., Albert, A., Díaz, F., and Morales, L. (1997). Effect of the environment on fetal skin wound healing. *J Pediatr Surg* **32**: 663-666.

Sanguinetti, C. J., Dias, N. E., and Simpson, A. J. (1994). Rapid silver staining and recovery of PCR products separated on polyacrylamide gels. *Biotechniques* **17**: 914-921.

Santiago, A., Satriano, J., DeCandido, S., Holthofer, H., Schreiber, R., Unkeless, J., and Schlondorff, D. (1989). A specific Fc gamma receptor on cultured rat mesangial cells. *J Immunol* **143**: 2575-2582.

Sappino, A. P., Schurch, W., and Gabbiani, G. (1990). Differentiation repertoire of fibroblastic cells: expression of cytoskeletal proteins as marker of phenotypic modulations. *Lab Invest* **63**: 144-161.

Sarkar, G. and Sommer, S. (1990b). More light on PCR contamination [letter]. *Nature* **347**: 340-341.

Sarkar, G. and Sommer, S. S. (1990a). Shedding light on PCR contamination [letter]. *Nature* **343**: 27.

Sawai, T., Usui, N., Sando, K., Fukui, Y., Kamata, S., Okada, A., Taniguchi, N., Itano, N., and Kimata, K. (1997). Hyaluronic acid of wound fluid in adult and fetal rabbits. *J Pediatr Surg* **32**: 41-43.

Scallon, B. J., Scigliano, E., Freedman, V. H., Miedel, M. C., Pan, Y. C., Unkeless, J. C., and Kochan, J. P. (1989). A human immunoglobulin G receptor exists in both polypeptide-anchored and phosphatidylinositol-glycan-anchored forms. *Proc Natl Acad Sci USA* **86**: 5079-5083.

Schaffer, C. J. and Nanney, L. B. (1996). Cell biology of wound healing. *Int Rev Cytol* **169**: 151-181.

Schilling, J. A. (1976). Wound healing. *Surg Clin of Nth Amer* **56**: 859-874.

Schilling, J. A., Joel, W., and Shurley, H. M. (1959). Wound Healing: A comparative study of the histochemical changes in granulation tissue contained in stainlesss steel wire mesh and polyvinyl sponge cylinders. *Surgery* **46**: 702-710.

Schmid, P., Kunz, S., Cerletti, N., McMaster, G., and Cox, D. (1993). Injury induced expression of TGF-β1 mRNA is enhanced by exogenously applied TGF-βs. *Biochem Biophys Res Commun* **194**: 399-406.

Schor, S. L., Ellis, I., Irwin, C. R., Banyard, J., Seneviratne, K., Dolman, C., Gilbert, A. D., and Chisholm, D. M. (1996). Subpopulations of fetal-like gingival fibroblasts: Characterisation and potential significance for wound healing and the progression of periodontal disease. *Oral Diseases*155-166.

Schor, S. L., Schor, A. M., Grey, A. M., Chen, J., Rushton, G., Grant, M. E., and Ellis, I. (1989). Mechanism of action of the migration stimulating factor produced by fetal and cancer patient fibroblasts: Effect on hyaluronic acid synthesis. *In Vitro Cell & Dev Biol* **25**: 737-746.

Schor, S. L., Schor, A. M., Grey, A. M., and Rushton, G. (1988). Foetal and cancer patient fibroblasts produce and autocrine migration-stimulating factor not made by normal adult cells. *J Cell Sci* **90**: 391-399.

Schultz, G. S., White, M., Mitchell, R., Brown, G., Lynch, J., Twardzik, D. R., and Todaro, G. J. (1987). Epithelial wound healing enhanced by transforming growth factor-α and Vaccinia growth factor. *Science* **235**: 350-351.

Schultz, J., Copley, R. R., Doerks, T., Ponting, C. P., and Bork, P. (2000). SMART: A web-based tool for the study of genetically mobile domains. *Nucleic Acids Res* **28**: 231-234.

Schultz, J., Milpetz, F., Bork, P., and Ponting, C. P. (1998). SMART, a simple modular architecture research tool: identification of signaling domains. *Proc Natl Acad Sci USA* **95**: 5857-5864.

Scott, J. E. and Hughes, E. W. (1986). Proteoglycan-collagen relationships in developing chick and bovine tendons. Influence of the physiological environment [published erratum appears in Connect Tissue Res 1986; 15(4): 304]. *Connect Tissue Res* **14**: 267-278.

Serini, G. and Gabbiani, G. (1996). Modulation of α -smooth muscle actin expression in fibroblasts by transforming growth factor-β isoforms: an *in vivo* and *in vitro* study. *Wound Rep Reg* **4**: 278-287.

Shah, M., Foreman, D. M., and Ferguson, M. W. (1992). Control of scarring in adult wounds by neutralising antibody to transforming growth factor beta. *Lancet* **339**: 213-214.

Shah, M., Foreman, D. M., and Ferguson, M. W. (1995). Neutralisation of TGF-beta 1 and TGF-beta 2 or exogenous addition of TGF-beta 3 to cutaneous rat wounds reduces scarring. *J Cell Sci* **108**: 985-1002.

Shah, M., Foreman, D. M., and Ferguson, M. W. J. (1994). Neutralising antibody to TGF-$\beta_{1,2}$ reduces cutaneous scarring in adult rodents. *J Cell Sci* **107**: 1137-1157.

Shah, M., Revis, D., Jr., Herrick, S., Baillie, R., Thorgeirson, S., Ferguson, M., and Roberts, A. (1999). Role of elevated plasma transforming growth factor-β1 levels in wound healing. *Am J Pathol* **154**: 1115-1124.

Shah, M., Roberts, A. B., Gold, L. I., and Ferguson, M. W. J. (1993). Immunolocalisation of TGFβ isoforms in normal and experimentally modulated incisional wounds in adult rodents. *Wound Rep Reg* **2**: 124.

Shelton, D. N., Chang, E., Whittier, P. S., Choi, D., and Funk, W. D. (1999). Microarray analysis of replicative senescence. *Curr Biol* **9**: 939-945.

Siebert, J. W., Burd, A. R., McCarthy, J. G., Weinzweig, J., and Ehrlich, H. P. (1990). Fetal wound healing: A biochemical study of scarless healing. *Plast Reconstr Surg* **85**: 495-502.

Simmons, D. and Seed, B. (1988). The Fc gamma receptor of natural killer cells is a phospholipid-linked membrane protein. *Nature* **333**: 568-570.

Simpson, D. M. and Ross, R. (1972). The neutrophilic leukocyte in wound repair: A study with antineutrophil serum. *J Clin Invest* **51**: 2009-2023.

Singer, A. J. and Clark, R. A. F. (1999). Mechanisms of disease - Cutaneous wound healing. *New Eng J Med* **341**: 738-746.

Sloan, P. (1991). Current concepts of the role of fibroblasts and extracellular matrix in wound healing and their relevance to oral implantology. *J Dent* **19**: 107-109.

Smedley, M. J. and Stanisstreet, M. (1984). Scanning electron microscopy of wound healing in rat embryos. *J Embryol Exp Morphol* **83**: 109-117.

Sokolov, B. P. and Prockop, D. J. (1994). A rapid and simple PCR-based method for isolation of cDNAs from differentially expressed genes. *Nucleic Acids Res* **22**: 4009-4015.

Somasundaram, K. and Prathap, K. (1970). Intra-uterine healing of skin wounds in rabbit foetuses. *J Pathol* **100**: 81-86.

Somasundaram, K. and Prathap, K. (1972). The effect of exclusion of amniotic fluid on intra-uterine healing of skin wounds in rabbit foetuses. *J Pathol* **107**: 127-130.

Sondermann, P., Huber, R., and Jacob, U. (1999). Crystal structure of the soluble form of the human fcgamma-receptor IIb: A new member of the immunoglobulin superfamily at 1.7 A resolution. *EMBO J* **18**: 1095-1103.

Sondermann, P., Huber, R., Oosthuizen, V., and Jacob, U. (2000). The 3.2-A crystal structure of the human IgG1 Fc fragment-Fc gammaRIII complex. *Nature* **406**: 267-273.

Songyang, Z., Shoelson, S. E., Chaudhuri, M., Gish, G., Pawson, T., Haser, W. G., King, F., Roberts, T., Ratnofsky, S., Lechleider, R. J., and . (1993). SH2 domains recognize specific phosphopeptide sequences. *Cell* **72**: 767-778.

Soo, C., Hu, F. Y., Zhang, X., Wang, Y., Beanes, S. R., Lorenz, H. P., Hedrick, M. H., Mackool, R. J., Plaas, A., Kim, S. J., Longaker, M. T., Freymiller, E., and Ting, K. (2000). Differential expression of fibromodulin, a transforming growth factor-beta modulator, in fetal skin development and scarless repair. *Am J Pathol* **157**: 423-433.

Soo, C., Shaw, W. W., Freymiller, E., Longaker, M. T., Bertolami, C. N., Chiu, R., Tieu, A., and Ting, K. (1999). Cutaneous rat wounds express *C49a*, a novel gene with homology to the human melanoma differentiation associated gene, *Mda-7*. *J Cell Biochem* **74**: 1-10.

Sopher, D. (1975a). A study of wound healing in the fetal tissues of the cynomologus monkey. *Lab Anim Handb* **6**: 327.

Sopher, D (1975b). "Future prospects for fetal sugery in teratology: Trends and applications," Springer-Verlag, New York / Berlin.

Sporn, M. B. and Roberts, A. B. (1992). Transforming growth factor-β: Recent progress and new challenges. *J Cell Biol* **119**: 1017-1021.

Steffan, A. M., Gendrault, J. L., McCuskey, R. S., McCuskey, P. A., and Kirn, A. (1986). Phagocytosis, an unrecognized property of murine endothelial liver cells. *Hepatology* **6**: 830-836.

Stelnicki, E. J., Arbeit, J., Cass, D. L., Saner, C., Harrison, M., and Largman, C. (1998). Modulation of the human homeobox genes *PRX-2* and *HOXB13* in scarless fetal wounds. *J Invest Dermatol* **111**: 57-63.

Stenn, K. S. and Malhotra, R. (1992). Epithelialization. *In* "Wound Healing Biochemical and Clinical Aspects" (I. K. Cohen, R. F. Diegelmann, and W. J. Lindblad, Eds.), pp. 115-127, W.B. Sauders Company, Philadelphia.

Stern, M., Schmidt, B., Dodson, T. B., Stern, R., and Kaban, L. B. (1992). Fetal cleft lip repair in rabbits: Histology and role of hyaluronic acid. *J Oral Maxillofac Surg* **50**: 263-268.

Stocum, D. L. (1998). Regenerative biology and engineering: Strategies for tissue restoration. *Wound Rep Reg* **6**: 276-290.

Stricklin, G. P., Li, L., Jancic, V., Wenczak, B. A., and Nanney, L. B. (1993). Localization of mRNAs representing collagenase and TIMP in sections of healing human burn wounds. *Am J Pathol* **143**: 1657-1666.

Stuart, S. G., Simister, N. E., Clarkson, S. B., Kacinski, B. M., Shapiro, M., and Mellman, I. (1989). Human IgG Fc receptor (hFcRII; CD32) exists as multiple isoforms in macrophages, lymphocytes and IgG-transporting placental epithelium. *EMBO J* **8**: 3657-3666.

Suh, D. Y., Hunt, T. K., and Spencer, E. M. (1992). Insulin-like growth factor-I reverses the impairment of wound healing induced by corticosteroids in rats. *Endocrinology* **131**: 2399-2403.

Sullivan, K. M., Lorenz, H. P., Meuli, M., Lin, R. Y., and Adzick, N. S. (1995b). A model of scarless human fetal wound repair is deficient in transforming growth factor beta. *J Pediatr Surg* **30**: 198-202.

Sullivan, K. M., Meuli, M., MacGillivray, T. E., and Adzick, N. S. (1995a). An adult-fetal skin interface heals without scar formation in sheep. *Surgery* **118**: 82-86.

Suzuki, T., Kono, H., Hirose, N., Okada, M., Yamamoto, T., Yamamoto, K., and Honda, Z. (2000). Differential involvement of Src family kinases in Fc gamma receptor-mediated phagocytosis. *J Immunol* **165**: 473-482.

Suzuki, Y., Itakura, M., Kashiwagi, M., Nakamura, N., Matsuki, T., Sakuta, H., Naito, N., Takano, K., Fujita, T., and Hirose, S. (1999). Identification by differential display of a hypertonicity-inducible inward rectifier potassium channel highly expressed in chloride cells. *J Biol Chem* **274**: 11376-11382.

Swofford, D. L. (1999). PAUP: Phylogenetic analysis using parsimony. [Computer Program 4.0b4A]. Champaign, Illinois Natural History Survey.

Tassava, R. A., Nace, J. D., and Wei, Y. (1996). Extracellular matrix protein turnover during salamander limb regeneration. *Wound Rep Reg* **4**: 75-81.

Thomasson, B., Viljanto, J., Jaaskelainen, A., and Raekallio, J. (1973). Enzyme-histochemical observations on the formation of granulation tissue in rabbit fetuses and does. *Acta Chir Scand* **139**: 327-333.

Thompson, J. D., Higgins, D. G., and Gibson, T. J. (1994). CLUSTAL W: Improving the sensitivity of progressive multiple sequence alignment through sequence weighting, position-specific gap penalties and weight matrix choice. *Nucleic Acids Res* **22**: 4673-4680.

Trenkle, T., Welsh, J., Jung, B., Mathieu-Daude, F., and McClelland, M. (1998). Non-stoichiometric reduced complexity probes for cDNA arrays. *Nucleic Acids Res* **26**: 3883-3891.

Tsou, R., Cole, J. K., Nathens, A. B., Isik, F. F., Heimbach, D. M., Engrav, L. H., and Gibran, N. S. (2000). Analysis of hypertrophic and normal scar gene expression with cDNA microarrays. *J Burn Care Rehabil* **21**:

541-550.

Tsuboi, R., Sato, C., Kurita, Y., Ron, D., Rubin, J. S., and Ogawa, H. (1993). Keratinocyte growth factor (FGF-7) stimulates migration and plasminogen activator activity of normal human keratinocytes. *J Invest Dermatol* **101**: 49-53.

Tuijnman, W. B., Capel, P. J., and van de Winkel, J. G. (1992b). Human low-affinity IgG receptor Fc gamma RIIa (CD32) introduced into mouse fibroblasts mediates phagocytosis of sensitized erythrocytes. *Blood* **79**: 1651-1656.

Tuijnman, W. B., Wijngaard, P. L., van Wichen, D., van de Winkel, J. G., Capel, P. J., and Schuurman, H. J. (1992a). Presence of CD16 on endothelial cells in heart transplant rejection: An immunohistochemical study. *Scand J Immunol* **35**: 569-573.

Tusnady, G. E. and Simon, I. (1998). Principles governing amino acid composition of integral membrane proteins: Application to topology prediction. *J Mol Biol* **283**: 489-506.

Uhl, E., Barker, J. H., Bondàr, I., Galla, T. J., Leiderer, R., Lehr, H.-A., and Messmer, K. (1993). Basic fibroblast growth factor accelerates wound healing in chronically ischaemic tissue. *Br J Surg* **80**: 977-980.

Utans, U., Liang, P., Wyner, L. R., Karnovsky, M. J., and Russell, M. E. (1994). Chronic cardiac rejection: Identification of five upregulated genes in transplanted hearts by differential mRNA display. *Proc Natl Acad Sci USA* **91**: 6463-6467.

Vaalamo, M., Leivo, T., and Saarialho-Kere, U. (1999). Differential expression of tissue inhibitors of metalloproteinases (TIMP-1,-2,-3, and-4) in normal and aberrant wound healing. *Hum Pathol* **30**: 795-802.

Vaalamo, M., Mattila, L., Johansson, N., Kariniemi, A. L., Karjalainen-Lindsberg, M. L., Kähäri, V. M., and Saarialho-Kere, U. K. (1997). Distinct populations of stromal cells express collagenase-3 (MMP- 13) and collagenase-1 (MMP-1) in chronic ulcers but not in normally healing wounds. *J Invest Dermatol* **109**: 96-101.

van Velthuysen, M. L., Mayen, A. E., Prins, F. A., De Heer, E., Bruijn, J. A., and Fleuren, G. J. (1994). Phagocytosis by glomerular endothelial cells in infection-related glomerulopathy. *Nephrol Dial Transplant* **9**: 1077-1083.

Van den Herik-Oudijk, I.E., Capel, P. J., van der Bruggen, T., and Van de Winkel, J. G. (1995b). Identification of signaling motifs within human Fc gamma RIIa and Fc gamma RIIb isoforms. *Blood* **85**: 2202-2211.

Van den Herik-Oudijk, I.E., Ter Bekke, M. W., Tempelman, M. J., Capel, P. J., and Van de Winkel, J. G. (1995a). Functional differences between two Fc receptor ITAM signaling motifs. *Blood* **86**: 3302-3307.

Venter, J. C., Adams, M. D., Myers, E. W., Li, P. W., and Mural, R. J. *et. al.* (2001). The sequence of the human genome. *Science* **291**: 1304-1351.

Verkoczy, L. K. and Berinstein, N. L. (1998). Isolation of genes negatively or positively co-expressed with

human recombination activating gene 1 (RAG1) by differential display PCR (DD RT-PCR). *Nucleic Acids Res* **26**: 4497-4507.

Viljanto, J. (1976). Cellstic: A device for wound healing studies in man. Description of the method. *J Surg Res* **20**: 115-119.

von Heijne, G. (1992). Membrane protein structure prediction. Hydrophobicity analysis and the positive-inside rule. *J Mol Biol* **225**: 487-494.

Vora, M. and Karasek, M. A. (1994). Retinoids upregulate phagocytosis by human dermal microvascular endothelial cells. *J Cell Physiol* **159**: 450-456.

Wan, J. S., Sharp, S. J., Poirier, G. M., Wagaman, P. C., Chambers, J., Pyati, J., Hom, Y. L., Galindo, J. E., Huvar, A., Peterson, P. A., Jackson, M. R., and Erlander, M. G. (1996). Cloning differentially expressed mRNAs. *Nat Biotechnol* **14**: 1685-1691.

Wang, J. F., Bown, C., and Young, L. T. (1999). Differential display PCR reveals novel targets for the mood-stabilizing drug valproate including the molecular chaperone GRP78. *Mol Pharmacol* **55**: 521-527.

Wang, X., Brownstein, M. J., and Young III, W. S. (1996). Sequence analysis of PG10.2, a gene expressed in the pineal gland and the outer nuclear layer of the retina. *Mol Brain Res* **41**: 269-278.

Wang, X., Brownstein, M. J., and Young, W. S. (1997). PG25, a pineal-specific cDNA, cloned by differential display PCR (DDPCR) and rapid amplification of cDNA ends (RACE). *J Neurosci Meth* **73**: 187-191.

Wearing, H. J. and Sherratt, J. A. (2000). Keratinocyte growth factor signalling: A mathematical model of dermal-epidermal interaction in epidermal wound healing. *Math Biosci* **165** : 41-62.

Weeks, P. M. and Nath, R. K. (1993). Fetal wound repair: a new direction [editorial]. *Plast Reconstr Surg* **91**: 922-924.

Weigel, P. H., Fuller, G. M., and LeBoeuf, R. D. (1986). A model for the role of hyaluronic acid and fibrin in the early events during the inflammatory response and wound healing. *J Theor Biol* **119**: 219-234.

Welch, M. P., Odland, G. F., and Clark, R. A. (1990). Temporal relationships of F-actin bundle formation, collagen and fibronectin matrix assembly, and fibronectin receptor expression to wound contraction. *J Cell Biol* **110**: 133-145.

Welgus, H. G., Fliszar, C. J., Seltzer, J. L., Schmid, T. M., and Jeffrey, J. J. (1990). Differential susceptibility of type X collagen to cleavage by two mammalian interstial collagenases and 72-kDa type IV collagenase. *J Biol Chem* **265**: 13521-13527.

Welgus, H. G., Jeffrey, J. J., and Eisen, A. Z. (1981b). Human skin fibroblast collagenase. *J Biol Chem* **256**: 9516-9521.

Welgus, H. G., Jeffrey, J. J., and Eisen, A. Z. (1981a). The collagen substrate specificity of human skin fibroblast collagenase. *J Biol Chem* **256**: 9511-9515.

Welsh, J., Chada, K., Dalal, S. S., Cheng, R., Ralph, D., and McClelland, M. (1992). Arbitrarily primed PCR fingerprinting of RNA. *Nucleic Acids Res* **20**: 4965-4970.

Werner, S., Peters, K. G., Longaker, M. T., Fuller-Pace, F., Banda, M. J., and Williams, L. T. (1992). Large induction of keratinocyte growth factor expression in the dermis during wound healing. *Proc Natl Acad Sci USA* **89**: 6896-6900.

Werner, S., Werner, S., and Munz, B. (2000). Suppression of keratin 15 expression by transforming growth factor beta *in vitro* and by cutaneous injury *in vivo*. *Exp Cell Res* **254**: 80-90.

West, D. C., Shaw, D. M., Lorenz, P., Adzick, N. S., and Longaker, M. T. (1997). Fibrotic healing of adult and late gestation fetal wounds correlates with increased hyaluronidase activity and removal of hyaluronan. *Int J Biochem Cell Biol* **29**: 201-210.

Whitby, D. J. and Ferguson, M. W. (1991a). Immunohistochemical localization of growth factors in fetal wound healing. *Dev Biol* **147**: 207-215.

Whitby, D. J. and Ferguson, M. W. (1991b). The extracellular matrix of lip wounds in fetal, neonatal and adult mice. *Development* **112**: 651-668.

Whitby, D. J. and Ferguson, M. W. J. (1991c). Immunohistochemical studies of the extracellular matrix and soluble growth factors in fetal and adult wound healing. *In* "Fetal wound healing." (N. S. Adzick and MT. Longaker, Eds.), pp. 161-175, Elsevier, New York.

Whitby, D. J., Longaker, M. T., Harrison, M. R., Adzick, N. S., and Ferguson, M. W. (1991). Rapid epithelialisation of fetal wounds is associated with the early deposition of tenascin. *J Cell Sci* **99**: 583-586.

Whitby, D. J., McMullen, H. F., Sung, J. J., Gold, L. I., Siebert, J. W., and Longaker, M. T. (1994). Localization of TGF-β isoforms in adult and fetal mouse lip wounds. *Surg Forum* **45**: 651-653.

Wickens, M. (1990). How the message got its tail. *Trends Biochem Sci* **15**: 277-281.

Wider, T. M., Yager, J. S., Rittenberg, T., Hugo, N. E., and Ehrlich, H. P. (1993). The inhibition of fibroblast-populated collagen lattice contraction by human amniotic fluid: A chronologic examination. *Plast Reconstr Surg* **91**: 1287-1293.

Williams, A. F. and Barclay, A. N. (1988). The immunoglobulin superfamily - Domains for cell surface recognition. *Annu Rev Immunol* **6**: 381-405.

Woessner, J. F., Jr. (1991). Matrix metalloproteinases and their inhibitors in connective tissue remodeling. *FASEB J* **5**: 2145-2154.

Wu, L. C., Siddiqui, A., Morris, D. E., Cox, D. A., Roth, S. I., and Mustoe, T. A. (1997). Transforming growth factor β3 (TGFβ3) accelerates wound healing without alteration of scar prominence - Histologic and competitive reverse-transcription polymerase chain reaction studies. *Arch Surg* **132**: 753-760.

Yamada, K. M. and Clark, R. A. F. (1996). Provisional Matrix. *In* "The Molecular and Cellular Biology of Wound Repair" (R. A. F. Clark, Ed.), pp. 51-92, Plenum Press, New York.

Yamada, K. M., Gailit, J., and Clark, R. A. F. (1996). Integrins in Wound Repair. *In* "The Molecular and Cellular Biology of Wound Repair" (R. A. F. Clark, Ed.), pp. 311-338, Plenum Press, New York.

Yang, L. J., Qiu, C. X., Ludlow, A., Ferguson, M. W. J., and Brunner, G. (1999). Active transforming growth factor-β in wound repair - Determination using a new assay. *Am J Pathol* **154**: 105-111.

Yeo, T. K., Brown, L., and Dvorak, H. F. (1991). Alterations in proteoglycan synthesis common to healing wounds and tumors. *Am J Pathol* **138**: 1437-1450.

Yi, X. J., Li, X. F., and Yu, F. S. (2000). A novel epithelial wound-related gene is abundantly expressed in developing rat cornea and skin. *Curr Eye Res* **20**: 430-440.

Zeger, D. L., Hogarth, P. M., and Sears, D. W. (1990). Characterization and expression of an Fc gamma receptor cDNA cloned from rat natural killer cells. *Proc Natl Acad Sci USA* **87**: 3425-3429.

Zhao, S., Ooi, S. L., and Pardee, A. B. (1995). New primer strategy improves precision of differential display. *Biotechniques* **18**: 842-850.

Zhao, S., Ooi, S. L., Yang, F. C., and Pardee, A. B. (1996). Three methods for identification of true positive cloned cDNA fragments in differential display. *Biotechniques* **20**: 400-404.

Addendum

Acknowledgements

Page xv – Third paragraph, ninth line "Dr. Grant Brooker" should read "Dr. Grant Booker".

Chapter 1

Page 6 – Third paragraph, third line "indifferent" should read "undifferentiated".

Page 38 – First paragraph, first line "in that of their constituent glycosaminoglycans" should read "in the synthesis of their constituent glycosaminoglycans".

- Second line "correlates" should read "correlate".

Page 59 – Fifth line "occurs" should read "occur".

Chapter 3

Page 116 – In section 3.3.1.1, Figure 3.4 incorrectly follows Figure 3.2 and is, therefore, referenced out of sequence.

Page 157 – Third paragraph, second sentence explains that the *HindIII* restriction sites were originally included in the primers used in this thesis to facilitate cloning of the DD-PCR products. However, these sites did not need to be utilised as the DD-PCR product of interest could be easily cloned using the pGEM-T vector system.

Page 158 – Last paragraph, first line "13" should read "11".

Chapter 4

The discussion suggests that differential expression of the 2VG2 gene is directly related to the functional differences between E17 and E19 skin. However, it is acknowledged that the upregulation of the 2VG2 gene in E17 skin may be a downstream result of another differentially expressed gene that may be involved in fetal wound repair. This is supported to some degree by the fact that another 52 differentially expressed candidates were observed in the original DD-PCR experiments, with 10 more detected in the modified protocol.

References

Page 254 – Third reference "alfa" should read "alpha".

Page 263 – Fourth reference "additons" should read "additions".

Page 279 – Third reference "fcgamma" should read "Fc gamma".